UNIVERSIDADE FEDERAL DE UBERLÂNDIA

INSTITUTO DE CIÊNCIAS BIOMÉDICAS

PROGRAMA DE PÓS-GRADUAÇÃO EM IMUNOLOGIA E PARASITOLOGIA
APLICADAS

FOSFOLIPASE A2 ISOLADA DA SERPENTE *Crotalus durissus terrificus* **INIBE
O VÍRUS CHIKUNGUNYA** *in vitro*

IGOR DE ANDRADE SANTOS

UBERLÂNDIA

Junho - 2020

UNIVERSIDADE FEDERAL DE UBERLÂNDIA

INSTITUTO DE CIÊNCIAS BIOMÉDICAS

PROGRAMA DE PÓS-GRADUAÇÃO EM IMUNOLOGIA E PARASITOLOGIA

APLICADAS

FOSFOLIPASE A2 ISOLADA DA SERPENTE *Crotalus durissus terrificus* INIBE O VÍRUS CHIKUNGUNYA *in vitro*

IGOR DE ANDRADE SANTOS

<div style="text-align: right">

Dissertação apresentada ao colegiado do Programa de Pós-Graduação em Imunologia e Parasitologia Aplicadas como parte de obtenção do título de Mestre.

Orientadora: Ana Carolina Gomes Jardim

</div>

UBERLÂNDIA

Junho – 2020

UNIVERSIDADE FEDERAL DE UBERLÂNDIA
Coordenação do Programa de Pós-Graduação em Imunologia e Parasitologia
Aplicada
Av. Amazonas, s/n, Bloco 4C, Sala 4C218 - Bairro Umuarama, Uberlândia-MG, CEP 38400-902
Telefone: (34) 3225-8672 - www.imunoparasito.ufu.br - coipa@ufu.br

ATA DE DEFESA - PÓS-GRADUAÇÃO

Programa de Pós-Graduação em:	Imunologia e Parasitologia Aplicadas				
Defesa de:	Dissertação de Mestrado número 264 do PPIPA				
Data:	Vinte e quatro de junho de dois mil e vinte	Hora de início:	14h20	Hora de encerramento:	18h25
Matrícula do Discente:	11912IPA001				
Nome do Discente:	Igor de Andrade Santos				
Título do Trabalho:	Fosfolipase A2 isolada da serpente *Crotalus durissus terrificus* inibe o vírus chikungunya *in vitro*				
Área de concentração:	Imunologia e Parasitologia Aplicadas				
Linha de pesquisa:	Biologia das interações entre patógenos e seus hospedeiros e Biotecnologia empregada no diagnóstico e controle de doenças				
Projeto de Pesquisa de vinculação:	Terapia Antiviral: a solução esta na natureza?				

Reuniu-se, por vídeo conferência web, a Banca Examinadora designada pelo Colegiado do Programa de Pós-graduação em Imunologia e Parasitologia Aplicadas, assim composta pelos Titulares**:** Prof. Dr. Pedro Paulo Corbi – UNICAMP; Prof. Dr. Diego Pandeló José – UFTM; Profª Drª Ana Carolina Gomes Jardim – ICBIM/UFU (Presidente) e Orientadora do candidato.

Iniciando os trabalhos a presidente da mesa, Profª Drª Ana Carolina Gomes Jardim, apresentou a Comissão Examinadora e o candidato, agradeceu a presença do público, e concedeu ao discente a palavra para a exposição do seu trabalho. A duração da apresentação do discente, o tempo de arguição e de resposta foram conforme as normas do programa.

A seguir o senhor(a) presidente concedeu a palavra, pela ordem sucessivamente, aos(às) examinadores(as), que passaram a arguir o(a) candidato(a). Ultimada a arguição, que se desenvolveu dentro dos termos regimentais, a Banca, em sessão secreta, atribuiu o resultado final, considerando o(a) candidato(a):

Aprovado(a).

Esta defesa faz parte dos requisitos necessários à obtenção do título de Mestre.

O competente diploma será expedido após cumprimento dos demais requisitos, conforme as normas do Programa, a legislação pertinente e a regulamentação interna da UFU.

Nada mais havendo a tratar foram encerrados os trabalhos. Foi lavrada a presente ata que após lida e achada conforme foi assinada pela Banca Examinadora.

Documento assinado eletronicamente por **Ana Carolina Gomes Jardim**, **Professor(a) do Magistério Superior**, em 25/06/2020, às 17:22, conforme horário oficial de Brasília, com fundamento no art. 6º,

§ 1º, do Decreto nº 8.539, de 8 de outubro de 2015.

Documento assinado eletronicamente por **Diego Pandeló José**, **Usuário Externo**, em 25/06/2020, às 17:42, conforme horário oficial de Brasília, com fundamento no art. 6º, § 1º, do Decreto nº 8.539, de 8 de outubro de 2015.

Documento assinado eletronicamente por **Pedro Paulo Corbi**, **Usuário Externo**, em 26/06/2020, às 17:04, conforme horário oficial de Brasília, com fundamento no art. 6º, § 1º, do Decreto nº 8.539, de 8 de outubro de 2015.

A autenticidade deste documento pode ser conferida no site https://www.sei.ufu.br/sei/controlador_externo.php?acao=documento_conferir&id_orgao_acesso_externo=0, informando o código verificador **2096524** e o código CRC **984F8847**.

Referência: Processo nº 23117.036175/2020-03   SEI nº 2096524

AGRADECIMENTOS

LISTA DE ABREVIATURAS E SIGLAS

C	Proteína do capsídeo
CHIKV	Vírus do Chikungunya
DENV	Vírus da Dengue
DMEM	Do Inglês, Dulbecco's Modified Eagle Medium (Meio básico modificado por Dulbecco)
DMSO	Dimetilsulfóxido
E	Proteína do envelope
ECA	Enzima conversora de angiotensina
ECSA	Do Inglês, East/Central/South Africa (Leste/Centro/Sul da África)
HIV	Vírus da Imunodeficiência Humana
HCV	Hacivírus C
HSV	Vírus do Herpes simplex
MAYV	Vírus do Mayaro
MOI	Do Inglês, Multiplicity of infection (Multiplicidade de infecção)
MTT	3-(4,5-dimethylthiazol-2-yl)-2,5-diphenyltetrazolium-bromide (Brometo de 3-(4',5'-dimetiltiazol-2'-ila)-2,5-difeniltetrazol)
mL	Mililitros
nsP	Do Inglês, non-structural proteins (Proteínas não estruturais)
OMS	Organização Mundial da Saúde
ORFs	Do Inglês, Open Reading Frame (Regiões de leitura aberta)
PLA2$_{CB}$	Fosfolipase A2 *Crotalus durissus terrificus*
pH	Potencial hidrogênico
RE	Retículo endoplasmático
RNA	Do Inglês, Ribonucleicacid (Ácido ribonucleico)
WA	Do Inglês, West African (Oeste Africano)
YFV	Vírus da Febre Amarela
µL	Microlitro
µg	Microgramas

SUMÁRIO

RESUMO

O vírus Chikungunya (CHIKV) é o agente etiológico da febre de Chikungunya, uma doença transmitida globalmente através de mosquitos do gênero *Aedes* sp. Até o momento, não há tratamento antiviral ou vacina aprovados contra o CHIKV, sendo mandatório o desenvolvimento de novas estratégias terapêuticas. Nesse contexto, as proteínas isoladas dos venenos de serpentes têm demonstrado atividade antiviral contra diversos vírus, incluindo arboviroses relevantes para o sistema público de saúde. A fosfolipase A2$_{CB}$ (PLA2$_{CB}$), uma proteína isolada da peçonha de *Crotalus durissus terrificus*, demonstrou possuir atividades anti-inflamatórias, antiparasitárias, antibacterianas e antivirais. Neste estudo, nós investigamos os vários efeitos da PLA2$_{CB}$ no ciclo replicativo do CHIKV *in vitro*. A atividade antiviral da PLA2$_{CB}$ foi avaliada usando CHIKV-*nanoluciferase*, uma construção viral inserida de um gene repórter (-*nanoluc*), para infectar células de rim de hamster bebê (BHK-21) e avaliar a viabilidade celular (ensaio MTT) e as taxas de infectividade (níveis de luminescência). Os resultados demostraram que a PLA2$_{CB}$ possui uma potente atividade antiviral, avaliada pelo índice de seletividade de 128 (razão de citotoxicidade por atividade antiviral). Identificamos que o tratamento com PLA2$_{CB}$ protegeu as células contra a infecção pelo CHIKV em 84%, e reduziu significativamente a entrada do vírus nas células hospedeiras por um efeito virucida maior que 99%, ou reduzindo a adsorção e desnudamento em 98 e 95%, respectivamente. Adicionalmente, a PLA2$_{CB}$ apresentou um efeito moderado, porém significante, inibindo 64% das etapas pós-entrada do ciclo replicativo do CHIKV. Cálculos envolvendo ancoramento molecular foram realizados, e os resultados sugerem interações entre PLA2$_{CB}$ e as glicoproteínas do CHIKV, principalmente com a E1, por meio de interações hidrofóbicas. Adicionalmente, análises de espectroscopia no infravermelho indicou interações da PLA2$_{CB}$ com glicoproteínas do CHIKV, corroborando com os dados das análises *in silico*. Nossos dados demonstraram os múltiplos efeitos antivirais da PLA2$_{CB}$ no ciclo replicativo do CHIKV, e sugerem as interações da PLA2$_{CB}$ com glicoproteínas do CHIKV como um modo de ação desse composto bloqueando a entrada do vírus nas células hospedeiras.

ABSTRACT

Chikungunya virus (CHIKV) is the etiologic agent of Chikungunya fever, a globally spreading mosquito-borne disease. To date, there is no approved antiviral treatment or vaccine against CHIKV, being mandatory the development of new therapeutic strategies. In this context, proteins isolated from snake venoms have demonstrated antiviral activity against several virus, including arbovirus which are relevant the public health system. The phospholipase $A2_{CB}$ ($PLA2_{CB}$), a protein isolated from the venom of *Crotalus durissus terrificus*, demonstrated to possess anti-inflammatory, antiparasitic, antibacterial, and antiviral activities. In this study, we investigated the multiple effects of $PLA2_{CB}$ on the CHIKV replicative cycle *in vitro*. The antiviral activity of $PLA2_{CB}$ was assessed using CHIKV-*nanoluciferase*, a viral construct inserted of a reporter gene (-*nanoluc*), to infect baby hamster kidney cells (BHK-21) cells and evaluate cell viability (MTT assay) and infectivity rates (luminescence levels). The results demonstrated that $PLA2_{CB}$ possess a strong antiviral activity judged by the selective index of 128 (ratio of cytotoxicity to antiviral activity). We identified that the treatment with $PLA2_{CB}$ protected the cells against CHIKV infection in 84% and strongly impaired virus entry to the host cells by a virucidal effect of over 99%, or by reducing adsorption and uncoating in 98 and 95 %, respectively. Moreover, $PLA2_{CB}$ presented a modest yet significant activity inhibiting 64 % of post-entry stages of CHIKV replicative cycle. Molecular docking calculations were performed and results suggested binding interactions between $PLA2_{CB}$ and CHIKV glycoprotein, mainly with E1 through hydrophobic interactions. In addition, infrared spectroscopy spectral analysis indicated interactions of $PLA2_{CB}$ and CHIKV glycoproteins, corroborating with data from *in silico* analyzes. Our data demonstrated the multiple antiviral effects of $PLA2_{CB}$ on the CHIKV replicative cycle, and suggest the interactions of $PLA2_{CB}$ with CHIKV glycoproteins as a mode of action of this compound on blocking virus entry to the host cells.

CAPÍTULO I

Fundamentação Teórica

Vírus Chikungunya

INTRODUÇÃO

Histórico e Epidemiologia

O vírus da Chikungunya (CHIKV) foi descoberto em 1950 na região da Tanzânia (HALSTEAD, 2015; LUMSDEN, 1955) e sua identificação como o agente etiológico da Febre do Chikungunya ocorreu somente em 1955 (ROSS, 1955; WEAVER; FORRESTER, 2015a). O nome "chikungunya" originou-se do idioma Makonde, e significa 'aqueles que se dobram", referindo aos pacientes que possuíam uma aparência curvada durante a primeira epidemia documentada entre 1952 e 1953 (MONATH, 2019).

Por muitos anos, casos esporádicos de CHIKV permaneceram restritos às regiões da África e Ásia (COHEN et al., 1969; NJENGA et al., 2008). Entretanto, um surto global teve início em 2005, com alguns casos em ilhas do oceano Índico, e notificações em países como Itália e França, associados à intensa circulação de pessoas nestas regiões (RAVI, 2006; SAMBRI et al., 2008). O surto de febre Chikungunya atingiu também as Américas, onde o vírus se espalhou com grande facilidade, em consequência do clima favorável e a presença de vetores suscetíveis (GRATZ, 2004; PAGÈS et al., 2009; RASHAD; MAHALINGAM; KELLER, 2013) **(Figura 1)**.

Figura 1: Locais com transmissão do CHIKV. Países que registraram casos de Chikungunya (verde escuro) de acordo com o Centro de Controle e Prevenção de Doenças (CDC). Países e/ou territórios com casos importados não estão inclusos.

Adaptado de ("Geographic Distribution | Chikungunya virus | CDC", 2019)

Estudos filogenéticos identificaram duas cepas distintas do CHIKV, originadas a partir de uma linhagem comum, sendo uma a do Oeste Africano (WA) e outra do Leste/Centro/Sul da África (ECSA) (VOLK et al., 2010; WEAVER; FORRESTER, 2015b). Relatos históricos identificaram a ocorrência de um surto na Ásia cerca de 150 anos atrás, causado pela cepa ECSA, a qual possivelmente propiciou a sua diferenciação em um genótipo diferente, conhecido como a Linhagem Urbana Asiática (AUL) (BURT et al., 2017; VOLK et al., 2010). Adicionalmente, a inserção de uma linhagem ECSA nas regiões do Oceano Índico deu origem a outro genótipo, a linhagem do Oceano Índico (IOL), entretanto, estima-se que essa linhagem tenha se extinguido (BURT et al., 2017; VOLK et al., 2010). No Brasil, os primeiros casos da febre do Chikungunya foram relatados no Amapá e na Bahia em 2014, causados pelas cepas ECSA e AUL, as quais foram rapidamente difundidas para os demais estados do território brasileiro (MINISTÉRIO DA SAÚDE, 2015; SILVA et al., 2017). Desde então, essas cepas foram responsáveis por mais de 650 mil casos de febre Chikungunya entre os anos de 2014 e 2019 (MINISTÉRIO DA SAÚDE, 2017, 2018; SILVA et al., 2018). No ano de 2020, foram registrados até a semana epidemiológica 21, 34.751 casos prováveis de febre Chikungunya, com uma incidência de 16,5 casos por 100 mil habitantes, e 8 óbitos confirmados (MINISTÉRIO DA SAÚDE, 2020b).

Transmissão

O CHIKV é transmitido por meio da picada de mosquitos fêmeas infectados pelo CHIKV, sendo os principais vetores o *Aedes aegypti* e *Aedes albopictus* (NGOAGOUNI et al., 2017; POWERS et al., 2000). Regiões com clima tropical facilitam o aumento da densidade de vetores e, consequentemente, a transmissão do vírus, especialmente durante períodos chuvosos (MAVALE et al., 2010) **(Figura 2)**. De maneira agravante, outros vetores, como *Haemagogus leucocelaenus* e *Aede terrens*, possuem alta susceptibilidade pelo vírus, podendo se tornar potenciais vetores transmissores, e assim, facilitar novos surtos da infecção (LOURENÇO-DE-OLIVEIRA; FAILLOUX, 2017). A transmissão vertical do CHIKV é classificada como rara, mas devido à patologia, pode provoca abortos em fases iniciais, bem como altas taxas de morbidade infantil, o que pode impactar diretamente na documentação desses casos (GUPTA; GUPTA, 2019). Entretanto, em 2018 foi relatado o primeiro caso de morte de recém-nascido no Brasil após infecção por CHIKV (OLIVEIRA et al., 2018).

Figura 2: Distribuição dos vetores do CHIKV no mundo. Mapa demonstrando a possível distribuição dos vetores *Aedes aegypti* (A) e *Aedes albopictus* (B). Regiões em azul indicam baixa densidade e em vermelho alta densidade da distribuição dos vetores. Pontos em preto significam os locais onde a presença desses vetores foi confirmada.
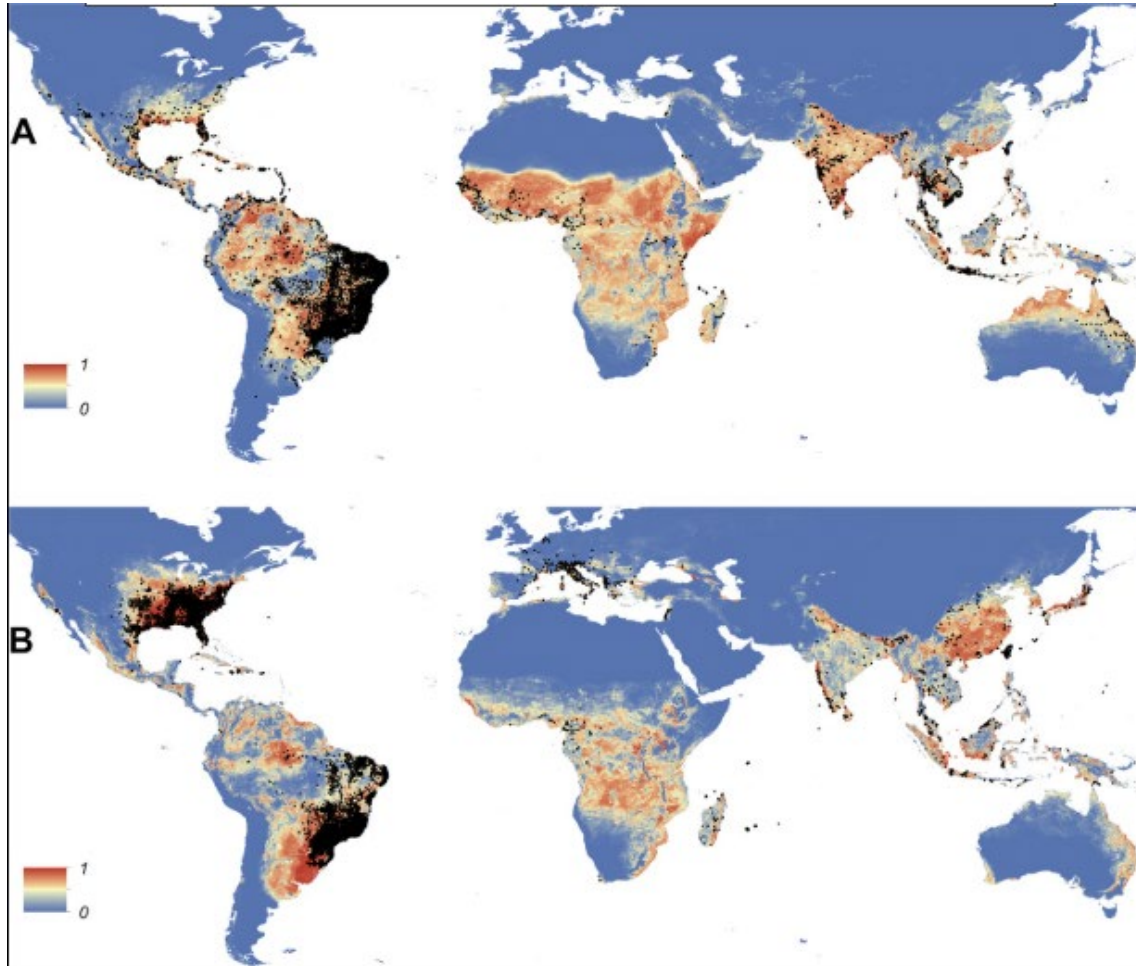

Adaptado de (KRAEMER et al., 2015)

Vírus Chikungunya

O CHIKV pertence à família *Togaviridae* e gênero *Alphavirus* (GAY et al., 2016; ROSS, 1955). É um vírus envelopado, com aproximadamente 70 nm de diâmetro e uma fita simples de RNA de polaridade positiva com aproximadamente 12 kB (ROBERTS et al., 2017; SOLIGNAT et al., 2009a) **(Figura 3A)**. O genoma viral apresenta uma região não-codificante 5', seguida de uma região aberta de leitura (*Open Reading frame*, ORF) codificante das 4 proteínas não estruturais (nsP1 a nsP4), relacionadas ao complexo replicativo, seguida da ORF codificante das 5 proteínas estruturais (C, E1, E2, E3 e 6K), presentes no capsídeo ou envelope do vírus, e por fim de uma região não-codificante 3' (LUM; NG, 2015; POWERS, 2017) **(Figura 3B)**.

Figura 3: Estrutura da partícula viral e Genoma do CHIKV. Esquema representativo da partícula viral do CHIKV (A). Ilustração do genoma do CHIKV (B).
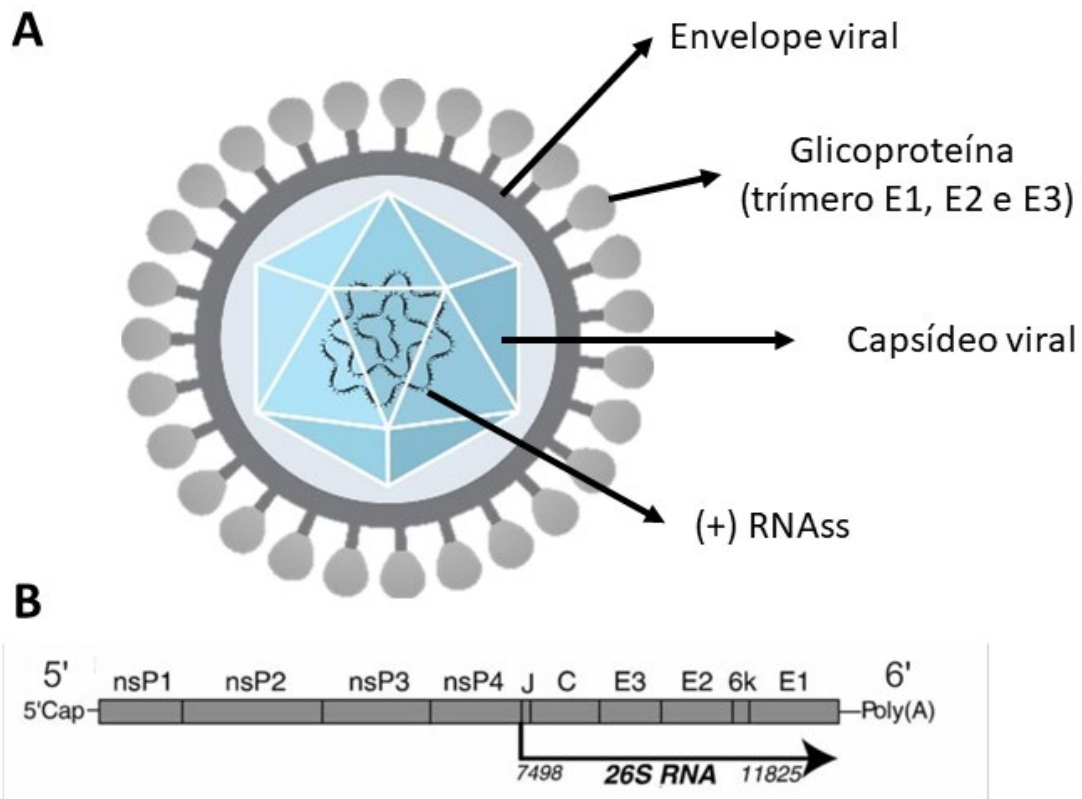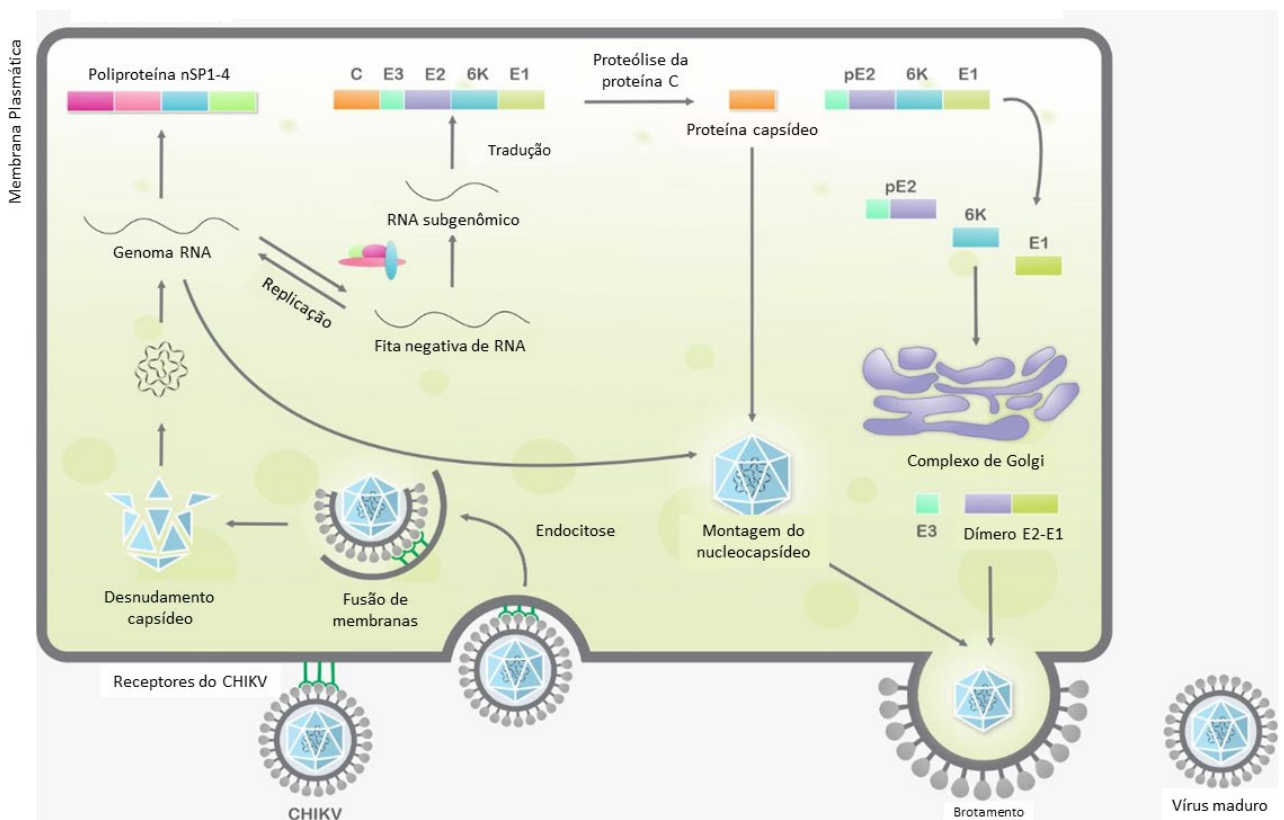

Adaptado de (MARTINS et al., 2020; SOLIGNAT et al., 2009b)

O ciclo replicativo do vírus ocorre em hospedeiros vertebrados e células de artrópodes, sendo assim classificada como uma arbovirose (BORGHERINI et al., 2007). A replicação viral se inicia pela adsorção do vírus à célula hospedeira, através da ligação da glicoproteína E2 do envelope viral com os glicosaminoglicanos e receptores TIM-1, DC-SIGN e Mxra8 da membrana da célula hospedeira, que promove a entrada do vírus por endocitose (SCHNIERLE, 2019). O pH se torna ácido no interior do endossomo, provocando mudanças conformacionais que permitem a fusão entre as membranas do endossomo e do envelope viral. Esse processo é mediado pela glicoproteína E1, promovendo a liberação do capsídeo viral no citoplasma da célula infectada e posterior liberação do RNA viral. O RNA de polaridade positiva é rapidamente traduzido em uma poliproteína não-estrutural (NSP1234), a qual interage com proteínas do hospedeiro e, posteriormente são clivadas em NSP1, NSP2, NSP3 e NSP4. Estas, formam um complexo conhecido como Replicase Viral, o qual é responsável por sintetizar uma fita de RNA polaridade negativa a partir do RNA de polaridade positiva, e produzir um RNA subgenômico a partir da segunda região de leitura aberta. Este RNA subgenômico será

utilizado como RNAm para sintetizar uma poliproteína estrutural do vírus (C-pE2-6K-E1). A poliproteína estrutural é clivada por auto proteólise em proteína C do capsídeo (proteínas de automontagem), enquanto as proteínas do complexo E2-6K-E1 serão processadas no retículo endoplasmático e posteriormente inseridas na membrana da célula hospedeira. Finalmente, os capsídeos formados se agrupam no citoplasma e deixam as células por brotamento, levando a região da membrana celular com as proteínas E1 e E2, como envelope viral (ABDELNABI; NEYTS; DELANG, 2015; GOULD et al., 2010; SOLIGNAT et al., 2009a) **(Figura 4).**

Figura 4: Esquema representativo do ciclo replicativo do CHIKV.

Adaptado de (MARTINS et al., 2020)

Febre Chikungunya e Patogênese

A febre Chikungunya é uma doença viral que apresenta fase aguda com duração entre 5 a 7 dias (WHO, 2019). Os sintomas gerais são muito semelhantes aos de outras arboviroses como a dengue e incluem febre, dores musculares, fadiga e manchas vermelhas sobre a pele (MOIZÉIS et al., 2018). Entretanto, as fortes dores nas articulações são características da infecção pelo CHIKV (LEE et al., 2012). Em alguns casos raros são observadas encefalopatias, hepatites e miocardites, podendo também levar

a óbito (DAS et al., 2010) **(Figura 5)**. Apesar de ser uma doença aguda e ocasionalmente assintomática, 43% dos pacientes diagnosticados com CHIKV desenvolvem a infecção crônica, permanecendo de alguns meses até anos (ALESSANDRA LO PRESTI1 et al., 2014; HOARAU et al., 2010; PAIXÃO et al., 2018; PIALOUX G, GAÜZÈRE BA, JAURÉGUIBERRY S, 2007).

Após a picada por um mosquito infectado, o CHIKV é liberado na derme e na corrente sanguínea do hospedeiro vertebrado, inicialmente infectando células suscetíveis ao vírus como as do tecido conjuntivo, células epiteliais e fibroblastos (THON-HON et al., 2012). O vírus atinge sítios de infecção secundários por meio da circulação linfática e sanguínea, como fígado, articulações e tecidos musculares (DUPUIS-MAGUIRAGA et al., 2012) **(Figura 5)**. A associação de processos inflamatórios causados pela replicação viral persistente e a resposta imune do hospedeiro resultam em manifestações relacionadas à mialgia e poliartralgia em articulações distais, provocando fortes dores articulares e musculares (SILVA et al., 2017).

Figura 5: Esquema demonstrativo da infecção do CHIKV e sintomas da infecção.
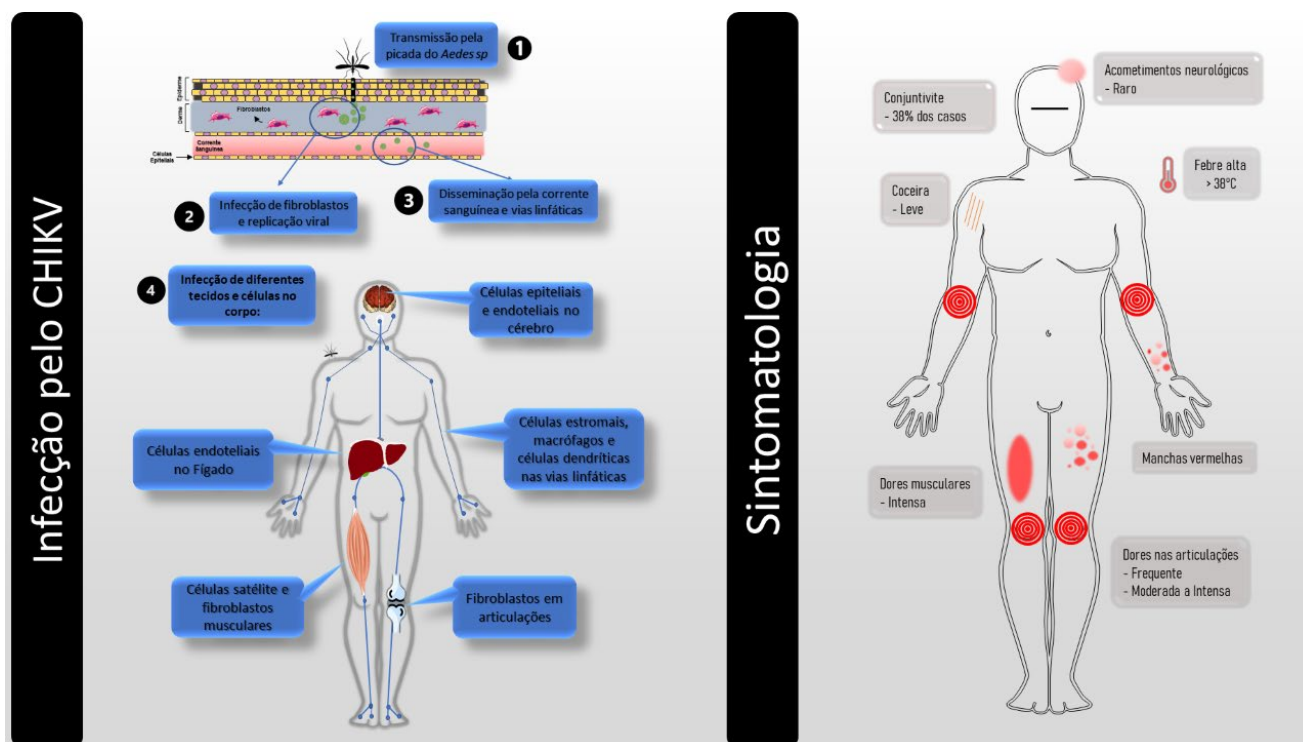
Adaptado de (MINISTÉRIO DA SAÚDE, 2020a)

Resposta Imune

A resposta imune contra a infecção pelo CHIKV é baseada inicialmente em uma resposta imune inata (WAUQUIER et al., 2011). No local de inoculação viral, as células

infectadas identificam o RNA viral por meio de receptores de reconhecimento padrão (PPRs), como os receptores *toll-like* 3 e 7 (VAN DUIJL-RICHTER et al., 2015), e produzem quimiocinas, como a proteína quimiotática de monócitos (CCL2), que estimulam a migração e diferenciação de monócitos em macrófagos no local de replicação viral (WHITE et al., 2011, p. 1). Apesar dos macrófagos residentes e infiltrados serem importantes para a produção de citocinas e garantir a eliminação da infecção, esses também são suscetíveis a infecção pelo CHIKV e podem funcionar como um reservatório em pacientes com infecção crônica, facilitando a disseminação do vírus (VERMA et al., 2018).

A resposta imune adaptativa é baseada no reconhecimento das células T CD4$^+$, as quais estão presentes na primeira semana de infecção (WAUQUIER et al., 2011). As células infectadas apresentam o antígeno viral por meio do complexo de histocompatibilidade humano (MHC) tipo II para os receptores de células T (ROLPH; FOO; MAHALINGAM, 2015). Essas também migram para capsulas sinoviais em articulações, sendo responsáveis pela produção de interferon gama (IFN-γ) para controle da viremia (TEO et al., 2013). As células T CD4$^+$ junto com as células Treg são responsáveis pela diferenciação da resposta em Th1, essencial para a ativação de células B produtoras de imunoglobulinas anti-CHIKV (VERMA et al., 2018). Em alguns indivíduos pode haver a produção de citocinas em ambas as vias Th1 e Th2, possivelmente comprometendo a eliminação viral e recuperação clínica (FOX; DIAMOND, 2020). Além disso, as células T CD4$^+$ participam ativamente no recrutamento e ativação de células T CD8$^+$ citotóxicas nos períodos iniciais da infecção (WAUQUIER et al., 2011).

Em relação às células B, essas são ativadas pelas células T CD4$^+$ e estimuladas a produzir imunoglobulinas para neutralização viral (LUM et al., 2013). Os anticorpos do tipo IgM são detectáveis no início da fase aguda, e após alguns dias ocorre o desenvolvimento de anticorpos do tipo IgG, permanecendo após o fim da fase aguda. Nos casos de cronificação, os níveis de IgG permanecem altos durante toda a fase crônica (LUM et al., 2013). Isso demonstra que os níveis de anticorpos são necessários para o controle, mas não são capazes de eliminar a infecção (FOX et al., 2015; FOX; DIAMOND, 2020).

Tratamento

Atualmente, o tratamento para a febre Chikungunya é baseado em medidas paliativas, visando mitigar os sintomas, tendo como base o uso de analgésicos, antitérmicos, repouso e hidratação (BRASIL. MINISTÉRIO DA SAÚDE. SECRETARIA DE VIGILÂNCIA EM SAÚDE, 2015; OMS, 2017). Além disso, também não existem vacinas capazes de levar a uma imunização satisfatória da população (ROUGERON et al., 2015). Desta forma, novas abordagens terapêuticas necessitam ser desenvolvidas, que incluem a investigação da atividade antivirais de compostos isolados de plantas, microrganismos e animais.

Compostos naturais e as toxinas de animais

Produtos naturais (PNs) apresentam uma vasta aplicação, apresentando importante papel na produção de temperos e condimentos e até mesmo inseticidas. A capitalização de PNs, entretanto, vem se mostrando promissora principalmente no desenvolvimento de fármacos, permitindo a sobrevivência e sobrevida de populações às doenças (VIEGAS; DA SILVA BOLZANI; BARREIRO, 2006). Historicamente, há relatos da utilização empírica de plantas com propriedades medicinais há milênios e em diferentes locais do mundo (CRAGG; NEWMAN, 2014). Os compostos naturais podem ser derivados de plantas, microrganismos e animais (GANESAN, 2008), e suas atividades biológicas resultaram na identificação e desenvolvimento de fármacos para o tratamento de doenças crônicas como câncer, diabetes, hipertensão arterial, e infecciosas, como as causadas por vírus, bactérias e fungos (HARVEY, 2008). Adicionalmente, entre 1994 a 2007, mais da metade dos fármacos aprovados pelas agências reguladoras envolvem moléculas sintéticas e semissintéticas baseadas em PNs (BUTLER; ROBERTSON; COOPER, 2014).

Dentre os compostos naturais, as peçonhas de serpente vêm se mostrando uma fonte terapêutica inovadora, por ser uma mistura complexa de lectinas, oxidases, metaloproteínas, desintegrinas, fosfolipases A2 (PLA2) e enzimas proteolíticas (BAILEY; WILCE, 2001; FABIAN VILLALTA-ROMERO, 2017). O isolamento de algumas destas macromoléculas permitiu a identificação de um peptídeo da peçonha de *Bothrops jararaca*, responsável pela inibição da Enzima Conversora de Angiotensina (ECA), a qual é amplamente utilizada como agente anti-hipertensivo (Captopril®) (ONDETTI et al., 1971; RUPAMONI THAKUR; ASHIS K. MUKHERJEEA, 2017).

As fosfolipases do tipo A2 (PLA2) são os constituintes mais estudados da peçonha de serpentes (FILKIN; LIPKIN; FEDOROV, 2020), devido a sua atividade enzimática em fosfolipídeos de membrana, produzindo ácido aracdônico e lisofosfolipídeos (BURKE; DENNIS, 2009; FILKIN; LIPKIN; FEDOROV, 2020). Os metabolitos produzidos exercem diversas atividades na inflamação, ativação de plaquetas e sinalização intracelular (SCHALOSKE; DENNIS, 2006). As PLA2 são classificadas como secretadas (sPLA2), citosólica (cPLA2), Ca^{2+}-independente (iPLA2), fator plaquetário por acetilhidrolases (PAF-AH), lisossomal (LyPLA2) e adipose-específica (AdPLA2) (BURKE; DENNIS, 2009). As sPLA2 são proteínas com massa molecular aproximada de 14 kDa, com uma atividade catalítica conservada (SCHALOSKE; DENNIS, 2006), e podem agir sobre membranas celulares em diversos tecidos causando citotoxicidade em músculos cardíacos e esquelético, neurotoxicidade, hipotensão e edema (LOMONTE; RANGEL, 2012).

PLA2 de *Crotalus durissus terrificus*

A peçonha da *Crotalus durissus terrificus*, uma serpente da América do Sul, é composta por diversas macromoléculas como a crotoxina, crotamina, convulxina, neurotoxina, dentre outras (SCHALOSKE; DENNIS, 2006; SIX; DENNIS, 2000). A crotoxina é o maior constituinte da peçonha de *C. d. terrificus*, sendo composta por duas principais subunidades, a crotapotina (proteína cataliticamente inativa) e a PLA2$_{CB}$ (cadeia base da crotoxina e cataliticamente ativa) **(Figura 6)** (FAURE; XU; SAUL, 2011; LOMONTE; RANGEL, 2012, p. 49). A crotoxina demonstrou possuir atividade antiviral contra o vírus da imunodeficiência humana (HIV) (VILLARRUBIA; COSTA; DÍEZ, 2004), interagindo diretamente com o vírus e impedindo sua entrada nas células alvo. Entretanto, quando separados os constituintes da crotoxina, a PLA2$_{CB}$ demonstrou atividades biológicas importantes (MULLER et al., 2012).

A PLA2$_{CB}$ faz parte da família de fosfolipases secretadas (KINI; EVANS, 1989) com atividades catalíticas (CALDERON et al., 2014), que apresentam diversas atividades biológicas descritas, as quais incluem as atividades anti-inflamatórias, bactericida e antiparasitária (ALMEIDA et al., 2016; DE CARVALHO et al., 2019). Adicionalmente, PLA2$_{CB}$ demonstrou atividade antiviral contra DENV-2 e DENV-3, HIV, vírus da febre amarela (YFV), hepacivírus C (HCV) e vírus Mayaro (MAYV) (CLEYSE et al., 2017;

MULLER et al., 2014; SHIMIZU et al., 2017; VERA L. PETRICEVICH; RONALDO Z. MENDONÇA, 2003).

Figura 6: Estrutura da PLA2_{CB} isolada de *Crotalus durissus terrificus* (PDB:3R0L).
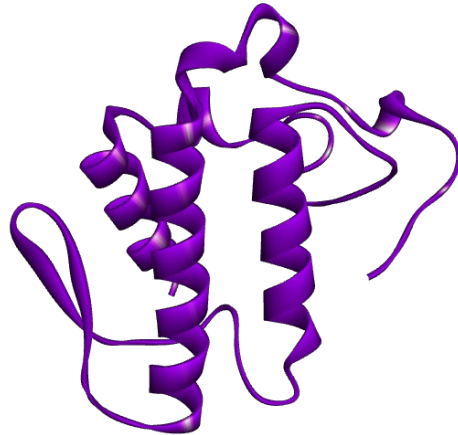
Adaptado de (FAURE; XU; SAUL, 2011)

As proteínas isoladas de veneno de serpente se apresentam como uma fonte promissora para o desenvolvimento de novos antivirais contra o CHIKV, visto que já demonstraram efeitos contra outros arbovírus. Portanto, a PLA2_{CB} se apresenta como uma fonte de informações para o desenvolvimento de tratamentos futuros contra a febre Chikungunya, o que poderá resultar na melhora da qualidade de vida da população infectada, e redução dos gastos públicos devido aos tratamentos paliativos de longo prazo e a incapacitação dos indivíduos infectados.

OBJETIVOS

O presente trabalho teve como objetivo avaliar a atividade da fosfolipase A_2 (PLA2$_{CB}$) isolada da peçonha da serpente *Crotalus durissus terrificus* no ciclo replicativo do CHIKV *in vitro*.

Objetivos específicos

- Determinar a concentração efetiva de 50% (EC$_{50}$), concentração citotóxica em 50% (CC$_{50}$) e índice de seletividade (IS=CC$_{50}$/EC$_{50}$) da PLA2$_{CB}$, de forma a estabelecer os valores ótimos de concentração para o tratamento celular e avaliar o potencial antiviral desta molécula;

- Avaliar a atividade da PLA2$_{CB}$ em diferentes etapas do ciclo replicativo do CHIKV, para um melhor entendimento das etapas do ciclo viral inibidas por essa molécula.

- Investigar as interações da PLA2$_{CB}$ com proteínas do CHIKV por meio de ancoragem molecular, para identificar potenciais mecanismos de ação antiviral;

- Analisar por espectroscopia no infravermelho (FTIR) as interações químicas da PLA2$_{CB}$ com constituintes da partícula viral do CHIKV, afim de investigar o modo de ação desta molécula.

REFERÊNCIAS

ABDELNABI, R.; NEYTS, J.; DELANG, L. Towards antivirals against chikungunya virus. **Antiviral Research**, v. 121, p. 59–68, 2015. https://doi.org/10.1016/j.antiviral.2015.06.017

ALESSANDRA LO PRESTI1 et al. Chikungunya virus, epidemiology, clinics and phylogenesis: A review. **Asian Pacific Journal of Tropical Medicine**, v. 7, n. 12, p. 925–932, 1 dez. 2014. https://doi.org/10.1016/S1995-7645(14)60164-4

ALMEIDA, J. R. et al. CoaTx-II, a new dimeric Lys49 phospholipase A2 from Crotalus oreganus abyssus snake venom with bactericidal potential: Insights into its structure and biological roles. **Toxicon**, v. 120, p. 147–158, 15 set. 2016. https://doi.org/10.1016/j.toxicon.2016.08.007

ASTANI, A.; REICHLING, J.; SCHNITZLER, P. Comparative study on the antiviral activity of selected monoterpenes derived from essential oils. **Phytotherapy Research**, v. 23, n. 9, p. n/a-n/a, 2009. https://doi.org/10.1002/ptr.2955

BAILEY, P.; WILCE, J. Venom as a source of useful biologically active molecules. **Emergency Medicine Australasia**, v. 13, n. 1, p. 28–36, 1 mar. 2001. https://doi.org/10.1046/j.1442-2026.2001.00174.x

BENNETT, M. A. et al. 16. (η^6-Hexamethylbenzene)Ruthenium Complexes. In: [s.l: s.n.]. p. 74–78. https://doi.org/10.1002/9780470132524.ch16

BORGHERINI, G. et al. Outbreak of Chikungunya on Reunion Island: Early Clinical and Laboratory Features in 157 Adult Patients. **Clinical Infectious Diseases**, v. 44, n. 11, p. 1401–1407, 1 jun. 2007. https://doi.org/10.1086/517537

BRASIL. MINISTÉRIO DA SAÚDE. SECRETARIA DE VIGILÂNCIA EM SAÚDE. Febre de Chikungunya manejo clínico Febre de chikungunya: manejo clínico. 2015.

BURKE, J. E.; DENNIS, E. A. Phospholipase A2 biochemistry. **Cardiovascular Drugs and Therapy**, v. 23, n. 1, p. 49–59, fev. 2009. https://doi.org/10.1007/s10557-008-6132-9

BURT, F. J. et al. Chikungunya virus: an update on the biology and pathogenesis of this emerging pathogen. **The Lancet Infectious Diseases**, v. 17, n. 4, p. e107–e117, 2017. https://doi.org/10.1016/S1473-3099(16)30385-1

BUTLER, M. S.; ROBERTSON, A. A. B.; COOPER, M. A. Natural product and natural product derived drugs in clinical trials. **Nat. Prod. Rep.**, v. 31, n. 11, p. 1612–1661, 2014. https://doi.org/10.1039/C4NP00064A

CALDERON, L. A. et al. Antitumoral Activity of Snake Venom Proteins: New Trends in Cancer Therapy. **BioMed Research International**, v. 2014, p. e203639, 2014. https://doi.org/10.1155/2014/203639

CARRAVILLA, P. et al. Effects of HIV-1 gp41-Derived Virucidal Peptides on Virus-like Lipid Membranes. **Biophysical Journal**, v. 113, n. 6, p. 1301–1310, 2017. https://doi.org/10.1016/j.bpj.2017.06.061

CARVALHO, R. G.; LOURENÇO-DE-OLIVEIRA, R.; BRAGA, I. A. Updating the geographical distribution and frequency of Aedes albopictus in Brazil with remarks regarding its range in the Americas. **Memorias do Instituto Oswaldo Cruz**, v. 109, n. 6, p. 787–796, 2014. https://doi.org/10.1590/0074-0276140304

CLARKE, M. J.; ZHU, F.; FRASCA, D. R. Non-platinum chemotherapeutic metallopharmaceuticals. **Chemical Reviews**, v. 99, n. 9, p. 2511–2533, 1999. https://doi.org/10.1021/cr9804238

CLEYSE, É. et al. Antiviral activity of animal venom peptides and related compounds. 2017. https://doi.org/10.1186/s40409-016-0089-0

COHEN, S. N. et al. Dengue and Chikungunya Virus Infection in Man in Thailand, 1962–1964. **The American Journal of Tropical Medicine and Hygiene**, v. 18, n. 6, p. 954–971, 1 nov. 1969. https://doi.org/10.4269/ajtmh.1969.18.954

CRAGG, G. M.; NEWMAN, D. J. NIH Public Access. v. 1830, n. 6, p. 3670–3695, 2014. https://doi.org/10.1016/j.bbagen.2013.02.008

CUNHA, R. V. DA; TRINTA, K. S. Chikungunya virus: clinical aspects and treatment - A Review. **Memórias do Instituto Oswaldo Cruz**, v. 112, n. 8, p. 523–531, 2017. https://doi.org/10.1590/0074-02760170044

CUNHA, M. S. et al. Autochthonous Transmission of East/Central/South African Genotype Chikungunya Virus, Brazil. **Emerging Infectious Diseases**, v. 23, n. 10, p. 2015–2017, 2017. https://doi.org/10.3201/eid2310.161855

DA SILVA-JÚNIOR, E. F. et al. The medicinal chemistry of Chikungunya virus. **Bioorganic & Medicinal Chemistry**, v. 25, n. 16, p. 4219–4244, 2017. https://doi.org/10.1016/j.bmc.2017.06.049

DAS, T. et al. Chikungunya fever: CNS infection and pathologies of a re-emerging arbovirus. **Progress in Neurobiology**, v. 91, n. 2, p. 121–129, jun. 2010. https://doi.org/10.1016/j.pneurobio.2009.12.006

DE ANDRADE, D. C. et al. Chronic pain associated with the Chikungunya Fever: long lasting burden of an acute illness. **BMC Infectious Diseases**, v. 10, n. 1, p. 31, 2010. https://doi.org/10.1186/1471-2334-10-31

DE CARVALHO, A. E. Z. et al. Crotalus durissus ruruima Snake Venom and a Phospholipase A2 Isolated from This Venom Elicit Macrophages to Form Lipid Droplets and Synthesize Inflammatory Lipid Mediators. **Journal of Immunology Research**, v. 2019, 4 nov. 2019. https://doi.org/10.1155/2019/2745286

DE OLIVEIRA, T. M. et al. Evaluation of p-cymene, a natural antioxidant. **Pharmaceutical Biology**, v. 53, n. 3, p. 423–428, 2015. https://doi.org/10.3109/13880209.2014.923003

DEY, D. et al. The effect of amantadine on an ion channel protein from Chikungunya virus. **PLOS Neglected Tropical Diseases**, v. 13, n. 7, p. e0007548, 2019. https://doi.org/10.1371/journal.pntd.0007548

DOUGAN, S. J.; SADLER, P. J. The design of organometallic ruthenium arene anticancer agents. **Chimia**, v. 61, n. 11, p. 704–715, 2007. https://doi.org/10.2533/chimia.2007.704

DUPUIS-MAGUIRAGA, L. et al. Chikungunya Disease: Infection-Associated Markers from the Acute to the Chronic Phase of Arbovirus-Induced Arthralgia. **PLoS Neglected Tropical Diseases**, v. 6, n. 3, p. e1446, 27 mar. 2012. https://doi.org/10.1371/journal.pntd.0001446

DYSON, P. J. Systematic design of a targeted organometallic antitumour drug in pre-clinical development. **Chimia**, v. 61, n. 11, p. 698–703, 2007. https://doi.org/10.2533/chimia.2007.698

FABIAN VILLALTA-ROMERO. Discovery of small molecule inhibitors for the snake venom metalloprotease BaP1 using in silico and in vitro tests. **Bioorganic & Medicinal Chemistry Letters**, v. 27, n. 9, p. 2018–2022, 1 maio 2017. https://doi.org/10.1016/j.bmcl.2017.03.007

FAURE, G.; XU, H.; SAUL, F. A. Crystal Structure of Crotoxin Reveals Key Residues Involved in the Stability and Toxicity of This Potent Heterodimeric β-Neurotoxin. **Journal of Molecular Biology**, v. 412, n. 2, p. 176–191, 16 set. 2011. https://doi.org/10.1016/j.jmb.2011.07.027

FILKIN, S. Y.; LIPKIN, A. V.; FEDOROV, A. N. Phospholipase Superfamily: Structure, Functions, and Biotechnological Applications. **Biochemistry. Biokhimiia**, v. 85, n. Suppl 1, p. S177–S195, jan. 2020. https://doi.org/10.1134/S0006297920140096

FONGSARAN, C. et al. Involvement of ATP synthase β subunit in chikungunya virus entry into insect cells. **Archives of Virology**, v. 159, n. 12, p. 3353–3364, 2014. https://doi.org/10.1007/s00705-014-2210-4

FOX, J. M. et al. Broadly Neutralizing Alphavirus Antibodies Bind an Epitope on E2 and Inhibit Entry and Egress. **Cell**, v. 163, n. 5, p. 1095–1107, 19 nov. 2015. https://doi.org/10.1016/j.cell.2015.10.050

FOX, J. M.; DIAMOND, M. S. Immune-Mediated Protection and Pathogenesis of Chikungunya Virus. **The Journal of Immunology**, p. 10, 2020. https://doi.org/10.4049/jimmunol.1601426

GANESAN, A. The impact of natural products upon modern drug discovery. **Current Opinion in Chemical Biology**, v. 12, n. 3, p. 306–317, 1 jun. 2008. https://doi.org/10.1016/j.cbpa.2008.03.016

GAROZZO, A. et al. In vitro antiviral activity of Melaleuca alternifolia essential oil. **Letters in Applied Microbiology**, v. 49, n. 6, p. 806–808, dez. 2009. https://doi.org/10.1111/j.1472-765X.2009.02740.x

GAY, N. et al. Seroprevalence of asian lineage chikungunya virus infection on saint martin Island, 7 months after the 2013 emergence. **American Journal of Tropical Medicine and Hygiene**, v. 94, n. 2, p. 393–396, 2016. https://doi.org/10.4269/ajtmh.15-0308

Geographic Distribution | Chikungunya virus | CDC. Disponível em: <https://www.cdc.gov/chikungunya/geo/index.html>. Acesso em: 3 jun. 2020.

GOULD, E. et al. Emerging arboviruses: Why today? **One Health**, v. 4, n. April, p. 1–13, 2017. https://doi.org/10.1016/j.onehlt.2017.06.001

GOULD, E. A. et al. Understanding the alphaviruses: Recent research on important emerging pathogens and progress towards their control. **Antiviral Research**, v. 87, n. 2, p. 111–124, ago. 2010. https://doi.org/10.1016/j.antiviral.2009.07.007

GRATZ, N. G. Critical review of the vector status of Aedes albopictus. **Medical and veterinary entomology**, v. 18, n. 3, p. 215–27, set. 2004. https://doi.org/10.1111/j.0269-283X.2004.00513.x

GUPTA, S.; GUPTA, N. Short-term pregnancy outcomes in patients chikungunya infection: An observational study. **Journal of Family Medicine and Primary Care**, v. 8, n. 3, p. 985–987, mar. 2019. https://doi.org/10.4103/jfmpc.jfmpc_274_18

HABTEMARIAM, A. et al. Structure-activity relationships for cytotoxic ruthenium(II) arene complexes containing N,N-, N,O-, and O,O-chelating ligands. **Journal of Medicinal Chemistry**, v. 49, n. 23, p. 6858–6868, 2006. https://doi.org/10.1021/jm060596m

HALSTEAD, S. B. Reappearance of chikungunya, formerly called Dengue, in the Americas. **Emerging Infectious Diseases**, v. 21, n. 4, p. 557–561, 2015. https://doi.org/10.3201/eid2104.141723

HARVEY, A. Natural products in drug discovery. **Drug Discovery Today**, v. 13, n. 19–20, p. 894–901, out. 2008. https://doi.org/10.1016/j.drudis.2008.07.004

HOARAU, J.-J. et al. Persistent Chronic Inflammation and Infection by Chikungunya Arthritogenic Alphavirus in Spite of a Robust Host Immune Response. **The Journal of Immunology**, v. 184, n. 10, p. 5914–5927, 15 maio 2010. https://doi.org/10.4049/jimmunol.0900255

JENSEN, S. B.; RODGER, S. J.; SPICER, M. D. **Facile preparation of η6-p-cymene ruthenium diphosphine complexes. Crystal structure of [(η6-p-cymene)Ru(dppf)Cl]PF6Journal of Organometallic Chemistry**, 1998. https://doi.org/10.1016/S0022-328X(97)00776-6

KAUR, P.; CHU, J. J. H. Chikungunya virus: An update on antiviral development and challenges. **Drug Discovery Today**, v. 18, n. 19–20, p. 969–983, 2013. https://doi.org/10.1016/j.drudis.2013.05.002

KHAN, A. H. et al. Complete nucleotide sequence of chikungunya virus and evidence for an internal polyadenylation site. **The Journal of general virology**, v. 83, n. Pt 12, p. 3075–84, dez. 2002. https://doi.org/10.1099/0022-1317-83-12-3075

KINI, R. M.; EVANS, H. J. A model to explain the pharmacological effects of snake venom phospholipases A2. **Toxicon**, v. 27, n. 6, p. 613–635, 1 jan. 1989. https://doi.org/10.1016/0041-0101(89)90013-5

KONG, B. et al. Virucidal nano-perforator of viral membrane trapping viral RNAs in the endosome. **Nature Communications**, v. 10, n. 1, p. 1–10, 2019. https://doi.org/10.1038/s41467-018-08138-1

KORDALI, S. et al. Antifungal, phytotoxic and insecticidal properties of essential oil isolated from Turkish Origanum acutidens and its three components, carvacrol, thymol and p-cymene. **Bioresource Technology**, v. 99, n. 18, p. 8788–8795, 2008. https://doi.org/10.1016/j.biortech.2008.04.048

KRAEMER, M. U. et al. The global distribution of the arbovirus vectors Aedes aegypti and Ae. albopictus. **eLife**, v. 4, p. e08347, 30 jun. 2015. https://dx.doi.org/10.7554%2FeLife.08347

KUMMER, R. et al. Effect of p-cymene on chemotaxis, phagocytosis and leukocyte behaviors. **International Journal of Applied Research in Natural Products**, v. 8, n. 2, p. 20–27, 2015.

LEE, V. J. et al. Simple Clinical and Laboratory Predictors of Chikungunya versus Dengue Infections in Adults. 2012. https://doi.org/10.1016/j.ijid.2012.05.885

LOMONTE, B.; RANGEL, J. Snake venom Lys49 myotoxins: From phospholipases A2 to non-enzymatic membrane disruptors. **Toxicon**, Advancing in Basic and Translational Venomics. v. 60, n. 4, p. 520–530, 15 set. 2012. https://doi.org/10.1016/j.toxicon.2012.02.007

LOURENÇO-DE-OLIVEIRA, R.; FAILLOUX, A. B. High risk for chikungunya virus to initiate an enzootic sylvatic cycle in the tropical Americas. **PLoS Neglected Tropical Diseases**, v. 11, n. 6, p. 1–11, 2017. https://doi.org/10.1371/journal.pntd.0005698

LUM, F. M.; NG, L. F. P. Cellular and molecular mechanisms of chikungunya pathogenesis. **Antiviral Research**, v. 120, p. 165–174, 2015. https://doi.org/10.1016/j.antiviral.2015.06.009

LUM, F.-M. et al. An essential role of antibodies in the control of Chikungunya virus infection. **Journal of Immunology (Baltimore, Md.: 1950)**, v. 190, n. 12, p. 6295–6302, 15 jun. 2013. https://doi.org/10.4049/jimmunol.1300304

LUMSDEN, W. H. R. An epidemic of virus disease in Southern Province, Tanganyika territory, in 1952–1953 II. General description and epidemiology. **Transactions of the Royal Society of Tropical Medicine and Hygiene**, v. 49, n. 1, p. 33–57, 1 jan. 1955. https://doi.org/10.1016/0035-9203(55)90081-X

MARTINS, D. O. S. et al. Antivirals Against Chikungunya Virus: Is the Solution in Nature? **Viruses**, v. 12, n. 3, p. 272, mar. 2020. https://doi.org/10.3390/v12030272

MATHEW, A. J. et al. Chikungunya Infection : a Global Public Health Menace. p. 1–9, 2017. https://doi.org/10.1007/s11882-017-0680-7

MATKOVIC, R. et al. The Host DHX9 DExH-Box Helicase Is Recruited to Chikungunya Virus Replication Complexes for Optimal Genomic RNA Translation. **Journal of Virology**, v. 93, n. 4, p. 1–17, 2018. https://doi.org/10.1128/JVI.01764-18

MAVALE, M. et al. Venereal transmission of chikungunya virus by Aedes aegypti mosquitoes (Diptera: Culicidae). **American Journal of Tropical Medicine and Hygiene**, v. 83, n. 6, p. 1242–1244, 2010. https://doi.org/10.4269/ajtmh.2010.09-0577

MINISTÉRIO DA SAÚDE. **Monitoramento dos casos de dengue, febre de chikungunya e febre pelo vírus Zika até a Semana Epidemiológica 52, 2016**. Disponível em: <https://www.saude.gov.br/images/pdf/2017/abril/06/2017-002-Monitoramento-dos-casos-de-dengue--febre-de-chikungunya-e-febre-pelo-v--rus-Zika-ate-a-Semana-Epidemiologica-52--2016.pdf>. Acesso em: 3 jun. 2020.

MINISTÉRIO DA SAÚDE. **Monitoramento dos casos de dengue, febre de chikungunya e doença aguda pelo vírus Zika até a Semana Epidemiológica 49 de 2018**. Disponível em: <http://www.saude.gov.br/images/pdf/2019/janeiro/02/2018-067.pdf>. Acesso em: 3 jun. 2020.

MINISTÉRIO DA SAÚDE. **Chikungunya: causas, sintomas, tratamento e prevenção**. Disponível em: <http://www.saude.gov.br/saude-de-a-z/chikungunya>. Acesso em: 3 jun. 2020a.

MINISTÉRIO DA SAÚDE. **Monitoramento dos casos de arboviroses urbanas transmitidas pelo Aedes Aegypti (dengue, chikungunya e zika), Semanas Epidemiológicas 1 a 21, 2020**. Disponível em: <https://www.saude.gov.br/images/pdf/2020/May/29/Boletim-epidemiologico-SVS-22.pdf>. Acesso em: 3 jun. 2020b.

MINISTÉRIO DA SAÚDE, S. DE V. EM S. Monitoramento-dos-casos-de-dengue-e-febre-de-chikungunya-20.pdf. **Boletim Epidemiológico**, v. 46, 2015.

MOIZÉIS, R. N. C. et al. Chikungunya fever: a threat to global public health. **Pathogens and Global Health**, v. 112, n. 4, p. 182–194, 19 maio 2018. https://doi.org/10.1080/20477724.2018.1478777

MOLLER-TANK, S. et al. Role of the Phosphatidylserine Receptor TIM-1 in Enveloped-Virus Entry. v. 87, n. 15, p. 8327–8341, 2013. https://doi.org/10.1128/JVI.01025-13

MONATH, T. P. **The Arboviruses: Epidemiology and Ecology**. CRC Press, 2019. https://doi.org/10.1201/9780429289170 MULLER, V. D. et al. Phospholipase A2 isolated from the venom of Crotalus durissus terrificus inactivates dengue virus and other enveloped viruses by disrupting the viral envelope. **PLoS ONE**, v. 9, n. 11, p. 1–10, 2014. https://doi.org/10.1371/journal.pone.0112351

MULLER, V. D. M. et al. Crotoxin and phospholipases A2 from Crotalus durissus terrificus showed antiviral activity against dengue and yellow fever viruses. **Toxicon**, From venoms to drugs. v. 59, n. 4, p. 507–515, 15 mar. 2012. https://doi.org/10.1016/j.toxicon.2011.05.021

NGOAGOUNI, C. et al. Potential of Aedes aegypti and Aedes albopictus populations in the Central African Republic to transmit enzootic chikungunya virus strains. **Parasites & Vectors**, v. 10, n. 1, p. 164, 2017. https://doi.org/10.1186/s13071-017-2101-0

NJENGA, M. K. et al. Tracking epidemic Chikungunya virus into the Indian Ocean from East Africa. **Journal of General Virology**, v. 89, n. 11, p. 2754–2760, 2008. https://doi.org/10.1099/vir.0.2008/005413-0

OLIVEIRA, R. DE M. A. B. et al. Maternal and infant death after probable vertical transmission of chikungunya virus in Brazil – case report. **BMC Infectious Diseases**, v. 18, n. 1, p. 333, 16 dez. 2018. https://doi.org/10.1186/s12879-018-3243-1

OMS. **Chikungunya**. Disponível em: <http://www.who.int/es/news-room/fact-sheets/detail/chikungunya>. Acesso em: 23 out. 2018.

ONDETTI, M. A. et al. Angiotensin-converting enzyme inhibitors from the venom of Bothrops jararaca. Isolation, elucidation of structure, and synthesis. **Biochemistry**, v. 10, n. 22, p. 4033–4039, out. 1971. https://doi.org/10.1021/bi00798a004

PAGÈS, F. et al. Correction: Aedes albopictus Mosquito: The Main Vector of the 2007 Chikungunya Outbreak in Gabon. **PLoS ONE**, v. 4, n. 5, 27 maio 2009. https://doi.org/10.1371/annotation/4145c2b9-dca1-4eef-996a-8e79de4dc1f5

PAIXÃO, E. S. et al. Chikungunya chronic disease: A systematic review and meta-analysis. **Transactions of the Royal Society of Tropical Medicine and Hygiene**, v. 112, n. 7, p. 301–316, 2018. https://doi.org/10.1093/trstmh/try063

PARASHAR, D.; CHERIAN, S. Antiviral perspectives for chikungunya virus. **BioMed Research International**, v. 2014, 2014. https://doi.org/10.1155/2014/631642PAVAN, F. R. et al. Ruthenium (II) phosphine/picolinate complexes as antimycobacterial agents. **European Journal of Medicinal Chemistry**, v. 45, n. 2, p. 598–601, 2010. https://doi.org/10.1016/j.ejmech.2009.10.049

PIALOUX G, GAÜZÈRE BA, JAURÉGUIBERRY S, S. M. Chikungunya, an epidemic arbovirosis. **The Lancet Infectious Diseases**, v. 7, n. 5, p. 319–327, 1 maio 2007. https://doi.org/10.1016/S1473-3099(07)70107-X

POHJALA, L. et al. Inhibitors of alphavirus entry and replication identified with a stable Chikungunya replicon cell line and virus-based assays. **PLoS ONE**, v. 6, n. 12, 2011. https://doi.org/10.1371/journal.pone.0028923

POWERS, A. M. et al. Re-emergence of chikungunya and o'nyong-nyong viruses: Evidence for distinct geographical lineages and distant evolutionary relationships. **Journal of General Virology**, v. 81, n. 2, p. 471–479, 2000. https://doi.org/10.1099/0022-1317-81-2-471

POWERS, A. M. Vaccine and Therapeutic Options To Control Chikungunya Virus. **Clinical Microbiology Reviews**, v. 31, n. 1, p. e00104-16, /cmr/31/1/e00104- 16.atom, 13 dez. 2017. https://doi.org/10.1128/CMR.00104-16

RASHAD, A. A.; KELLER, P. A. Structure based design towards the identification of novel binding sites and inhibitors for the chikungunya virus envelope proteins. **Journal of Molecular Graphics and Modelling**, v. 44, p. 241–252, 2013. https://doi.org/10.1016/j.jmgm.2013.07.001

RASHAD, A. A.; MAHALINGAM, S.; KELLER, P. A. Chikungunya Virus: Emerging Targets and New Opportunities for Medicinal Chemistry. 2013. https://doi.org/10.1021/jm400460d

RAVI, V. Re-emergence of chikungunya virus in India. **Indian journal of medical microbiology**, v. 24, n. 2, p. 83–4, abr. 2006. https://doi.org/10.4103/0255-0857.25175

ROBERTS, G. C. et al. Evaluation of a range of mammalian and mosquito cell lines for use in Chikungunya virus research. **Scientific Reports**, v. 7, n. 1, p. 14641, 7 dez. 2017. https://doi.org/10.1038/s41598-017-15269-w

ROBINSON, M. C. An epidemic of virus disease in Southern Province, Tanganyika Territory, in 1952-53. I. Clinical features. **Transactions of the Royal Society of Tropical Medicine and Hygiene**, v. 49, n. 1, p. 28–32, jan. 1955. https://doi.org/10.1016/0035-9203(55)90080-8

ROLPH, M. S.; FOO, S. S.; MAHALINGAM, S. Emergent chikungunya virus and arthritis in the Americas. **The Lancet Infectious Diseases**, v. 15, n. 9, p. 1007–1008, 1 set. 2015. https://doi.org/10.1016/S1473-3099(15)00231-5

ROSS, B. Y. R. W. the Newala Epidemic and Relationship To the Epidemic. p. 177–191, 1955. https://doi.org/10.1017/S0022172400044442

ROUGERON, V. et al. Chikungunya, a paradigm of neglected tropical disease that emerged to be a new health global risk. **Journal of Clinical Virology**, v. 64, p. 144–152, mar. 2015. https://doi.org/10.1016/j.jcv.2014.08.032

RUPAMONI THAKUR; ASHIS K. MUKHERJEEA. Pathophysiological significance and therapeutic applications of snake venom protease inhibitors. **Toxicon**, v. 131, p. 37–47, 1 jun. 2017. https://doi.org/10.1016/j.toxicon.2017.03.011

RUSSO, R. R. et al. Expression, purification and virucidal activity of two recombinant isoforms of phospholipase A2 from Crotalus durissus terrificus venom. **Archives of Virology**, v. 164, n. 4, p. 1159–1171, 26 abr. 2019. https://doi.org/10.1007/s00705-019-04172-6

SAMBRI, V. et al. The 2007 epidemic outbreak of Chikungunya virus infection in the Romagna region of Italy: A new perspective for the possible diffusion of tropical diseases in temperate areas? **New Microbiologica**, v. 31, n. 3, p. 303–304, 2008.

SAVIĆ, A. et al. Antitumor activity of organoruthenium complexes with chelate aromatic ligands, derived from 1,10-phenantroline: Synthesis and biological activity. **Journal of Inorganic Biochemistry**, v. 202, n. September 2019, p. 110869, 2020. https://doi.org/10.1016/j.jinorgbio.2019.110869

SCHALOSKE, R. H.; DENNIS, E. A. The phospholipase A2 superfamily and its group numbering system. **Biochimica Et Biophysica Acta**, v. 1761, n. 11, p. 1246–1259, nov. 2006. https://doi.org/10.1016/j.bbalip.2006.07.011SCHNIERLE, B. S. Cellular Attachment and Entry Factors for Chikungunya Virus. **Viruses**, v. 11, n. 11, 19 nov. 2019. https://doi.org/10.3390/v11111078

SCHUFFENECKER, I. et al. Genome Microevolution of Chikungunya Viruses Causing the Indian Ocean Outbreak. **PLoS Medicine**, v. 3, n. 7, p. 1058–1070, 2006. https://doi.org/10.1371/journal.pmed.0030263

SCHUHMACHER, A.; REICHLING, J.; SCHNITZLER, P. Virucidal effect of peppermint oil on the enveloped viruses herpes simplex virus type 1 and type 2 in vitro. **Phytomedicine**, v. 10, n. 6–7, p. 504–510, jan. 2003. https://doi.org/10.1078/094471103322331467

SHARIFI-RAD, J. et al. Susceptibility of herpes simplex virus type 1 to monoterpenes thymol, carvacrol, p-cymene and essential oils of Sinapis arvensis L., Lallemantia royleana Benth. and Pulicaria vulgaris Gaertn. **Cellular and molecular biology (Noisy-le-Grand, France)**, v. 63, n. 8, p. 42–47, 30 ago. 2017. https://doi.org/10.14715/cmb/2017.63.8.10

SHIMIZU, J. F. et al. Multiple effects of toxins isolated from Crotalus durissus terrificus on the hepatitis C virus life cycle. **PLOS ONE**, v. 12, n. 11, p. e0187857, 15 nov. 2017. https://doi.org/10.1371/journal.pone.0187857

SILVA, N. M. DA et al. Vigilância de chikungunya no Brasil: desafios no contexto da Saúde Pública. **Epidemiologia e Serviços de Saúde**, v. 27, n. 3, p. e2017127, 2018. https://doi.org/10.5123/S1679-49742018000300003

SILVA, L. A. et al. A Single-Amino-Acid Polymorphism in Chikungunya Virus E2 Glycoprotein Influences Glycosaminoglycan Utilization. **Journal of Virology**, v. 88, n. 5, p. 2385–2397, 2014. https://doi.org/10.1128/JVI.03116-13

SILVA, L. A. et al. Chikungunya virus: epidemiology, replication, disease mechanisms, and prospective intervention strategies Find the latest version: Chikungunya virus: epidemiology, replication, disease mechanisms, and prospective intervention strategies. v. 127, n. 3, p. 737–749, 2017. https://doi.org/10.1172/JCI84417

SIMON, F. et al. Chikungunya virus infection. **Current Infectious Disease Reports**, v. 13, n. 3, p. 218–228, 2011. https://doi.org/10.1007/s11908-011-0180-1

SIX, D. A.; DENNIS, E. A. The expanding superfamily of phospholipase A (2) enzymes: classification and characterization. **Biochimica Et Biophysica Acta**, v. 1488, n. 1–2, p. 1–19, 31 out. 2000. https://doi.org/10.1016/S1388-1981(00)00105-0

SOLIGNAT, M. et al. Replication cycle of chikungunya: A re-emerging arbovirus. **Virology**, v. 393, n. 2, p. 183–197, out. 2009. https://doi.org/10.1016/j.virol.2009.07.024

STEGMANN-PLANCHARD, S. et al. Chikungunya, a Risk Factor for Guillain-Barré Syndrome. **Clinical Infectious Diseases**, v. 66, p. 37–39, 9 jul. 2019. https://doi.org/10.1093/cid/ciz625

TANG, J. et al. Virucidal activity of hypericin against enveloped and non-enveloped DNA and RNA viruses. **Antiviral Research**, v. 13, n. 6, p. 313–325, jun. 1990. https://doi.org/10.1016/0166-3542(90)90015-Y

TEIXEIRA, R. R. et al. Natural Products as Source of Potential Dengue Antivirals. **Molecules**, v. 19, p. 8151–8176, 2014. https://doi.org/10.3390/molecules19068151

TEO, T.-H. et al. A pathogenic role for CD4+ T cells during Chikungunya virus infection in mice. **Journal of Immunology (Baltimore, Md.: 1950)**, v. 190, n. 1, p. 259–269, 1 jan. 2013. https://doi.org/10.4049/jimmunol.1202177

THIBERVILLE, S. D. et al. Chikungunya fever: Epidemiology, clinical syndrome, pathogenesis and therapy. **Antiviral Research**, v. 99, n. 3, p. 345–370, 2013. https://doi.org/10.1016/j.antiviral.2013.06.009

THON-HON, V. G. et al. Deciphering the differential response of two human fibroblast cell lines following Chikungunya virus infection. p. 1–10, 2012. https://doi.org/10.1186/1743-422X-9-213

VAJS, J. et al. The 1,3-diaryltriazenido(p-cymene)ruthenium(II) complexes with a high in vitro anticancer activity. **Journal of Inorganic Biochemistry**, v. 153, p. 42–48, 2015. https://doi.org/10.1016/j.jinorgbio.2015.09.005

VAN DUIJL-RICHTER, M. K. S. et al. Early Events in Chikungunya Virus Infection-From Virus Cell Binding to Membrane Fusion. **Viruses**, v. 7, n. 7, p. 3647–3674, 7 jul. 2015. https://doi.org/10.3390/v7072792

VERA L. PETRICEVICH; RONALDO Z. MENDONÇA. Inhibitory potential of Crotalus durissus terrificus venom on measles virus growth. **Toxicon**, v. 42, n. 2, p. 143–153, 1 ago. 2003. https://doi.org/10.1016/S0041-0101(03)00124-7

VERMA, P. et al. Chikungunya Infection and Immunity: An Overview. **Current Immunology Reviews**, v. 14, n. 1, p. 31–39, 1 abr. 2018. https://doi.org/10.2174/1573395514666180417143739

VIEGAS, C.; DA SILVA BOLZANI, V.; BARREIRO, E. J. OS produtos naturais e a química medicinal moderna. **Quimica Nova**, v. 29, n. 2, p. 326–337, 2006. https://doi.org/10.1590/S0100-40422006000200025

VILLARRUBIA, V. G.; COSTA, L. A.; DÍEZ, R. A. Fosfolipasas A2 segregadas (sPLA2):¿amigas o enemigas? ¿Actores de la resistencia antibacteriana y antivirus de la inmunodeficiencia humana? **Medicina Clínica**, v. 123, n. 19, p. 749–757, 1 out. 2004. https://doi.org/10.1016/S0025-7753(04)74656-4

VOLK, S. M. et al. Genome-Scale Phylogenetic Analyses of Chikungunya Virus Reveal Independent Emergences of Recent Epidemics and Various Evolutionary Rates. **Journal of Virology**, v. 84, n. 13, p. 6497–6504, 2010. https://doi.org/10.1128/JVI.01603-09

VU, D. M.; JUNGKIND, D.; LABEAUD, A. D. Chikungunya Virus. **Clinics in Laboratory Medicine**, v. 37, n. 2, p. 371–382, 2017. https://doi.org/10.1016/j.cll.2017.01.008

WAUQUIER, N. et al. The Acute Phase of Chikungunya Virus Infection in Humans Is Associated With Strong Innate Immunity and T CD8 Cell Activation. **The Journal of Infectious Diseases**, v. 204, n. 1, p. 115–123, 1 jul. 2011. https://doi.org/10.1093/infdis/jiq006

WEAVER, S. C.; FORRESTER, N. L. Chikungunya: Evolutionary history and recent epidemic spread. **Antiviral Research**, v. 120, p. 32–39, ago. 2015. https://doi.org/10.1016/j.antiviral.2015.04.016

WHITE, L. K. et al. Chikungunya virus induces IPS-1-dependent innate immune activation and protein kinase R-independent translational shutoff. **Journal of Virology**, v. 85, n. 1, p. 606–620, jan. 2011. https://doi.org/10.1128/JVI.00767-10

WHO. **What is chikungunya fever?** Disponível em: <https://www.who.int/news-room/q-a-detail/what-is-chikungunya-fever>. Acesso em: 17 jun. 2020.

WINTACHAI, P. et al. Identification of Prohibitin as a Chikungunya Virus Receptor Protein. **Journal of Medical Virology**, v. 84, p. 1757–1770, 2012. https://doi.org/10.1002/jmv.23403

YANG, S. et al. Regulatory considerations in development of vaccines to prevent disease caused by Chikungunya virus q. **Vaccine**, v. 35, n. 37, p. 4851–4858, 2017. https://doi.org/10.1016/j.vaccine.2017.07.065

CAPÍTULO II

Manuscript:

CHIKUNGUNYA VIRUS IS STRONGLY INHIBITED BY PHOSPHOLIPASE A2 isolated from *Crotalus durissus terrificus*

*Este capítulo está em formato de manuscrito com algumas alterações estruturais para melhor se adequar ao formato da dissertação. O artigo em questão será submetido à revista **Antiviral Research.**

CHIKUNGUNYA VIRUS IS STRONGLY INHIBITED BY PHOSPHOLIPASE
A2 isolated from *Crotalus durissus terrificus*

Igor de Andrade Santos[a], Jacqueline Farinha Shimizu[a,b], Débora Moraes de Oliveira[a], Daniel Oliveira Silva Martins[a,b], Adélia Cristina Oliveira Cintra[c], Suely Vilela Sampaio[c], Léia Cardoso Sousa[a], Robinson Sabino da Silva[a], Nilson Nicolau Junior[d], Andres Merits[e], Mark Harris[f], Ana Carolina Gomes Jardim[a,b].

[a]Federal University of Uberlândia (UFU), Institute of Biomedical Science, Uberlândia, MG, Brazil.

[b]São Paulo State University (UNESP), Institute of Bioscience, Language and Exact Sciences, São José do Rio Preto, SP, Brazil.

[c]São Paulo University (USP), Department of Clinical, Toxicological and Bromatological Analyses, Ribeirão Preto, SP, Brazil.

[d]Federal University of Uberlândia (UFU), Institute of Biotechnology, Uberlândia, MG, Brazil.

[e]University of Tartu, Institute of Technology, Tartu, Estonia

[f]University of Leeds, Faculty of Biological Sciences and Centre for Structural Molecular Biology, Leeds, United Kingdon

Corresponding author**:** Professor Ana Carolina Gomes Jardim, Institute of Biomedical Science (ICBIM), Federal University of Uberlandia (UFU), Avenida Amazonas, 4C-Room 216, Umuarama, Uberlândia, Minas Gerais, Brazil, CEP: 38405-302

Tel: +55 (34) 3225-8682

E-mail: jardim@ufu.br

ABSTRACT

Chikungunya virus (CHIKV) is the etiologic agent of Chikungunya fever, a globally spreading mosquito-borne disease. There is no approved antiviral or vaccine against CHIKV, which leads to a mandatory need for development of new therapies. In this context, proteins isolated from snake venoms have demonstrated antiviral activity against several virus, including arbovirus which are relevant the public health system. The phospholipase A2$_{CB}$ (PLA2$_{CB}$), a protein isolated from the venom of *Crotalus durissus terrificus*, presented several biological activities such as anti-inflammatory, antiparasitic, antibacterial and antiviral. In this study, we investigated the multiple effects of PLA2$_{CB}$ on the CHIKV replicative cycle *in vitro*. The antiviral activity of PLA2$_{CB}$ was assessed using CHIKV-*nanoluciferase*, a viral construct inserted of a reporter gene (-*nanoluc*), to infect baby hamster kidney cells (BHK-21) cells and evaluate cell viability (MTT assay) and infectivity rates (luminescence levels). The results demonstrated that PLA2$_{CB}$ possess a strong antiviral activity judged by its selectivity index of 128. We identified that the treatment with PLA2$_{CB}$ protected the cells against CHIKV infection in 84% and strongly impaired virus entry to the host cells by a virucidal effect of over 99 %, or by reducing adsorption and uncoating in 98 and 95 %, respectively. Moreover, PLA2$_{CB}$ presented a modest yet significant activity towards post-entry stages of CHIKV replicative cycle, with inhibition rate of 64 %. Molecular docking calculations were performed and results suggested binding interactions between PLA2$_{CB}$ and CHIKV glycoprotein, mainly with E1 through hydrophobic interactions. In addition, infrared spectroscopy measurements indicated interactions of PLA2$_{CB}$ and CHIKV glycoproteins, corroborating with data from *in silico* analyzes. Our data demonstrated the multiple antiviral effects of PLA2$_{CB}$ on the CHIKV replicative cycle, and suggest the interactions of PLA2$_{CB}$ with CHIKV glycoproteins as the potential target of this compound on blocking virus entry to the host cells.

1. INTRODUCTION

Chikungunya virus (CHIKV), a member of the genus *Alphavirus*, family *Togaviridae* (ICTV, 2019), is the causative agent of the Chikungunya fever epidemics (Mayer et al., 2017). CHIKV particle is constituted by an icosahedral capsid with a positive single strain RNA genome of approximately 12 kb (Burt et al., 2017), involved by a lipid envelope encompassing E1 and E2 glycoproteins in its surface (Strauss and Strauss, 1994; Yap et al., 2017).

CHIKV was first identified in 1950 in Tanzania, Africa, however, it was only related to Chikungunya fever in 1955 (Mason and Haddow, 1957; Weaver and Forrester, 2015). Since then, CHIKV outbreaks were identified in several countries, of Oceanic Indic islands, France, Italy and from the Americas (Silva and Dermody, 2017). In Brazil, the first cases of Chikungunya fever were identified in 2014, and since then, became an endemic disease (Nunes et al., 2015). From January to April of 2020, 22.786 cases and 4 deaths by CHIKV were notified (Ministério da Saúde and Secretaria de Vigilância em Saúde, 2020). This virus is transmitted through the bite of *Aedes aegypty* and *Aedes albopictus* female mosquito (Geevarghese et al., 2010; Ngoagouni et al., 2017), and, therefore, have been associated to the epidemics in tropical and subtropical regions (Kraemer et al., 2015).

Chikungunya fever symptoms include fever, nausea, and fatigue (Das et al., 2010). However, the arthralgia and polyarthralgia caused by the persistent viral replication associated with the host immune response are characteristic of this disease (Brault et al., 2000). In some rare cases, infected individuals can develop hepatitis, myocarditis, and encephalopathy, ultimately leading to death of patients (Das et al., 2010). Unlike other arboviruses, CHIKV infection can progress from acute to chronic condition for months or years, resulting in a disabling disease (Dupuis-Maguiraga et al., 2012; Gardner et al., 2010). In front of the lack of effective Food and Drug Administration (FDA) approved treatments towards CHIKV infection as well as vaccines, CHIKV treatment is often palliative and symptomatic, based on analgesics, non-steroidal anti-inflammatory, rest, and hydration (FDA, 2019).

Given that many approved drugs employed in the treatment of several infectious and chronic diseases originated or derived from natural sources (Dias et al., 2012; Newman

and Cragg, 2020), it is reasonable to hypothesize that natural compounds may also be exploited onto generation of antiviral drugs. In this context,proteins isolated from snake venoms are very promising, since they are a complex mixture of lectins, oxidases, disintegrins, metalloproteins, and phospholipases A2 (Bailey and Wilce, 2001; Villalta-Romero et al., 2017). Phospholipases A2 (PLA2s), in its turn are members of a secreted phospholipases family with catalytic activities, which can act in the cell membranes of several tissues and play several roles in biological systems (Burke and Dennis, 2009; Calderon et al., 2014; Filkin et al., 2020).

The snake venom isolated from *Crotalus durissus terrificus* has numerous constituents such as crotoxin, crotamin, neurotoxin, among others (Schaloske and Dennis, 2006; Six and Dennis, 2000). Crotoxin is the major part of the *C. d. terrificus* venom and is composed of crotapotin and phospholipase A2 (PLA2$_{CB}$) (Hendon and Fraenkel-Conrat, 1971). Subsequently, PLA2$_{CB}$ is a protein with approximately 14 kDa which possess described anti-inflammatory, antiparasitic, and antibacterial properties (Almeida et al., 2016; de Carvalho et al., 2019). PLA2$_{CB}$ have also presented activity towards viruses such as Rocio (ROCV), Mayaro (MAYV) (Muller et al., 2014, 2012), Hepacivirus C (HCV) (Shimizu et al., 2017), Dengue (DENV) and Yellow Fever (YFV) (Muller et al., 2012).

Russo and coworkers expressed and purified two recombinant PLA2$_{CB}$ (rPLA2$_{CB}$) and partially assessed its anti-CHIKV activity. Nevertheless, rPLA2$_{CB}$ proteins presented lower antiviral activity and higher cytotoxicity profile than the native protein, probably due to the nine additional amino acid residues present in their sequences (Russo et al., 2019). Considering these previous results, herein we present and thorough *in vitro* evaluation of the effects of the native PLA2$_{CB}$ towards CHIKV replication cycle. Furthermore, we present possible targets and antiviral mechanism of action of this protein.

2. METHODS

2.1. Compound

The crude venom of *Crotalus durissus terrificus* was obtained from the "Animal Toxin Extraction Center" (CETA), duly registered with the Ministry of the Environment under de process number 3002678. The poison was collected from 28 specimens from the Morungaba-SP collection (IBAMA authorization: 1/35/1998/000846-1) and extraction

was performed by Jairo Marques do Vale (CETA). The isolation and purification of phospholipase PLA2$_{CB}$ **(Figure 1A)** from the venom of *Crotalus durissus terrificus* snakes were carried out at the Toxinology Laboratory of the School of Pharmaceutical Sciences of Ribeirão Preto, University of São Paulo (IBAMA authorization: 1/35/1998/000846-1), as previously described (Hendon and Fraenkel-Conrat, 1971; Muller et al., 2012). The lyophilized protein was dissolved in PBS (phosphate buffer solution), filtered, and stored at -80°C. Dilutions of the stock solution containing protein in complete medium were made immediately prior to the experiments. For all the performed assays, PBS was used as the untreated control.

2.2. Cell culture

BHK-21 cells (ATCC® CCL-10™), derived from baby hamster kidney, were maintained in Dulbecco's modified Eagle's medium (DMEM, Sigma-Aldrich) supplemented with 100U/mL of penicillin (Hyclone Laboratories), 100 mg/mL of streptomycin (Hyclone Laboratories), 1% of non-essential amino acids (Hyclone 28 Laboratories) and 1% of fetal bovine serum (FBS, Hyclonen Laboratoires) in a humidified 5% CO_2 incubator at 37°C. Subgenomic replicon (SGR) harboring cell lines (BHK-CHIKV-NCT) (Pohjala et al., 2011) were maintained under the same conditions of BHK-21 cells (ATCC® CCL-10™), except for the addition of G418 (Sigma-Aldrich) at 5 mg/mL.

2.3. CHIKV construct

The CHIKV-*nanoluciferase* (CHIKV-*nanoluc*) construct **(Figure 1B)** used for the antiviral assays was designed based on the sequence of CHIKV LR (*Lá reunion*) inserted of the CMV promoter and *nanoluciferase* protein sequence (Matkovic et al., 2018; Pohjala et al., 2011). To produce CHIKV-*nanoluc* virus particles, 2.3 x 10^7 BHK-21 cells seeded in a T175 cm^2 flask were transfected with 1.5 µg of CHIKV-CMV-*nanoluc* plasmid using lipofectamine 3000® and Opti-Mem medium. Forty-eight hours post-transfection the supernatant was collected and stored at -80°C. To determine viral titers, 1 x 10^5 BHK-21 cells were seeded in each of 24 wells plate 24 hours prior to the infection. Then, the cells were infected with 10-fold serially dilutions of CHIKV-*nanoluc* for 1 hour at 37°C. The inoculums were removed, cells were washed with PBS to remove the unbound virus, and added fresh medium supplemented with 1% penicillin, 1% streptomycin, 2% FBS and 1% carboxymethyl cellulose (CMC). Infected cells were incubated for 2 days in a humidified 5% CO_2 incubator at 37°C, followed by fixation with

4% formaldehyde and stained with 0.5% violet crystal. The viral foci were counted to determine viral titer.

2.4. Cell viability

Cell viability was measured by MTT [3-(4,5-dimethylthiazol-2-yl)-2,5-diphenyl tetrazolium bromide] (Sigma-Aldrich) assay. BHK-21 cells were cultured in 48 well plates at a density of 5 x 10^4 cells per well and incubated overnight at 37 °C in a humidified 5% CO_2 incubator. PLA2$_{CB}$-containing medium at concentrations ranging from 0.195 to 200 µg/mL in two-fold serial dilutions was added to the cell culture for 16h at 37°C with 5% of CO_2. After treatment, the compound-containing medium was removed and MTT solution at 1 mg/mL was added to each well, incubated for 30 minutes, and replaced with 100 µL of DMSO (dimethyl sulfoxide) to solubilize the formazan crystals. The absorbance was measured at 560 nm on the Glomax microplate reader (Promega). Cell viability was calculated according to the equation (T/C) × 100%, where T and C represent the mean optical density of the treated and untreated control groups, respectively. The cytotoxic concentration of 50% (CC_{50}) was calculated using GraphPad Prism 8.

2.5. The effective concentration of 50% inhibition (EC50)

To assess the antiviral activity of PLA2$_{CB}$, BHK-21 cells were seeded at a density of 5 x 10^4 cells per well into 48 well plates 24 hours before the infection. Cells were infected with CHIKV-*nanoluc* at a multiplicity of infection (MOI) of 0.1 in the presence of PLA2$_{CB}$ at concentrations ranging 0.195 to 200 µg/mL in two-fold serial dilutions. Samples were harvested in Renilla-luciferase lysis buffer (Promega) at 16 hours post-infection (h.p.i.) and virus replication levels were quantified by measuring *nanoluciferase* activity using the Renilla luciferase Assay System (Promega). The effective concentration of 50% inhibition (EC_{50}) was calculated using GraphPad Prism 8. The values of CC_{50} and EC_{50} were used to calculate the selectivity index (SI = CC_{50}/EC_{50}).

2.6. Time-of-addition assays.

To investigate in which step of CHIKV replicative cycle PLA2$_{CB}$ was active, BHK-21 cells at the density of 5 x 10^4 cells per well were seeded in 48 well plates 24 hours before infection and treatment. All experiments were conducted with the virus at MOI of 0.1 and luminescence levels were accessed 16 h.p.i. to analyze the virus replication rates.

2.6.1. Pretreatment assay

To evaluate the protective activity of PLA2$_{CB}$, cells were treated for 1 hour with the compound prior to the CHIKV infection, extensively washed with PBS to the complete removal of the compound, and added of CHIKV-*nanoluc* for 1h. Then, cells were washed with PBS to remove unbound virus and added fresh medium **(Figure 2A)**.

To further investigate the pretreatment stage, further assays were performed: i) cells were treated for 1h with the compound, washed with PBS and infected with CHIKV-*nanoluc* in the presence of PLA2$_{CB}$ for 16h **(Figure 2B)**, and ii) cells were treated with the compound for 1h, then extensively washed with PBS to remove medium containing PLA2$_{CB}$ and infected with CHIKV-*nanoluc* for 16h **(Figure 2C)**.

2.6.2. Entry inhibition assay

The activity of PLA2$_{CB}$ in blocking CHIKV entry to the host cells was assessed by incubating the compound-containing medium and virus with the cells for 1h. Then, cells were extensively washed with PBS and incubated with medium for 16h **(Figure 3A)**. For further analyzes, the following procedures were carried out: i) the virucidal activity was investigated by previously incubating CHIKV and PLA2$_{CB}$ for 1 hour and then adding to the cells for an extra 1 hour. The compound was removed by extensively washing cells with PBS, followed by the replacement with fresh medium **(Figure 3B)**; ii) to evaluate the attachment step, the supernatant containing virus and compound was added to the cells for 1 hour at 4°C, and then the cells were washed to the supernatant removal and replaced by fresh medium **(Figure 3C)**, and iii) to access the effects on the uncoating step, CHIKV and PLA2$_{CB}$ were incubated for 1 hour at 4°C followed by 30 minutes at 37°C. Cells were then washed and replaced by fresh medium **(Figure 3D)**.

2.6.3. Post-entry assay

To investigate the activity of the compound on post-entry stages of the viral replicative cycle, cells were infected with CHIKV for 1 hour, washed extensively with PBS to remove unbound virus, and added with compound-containing medium for 16h **(Figure 4A)**.

2.7. Replication assay using BHK-21-CHIKV-NCT cells

BHK-21 cells harboring the non-cytotoxic CHIKV-LR RNA replicon (BHK-CHIKV-NCT) (Pohjala et al., 2011), that express CHIKV nonstructural proteins, a selection marker (puromycin acetyltransferase, Pac) and two reporters genes (*Renilla* luciferase,

Rluc, and EGFP), were used to assess the activity of PLA2$_{CB}$ on CHIKV replication stage. Cells were seed at a density of 7 x 10^3 in a 96 well plate. After 24h, cells were treated with the PLA2$_{CB}$ at 12.5 µg/mL for 72h **(Figure 4B)**. Then, luminescence levels were accessed to analyze the CHIKV replication rates. The fluorescence was analyzed by placing plates directly in the fluorescence microscopy EVOS$^®$ (Thermo-Fischer) in a 20x lens (scale 400µm) and GFP filter.

2.8. Molecular Docking analysis

The interaction between PLA2$_{CB}$ from the venom of the *Crotalus durissus terrificus* (PDB: 3R0L) and the envelope glycoprotein of the Chikungunya virus (PDB: 3N42) was performed through blind docking performed in the PatchDock server (Schneidman-Duhovny et al., 2005), using the parameters predefined by the program and refined by the FireDock algorithm (Andrusier et al., 2007). The best docking positions were evaluated by the geometric complementarity score defined by PatchDock, with results refined and ranked by the global energy after refinement. The post-docking 3D image was generated in the DS Visualizer program, Dassault Systèmes BIOVIA, Discovery Studio Visualizer, version 17, San Diego: Dassault Systèmes, 2016, and a 2D diagram of the interactions interface between the molecules was generated with the aid of the LigPlot + program (Laskowski and Swindells, 2011).

2.9. Infrared spectroscopy Spectral data analysis

An Fourrier Transformed Infrared (FTIR) spectrophotometer Vertex 70 (Bruker Optics, Reinstetten, Germany) connected to a micro-attenuated total reflectance (ATR) platform was used to record sample signature at 1800 cm^{-1} to 400 cm^{-1} regions. The ATR unit is composed of a diamond disc as an internal-reflection element. The sample dehydrated pellicle penetration depth ranges between 0.1 and 2 µm and depends on the wavelength, incidence angle of the beam, and the refractive index of ATR-crystal material. The infrared beam is reflected at the interface toward sample in the ATR-crystal. All samples (2µL) were dried using airflow on ATR-crystal for 3 min before sample spectra recorded in triplicate. The air spectrum was used as a background in all ATR-FTIR analysis. Sample spectra and background were taken with 4 cm^{-1} of resolution and 32 scans were performed for analysis. The spectra were normalized by the vector method and adjusted to rubber band baseline correction. The original data were plotted in the Origin Pro 9.0 (OriginLab, Northampton, MA, USA) software to create the second

derivative analysis. The second derivative was obtained by applying the Savitzky-Golay algorithm with polynomial order 5 and 20 points of the window. The value heights indicated the intensity of the functional group evaluated.

2.10.　　Statistical analysis

Individual experiments were performed in triplicate and all assays were performed a minimum of three times to confirm the reproducibility of the results. GraphPad Prism 8 software (Graph Pad Software) was used to assess differences between unpaired means of readings using t-Student's for parametric tests, and Mann-Whitney for nonparametric tests. P values < 0.01 were considered to be statistically significant.

3.　RESULTS

3.1. Phospholipase A2$_{CB}$ (PLA2$_{CB}$) strongly impairs Chikungunya virus (CHIKV) infection *in vitro*

We investigated the anti-CHIKV activity of the PLA2$_{CB}$ **(Figure 1A)** using BHK-21 cells and a recombinant CHIKV that expresses a *nanoluciferase* reporter (CHIKV-*nanoluc*) **(Figure 1B)** (Matkovic et al., 2018; Pohjala et al., 2011). First, the PLA2$_{CB}$ antiviral activity was evaluated by performing a dose-response assay to determine the effective concentration of 50% (EC$_{50}$) and cytotoxicity of 50% (CC$_{50}$). BHK-21 cells were infected with CHIKV-*nanoluc* and simultaneously treated with PLA2$_{CB}$ at concentrations ranging from 0.195 to 200 µg/mL in two-fold serial dilutions, and viral replication was assessed 16 hours post-infection (h.p.i.) **(Figure 1C)**. In parallel, cell viability was assessed by an MTT assay. Our data showed that PLA2$_{CB}$ was able to inhibit > 99% of virus replication, while the minimum cell viability remained above 72%. From this range of concentrations, it was determined that PLA2$_{CB}$ has the EC50 of 1.34 µg/mL, CC50 of 172 µg/mL, and the Selectivity Index (SI) of 128 **(Figure 1D)**. This data demonstrated that PLA2$_{CB}$ strongly blocked the CHIKV infection judged by the high SI value. To analyze the PLA2$_{CB}$ antiviral activity on different stages of CHIKV replication, time-based assays were performed. For these further assays, cells were treated with PLA2$_{CB}$ at 12.5 µg/mL which inhibited 91% (p < 0.01) of the virus infection and presented cell viability of 100%.

3.2. PLA2$_{CB}$ protects cells against CHIKV infection

To assess the protective effects of PLA2$_{CB}$ against CHIKV infection, cells were pretreated with PLA2$_{CB}$ for 1 hour at 37°C, washed extensively with PBS to remove the compound and infected with CHIKV-*nanoluc* for 1 hour. Then, the supernatant was removed, cells were added of fresh medium and luminescence levels were measured 16 h.p.i. **(Figure 2A)**. PLA2$_{CB}$ significantly reduced 84% of CHIKV-*nanoluc* infection, demonstrating a robust antiviral effect when cells were treated prior to the infection ($p < 0.01$) **(Figure 2A)**.

In view of this result, two additional assays were performed to further investigate the protective effect of PLA2$_{CB}$. In the first assay, BHK-21 cells were treated with PLA2$_{CB}$ for 1h, washed with PBS and infected with CHIKV in the presence of PLA2$_{CB}$ for 16h. As a result, PLA2$_{CB}$ also protected the cells from CHIKV-*nanoluc* infection, reducing 84% of luminescence levels ($p < 0.01$) **(Figure 2B)**. In the second assay, BHK-21 cells were treated with PLA2$_{CB}$ for 1 hour before the infection, washed with PBS to remove the compounds, and infected with CHIKV for 16h **(Figure 2C)**. The result demonstrated that PLA2$_{CB}$ reduced 96% of CHIKV infection ($p < 0.01$) **(Figure 2C)**, suggesting that PLA2$_{CB}$ was able to protect cells over periods of infection longer than 1 hour. Besides the variation in the values of antiviral activity, no statistical difference was observed among data from these assays, suggesting that the treatment of cells with PLA2$_{CB}$ for more than 1 hour did not enhance the protective effect **(Figure 2D)**.

3.3. CHIKV entry to the host cells is knocked down by PLA2$_{CB}$

To evaluate the PLA2$_{CB}$ effect on CHIKV entry to the host cells, virus and PLA2$_{CB}$ were simultaneously added to BHK-21 cells for 1 hour at 37°C, cells were washed with PBS and replaced with fresh medium **(Figure 3A)**. Luminescence levels were assessed at 16 h.p.i. and demonstrated that PLA2$_{CB}$ decreased 95.3% of virus infection ($p < 0.01$), significantly inhibiting the CHIKV-*nanoluc* entry to the host cells **(Figure 3A)**.

Additional assays were performed for a better understanding of the virucidal effect, and activity of PLA2$_{CB}$ on viral attachment and or uncoating. To evaluate the virucidal activity, an inoculum containing PLA2$_{CB}$ and CHIKV was incubated at 37°C for 1h. Then, the inoculum was added to naive BHK-21 cells and incubated for an additional hour. Cells were extensively washed, replaced with fresh medium, and luminescence levels assessed **(Figure 3B)**. PLA2$_{CB}$ showed strong virucidal activity, blocking over 99% of virus entry to the host cells ($p < 0.01$) **(Figure 3B)**. To analyze the

PLA2$_{CB}$ effect on CHIKV attachment, virus and compound were first incubated with the cells at 4°C for 1h. At this temperature, virus particles were able to attach to the cellular receptors, but not entry into the host cells. Cells were then washed with PBS, added of fresh medium, and incubated at 37°C **(Figure 3C)**, to allow the continuation of the entry process. Data obtained from this assay also showed strong inhibition of CHIKV attachment by reducing 98.2% of virus entry to the cells ($p < 0.01$) **(Figure 3C)**. In the uncoating assay, cells were incubated with the virus and compound inoculum at 4°C for 1 hour, followed by incubation for 30 minutes at 37°C in an attempt to focus on the effect of PLA2$_{CB}$ on the uncoating step **(Figure 3D)**. The results demonstrated that PLA2$_{CB}$ decreased luminescence levels up to 95.2% ($p < 0.01$), suggesting a robust inhibition of the CHIKV entry **(Figure 3D)**.

3.4. PLA2$_{CB}$ moderately affect post-entry steps of CHIKV replicative cycle

For the post-entry steps analysis, cells were first infected with CHIKV-*nanoluc* for 1 hour at 37°C, washed extensively with PBS to remove the unbounded virus, and then added fresh medium containing PLA2$_{CB}$ **(Figure 4A)**. The results showed that PLA2$_{CB}$ significantly reduced of 64% of CHIKV replication ($p < 0.01$) **(Figure 4A)**. An additional antiviral assay was performed to investigate the effects of PLA2$_{CB}$ on virus replication using BHK-CHIKV-NCT cells. This stable replicon cell line continuously expresses CHIKV nonstructural proteins and two reporter genes (*Renilla* luciferase and EGFP), allowing the evaluation of the effect of PLA2$_{CB}$ on replication complexes formed during the replication stage. For this analysis, BHK-CHIKV-NCT cells were treated with PLA2$_{CB}$ at 12.5 µg/mL and replication rates were assessed 72h after treatment **(Figure 4B)**. Corroborating the post-entry data, PLA2$_{CB}$ significantly decreased CHIKV replication levels in 58% without cytotoxicity **(Figure 4B)**. The levels in EGFP expression were also decrease as seen in **Figure 4C**. These results suggest that the observed post-entry inhibition can be also associated with an effect on nonstructural proteins, impairing the CHIKV replication cycle.

Altogether, these data suggest that PLA2$_{CB}$ can inhibit multiple steps of CHIKV replication. However, the strongest effect of PLA2$_{CB}$ was related to virus entry inhibition, more specifically as virucidal and/or on attachment step. It suggests that the mechanism of action of PLA2$_{CB}$ as anti-CHIKV might be related to a direct action on the virus structure.

3.5. Possible interactions between PLA2$_{CB}$ and CHIKV glycoproteins

In view of the results of PLA2$_{CB}$ impairing CHIKV entry on host cells, a molecular docking assay was performed to investigate interactions and binging mode between PLA2$_{CB}$ and CHIKV glycoproteins. In a blind molecular docking, PLA2$_{CB}$ interacted with the E1 and E2 of the glycoprotein complex, with global energy of 0.57 kJ/mol after refining **(Figure 5).**

The 2D interactions between PLA2$_{CB}$ and CHIKV glycoproteins showed that PLA2$_{CB}$ mainly interacted with E1 glycoprotein, forming thirty hydrophobic interactions (residues He63, Gln33, Pro19, Phe109, Gly31, Ala55, Val18, Lys60, Arg114, Phe23, Trp30, Trp61, Leu3 in PLA2$_{CB}$ and residues Gln353, Lys132, Leu34, Val269, Ser35, Asn389, Arg134, Asn140, Tyr390, Leu136, Gln260, Gly12, He344, Glu32, Arg340, Ser355 in E1 glycoprotein) **(Figure 6)**. Also, PLA2$_{CB}$ formed 3 hydrogens bonds with E1, being one between Ser113 and Asn270 (2.30 Å), one among Asn58 and Glu343 (2.95 Å) and one between His1 and Glu341 (2.18 Å) **(Figure 6)**. Regarding the interaction among PLA2$_{CB}$ and E2 glycoprotein, one hydrogen bond was formed between Arg11 and Glu 334 (2.07 Å), plus five hydrophobic interactions (Asn105, Lys104, Gly106 in PLA2$_{CB}$ and Asn273, Lys270 in E1) **(Figure 7)**.

3.6. PLA2$_{CB}$ causes molecular changes in CHIKV glycoprotein

To further investigate the interactions between PLA2$_{CB}$ and CHIKV particles, infrared spectroscopy spectral analysis was performed and vibrational analysis among the virus and PLA2$_{CB}$. Representative means of the infrared spectrum of CHIKV, PLA2$_{CB,}$ and CHIKV plus PLA2$_{CB}$, which is the bio fingerprint region representing proteins, lipids, nucleic acids, and glycoproteins are shown in **Figure 8A**. We focused on the molecular analysis in the interaction of PLA2$_{CB}$ with CHIKV. A representative infrared average spectrum of second derivative analysis from CHIKV, PLA2$_{CB,}$ and CHIKV plus PLA2$_{CB}$ was displayed in **Figure 8A**. In the second derivative analysis, the value heights indicate parallel changes in the intensity of each functional group. The binding interaction between CHIKV and PLA2$_{CB}$ was mainly revealed by the increase in the vibrational mode at 1068 cm^{-1}, which indicates detection of additional stretching of C-O ribose present in glycoprotein derived from the association CHIKV and PLA2$_{CB}$ (Derenne et al., 2020; Khajehpour et al., 2006; Movasaghi et al., 2008) **(Figure 8B).** Furthermore, the Stacked Walls **(Figure 9A)** and split heat map **(Figure 9B)** reinforces

the additional expression of vibrational mode at 1068 cm^{-1} under CHIKV plus PLA2$_{CB}$ association.

4. DISCUSSION

Phospholipase A2 from *Crotalus durissus terrificus* (PLA2$_{CB}$) is a molecule described to possess antiviral activity against virus as the Yellow-fever (YFV), Dengue (DENV) (Muller et al., 2014, 2012), and Hepacivirus C (HCV) (Shimizu et al., 2017). Additionally, two recombinant forms of PLA2$_{CB}$ (rPLA2$_{CB}$) was partially described to possess anti-CHIKV activity (Russo et al., 2019), however, presented lower antiviral activity and higher cytotoxicity than the native protein, probably due to the nine additional amino acid residues present in their sequences. Here, we assessed the antiviral activity of the PLA2$_{CB}$ from *Crotalus durissus terrificus* against CHIKV, as well as sought comprehension on its mechanism of action.

Our results demonstrated that PLA2$_{CB}$ strongly inhibited CHIKV infectivity, corroborating with Russo and colleagues work, which demonstrated that rPLA2$_{CB}$ impaired CHIKV infection (Russo et al., 2019). Additionally, the results demonstrated that the treatment of naïve cells with PLA2$_{CB}$ for 1 hour or longer protected host cells against CHIKV infection in up to 84%. In accordance with our study, Chen and coworkers found that a similar phospholipase A2 isolated from the venom of the honeybee *Apis mellifera* was able to protect cells against the Human immunodeficiency virus (HIV) and DENV infections by performing a time-of -addiction assay (Chen et al., 2017). Fenard and colleagues, in their turn, also demonstrated that different phospholipases A2 isolated from several mammals protected the HIV target cells against virus infection (Fenard et al., 1999). The PLA2s from snake venoms are classified in the group II of a secreted family phospholipases and show homology to the mammalian inflammatory PLA2, which play different roles in the organism as an immune response to infectious diseases (Gutiérrez and Lomonte, 2013; Murakami et al., 2016; Palm et al., 2013; Sadekuzzaman et al., 2018). Therefore, our data might also suggest that PLA2$_{CB}$ plays a role in host cell metabolism and as a result protects cells against viral infection, by the possible mimetic effect of phospholipases found in host cells.

In our study, PLA2$_{CB}$ strongly inhibited CHIKV entry into the host cells by a virucidal effect (99.2%) and also by interfering with viral adsorption (98.2%) and uncoating (95.2%). It is consistent with previous findings for DENV and YFV, two other

arboviruses (Muller et al., 2012). By incubating the wild type DENV or YFV with PLA2$_{CB}$ before infection, the authors demonstrated that the compound inhibited early steps of viral infection probably by disrupting viral membrane and/or adsorption (Muller et al., 2014, 2012). Additionally, Russo and coworkers described that incubation of rPLA2$_{CB}$ with CHIKV prior to the infection of cells significantly impaired CHIKV infectivity (Russo et al., 2019). Therefore, our results are in agreement with previous data that suggested that the PLA2$_{CB}$ main activity is due to its virucidal effect, probably by acting on the virus particle. Several PLA2s isolated from snake venoms has been described to possess antiviral activity against DENV, YFV, Herpes simples types 1 and 2 and Influenza A (H3N2) by interacting with lipid membrane founded in a pocket between glycoproteins and/or through attachment to the glycoproteins in the viral envelope surface (Brenes et al., 2020; Chen et al., 2017; Muller et al., 2014, 2012). Based on this data, we performed a blind molecular docking using PLA2$_{CB}$ and the glycoproteins complex (E1, E2, and E3) to assess the possible interaction among then. The results demonstrated that PLA2$_{CB}$ bonded to E1 and E2 (mainly with E1) with low global energy (0.57 kJ/mol), suggesting possible interactions. These results are also consistent with the virucidal effect described here and corroborate previously published data (Russo et al., 2019). The glycoproteins E1 and E2 are essential during the early stages of CHIKV infection. The glycoprotein E2 is responsible for binding to cells receptors as TIM-1 and glycosaminoglycans (Fongsaran et al., 2014; Moller-Tank et al., 2013; Silva et al., 2014) and E1 is a viral fusion protein that ensures the envelope fusion with host cells membranes (Salvador et al., 2009; Wengler et al., 2003). Thus, molecules that can interact with E1 and/or E2 attachment sites can prevent them of entering into host cells (Rashad and Keller, 2013). To the best of our knowledge, there is no description of PLA2$_{CB}$ mode of action against CHIKV. Therefore, we propose that this macromolecule might be binding to E1 and/or E2 glycoproteins and preventing its entry on cells by impairing attachment and/or membrane fusion. An infrared spectrum assay was also performed to further characterize PLA2$_{CB}$/glycoproteins interaction. As a result, glycoproteins sites seem to be affected by PLA2$_{CB}$, mainly revealed by the increase in the vibrational mode at 1068 cm^{-1}, which indicates the detection of stretching of C-O ribose present in glycoproteins derived from the association CHIKV and PLA2$_{CB}$, reinforcing the interaction between CHIKV envelope and PLA2$_{CB}$.

Moreover, in our data, PLA2$_{CB}$ demonstrated a modest yet significant anti-CHIKV activity on post-entry steps. We used a subgenomic replicon expressing CHIKV nonstructural proteins to investigate the activity of PLA2$_{CB}$ on the CHIKV replication stage. The results also showed a moderate antiviral effect of 58%, suggesting that the observed post-entry inhibition can be associated with an effect on the replication process, which also occurs in the presence of cells membranes. Shimizu and coworkers identified that PLA2$_{CB}$ also affected the HCV post-entry steps using a subgenomic replicon system (Shimizu et al., 2017), corroborating with our findings. However, a residual activity cannot be completely discarded due to the strong virucidal effect presented by PLA2$_{CB}$.

CONCLUSIONS

In summary, our study evidenced that PLA2$_{CB}$ isolated from *Crotalus durissus terrificus* inhibited multiple steps of CHIKV infection. This compound was able to protect the target cells against CHIKV infection, impaired virus entry to the host cells, mainly by virucidal activity, and also disturbed post-entry steps of the CHIKV replication cycle. Therefore, this data might be useful for further development of new antiviral therapy against CHIKV and provide a relevant advance to the public health to treat Chikungunya fever.

5. REFERENCES

Almeida, J.R., Lancellotti, M., Soares, A.M., Calderon, L.A., Ramírez, D., González, W., Marangoni, S., Da Silva, S.L., 2016. CoaTx-II, a new dimeric Lys49 phospholipase A2 from Crotalus oreganus abyssus snake venom with bactericidal potential: Insights into its structure and biological roles. Toxicon 120, 147–158. https://doi.org/10.1016/j.toxicon.2016.08.007

Andrusier, N., Nussinov, R., Wolfson, H.J., 2007. FireDock: Fast interaction refinement in molecular docking. Proteins Struct. Funct. Bioinforma. 69, 139–159. https://doi.org/10.1002/prot.21495

Bailey, P., Wilce, J., 2001. Venom as a source of useful biologically active molecules. Emerg. Med. 13, 28–36. https://doi.org/10.1046/j.1442-2026.2001.00174.x

Brault, A.C., Tesh, R.B., Powers, A.M., Weaver, S.C., 2000. Re-emergence of chikungunya and o'nyong-nyong viruses: evidence for distinct geographical lineages and distant evolutionary relationships. J. Gen. Virol. 81, 471–479. https://doi.org/10.1099/0022-1317-81-2-471

Brenes, H., Loría, G.D., Lomonte, B., 2020. Potent virucidal activity against Flaviviridae of a group IIA phospholipase A2 isolated from the venom of Bothrops asper. Biol. J. Int. Assoc. Biol. Stand. 63, 48–52. https://doi.org/10.1016/j.biologicals.2019.12.002

Burke, J.E., Dennis, E.A., 2009. Phospholipase A2 biochemistry. Cardiovasc. Drugs Ther. 23, 49–59. https://doi.org/10.1007/s10557-008-6132-9

Burt, F.J., Chen, W., Miner, J.J., Lenschow, D.J., Merits, A., Schnettler, E., Kohl, A., Rudd, P.A., Taylor, A., Herrero, L.J., Zaid, A., Ng, L.F.P., Mahalingam, S., 2017. Chikungunya virus: an update on the biology and pathogenesis of this emerging pathogen. Lancet Infect. Dis. 17, e107–e117. https://doi.org/10.1016/S1473-3099(16)30385-1

Calderon, L.A., Sobrinho, J.C., Zaqueo, K.D., de Moura, A.A., Grabner, A.N., Mazzi, M.V., Marcussi, S., Nomizo, A., Fernandes, C.F.C., Zuliani, J.P., Carvalho, B.M.A., da Silva, S.L., Stábeli, R.G., Soares, A.M., 2014. Antitumoral Activity of Snake Venom Proteins: New Trends in Cancer Therapy. BioMed Res. Int. 2014, e203639. https://doi.org/10.1155/2014/203639

Chen, M., Aoki-Utsubo, C., Kameoka, M., Deng, L., Terada, Y., Kamitani, W., Sato, K., Koyanagi, Y., Hijikata, M., Shindo, K., Noda, T., Kohara, M., Hotta, H., 2017. Broad-spectrum antiviral agents: secreted phospholipase A 2 targets viral envelope lipid bilayers derived from the endoplasmic reticulum membrane. Sci. Rep. 7, 15931. https://doi.org/10.1038/s41598-017-16130-w

Costa Torres, A.F., Dantas, R.T., Toyama, M.H., Filho, E.D., Zara, F.J., Rodrigues de Queiroz, M.G., Pinto Nogueira, N.A., Rosa de Oliveira, M., de Oliveira Toyama, D., Monteiro, H.S.A., Martins, A.M.C., 2010. Antibacterial and antiparasitic effects of Bothrops marajoensis venom and its fractions: Phospholipase A2 and l-amino acid oxidase. Toxicon 55, 795–804. https://doi.org/10.1016/j.toxicon.2009.11.013

Das, T., Jaffar-Bandjee, M.C., Hoarau, J.J., Krejbich Trotot, P., Denizot, M., Lee-Pat-Yuen, G., Sahoo, R., Guiraud, P., Ramful, D., Robin, S., 2010. Chikungunya fever: CNS infection and pathologies of a re-emerging arbovirus. Prog. Neurobiol. 91, 121–129. https://doi.org/10.1016/j.pneurobio.2009.12.006

de Carvalho, A.E.Z., Giannotti, K., Junior, E.L., Matsubara, M., Santos, M.C.D., Fortes-Dias, C.L., Teixeira, C., 2019. Crotalus durissus ruruima Snake Venom and a Phospholipase A2 Isolated from This Venom Elicit Macrophages to Form Lipid Droplets and Synthesize Inflammatory Lipid Mediators. J. Immunol. Res. 2019. https://doi.org/10.1155/2019/2745286

Derenne, A., Derfoufi, K.-M., Cowper, B., Delporte, C., Goormaghtigh, E., 2020. FTIR spectroscopy as an analytical tool to compare glycosylation in therapeutic monoclonal antibodies. Anal. Chim. Acta 1112, 62–71. https://doi.org/10.1016/j.aca.2020.03.038

Dias, D.A., Urban, S., Roessner, U., 2012. A Historical Overview of Natural Products in Drug Discovery. Metabolites 2, 303–336. https://doi.org/10.3390/metabo2020303

Dupuis-Maguiraga, L., Noret, M., Brun, S., Le Grand, R., Gras, G., Roques, P., 2012. Chikungunya Disease: Infection-Associated Markers from the Acute to the Chronic Phase of Arbovirus-Induced Arthralgia. PLoS Negl. Trop. Dis. 6, e1446. https://doi.org/10.1371/journal.pntd.0001446

FDA, 2019. Vaccines and Related Biological Products Advisory Committee Meeting 08 November 2019.

Fenard, D., Lambeau, G., Valentin, E., Lefebvre, J.-C., Lazdunski, M., Doglio, A., 1999. Secreted phospholipases A2, a new class of HIV inhibitors that block virus entry into host cells. J. Clin. Invest. 104, 611–618.

Filkin, S.Y., Lipkin, A.V., Fedorov, A.N., 2020. Phospholipase Superfamily: Structure, Functions, and Biotechnological Applications. Biochem. Biokhimiia 85, S177–S195. https://doi.org/10.1134/S0006297920140096

Fongsaran, C., Jirakanwisal, K., Kuadkitkan, A., Wikan, N., Wintachai, P., Thepparit, C., Ubol, S., Phaonakrop, N., Roytrakul, S., Smith, D.R., 2014. Involvement of ATP synthase β subunit in chikungunya virus entry into insect cells. Arch. Virol. 159, 3353–3364. https://doi.org/10.1007/s00705-014-2210-4

Gardner, J., Anraku, I., Le, T.T., Larcher, T., Major, L., Roques, P., Schroder, W.A., Higgs, S., Suhrbier, A., 2010. Chikungunya Virus Arthritis in Adult Wild-Type Mice. J. Virol. 84, 8021–8032. https://doi.org/10.1128/JVI.02603-09

Geevarghese, G., Ghodke, Y., Sudeep, A., Arankalle, V., Mavale, M., Gokhale, M., Parashar, D., Mishra, A.C., 2010. Venereal Transmission of Chikungunya Virus by Aedes aegypti Mosquitoes (Diptera: Culicidae). Am. J. Trop. Med. Hyg. 83, 1242–1244. https://doi.org/10.4269/ajtmh.2010.09-0577

Gutiérrez, J.M., Lomonte, B., 2013. Phospholipases A2: unveiling the secrets of a functionally versatile group of snake venom toxins. Toxicon Off. J. Int. Soc. Toxinology 62, 27–39. https://doi.org/10.1016/j.toxicon.2012.09.006

Hendon, R.A., Fraenkel-Conrat, H., 1971. Biological roles of the two components of crotoxin. Proc. Natl. Acad. Sci. U. S. A. 68, 1560–1563. https://doi.org/10.1073/pnas.68.7.1560

ICTV, 2019. Genus: Alphavirus - Togaviridae - Positive-sense RNA Viruses [WWW Document]. Int. Comm. Taxon. Viruses ICTV. URL https://talk.ictvonline.org/ictv-reports/ictv_online_report/positive-sense-rna-viruses/w/togaviridae/872/genus-alphavirus (accessed 5.19.20).

Khajehpour, M., Dashnau, J.L., Vanderkooi, J.M., 2006. Infrared spectroscopy used to evaluate glycosylation of proteins. Anal. Biochem. 348, 40–48. https://doi.org/10.1016/j.ab.2005.10.009

Kraemer, M.U., Sinka, M.E., Duda, K.A., Mylne, A.Q., Shearer, F.M., Barker, C.M., Moore, C.G., Carvalho, R.G., Coelho, G.E., Van Bortel, W., Hendrickx, G., Schaffner, F., Elyazar, I.R., Teng, H.-J., Brady, O.J., Messina, J.P., Pigott, D.M., Scott, T.W., Smith, D.L., Wint, G.W., Golding, N., Hay, S.I., 2015. The global distribution of the arbovirus vectors Aedes aegypti and Ae. albopictus. eLife 4, e08347. https://doi.org/10.7554/eLife.08347

Laskowski, R.A., Swindells, M.B., 2011. LigPlot+: Multiple ligand-protein interaction diagrams for drug discovery. J. Chem. Inf. Model. 51, 2778–2786. https://doi.org/10.1021/ci200227u

Lima Neto, A.S., Sousa, G.S., Nascimento, O.J., Castro, M.C., 2019. Chikungunya-attributable deaths: A neglected outcome of a neglected disease. PLoS Negl. Trop. Dis. 13. https://doi.org/10.1371/journal.pntd.0007575

Mason, P.J., Haddow, A.J., 1957. An Epidemic of Yirus Disease in Southern Province, Tanganyika Territory, in 1952-53. An Additional Note on Chlkungunya Yirus Isolations and Serum Antibodies. Trans. R. Soc. Trop. Med. Hyg. 51, 238–40.

Matkovic, R., Bernard, E., Fontanel, S., Eldin, P., Chazal, N., Hassan Hersi, D., Merits, A., Péloponèse, J.-M., Briant, L., 2018. The Host DHX9 DExH-Box Helicase Is Recruited to Chikungunya Virus Replication Complexes for Optimal Genomic RNA Translation. J. Virol. 93, e01764-18, /jvi/93/4/JVI.01764-18.atom. https://doi.org/10.1128/JVI.01764-18

Mayer, S.V., Tesh, R.B., Vasilakis, N., 2017. The emergence of arthropod-borne viral diseases: A global prospective on dengue, chikungunya and zika fevers. Acta Trop. 166, 155–163. https://doi.org/10.1016/j.actatropica.2016.11.020

Ministério da Saúde, Secretaria de Vigilância em Saúde, 2020. Monitoramento dos casos de arboviroses urbanas transmitidas pelo Aedes Aegypti (dengue, chikungunya e zika), Semanas Epidemiológicas 1 a 17, 2020 (No. 18). Ministério da Saúde.

Moller-Tank, S., Kondratowicz, A.S., Davey, R.A., Rennert, P.D., Maury, W., 2013. Role of the phosphatidylserine receptor TIM-1 in enveloped-virus entry. J. Virol. 87, 8327–8341. https://doi.org/10.1128/JVI.01025-13

Movasaghi, Z., Rehman, S., Rehman, D.I. ur, 2008. Fourier Transform Infrared (FTIR) Spectroscopy of Biological Tissues. Appl. Spectrosc. Rev. 43, 134–179. https://doi.org/10.1080/05704920701829043

Muller, V.D., Soares, R.O., dos Santos-Junior, N.N., Trabuco, A.C., Cintra, A.C., Figueiredo, L.T., Caliri, A., Sampaio, S.V., Aquino, V.H., 2014. Phospholipase A2 Isolated from the Venom of Crotalus durissus terrificus Inactivates Dengue virus and Other Enveloped Viruses by Disrupting the Viral Envelope. PLoS ONE 9, e112351. https://doi.org/10.1371/journal.pone.0112351

Muller, V.D.M., Russo, R.R., Oliveira Cintra, A.C., Sartim, M.A., De Melo Alves-Paiva, R., Figueiredo, L.T.M., Sampaio, S.V., Aquino, V.H., 2012. Crotoxin and phospholipases A2 from Crotalus durissus terrificus showed antiviral activity against dengue and yellow fever viruses. Toxicon, From venoms to drugs 59, 507–515. https://doi.org/10.1016/j.toxicon.2011.05.021

Murakami, M., Yamamoto, K., Miki, Y., Murase, R., Sato, H., Taketomi, Y., 2016. Chapter Four - The Roles of the Secreted Phospholipase A2 Gene Family in Immunology, in: Alt, F.W. (Ed.), Advances in Immunology. Academic Press, pp. 91–134. https://doi.org/10.1016/bs.ai.2016.05.001

Newman, D.J., Cragg, G.M., 2020. Natural Products as Sources of New Drugs over the Nearly Four Decades from 01/1981 to 09/2019. J. Nat. Prod. 83, 770–803. https://doi.org/10.1021/acs.jnatprod.9b01285

Ngoagouni, C., Kamgang, B., Kazanji, M., Paupy, C., Nakouné, E., 2017. Potential of Aedes aegypti and Aedes albopictus populations in the Central African Republic to transmit enzootic chikungunya virus strains. Parasit. Vectors 10. https://doi.org/10.1186/s13071-017-2101-0

Nunes, M.R.T., Faria, N.R., de Vasconcelos, J.M., Golding, N., Kraemer, M.U., de Oliveira, L.F., Azevedo, R. do S. da S., da Silva, D.E.A., da Silva, E.V.P., da Silva, S.P., Carvalho, V.L., Coelho, G.E., Cruz, A.C.R., Rodrigues, S.G., da Silva Gonçalves Vianez, J.L., Nunes, B.T.D., Cardoso, J.F., Tesh, R.B., Hay, S.I., Pybus, O.G., da Costa Vasconcelos, P.F., 2015. Emergence and potential for spread of Chikungunya virus in Brazil. BMC Med. 13, 102. https://doi.org/10.1186/s12916-015-0348-x

Palm, N.W., Rosenstein, R.K., Yu, S., Schenten, D.D., Florsheim, E., Medzhitov, R., 2013. Bee Venom Phospholipase A2 Induces a Primary Type 2 Response that Is Dependent on the Receptor ST2 and Confers Protective Immunity. Immunity 39, 976–985. https://doi.org/10.1016/j.immuni.2013.10.006

Pohjala, L., Utt, A., Varjak, M., Lulla, A., Merits, A., Ahola, T., Tammela, P., 2011. Inhibitors of alphavirus entry and replication identified with a stable Chikungunya replicon cell line and virus-based assays. PloS One 6, e28923. https://doi.org/10.1371/journal.pone.0028923

Rashad, A.A., Keller, P.A., 2013. Structure based design towards the identification of novel binding sites and inhibitors for the chikungunya virus envelope proteins. J. Mol. Graph. Model. 44, 241–252. https://doi.org/10.1016/j.jmgm.2013.07.001

Russo, R.R., dos Santos Júnior, N.N., Cintra, A.C.O., Figueiredo, L.T.M., Sampaio, S.V., Aquino, V.H., 2019. Expression, purification and virucidal activity of two recombinant isoforms of phospholipase A2 from Crotalus durissus terrificus venom. Arch. Virol. 164, 1159–1171. https://doi.org/10.1007/s00705-019-04172-6

Sadekuzzaman, M., Stanley, D., Kim, Y., 2018. Nitric Oxide Mediates Insect Cellular Immunity via Phospholipase A2 Activation. J. Innate Immun. 10, 70–81. https://doi.org/10.1159/000481524

Salvador, B., Zhou, Y., Michault, A., Muench, M.O., Simmons, G., 2009. Characterization of Chikungunya pseudotyped viruses: Identification of refractory cell lines and demonstration of cellular tropism differences mediated by mutations in E1 glycoprotein. Virology 393, 33–41. https://doi.org/10.1016/j.virol.2009.07.013

Schaloske, R.H., Dennis, E.A., 2006. The phospholipase A2 superfamily and its group numbering system. Biochim. Biophys. Acta 1761, 1246–1259. https://doi.org/10.1016/j.bbalip.2006.07.011

Schneidman-Duhovny, D., Inbar, Y., Nussinov, R., Wolfson, H.J., 2005. PatchDock and SymmDock: Servers for rigid and symmetric docking. Nucleic Acids Res. 33, 363–367. https://doi.org/10.1093/nar/gki481

Shimizu, J.F., Pereira, C.M., Bittar, C., Batista, M.N., Campos, G.R.F., Silva, S. da, Cintra, A.C.O., Zothner, C., Harris, M., Sampaio, S.V., Aquino, V.H., Rahal, P., Jardim, A.C.G., 2017. Multiple effects of toxins isolated from Crotalus durissus terrificus on the hepatitis C virus life cycle. PLOS ONE 12, e0187857. https://doi.org/10.1371/journal.pone.0187857

Silva, L.A., Dermody, T.S., 2017. Chikungunya virus: epidemiology, replication, disease mechanisms, and prospective intervention strategies. J. Clin. Invest. 127, 737–749. https://doi.org/10.1172/JCI84417

Silva, L.A., Khomandiak, S., Ashbrook, A.W., Weller, R., Heise, M.T., Morrison, T.E., Dermody, T.S., 2014. A single-amino-acid polymorphism in Chikungunya virus E2 glycoprotein influences glycosaminoglycan utilization. J. Virol. 88, 2385–2397. https://doi.org/10.1128/JVI.03116-13

Six, D.A., Dennis, E.A., 2000. The expanding superfamily of phospholipase A(2) enzymes: classification and characterization. Biochim. Biophys. Acta 1488, 1–19. https://doi.org/10.1016/s1388-1981(00)00105-0

Strauss, J.H., Strauss, E.G., 1994. The alphaviruses: gene expression, replication, and evolution. Microbiol. Rev. 58, 491–562.

Tsetsarkin, K.A., Vanlandingham, D.L., McGee, C.E., Higgs, S., 2007. A Single Mutation in Chikungunya Virus Affects Vector Specificity and Epidemic Potential. PLOS Pathog. 3, e201. https://doi.org/10.1371/journal.ppat.0030201

Villalta-Romero, F., Borro, L., Mandic, B., Escalante, T., Rucavado, A., Gutiérrez, J.M., Neshich, G., Tasic, L., 2017. Discovery of small molecule inhibitors for the snake venom metalloprotease BaP1 using in silico and in vitro tests. Bioorg. Med. Chem. Lett. 27, 2018–2022. https://doi.org/10.1016/j.bmcl.2017.03.007

Weaver, S.C., Forrester, N.L., 2015. Chikungunya: Evolutionary history and recent epidemic spread. Antiviral Res. 120, 32–39. https://doi.org/10.1016/j.antiviral.2015.04.016

Wengler, Gerd, Koschinski, A., Wengler, Gisela, Dreyer, F., 2003. Entry of alphaviruses at the plasma membrane converts the viral surface proteins into an ion-permeable pore that can

be detected by electrophysiological analyses of whole-cell membrane currents. J. Gen. Virol. 84, 173–181. https://doi.org/10.1099/vir.0.18696-0

Yap, M.L., Klose, T., Urakami, A., Hasan, S.S., Akahata, W., Rossmann, M.G., 2017. Structural studies of Chikungunya virus maturation. Proc. Natl. Acad. Sci. 114, 13703–13707. https://doi.org/10.1073/pnas.1713166114
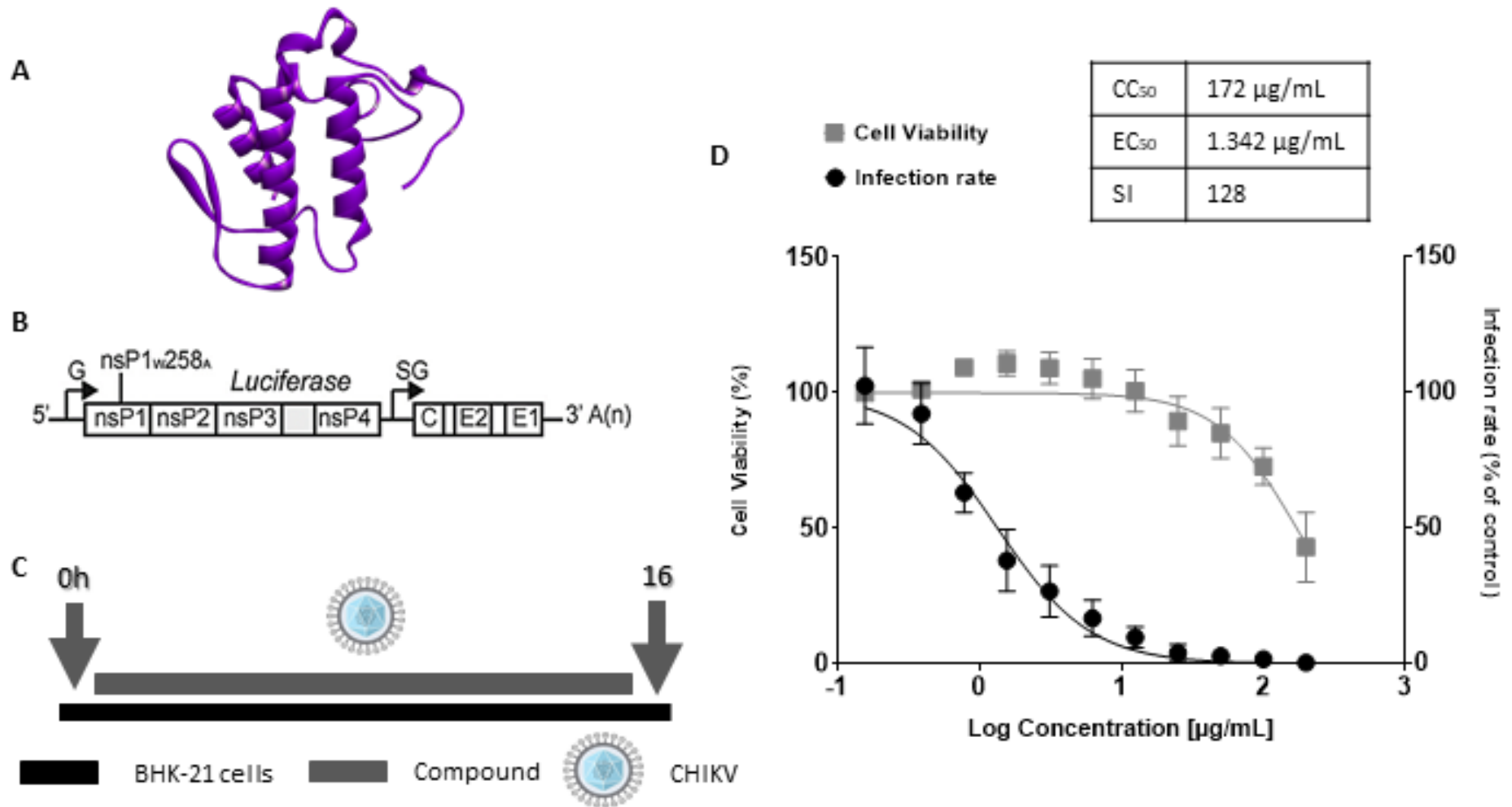
Figures

Figure 1. The activity of Phospholipase A2CB (PLA2CB) against CHIKV infection. (A) Phospholipase A2CB protein structure (PDB: 3R0L). (B) schematic representation of CHIKV-*nanoluc* replicon construction (Matkovic et al., 2018). (C) Schematic representation of infectivity assay. (D) BHK-21 cells were treated with concentrations of PLA2CB ranging from 0.195 to 200 µg/mL and the effective concentration of 50% (EC_{50}) and cytotoxic concentration of 50% (CC_{50}) were determined. CHIKV replication was measured by luciferase assay (indicated by •) and cellular viability measured using an MTT assay (indicated by ▢). The mean values of three independent experiments each measured in triplicate including the standard deviation are shown.
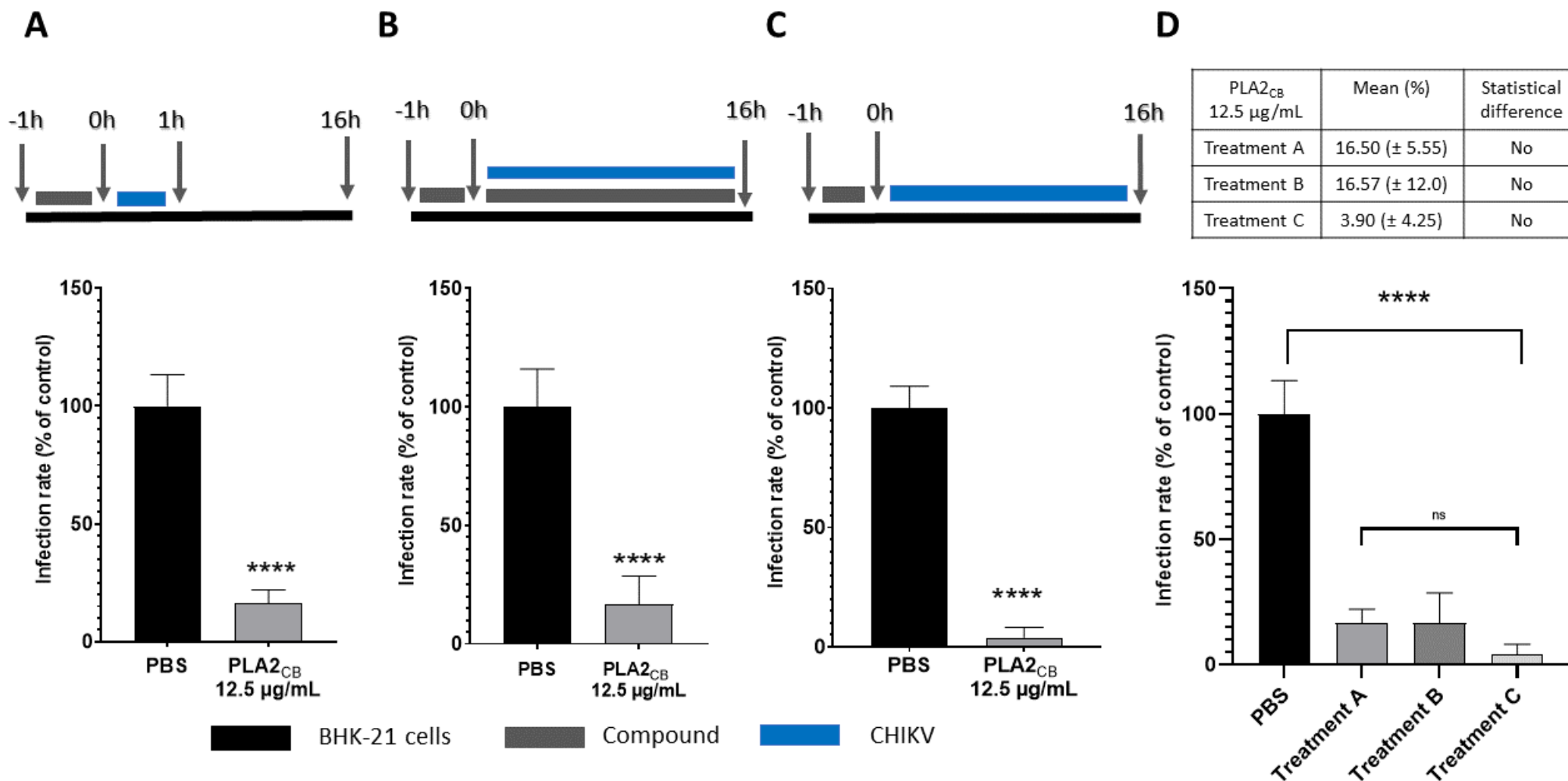
Figure 2. Protective effects of PLA2CB against CHIKV infection. (A) BHK-21 cells were treated with PLA2CB at 12.5 µg/mL for 1h. Then, cells were extensively washed and infected with CHIKV-*nanoluc* at MOI 0.1 for 1h. The compound-containing medium was removed and replaced with a fresh medium. (B) BHK-21 cells were treated with the PLA2CB at 12.5 µg/mL for 1h, then were extensively washed with PBS. The compound was removed and cells were infected with CHIKV-*nanoluc* in the presence of PLA2CB. (C) Cells were treated with the compound for 1h, then extensively washed with PBS and added fresh medium with CHIKV-*nanoluc*. (D) Comparisons among the three pretreatments assays. For all assays, CHIKV replication was measured by *nanoluc* activity at 16 h.p.i.. Schematic representation of each time-based assay as indicated by BHK-21 cells (black bars), PLA2CB (grey bars), and CHIKV-*nanoluc* (blue bars). Mean values of a minimum of three independent experiments each measured in triplicate, $p < 0.01$ was considered significant.
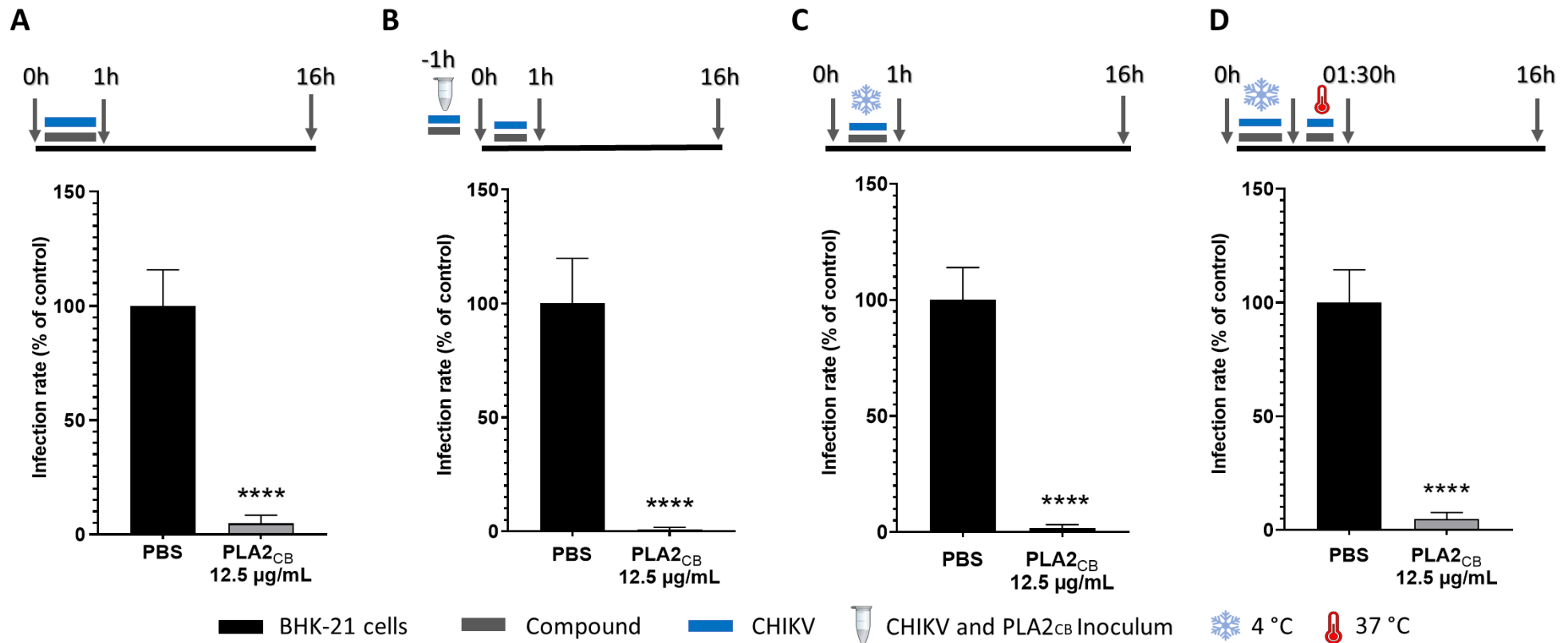
60

Figure 3. PLA2$_{CB}$ activity on CHIKV entry to the host cells. (A) BHK-21 cells were infected with CHIKV-*nanoluc* (MOI 0.1) and simultaneously treated with PLA2$_{CB}$ at 12.5 µg/mL for 1 h. Cells were extensively washed and replaced by fresh medium. (B) CHIKV-*nanoluc* and PLA2$_{CB}$ at 12.5 µg/mL were incubated for 1 h at 37°C and then for one extra hour with the cells. Then, virus and compound were removed, cells were extensively washed with PBS, and added fresh medium. (C) BHK-21 cells were infected with the virus and simultaneously treated with PLA2$_{CB}$ at 12.5 µg/mL for 1 h at 4°C. The cells were washed to remove virus and compound and replaced with fresh medium. (D) BHK-21 cells were infected with virus and simultaneously treated with PLA2$_{CB}$ at 12.5 µg/mL for 1 h at 4°C. Then, cells were incubated for a further 30 min with compound and virus at 37°C, washed with PBS to remove virus and compound, and replaced by fresh medium. For all assays, CHIKV replication was measured by *nanoluc* activity at 16 h.p.i.. Schematic representation of each time-based assay as indicated by BHK-21 cells (black bars), PLA2$_{CB}$ (grey bars), and CHIKV-*nanoluc* (blue bars), CHIKV and PLA2$_{CB}$ inoculum (microtube), incubation at 4 °C (ice crystal) and incubation at 37 °C (thermometer). Mean values of a minimum of three independent experiments each measured in triplicate, $p < 0.01$ was considered significant.
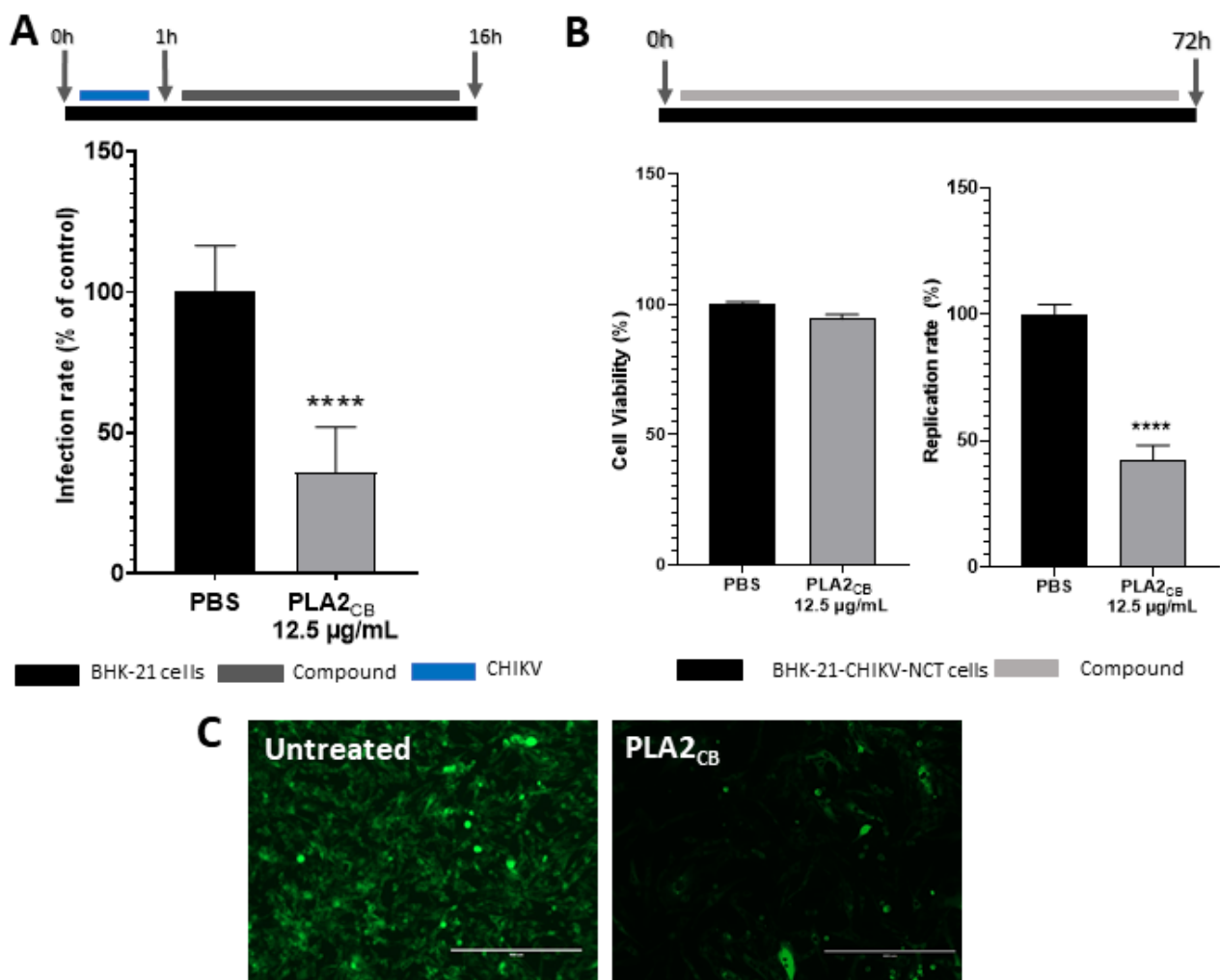
Figure 4. Post-entry activity of PLA2CB against CHIKV replication: (A) BHK-21 cells were first infected with CHIKV-*nanoluc* (MOI 0.1) for 1h, washed to remove unbound virus and added of medium containing PLA2$_{CB}$ at 12.5 μg/mL for 16h. Luminescence levels were assessed to analyze the CHIKV replication rates. (B) BHK-CHIKV-NCT cells that express CHIKV nonstructural proteins, a selection marker (puromycin acetyltransferase, Pac), and two reporter genes (*Renilla* luciferase, *Rluc,* and EGFP) were seed 24h prior treatment. Then, cells were treated with PLA2$_{CB}$ at 12,5 μg/mL for 72h. Luminescence levels were accessed to analyze the CHIKV replication rates and cellular viability measured using an MTT assay. (C) Fluorescence of untreated control and PLA2$_{CB}$ treatment in BHK-CHIKV-NCT, observed in fluorescence microscopy at 20x lens (scale 400μm), in GFP filter. Schematic representation of each assay as indicated by BHK-21 cells or BHK-CHIKV-NCT (black bars), PLA2$_{CB}$ (grey bars), and CHIKV-*nanoluc* (blue bars). Mean values of a minimum of three independent experiments each measured in triplicate, $p < 0.01$ was considered significant.
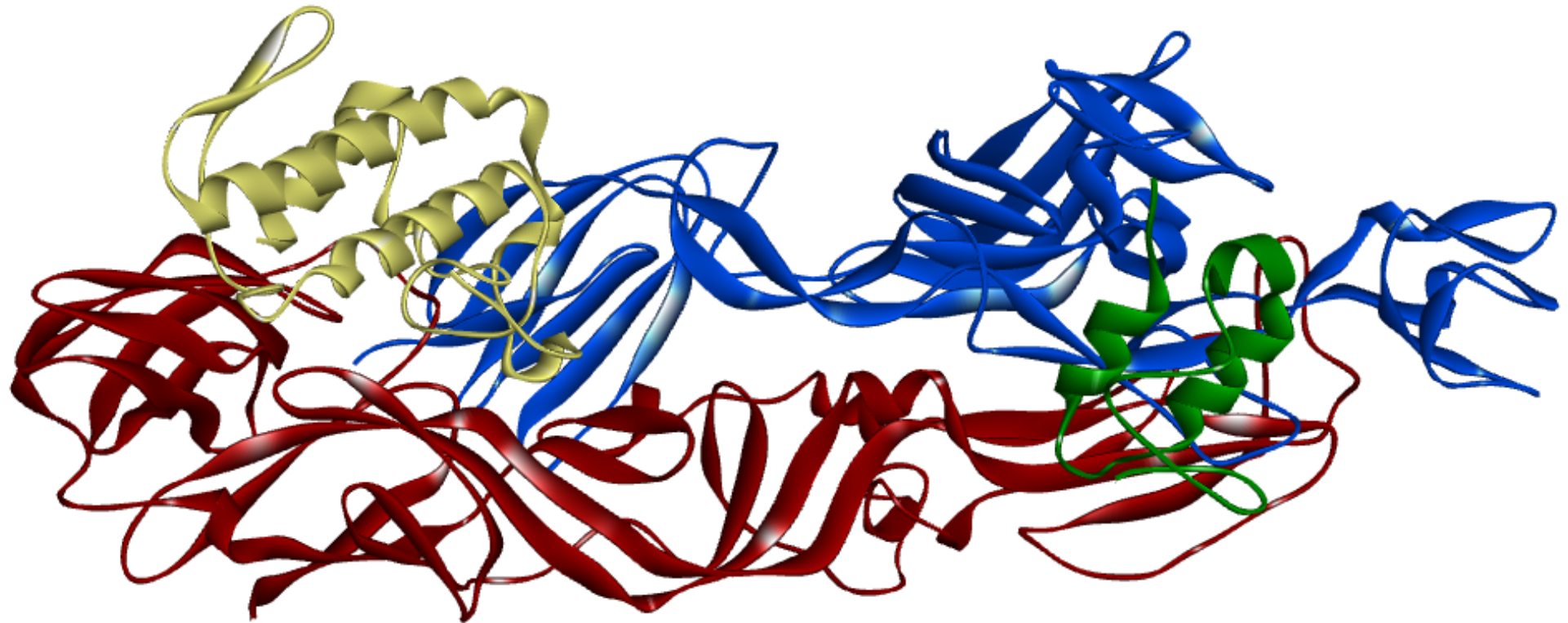
Figure 5. The CHIKV envelope glycoproteins composed by E1 (Red), E2 (Blue), E3 (green), complexed with PLA2$_{CB}$ (Yellow).

Figure 6. 2D diagram of the interactions of the envelope glycoprotein E1 protein with PLA2$_{CB}$. The hydrogen bonds (green dashes) are shown between PLA2$_{CB}$ (purple lines) and E1 glycoprotein (orange lines). Hydrophobic interactions are also shown between PLA2$_{CB}$ (purple bows) and E1 glycoprotein (red bows).
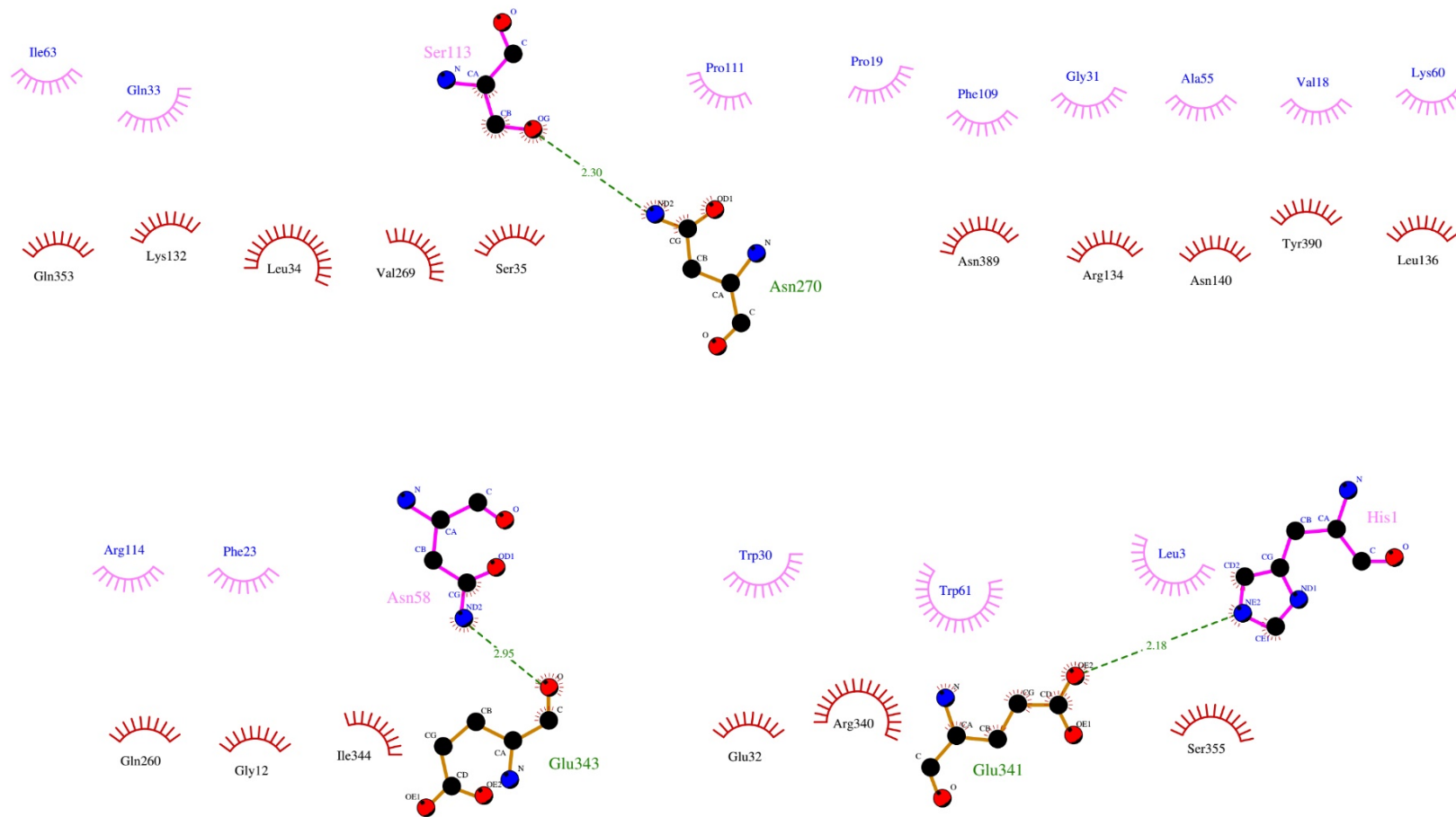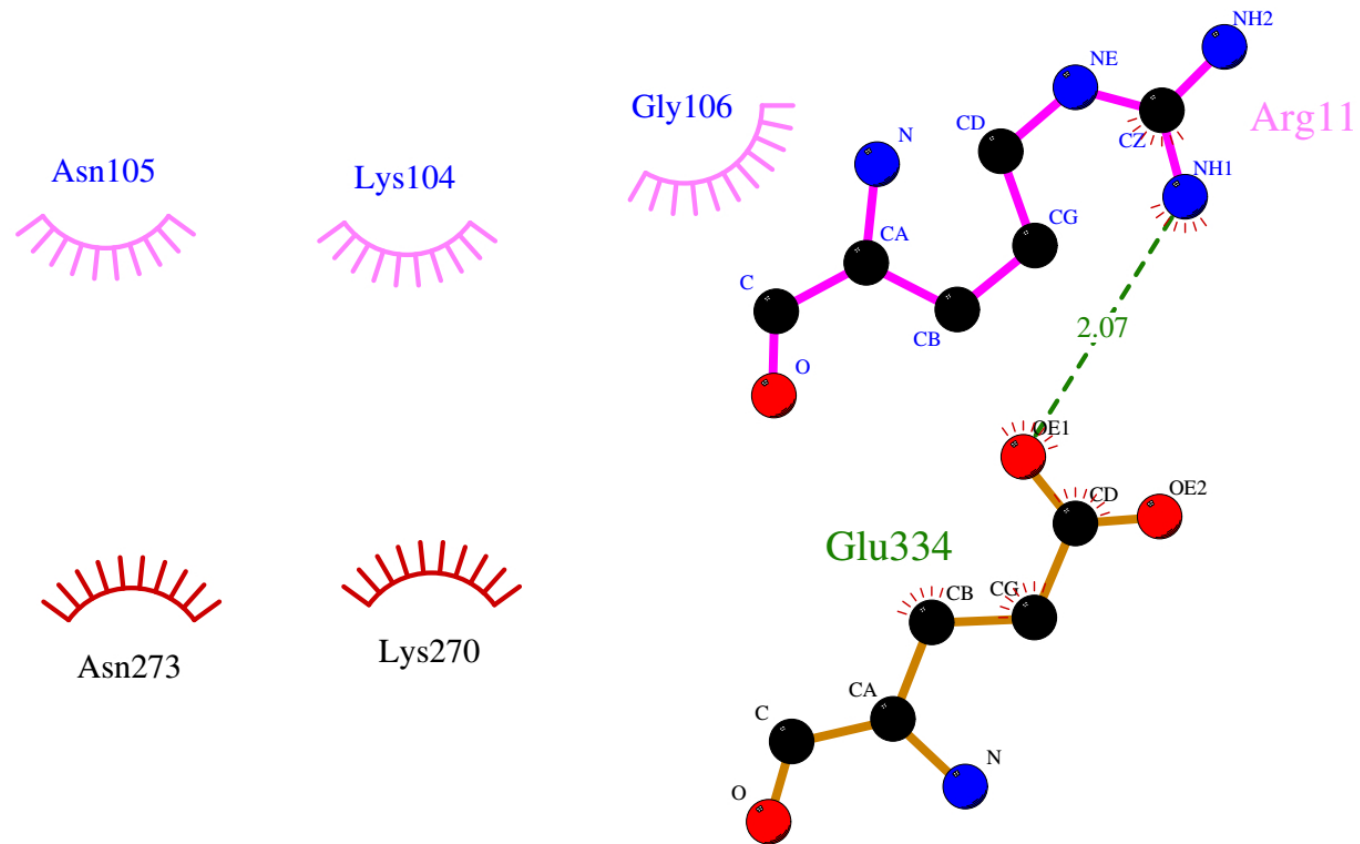
Figure 7. 2D diagram of the interactions of the envelope glycoprotein E2 protein with PLA2$_{CB}$. The hydrogen bonds (green dashes) are shown between PLA2$_{CB}$ (purple lines) and E1 glycoprotein (orange lines). Hydrophobic interactions are also shown between PLA2$_{CB}$ (purple bows) and E1 glycoprotein (red bows).
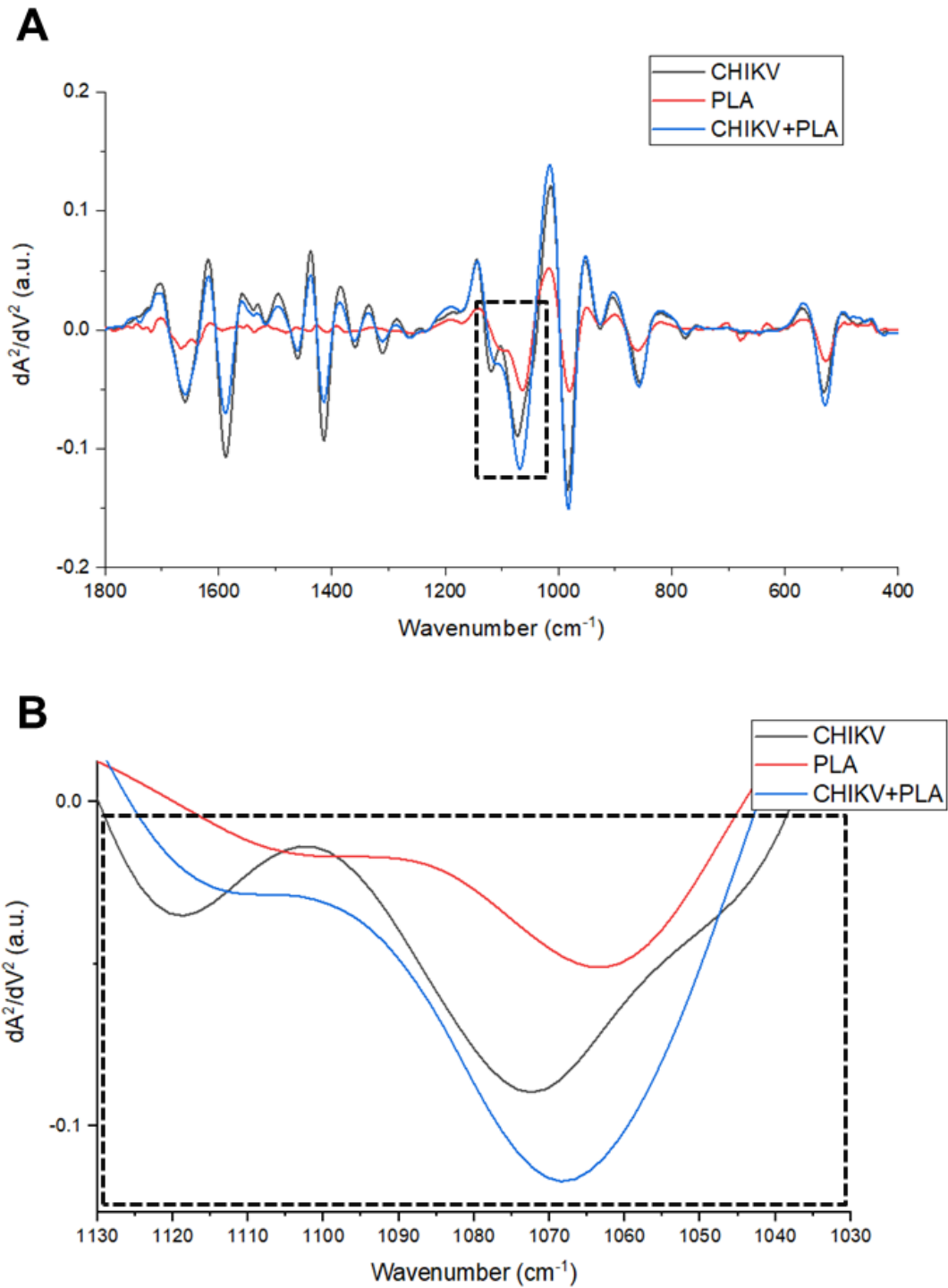
Figure 8. (A) Representative infrared average spectrum of second derivative analysis from PLA2$_{CB}$ (red line), CHIKV (black line), and PLA2$_{CB}$ plus CHIKV (blue line). (B) Second derivative analysis, which the value heights indicate the intensity of each functional group
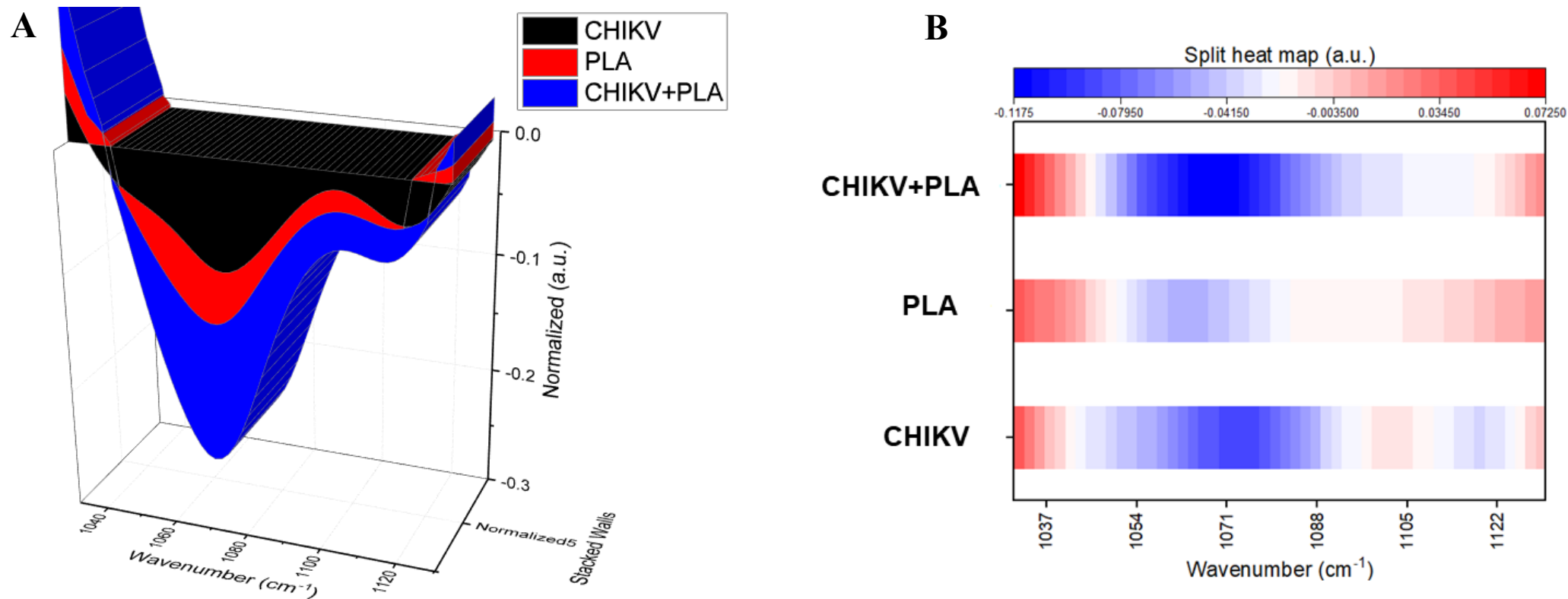
Figure 9. A representative Stacked Walls (A) and split heat map (B) of the infrared average spectrum of second derivative analysis from PLA2$_{CB}$ (red), CHIKV (black), and PLA2$_{CB}$ plus CHIKV (blue).

CAPÍTULO III

Considerações finais

Considerações finais

Os resultados deste estudo demonstram que a fosfolipase A2 isolada do veneno de *Crotalus durissus terrificus* (PLA2$_{CB}$) possui atividade anti-CHIKV e pode servir de base para próximos estudos na busca de novos antivirais. Mais estudos são necessários para avaliar a ação antiviral desse composto em testes *in vivo* e o estudo das vias de entrega desse composto.

Este trabalho fornecerá informação potencial para o desenvolvimento de novas terapias antivirais.

ANEXOS

Artigos submetidos e/ou publicados

ANEXO I: Organometallic complex strongly impairs CHIKV entry to the host cells

Débora Moraes de Oliveira[a], Igor de Andrade Santos[a], Daniel Oliveira Silva Martins[a,b], Yasmin Garcia Gonçalves[c], Léia Cardoso Sousa[d], Robinson Sabino da Silva[d], Carolina Colombelli Pacca[e], Nilson Nicolau Junior[h], Gustavo Von Poelhsitz[c], Andres Merits[f], Mark Harris[g], Ana Carolina Gomes Jardim[a,b].

[a]Laboratory of Virology, Institute of Biomedical Science, Federal University of Uberlândia, MG, Brazil
[b]São Paulo State University, IBILCE, São José do Rio Preto, SP, Brazil
[c]Institute of Chemistry, Federal University of Uberlândia, MG, Brazil
[d]Department of Physiology, Institute of Biomedical Sciences, Federal University of Uberlândia, Minas Gerais, Brazil
[e]Faculty of medicine, FACERES, São José do Rio Preto, SP, Brazil
[f]Institute of Technology, University of Tartu, Tartu, Estonia
[g]School of Molecular and Cellular Biology, Faculty of Biological Sciences and Centre for Structural Molecular Biology, University of Leeds, Leeds, United Kingdon
[h]Laboratory of Molecular Modeling, Institute of Biotechnology, Federal University of Uberlândia, MG, Brazil

Corresponding author: Professor Ana Carolina Gomes Jardim, Institute of Biomedical Science, ICBIM/UFU, Avenida Amazonas, 4C- Room 216, Umuarama, Uberlândia, Minas Gerais, Brazil, CEP: 38405-302
Tel: +55 (34) 3225−8682
E-mail: jardim@ufu.br

*Este capítulo está em formato de manuscrito com algumas alterações estruturais paramelhor se adequar ao formato da dissertação. O artigo em questão será submetido à revista **Antiviral Research.**

Abstract

Chikungunya fever is a disease caused by the Chikungunya virus (CHIKV) that is transmitted by the bite of the female of *Aedes* sp mosquito. The symptoms include fever, muscle aches, skin rash e and severe joint pains. The disease may develop into a chronic condition and joint pain that may last for months or years. Currently, there is no effective antiviral treatment against CHIKV infection, being necessary the development of novel therapies. Treatments based on natural compounds have been widely studied, as many drugs were produced by using natural molecules and their derivatives. *Para*-cymene (pCYM) is a naturally occurring aromatic organic compound that is a common ligand for ruthenium, forming the organometallic ruthenium and pCYM complex. Organometallic complexes have shown promising as a new generation of compounds that presented relevant biological properties, however, there is a lack of knowledge concerning the anti-CHIKV activity of these complexes. In this context, the present work evaluated the effects of the ruthenium and pCYM complex ($[Ru_2Cl_4(\eta^6\text{-p-cymene})_2]$) (RcP) and its precursors on CHIKV infection *in vitro*. To this, BHK21 cells were infected with CHIKV-*nanoluciferase* (CHIKV-*nanoluc*), a viral construct with the reporter gene -*nanoluc*, at the presence or absence of the compounds for 16 hours. Cytotoxicity and infectivity assays were performed. The results demonstrated that RcP exhibited a strong therapeutic index judged by the selective index of 43.1 (ratio of cytotoxicity to antiviral potency). Antiviral effects of RcP on different stages of the CHIKV replicative cycle were investigated and the results showed that it reduced 77% of virus entry to the host cells at non-toxic concentrations. Further assays demonstrated the virucidal activity of the compound that completely knocked down virus infectivity. Molecular docking calculations were performed in order to investigate possible interactions between pCYM and CHIKV glycoproteins and results suggested bindings between pCYM and a sitelocated behind the fusion loop between glycoproteins E3 and E2. Additionally, infrared spectroscopy spectral analysis indicated interactions of RcP with CHIKV glycoproteins. This data suggests that RcP may acts on CHIKV viral particles, disrupting virus entry to the host cells. Additional analyses are being performed to evaluate the mode of action of this complex.

1. Introduction

The Chikungunya virus (CHIKV) belongs to the genus *Alphavirus* of the family *Togaviridae* (ICTV, 2019). This virus is the causative agent of Chikungunya fever being related to epidemics mainly in tropical and subtropical regions (KHAN et al., 2002; PAIXÃO et al., 2018; STEGMANN-PLANCHARD et al., 2019).

CHIKV is a positive single strand RNA virus with a genome of approximately 12 kb (SCHUFFENECKER et al., 2006). The icosahedral capsid is covered by a lipid envelope derived from the host cell plasma membrane where the viral glycoproteins E1 and E2 are inserted into(KHAN et al., 2002; SCHUFFENECKER et al., 2006; THIBERVILLE et al., 2013).

CHIKV is transmitted through the bite of the female mosquito of *Aedes* sp (VU; JUNGKIND; LABEAUD, 2017). It was first isolated during an epidemic in Tanzania in 1953 (ROBINSON, 1955; WINTACHAI et al., 2012). In 2006, CHIKV outbreaks were reported on several Indian Ocean islands and about 250 people died from the disease on the French island of *La Réunion* (SCHUFFENECKER et al., 2006)*.* In 2013, the virus was detected in the Americas with reported cases in the Caribbean islands (KAUR; CHU, 2013). The first case in Brazil was reported in 2014 (CARVALHO; LOURENÇO-DE-OLIVEIRA; BRAGA, 2014).

Chikungunya fever presents symptoms as fever, prostration, muscle aches, lymphopenia and arthralgia, being the latest the main symptom related to this disease (CUNHA et al., 2017; PAIXÃO et al., 2018). Pain associated to arthralgia in the phalanges, wrists and ankles occurs in up to 98% of cases (THIBERVILLE et al., 2013).The infection can progress to a chronic infection in around 70 % of infected patients (DE ANDRADE et al., 2010; SIMON et al., 2011), causing muscle pain and persistent arthralgia for periods ranging from months to years (MATHEW et al., 2017).

Currently, there is no vaccine or specific therapy against CHIKV infection (DEY et al., 2019; YANG et al., 2017). The treatment of symptomatic infections is palliative, based on the use of non-salicylate analgesics and non-steroidal anti-inflammatory drugs (MATHEW et al., 2017; PARASHAR; CHERIAN, 2014). Several of the currently used drugs for different pathologies are either from natural origin synthesized based on natural scaffolds (DA SILVA-JÚNIOR et al., 2017; TEIXEIRA et al., 2014).

Para-cymene (pCYM) is a naturally occurring organic aromatic hydrocarbon from the monoterpene class that has shown to possess important biological activities as antioxidant (DE OLIVEIRA et al., 2015), anti-inflammatory (KUMMER et al., 2015), antifungal (KORDALI et al., 2008) and antiviral (ASTANI; REICHLING; SCHNITZLER, 2009). Ruthenium is a metal belonging to the iron group and studies have shown that the ruthenium complexed molecules possess effective biological properties as antimicrobial (PAVAN et al., 2010). pCYM is a common binder for ruthenium (BENNETT et al., 2007) and the antitumoral activity of this complex has also been described (CLARKE; ZHU; FRASCA, 1999; DOUGAN; SADLER, 2007; DYSON, 2007; HABTEMARIAM et al., 2006; SAVIĆ et al., 2020; VAJS et al., 2015).

Here we evaluated the activity of ruthenium and pCYM complex (RcP) and its precursors on the CHIKV replicative cycle. These data are the first description of the ruthenium and pCYM complex possessing anti-CHIKV activity.

2. Material and methods

2.1. Compounds

The ruthenium and *para*-cymene complex ($[Ru_2Cl_4(\eta^6$-p-cymene$)_2]$) (RcP) **(Figure 1A)** evaluated in this work was synthesized as previously described (JENSEN; RODGER; SPICER, 1998). The precursors ruthenium trichloride ($RuCl_3.3H_2O$) and *para*-cymene (α-phellandrene), used in the synthesis of complex were purchased by Sigma Aldrich. The complex was dissolved in dimethyl sulfoxide (DMSO) and stored at - 20°C. Dilutions of the compounds in complete media were made immediately prior to the experiments. For all the assays performed, control cells were treated with media added of DMSO at the final concentration of 0.3%.

2.2. Cell culture

BHK 21 cells (fibroblasts derived from Syrian golden hamster kidney) were a gift from Andres Merits (University of Tartu, Estonia). The cells were maintained in Dulbecco's modified Eagle's media (DMEM; Sigma-Aldrich) supplemented with 100U/mL of penicillin (Hyclone Laboratories, USA), 100 mg/mL of streptomycin (Hyclone Laboratories, USA), 1% of non-essential aminoacids (Hyclone 28 Laboratories, USA) and 1% of fetal bovine serum (FBS, HycloneLaboratoires, USA) in a humidified 5% CO_2 incubator at 37°C.

2.3.Virus

The CHIKV-*nanoluciferase* (CHIKV-*nanoluc*) construct **(Figure 1A)** used for the antiviral assays was designed from a CHIKV sequence based on CHIKV LR (*Lá reunion*) added of CMV promoter and *nanoluciferase* protein sequence (MATKOVIC et al., 2018; POHJALA et al., 2011). For virus production, 2.3×10^7 BHK 21 cells seeded in a T175 cm^2 were transfected with 1.5 μg of CHIKV-CMV-*nanoluc* plasmid, using lipofectamine 3000® and Opti-Mem media to produce CHIKV-*nanoluc* virus particles. Forty-eight hours post transfection the supernatant was collected and stored at -80°C. To determine viral titer, 5×10^5 BHK 21 cells were seeded in each of 6 wells plate 24 hours prior to the infection. Then, the cells were infected with 10-fold serially diluted of CHIKV-*nanoluc* for 1hour at 37°C. The inoculums were removed and the cells were washed with PBS to remove the unbound virus and added of cell culture media supplemented with 1% penicillin, 1% streptomycin, 2% FBS and 1% carboxymethyl cellulose (CMC). Infected cells were incubated for 2 days in a humidified 5% CO_2 incubator at 37°C, followed by fixation with 4% formaldehyde and stained with 0.5% violet crystal. The viral foci were counted to determine CHIKV-*nanoluc* titer.

2.4. Cell viability through MTT assay

Cell viability was measured by MTT [3-(4,5-dimethylthiazol-2-yl)-2,5-diphenyl tetrazolium bromide] (Sigma-Aldrich) assay. For viability assay, 5×10^4 BHK 21 cells were cultured in 48 well plates and treated with different concentrations of each compound for 16h at 37°C with 5% of CO_2. Sixteen hours post treatment, compound-containing media was removed and MTT solution at 1 mg/mL was added to each well, incubated for 1 hour and replaced with 100 μL of DMSO (dimethyl sulfoxide) to solubilize the formazan crystals. The absorbance was measured at 560 nm on Glomax microplate reader (Promega). Cell viability was calculated according to the equation (T/C) × 100%, which T and C represented the optical density of the treated well and control groups, respectively. DMSO was used as untreated control. The cytotoxic concentration of 50% (CC50) was calculated using using Graph Pad Prism 5.0 Software.

2.5. Antiviral assays

To access the antiviral activity of compounds, BHK 21 cells were seeded at density of 5×10^4 cells per well into 48 well plates 24 hours prior to the infection. CHIKV-*nanoluc* (MATKOVIC

et al., 2018) at a multiplicity of infection (MOI) of 0.1 and compounds were simultaneously added to cells. Samples were harvested in Renilla luciferase lysis buffer (Promega) at 16 hours post-infection (h.p.i.) and virus replication levels were quantified by measuring *nanoluciferase* activity using the Renilla luciferase Assay System (Promega). The effective concentration of 50% inhibition (EC50) was calculated using Graph Pad Prism 5.0 Software. The values of CC50 and EC50 were used to calculate the selectivity index (SI = CC50/EC50).

To investigate in which step of CHIKV replicative cycle the compound was active, BHK 21 cells at the density of 5×10^4 were seeded in 48 well plate 24 hours prior to infection and treatment. To evaluate if the compound possesses protective activity to the host cells, cells were treated for 1 hour with the compound before infection, extensively washed to remove compound and added CHIKV-*nanoluc*. The effect on the entry steps was analyzed by incubating virus and compound simultaneously with BHK 21 cells for 1 hour. To investigate the activity of the compound on postentry stages of viral replicative cycle, cells were infected with CHIKV for 1 hour, washed extensively with PBS (phosphate buffered saline) to remove unbound virus and added with compound containing media.

To further investigate entry stage, the virucidal activity was investigated by previously incubating virus and compound for 1 hour and then adding to the cells for extra 1 hour. Then, compound was removed and as cells added of media. To evaluate the attachment step, the cells were treated with virus and compound at for 1 hour at 4°C, and then the cells were washed to the complex removal and replaced by media. For the uncoating step, cell, virus and compound were also incubated for 1 hour at 4°C followed by 30 minutes at 37°Cand then washed and replaced by media. All experiments were conducted with virus at MOI of 0.1. Luminescence levels were accessed 16h.p.i. to analyze the virus replication rates.

2.6. Docking Protein Binder

The interaction of the *para*-cymene ligand with the envelope glycoprotein of the CHIKV (PDB: 3N42) was evaluated using the GOLD program, using the parameters predefined by the program except the flexibility of the ligand, which was defined as 200%. The seven glycoprotein binding sites defined by (RASHAD; KELLER, 2013) were defined for this purpose. Each docking was performed 10 times and the best docking positions were assessed using a ranking of the ChemPLP scoring function. The post-docking images were generated in the DS Visualizer program, Dassault Systèmes BIOVIA, Discovery Studio Visualizer, version

17, San Diego: Dassault Systèmes, 2016. The interaction between the ruthenium ligand and the complex was not evaluated due to the program not having parameters for loading metals.

2.7. Infrared spectroscopy Spectral data analysis

An ATR-FTIR spectrophotometer Vertex 70 (Bruker Optics, Reinstetten, Germany) connected to a micro-attenuated total reflectance (ATR) platform was used to record sample signature at 1800 cm^{-1} to 400 cm^{-1} regions. The ATR unit is composed by a diamond disc as internal-reflection element. The sample dehydrated pellicle penetration depth ranges between 0.1 and 2 μm and depends on the wavelength, incidence angle of the beam and the refractive index of ATR-crystal material. The infrared beam is reflected at the interface toward the sample in the ATR-crystal. All samples (1μL) were dried using airflow on ATR-crystal for 3 min before sample spectra recorded in triplicate. The air spectrum was used as a background in all ATR-FTIR analysis. Sample spectra and background was taken with 4 cm^{-1} of resolution and 32 scans were performed for sample analysis. The spectra were normalized by the vector method and adjusted to rubber band baseline correction. The original data were plotted in the Origin Pro 9.0 (OriginLab, Northampton, MA, USA) software to create the second derivative analysis. The second derivative was obtained by applying Savitzky-Golay algorithm with polynomial order 5 and 20 points of the window. The value heights indicated the intensity of functional group evaluated.

2.8. Statistical analysis

Individual experiments were performed in triplicate and all assays were performed a minimum of three times in order to confirm the reproducibility of the results. Differences between means of readings were compared using analysis of variance (one way or two-way ANOVA) or Student's t-test using Graph Pad Prism 5.0 software (Graph Pad Software). P values than < 0.01 were considered to be statistically significant.

3. Results

3.1. Ruthenium (Ru) and *para*-cymene (pCYM) complex (RcP) inhibits CHIKV *in vitro*

Since pCYM previously demonstrated antiviral activity (ASTANI; REICHLING; SCHNITZLER, 2009) and Ru complexed molecules showed to possess antimicrobial properties

(PAVAN et al., 2010), we aimed to investigated the anti-CHIKV activity of the RcP complex **(Figure 1A)** by using a recombinant CHIKV that expresses the *nanoluciferase* reporter (CHIKV-*nanoluc*) **(Figure 1B)**.

To assess the effect of RcP on cell viability and virus infection, we therefore performed a dose response assay to determine effective concentration 50% (EC50) and cytotoxicity 50% (CC50) values for RcP. BHK 21 cells were infected with CHIKV-*nanoluc* and treated with RcP at concentrations ranging from 500 to 3.9 µM and viral replication efficiency was evaluated at 16 h.p.i. **(Figure 1C)**. In parallel cell viability was measured by MTT assay. The results showed that the RcP was able to completely knocked down the virus infectivity while the minimum cell viability was 93% **(Figure 1D)**. By the use of this range of concentrations, it was determined that the RcP complex has an EC50 of 31,99 µM, CC50 of 1379 µM and Selective Index (SI) of 43.1 **(Figure 1D)**.

Since the complex showed to be strongly active against CHIKV at a concentration of 125 µM with no cytotoxicity, we also evaluated its precursors for cell viability and viral replication. For this, MTT and luminescence tests were performed. Cells were infected with CHIKV-*nanoluc* and treated with the RcP or its precursors at 125 µM. The efficiency of viral replication and cell viability were evaluated at 16 h.p.i. **(Figure 1C)**. The results showed that RcP complex significantly inhibited 91% of CHIKV infectivity and presented no toxicity to cells (p <0.01) **(Figure 1E)**. Alternatively, pCYM and Ru at the same concentration decreased cell viability and/or reduced antiviral activity compared to the complex (p <0.01) **(Figure 1E)**. This data demonstrated that RcP exhibited the best therapeutic index (favorable ratio of cytotoxicity to antiviral potency) and further analysis were performed only to this compound.

3.2. RcP inhibits CHIKV entry to the host cells

The antiviral activity of the RcP at different stages of CHIKV replication was analyzed. First, cells were pretreated with RcP for 1hour at 37 °C, washed with PBS to completely remove the compound and then were infected with CHIKV-*nanoluc*. Luminescence levels were measured 16 h.p.i. **(Figure 2A)**. The RcP demonstrated a modest yet significant reduction of 23 % of luminescence levels when cells were pretreated (p <0.01) **(Figure 2A)**

To evaluate virus entry to the host cells, virus and RcP were simultaneously added to BHK 21 cells for 1 hour, then washed with PBS and replaced with media. Luminescence levels were

measured 16 h.p.i. **(Figure 2B)**. The results showed that RcP at 125 µM significantly reduced 77% of the virus entry to the host cells (p <0.01) **(Figure 2B)**.

For the post-entry steps, the cells were first infected with CHIKV-*nanoluc* for 1 hour at 37 ° C, washed to remove unbound virus and then added with compound containing media. Luminescence levels were measured 16 h.p.i. **(Figure 2C)**. RcP also demonstrated a modest yet significant reduction of 21% of luminescence levels when the treatment was performed after virus entry to the cells (p <0.01) **(Figure 2C)**. Altogether, these data suggest that the main antiviral activity of RcP is related to its ability to inhibit the entry stage of the virus lifecycle.

Based on the results obtained, we further evaluated the activity of RcP on CHIKV entry to the cells. First, supernatant containing CHIKV-*nanoluc* was incubated with RcP125µM for 1 hour at 37 °C prior to the infection of cells to investigate virucidal effect. The inoculum of virus and RcP was transferred to the naïve cells and incubated for 1 hour. Cells were washed for the complete removal of the inoculum and replaced with fresh media for 16 h.p.i. **(Figure 3A)**. The results showed a strong significant virucidal activity of RcP by blocking100% of virus entry (p <0.01) **(Figure 3A)**.

We also analyzed RcP effect on the virus attachment. For this, virus and RcP were incubated with the cells at 4°C for 1 hour, when virus is able to attach to cell membrane receptor, but not to entry to the host cells. Then, cells were washed with PBS and a fresh media was added. Luminescence levels were measured 16 h.p.i. **(Figure 3B)**. Data obtained from this assay showed that RcP reduced 90% of virus entry to the host cells (p <0.01) **(Figure 3B)**.

Next, antiviral activity of RcP on virus uncoating was investigated by incubating virus and compound for 1 hour at 4°C and then at 37°C for 30 minutes. Therefore, the period of treatment may include virus attachment, entry and uncoating. Cells were washed with PBS and a fresh media was added. Luminescence levels were measured 16 h.p.i. **(Figure 3C)**. The results demonstrated that under this protocol of treatment, the complex inhibited up to55% of the virus entry to the host cells (p <0.01) **(Figure 3C)**. These data demonstrated that RcP was able to abrogate different stages of virus entry to the host cells **(Figure 3)**. However, the strongest effect was observed in virucidal and attachment protocol. This might suggest that an anti-CHIKV mechanism of action for this complex might be related to a direct action on the virus chemical structure.

3.3. Possible interactions between pCYM and CHIKV E2 glycoprotein

Based on the results that showed RcP interfering on CHIKV entry to the host cells, molecular docking calculations were performed in order to investigate possible binding mode and the interactions between pCYM and CHIKV glycoproteins. Docking analysis are not feasible with metallocenes as RcP because their chemical structure presents an unforeseen conformation named "half sandwich piano stool". Therefore, the pCYM ligand was used for *in silico* analysis, Seven possible glycoprotein complex binding sites were explored and the scores generated by the ChemPLP scoring function of the Gold program are presented in **Table 1.** The *p*-cymene showed the best result with site 4, score 39.71 **(Table 1)**. The best docking scores were obtained between the site 4, located behind the fusion loop between glycoproteins E3 and E2 **(Figure 4)**.

3.4. RcP causes molecular changes in CHIKV

To further investigate the interaction between RcP and CHIKV particles, infrared spectroscopy spectral analysis was performed. The vibrational analysis between virus and RcP are shown in **Table 2**. A representative infrared average spectrum of RcP, CHIKV or RcP plus CHIKV, which contains different biochemical functional groups such as lipids, proteins, glycoproteins and nucleic acid, are represented in **Figure 5**. We were particularly interested in the interaction of RcP with CHIKV. A representative infrared average spectrum of second derivative analysis from RcP, CHIKV or RcP plus CHIKV was displayed in **Figure 6A**. In the second derivative analysis, which the value heights indicated the intensity of each functional group, a reduction in intensity of Amide II [ν (N–H), ν (C–N)] at 1540 cm^{-1} with the association of RcP with CHIKV indicates interaction with proteins of CHIKV **(Figure 6B)**. The binding interaction was also revealed by spectral shifting of the 1013 cm^{-1} to 1005 cm^{-1}, which indicates interaction with vs (CO-O-C) presents in Glycoprotein derived from RcP and/or CHIKV **(Figure 6C)**. The binding interaction was also revealed by increase in intensity of 724 cm^{-1}, 679 cm^{-1}, 645 cm^{-1} and 609 cm^{-1} in RcP plus CHIKV, which indicate formation of C-H rocking of CH2 and S-O bending. The binding interaction was additionally confirmed by the decrease in intensity of 704 cm^{-1}, 652 cm^{-1} and 632 cm^{-1} in RcP plus CHIKV, which indicate reduction in the presence of OH out-of-plane bend **(Figure 6D)**.

4. Discussion

Chikungunya virus (CHIKV) has obtained attention from the public health worldwide due to the recent outbreaks (GOULD et al., 2017), but also because the infection may persist for

months or even years (CUNHA; TRINTA, 2017). CHIKV was first described in the 1950s (ROBINSON, 1955), however, there is still no specific treatment or vaccine against this virus (MATHEW et al., 2017; STEGMANN-PLANCHARD et al., 2019). Thus, the search for new molecules with anti-CHIKV activity is necessary.

In this study, the anti-CHIKV activity of the ruthenium (Ru) and *para*-cymene (pCYM) complex (RcP) was investigated. The pCYM molecule has already been described to demonstrate biological activities as antioxidant, anti-inflammatory and antifungal(DE OLIVEIRA et al., 2015; KORDALI et al., 2008; KUMMER et al., 2015). It was also demonstrated that pCYM in lower concentrations showed moderate antiviral activity against the Herpes simplex virus (HSV), partially inhibiting the viral infection in RC-37 cells(ASTANI; REICHLING; SCHNITZLER, 2009; GAROZZO et al., 2009). However, there is a lack of studies on the effects of pCYM against CHIKV.

Our results showed that RcP significant reduced virus entry to the host cells at non-toxic concentrations. As the complex demonstrated to interfere on virus entry, were evaluated the early stages of CHIKV infection.RcP demonstrated a moderate activity on the virus uncoating and strong action on inhibiting virus attachment or as a virucide. A recent study demonstrated that pCYM presented virucidal activity against HSV. The results showed that when p-cymene and HSV were incubated together, virus entry was reduced by 80% (SHARIFI-RAD et al., 2017).

The strong virucidal effect observed for RcP might suggest that an anti-CHIKV mechanism of action for this complex might be related to a direct action on the viral particle envelope(RUSSO et al., 2019; SCHUHMACHER; REICHLING; SCHNITZLER, 2003; TANG et al., 1990), which could also be responsible for the effect observed on virus attachment (CARRAVILLA et al., 2017; KONG et al., 2019).Possible interactions between Chikungunya envelope proteins and RcP could be a reasonable explanation for the observed virucidal effect. Based on this data, molecular docking calculations were performed in order to investigate possible binding mode and the interactions between pCYM and CHIKV glycoproteins. Our results suggested that pCYM may bind to a site located behind the fusion loop between glycoproteins E3 and E2. Glycoprotein E2 is responsible for binding the virus to cell receptors (FONGSARAN et al., 2014; MOLLER-TANK et al., 2013; SILVA et al., 2014). When small molecules attach to that site, the movement of the glycoprotein domains can be frozen and then prevent the virus from entering the cell (RASHAD; KELLER, 2013). We suggest that pCYM may be binding to such

a site and preventing the virus from binding to the cell. Similarly, we can suggest that, through molecular interactions observed by the FTIR methodology, the RcP compound alters CHIKV glycoprotein and lipid sites, reaffirming that there is an interaction between the viral envelope and the complex.

In summary, we showed that ruthenium and para-cymene complexis able to strongly inhibit CHIKV infectivity, acting mainly on the entry of virus to the host cells. This is the first description of the antiviral activity of an organometallic complex against CHIKV. This dada may be useful for the development of future antivirals against CHIKV that will provide a relevant advance to the public heath to treat Chikungunya fever.

5. References

ABDELNABI, R.; NEYTS, J.; DELANG, L. Towards antivirals against chikungunya virus. **Antiviral Research**, v. 121, p. 59–68, 2015.

ALESSANDRA LO PRESTI1 et al. Chikungunya virus, epidemiology, clinics and phylogenesis: A review. **Asian Pacific Journal of Tropical Medicine**, v. 7, n. 12, p. 925–932, 1 dez. 2014.

ALMEIDA, J. R. et al. CoaTx-II, a new dimeric Lys49 phospholipase A2 from Crotalus oreganus abyssus snake venom with bactericidal potential: Insights into its structure and biological roles. **Toxicon**, v. 120, p. 147–158, 15 set. 2016.

ASTANI, A.; REICHLING, J.; SCHNITZLER, P. Comparative study on the antiviral activity of selected monoterpenes derived from essential oils. **Phytotherapy Research**, v. 23, n. 9, p. n/a-n/a, 2009.

BAILEY, P.; WILCE, J. Venom as a source of useful biologically active molecules. **Emergency Medicine Australasia**, v. 13, n. 1, p. 28–36, 1 mar. 2001.

BENNETT, M. A. et al. 16. (η ^{6} -Hexamethylbenzene)Ruthenium Complexes. In: [s.l: s.n.]. p. 74–78.

BORGHERINI, G. et al. Outbreak of Chikungunya on Reunion Island: Early Clinical and Laboratory Features in 157 Adult Patients. **Clinical Infectious Diseases**, v. 44, n. 11, p. 1401–1407, 1 jun. 2007.

BRASIL. MINISTÉRIO DA SAÚDE. SECRETARIA DE VIGILÂNCIA EM SAÚDE. Febre de Chikungunya manejo clínico Febre de chikungunya: manejo clínico. 2015.

BURKE, J. E.; DENNIS, E. A. Phospholipase A2 biochemistry. **Cardiovascular Drugs and Therapy**, v. 23, n. 1, p. 49–59, fev. 2009.

BURT, F. J. et al. Chikungunya virus: an update on the biology and pathogenesis of this emerging pathogen. **The Lancet Infectious Diseases**, v. 17, n. 4, p. e107–e117, 2017.

BUTLER, M. S.; ROBERTSON, A. A. B.; COOPER, M. A. Natural product and natural product derived drugs in clinical trials. **Nat. Prod. Rep.**, v. 31, n. 11, p. 1612–1661, 2014.

CALDERON, L. A. et al. Antitumoral Activity of Snake Venom Proteins: New Trends in Cancer Therapy. **BioMed Research International**, v. 2014, p. e203639, 2014.

CARRAVILLA, P. et al. Effects of HIV-1 gp41-Derived Virucidal Peptides on Virus-like Lipid Membranes. **Biophysical Journal**, v. 113, n. 6, p. 1301–1310, 2017.

CARVALHO, R. G.; LOURENÇO-DE-OLIVEIRA, R.; BRAGA, I. A. Updating the geographical distribution and frequency of Aedes albopictus in Brazil with remarks regarding its range in the Americas. **Memorias do Instituto Oswaldo Cruz**, v. 109, n. 6, p. 787–796, 2014.

CLARKE, M. J.; ZHU, F.; FRASCA, D. R. Non-platinum chemotherapeutic metallopharmaceuticals. **Chemical Reviews**, v. 99, n. 9, p. 2511–2533, 1999.

CLEYSE, É. et al. Antiviral activity of animal venom peptides and related compounds. 2017.

COHEN, S. N. et al. Dengue and Chikungunya Virus Infection in Man in Thailand, 1962–1964. **The American Journal of Tropical Medicine and Hygiene**, v. 18, n. 6, p. 954–971, 1 nov. 1969.

CRAGG, G. M.; NEWMAN, D. J. NIH Public Access. v. 1830, n. 6, p. 3670–3695, 2014.

CUNHA, R. V. DA; TRINTA, K. S. Chikungunya virus: clinical aspects and treatment - A Review. **Memórias do Instituto Oswaldo Cruz**, v. 112, n. 8, p. 523–531, 2017.

CUNHA, M. S. et al. Autochthonous Transmission of East/Central/South African Genotype Chikungunya Virus, Brazil. **Emerging Infectious Diseases**, v. 23, n. 10, p. 2015–2017, 2017.

DA SILVA-JÚNIOR, E. F. et al. The medicinal chemistry of Chikungunya virus. **Bioorganic & Medicinal Chemistry**, v. 25, n. 16, p. 4219–4244, 2017.

DAS, T. et al. Chikungunya fever: CNS infection and pathologies of a re-emerging arbovirus. **Progress in Neurobiology**, v. 91, n. 2, p. 121–129, jun. 2010.

DE ANDRADE, D. C. et al. Chronic pain associated with the Chikungunya Fever: long lasting burden of an acute illness. **BMC Infectious Diseases**, v. 10, n. 1, p. 31, 2010.

DE CARVALHO, A. E. Z. et al. Crotalus durissus ruruima Snake Venom and a Phospholipase A2 Isolated from This Venom Elicit Macrophages to Form Lipid Droplets and Synthesize Inflammatory Lipid Mediators. **Journal of Immunology Research**, v. 2019, 4 nov. 2019.

DE OLIVEIRA, T. M. et al. Evaluation of p-cymene, a natural antioxidant. **Pharmaceutical Biology**, v. 53, n. 3, p. 423–428, 2015.

DEY, D. et al. The effect of amantadine on an ion channel protein from Chikungunya virus. **PLOS Neglected Tropical Diseases**, v. 13, n. 7, p. e0007548, 2019.

DOUGAN, S. J.; SADLER, P. J. The design of organometallic ruthenium arene anticancer agents. **Chimia**, v. 61, n. 11, p. 704–715, 2007.

DUPUIS-MAGUIRAGA, L. et al. Chikungunya Disease: Infection-Associated Markers from the Acute to the Chronic Phase of Arbovirus-Induced Arthralgia. **PLoS Neglected Tropical Diseases**, v. 6, n. 3, p. e1446, 27 mar. 2012.

DYSON, P. J. Systematic design of a targeted organometallic antitumour drug in pre-clinical development. **Chimia**, v. 61, n. 11, p. 698–703, 2007.

FABIAN VILLALTA-ROMERO. Discovery of small molecule inhibitors for the snake venom metalloprotease BaP1 using in silico and in vitro tests. **Bioorganic & Medicinal Chemistry Letters**, v. 27, n. 9, p. 2018–2022, 1 maio 2017.

FAURE, G.; XU, H.; SAUL, F. A. Crystal Structure of Crotoxin Reveals Key Residues Involved in the Stability and Toxicity of This Potent Heterodimeric β-Neurotoxin. **Journal of Molecular Biology**, v. 412, n. 2, p. 176–191, 16 set. 2011.

FILKIN, S. Y.; LIPKIN, A. V.; FEDOROV, A. N. Phospholipase Superfamily: Structure, Functions, and Biotechnological Applications. **Biochemistry. Biokhimiia**, v. 85, n. Suppl 1, p. S177–S195, jan. 2020.

FONGSARAN, C. et al. Involvement of ATP synthase β subunit in chikungunya virus entry into insect cells. **Archives of Virology**, v. 159, n. 12, p. 3353–3364, 2014.

GANESAN, A. The impact of natural products upon modern drug discovery. **Current Opinion in Chemical Biology**, v. 12, n. 3, p. 306–317, 1 jun. 2008.

GAROZZO, A. et al. In vitro antiviral activity of Melaleuca alternifolia essential oil. **Letters in Applied Microbiology**, v. 49, n. 6, p. 806–808, dez. 2009.

GAY, N. et al. Seroprevalence of asian lineage chikungunya virus infection on saint martin Island, 7 months after the 2013 emergence. **American Journal of Tropical Medicine and Hygiene**, v. 94, n. 2, p. 393–396, 2016.

Geographic Distribution | Chikungunya virus | CDC. Disponível em: <https://www.cdc.gov/chikungunya/geo/index.html>. Acesso em: 3 jun. 2020.

GOULD, E. et al. Emerging arboviruses: Why today? **One Health**, v. 4, n. April, p. 1–13, 2017.

GOULD, E. A. et al. Understanding the alphaviruses: Recent research on important emerging pathogens and progress towards their control. **Antiviral Research**, v. 87, n. 2, p. 111–124, ago. 2010.

GRATZ, N. G. Critical review of the vector status of Aedes albopictus. **Medical and veterinary entomology**, v. 18, n. 3, p. 215–27, set. 2004.

HABTEMARIAM, A. et al. Structure-activity relationships for cytotoxic ruthenium(II) arene complexes containing N,N-, N,O-, and O,O-chelating ligands. **Journal of Medicinal Chemistry**, v. 49, n. 23, p. 6858–6868, 2006.

HALSTEAD, S. B. Reappearance of chikungunya, formerly called Dengue, in the Americas. **Emerging Infectious Diseases**, v. 21, n. 4, p. 557–561, 2015.

HARVEY, A. Natural products in drug discovery. **Drug Discovery Today**, v. 13, n. 19–20, p. 894–901, out. 2008.

HOARAU, J.-J. et al. Persistent Chronic Inflammation and Infection by Chikungunya Arthritogenic Alphavirus in Spite of a Robust Host Immune Response. **The Journal of Immunology**, v. 184, n. 10, p. 5914–5927, 15 maio 2010.

JENSEN, S. B.; RODGER, S. J.; SPICER, M. D. **Facile preparation of η6-p-cymene ruthenium diphosphine complexes. Crystal structure of [(η6-p-cymene)Ru(dppf)Cl]PF6Journal of Organometallic Chemistry**, 1998.

KAUR, P.; CHU, J. J. H. Chikungunya virus: An update on antiviral development and challenges. **Drug Discovery Today**, v. 18, n. 19–20, p. 969–983, 2013.

KHAN, A. H. et al. Complete nucleotide sequence of chikungunya virus and evidence for an internal polyadenylation site. **The Journal of general virology**, v. 83, n. Pt 12, p. 3075–84, dez. 2002.

KINI, R. M.; EVANS, H. J. A model to explain the pharmacological effects of snake venom phospholipases A2. **Toxicon**, v. 27, n. 6, p. 613–635, 1 jan. 1989.

KONG, B. et al. Virucidal nano-perforator of viral membrane trapping viral RNAs in the endosome. **Nature Communications**, v. 10, n. 1, p. 1–10, 2019.

KORDALI, S. et al. Antifungal, phytotoxic and insecticidal properties of essential oil isolated from Turkish Origanum acutidens and its three components, carvacrol, thymol and p-cymene. **Bioresource Technology**, v. 99, n. 18, p. 8788–8795, 2008.

KRAEMER, M. U. et al. The global distribution of the arbovirus vectors Aedes aegypti and Ae. albopictus. **eLife**, v. 4, p. e08347, 30 jun. 2015.

KUMMER, R. et al. Effect of p-cymene on chemotaxis, phagocytosis and leukocyte behaviors. **International Journal of Applied Research in Natural Products**, v. 8, n. 2, p. 20–27, 2015.

LEE, V. J. et al. Simple Clinical and Laboratory Predictors of Chikungunya versus Dengue Infections in Adults. 2012.

LOMONTE, B.; RANGEL, J. Snake venom Lys49 myotoxins: From phospholipases A2 to non-enzymatic membrane disruptors. **Toxicon**, Advancing in Basic and Translational Venomics. v. 60, n. 4, p. 520–530, 15 set. 2012.

LOURENÇO-DE-OLIVEIRA, R.; FAILLOUX, A. B. High risk for chikungunya virus to initiate an enzootic sylvatic cycle in the tropical Americas. **PLoS Neglected Tropical Diseases**, v. 11, n. 6, p. 1–11, 2017.

LUM, F. M.; NG, L. F. P. Cellular and molecular mechanisms of chikungunya pathogenesis. **Antiviral Research**, v. 120, p. 165–174, 2015.

LUMSDEN, W. H. R. An epidemic of virus disease in Southern Province, Tanganyika territory, in 1952–1953 II. General description and epidemiology. **Transactions of the Royal Society of Tropical Medicine and Hygiene**, v. 49, n. 1, p. 33–57, 1 jan. 1955.

MARTINS, D. O. S. et al. Antivirals Against Chikungunya Virus: Is the Solution in Nature? **Viruses**, v. 12, n. 3, p. 272, mar. 2020.

MATHEW, A. J. et al. Chikungunya Infection : a Global Public Health Menace. p. 1–9, 2017.

MATKOVIC, R. et al. The Host DHX9 DExH-Box Helicase Is Recruited to Chikungunya Virus Replication Complexes for Optimal Genomic RNA Translation. **Journal of Virology**, v. 93, n. 4, p. 1–17, 2018.

MAVALE, M. et al. Venereal transmission of chikungunya virus by Aedes aegypti mosquitoes (Diptera: Culicidae). **American Journal of Tropical Medicine and Hygiene**, v. 83, n. 6, p. 1242–1244, 2010.

MINISTÉRIO DA SAÚDE. **Monitoramento dos casos de dengue, febre de chikungunya e febre pelo vírus Zika até a Semana Epidemiológica 52, 2016**. [s.l: s.n.]. Disponível em: <https://www.saude.gov.br/images/pdf/2017/abril/06/2017-002-Monitoramento-dos-casos-de-dengue--febre-de-chikungunya-e-febre-pelo-v--rus-Zika-ate-a-Semana-Epidemiologica-52--2016.pdf>. Acesso em: 3 jun. 2020.

MINISTÉRIO DA SAÚDE. **Monitoramento dos casos de dengue, febre de chikungunya e doença aguda pelo vírus Zika até a Semana Epidemiológica 49 de 2018**. [s.l: s.n.].

Disponível em: <http://www.saude.gov.br/images/pdf/2019/janeiro/02/2018-067.pdf>. Acesso em: 3 jun. 2020.

MINISTÉRIO DA SAÚDE. **Chikungunya: causas, sintomas, tratamento e prevenção**. Disponível em: <http://www.saude.gov.br/saude-de-a-z/chikungunya>. Acesso em: 3 jun. 2020a.

MINISTÉRIO DA SAÚDE. **Monitoramento dos casos de arboviroses urbanas transmitidas pelo Aedes Aegypti (dengue, chikungunya e zika), Semanas Epidemiológicas 1 a 21, 2020**. [s.l: s.n.]. Disponível em: <https://www.saude.gov.br/images/pdf/2020/May/29/Boletim-epidemiologico-SVS-22.pdf>. Acesso em: 3 jun. 2020b.

MINISTÉRIO DA SAÚDE, S. DE V. EM S. Monitoramento-dos-casos-de-dengue-e-febre-de-chikungunya-20.pdf. **Boletim Epidemiológico**, v. 46, 2015.

MOLLER-TANK, S. et al. Role of the Phosphatidylserine Receptor TIM-1 in Enveloped-Virus Entry. v. 87, n. 15, p. 8327–8341, 2013.

MULLER, V. D. et al. Phospholipase A2 isolated from the venom of Crotalus durissus terrificus inactivates dengue virus and other enveloped viruses by disrupting the viral envelope. **PLoS ONE**, v. 9, n. 11, p. 1–10, 2014.

MULLER, V. D. M. et al. Crotoxin and phospholipases A2 from Crotalus durissus terrificus showed antiviral activity against dengue and yellow fever viruses. **Toxicon**, From venoms to drugs. v. 59, n. 4, p. 507–515, 15 mar. 2012.

NGOAGOUNI, C. et al. Potential of Aedes aegypti and Aedes albopictus populations in the Central African Republic to transmit enzootic chikungunya virus strains. **Parasites & Vectors**, v. 10, n. 1, p. 164, 2017.

NJENGA, M. K. et al. Tracking epidemic Chikungunya virus into the Indian Ocean from East Africa. **Journal of General Virology**, v. 89, n. 11, p. 2754–2760, 2008.

OLIVEIRA, R. DE M. A. B. et al. Maternal and infant death after probable vertical transmission of chikungunya virus in Brazil – case report. **BMC Infectious Diseases**, v. 18, n. 1, p. 333, 16 dez. 2018.

OMS. **Chikungunya**. Disponível em: <http://www.who.int/es/news-room/fact-sheets/detail/chikungunya>. Acesso em: 23 out. 2018.

ONDETTI, M. A. et al. Angiotensin-converting enzyme inhibitors from the venom of Bothrops jararaca. Isolation, elucidation of structure, and synthesis. **Biochemistry**, v. 10, n. 22, p. 4033–4039, out. 1971.

PAGÈS, F. et al. Correction: Aedes albopictus Mosquito: The Main Vector of the 2007 Chikungunya Outbreak in Gabon. **PLoS ONE**, v. 4, n. 5, 27 maio 2009.

PAIXÃO, E. S. et al. Chikungunya chronic disease: A systematic review and meta-analysis. **Transactions of the Royal Society of Tropical Medicine and Hygiene**, v. 112, n. 7, p. 301–316, 2018.

PARASHAR, D.; CHERIAN, S. Antiviral perspectives for chikungunya virus. **BioMed Research International**, v. 2014, 2014.

PAVAN, F. R. et al. Ruthenium (II) phosphine/picolinate complexes as antimycobacterial agents. **European Journal of Medicinal Chemistry**, v. 45, n. 2, p. 598–601, 2010.

PIALOUX G, GAÜZÈRE BA, JAURÉGUIBERRY S, S. M. Chikungunya, an epidemic arbovirosis. **The Lancet Infectious Diseases**, v. 7, n. 5, p. 319–327, 1 maio 2007.

POHJALA, L. et al. Inhibitors of alphavirus entry and replication identified with a stable Chikungunya replicon cell line and virus-based assays. **PLoS ONE**, v. 6, n. 12, 2011.

POWERS, A. M. et al. Re-emergence of chikungunya and o'nyong-nyong viruses: Evidence for distinct geographical lineages and distant evolutionary relationships. **Journal of General Virology**, v. 81, n. 2, p. 471–479, 2000.

POWERS, A. M. Vaccine and Therapeutic Options To Control Chikungunya Virus. **Clinical Microbiology Reviews**, v. 31, n. 1, p. e00104-16, /cmr/31/1/e00104- 16.atom, 13 dez. 2017.

RASHAD, A. A.; KELLER, P. A. Structure based design towards the identification of novel binding sites and inhibitors for the chikungunya virus envelope proteins. **Journal of Molecular Graphics and Modelling**, v. 44, p. 241–252, 2013.

RASHAD, A. A.; MAHALINGAM, S.; KELLER, P. A. Chikungunya Virus : Emerging Targets and New Opportunities for Medicinal Chemistry. 2013.

RAVI, V. Re-emergence of chikungunya virus in India. **Indian journal of medical microbiology**, v. 24, n. 2, p. 83–4, abr. 2006.

ROBERTS, G. C. et al. Evaluation of a range of mammalian and mosquito cell lines for use in Chikungunya virus research. **Scientific Reports**, v. 7, n. 1, p. 14641, 7 dez. 2017.

ROBINSON, M. C. An epidemic of virus disease in Southern Province, Tanganyika Territory, in 1952-53. I. Clinical features. **Transactions of the Royal Society of Tropical Medicine and Hygiene**, v. 49, n. 1, p. 28–32, jan. 1955.

ROSS, B. Y. R. W. the Newala Epidemic and Relationship To the Epidemic. p. 177–191, 1955.

ROUGERON, V. et al. Chikungunya, a paradigm of neglected tropical disease that emerged to be a new health global risk. **Journal of Clinical Virology**, v. 64, p. 144–152, mar. 2015.

RUPAMONI THAKUR; ASHIS K. MUKHERJEEA. Pathophysiological significance and therapeutic applications of snake venom protease inhibitors. **Toxicon**, v. 131, p. 37–47, 1 jun. 2017.

RUSSO, R. R. et al. Expression, purification and virucidal activity of two recombinant isoforms of phospholipase A2 from Crotalus durissus terrificus venom. **Archives of Virology**, v. 164, n. 4, p. 1159–1171, 26 abr. 2019.

SAMBRI, V. et al. The 2007 epidemic outbreak of Chikungunya virus infection in the Romagna region of Italy: A new perspective for the possible diffusion of tropical diseases in temperate areas? **New Microbiologica**, v. 31, n. 3, p. 303–304, 2008.

SAVIĆ, A. et al. Antitumor activity of organoruthenium complexes with chelate aromatic ligands, derived from 1,10-phenantroline: Synthesis and biological activity. **Journal of Inorganic Biochemistry**, v. 202, n. September 2019, p. 110869, 2020.

SCHALOSKE, R. H.; DENNIS, E. A. The phospholipase A2 superfamily and its group numbering system. **Biochimica Et Biophysica Acta**, v. 1761, n. 11, p. 1246–1259, nov. 2006.

SCHUFFENECKER, I. et al. Genome Microevolution of Chikungunya Viruses Causing the Indian Ocean Outbreak. **PLoS Medicine**, v. 3, n. 7, p. 1058–1070, 2006.

SCHUHMACHER, A.; REICHLING, J.; SCHNITZLER, P. Virucidal effect of peppermint oil on the enveloped viruses herpes simplex virus type 1 and type 2 in vitro. **Phytomedicine**, v. 10, n. 6–7, p. 504–510, jan. 2003.

SHARIFI-RAD, J. et al. Susceptibility of herpes simplex virus type 1 to monoterpenes thymol, carvacrol, p-cymene and essential oils of Sinapis arvensis L., Lallemantia royleana Benth. and Pulicaria vulgaris Gaertn. **Cellular and molecular biology (Noisy-le-Grand, France)**, v. 63, n. 8, p. 42–47, 30 ago. 2017.

SHIMIZU, J. F. et al. Multiple effects of toxins isolated from Crotalus durissus terrificus on the hepatitis C virus life cycle. **PLOS ONE**, v. 12, n. 11, p. e0187857, 15 nov. 2017.

SILVA, N. M. DA et al. Vigilância de chikungunya no Brasil: desafios no contexto da Saúde Pública. **Epidemiologia e Serviços de Saúde**, v. 27, n. 3, p. e2017127, 2018.

SILVA, L. A. et al. A Single-Amino-Acid Polymorphism in Chikungunya Virus E2 Glycoprotein Influences Glycosaminoglycan Utilization. **Journal of Virology**, v. 88, n. 5, p. 2385–2397, 2014.

SILVA, L. A. et al. Chikungunya virus : epidemiology , replication , disease mechanisms , and prospective intervention strategies Find the latest version : Chikungunya virus : epidemiology , replication , disease mechanisms , and prospective intervention strategies. v. 127, n. 3, p. 737–749, 2017.

SIMON, F. et al. Chikungunya virus infection. **Current Infectious Disease Reports**, v. 13, n. 3, p. 218–228, 2011.

SIX, D. A.; DENNIS, E. A. The expanding superfamily of phospholipase A(2) enzymes: classification and characterization. **Biochimica Et Biophysica Acta**, v. 1488, n. 1–2, p. 1–19, 31 out. 2000.

SOLIGNAT, M. et al. Replication cycle of chikungunya: A re-emerging arbovirus. **Virology**, v. 393, n. 2, p. 183–197, out. 2009a.

SOLIGNAT, M. et al. Replication cycle of chikungunya: A re-emerging arbovirus. **Virology**, v. 393, n. 2, p. 183–197, out. 2009b.

STEGMANN-PLANCHARD, S. et al. Chikungunya, a Risk Factor for Guillain-Barré Syndrome. **Clinical Infectious Diseases**, v. 66, p. 37–39, 9 jul. 2019.

TANG, J. et al. Virucidal activity of hypericin against enveloped and non-enveloped DNA and RNA viruses. **Antiviral Research**, v. 13, n. 6, p. 313–325, jun. 1990.

TEIXEIRA, R. R. et al. Natural Products as Source of Potential Dengue Antivirals. **Molecules**, v. 19, p. 8151–8176, 2014.

THIBERVILLE, S. D. et al. Chikungunya fever: Epidemiology, clinical syndrome, pathogenesis and therapy. **Antiviral Research**, v. 99, n. 3, p. 345–370, 2013.

THON-HON, V. G. et al. Deciphering the differential response of two human fibroblast cell lines following Chikungunya virus infection. p. 1–10, 2012.

VAJS, J. et al. The 1,3-diaryltriazenido(p-cymene)ruthenium(II) complexes with a high in vitro anticancer activity. **Journal of Inorganic Biochemistry**, v. 153, p. 42–48, 2015.

VERA L. PETRICEVICH; RONALDO Z. MENDONÇA. Inhibitory potential of Crotalus durissus terrificus venom on measles virus growth. **Toxicon**, v. 42, n. 2, p. 143–153, 1 ago. 2003.

VIEGAS, C.; DA SILVA BOLZANI, V.; BARREIRO, E. J. OS produtos naturais e a química medicinal moderna. **Quimica Nova**, v. 29, n. 2, p. 326–337, 2006.

VILLARRUBIA, V. G.; COSTA, L. A.; DÍEZ, R. A. Fosfolipasas A2 segregadas (sPLA2):¿amigas o enemigas? ¿Actores de la resistencia antibacteriana y antivirus de la inmunodeficiencia humana? **Medicina Clínica**, v. 123, n. 19, p. 749–757, 1 out. 2004.

VOLK, S. M. et al. Genome-Scale Phylogenetic Analyses of Chikungunya Virus Reveal Independent Emergences of Recent Epidemics and Various Evolutionary Rates. **Journal of Virology**, v. 84, n. 13, p. 6497–6504, 2010.

VU, D. M.; JUNGKIND, D.; LABEAUD, A. D. Chikungunya Virus. **Clinics in Laboratory Medicine**, v. 37, n. 2, p. 371–382, 2017.

WEAVER, S. C.; FORRESTER, N. L. Chikungunya: Evolutionary history and recent epidemic spread. **Antiviral Research**, v. 120, p. 32–39, ago. 2015.

WINTACHAI, P. et al. Identification of Prohibitin as a Chikungunya Virus Receptor Protein. **Journal of Medical Virology**, v. 84, p. 1757–1770, 2012.

YANG, S. et al. Regulatory considerations in development of vaccines to prevent disease caused by Chikungunya virus q. **Vaccine**, v. 35, n. 37, p. 4851–4858, 2017.

Tables

Table 1. Maximum score resulting from the dosage for each evaluated site.

	Binder color	ChemPLP	Coordinates (x, y, z)	Volume ($\mathrm{Å}^3$)	Localization
Site 1	Yellow	32.53	−15.687, 2.019, −19.939	651.375	Between E1 domain II and E2 domain
Site 2	Green	38.98	−33.937, −18.731, −31.939	357.375	Between E1 domain II and E2 beta-sheet
Site 3	Blue	37.10	−33.437, −6.731, −33.189	156.125	Adjacentto site 2
Site 4	Purple	39.71	−42.937, −28.731, −22.939	183.875	Behind the fusion loop, between E3 B domains, E2 domain B, and E2 domain A
Site 5	Brown	18.38	−44.437, −14.731, −23.439	124	Between the E2 and E3 beta sheet
Site 6	-	*	−16.187, −18.231, −36.439	20.5	Insidethe E3 cavity
Site 7	Black	4.56	−59.187, −15.731,−26.189	22.5	Replacingthefurin loop

* No docking results
FONT: Adapted (RASHAD E KELLER, 2013)

Table 2. Vibrational modes present in each vibrational mode and identification of the respective functional group in the sample.

Vibrational mode (cm^1)	Proposed vibrational mode	Molecular source
1540	Amide II [ν (N–H), ν (C–N)]	Protein
1013	vs (CO-O-C)	Glycoprotein/ Carbohydrates
1005	vs (CO-O-C)	Glycoprotein/ Carbohydrates
724	C-H rocking of CH2	Fattyacids, proteinsInespecific
704	Unsaigment band	Sulphates components
679	S-O bending	Protein and lipids
652	OH out-of-plane bend	Inespecific

645	Unsaigment band	Protein, Lipids
632	OH out-of-plane bend	Sulphates components
609	S-O bending	

Assignments of main wavenumbers of sample ATR-FTIR spectra. Abbreviations: v = stretching vibrations, δ = bending vibrations, s= symmetric vibrations and as = asymmetric vibrations.
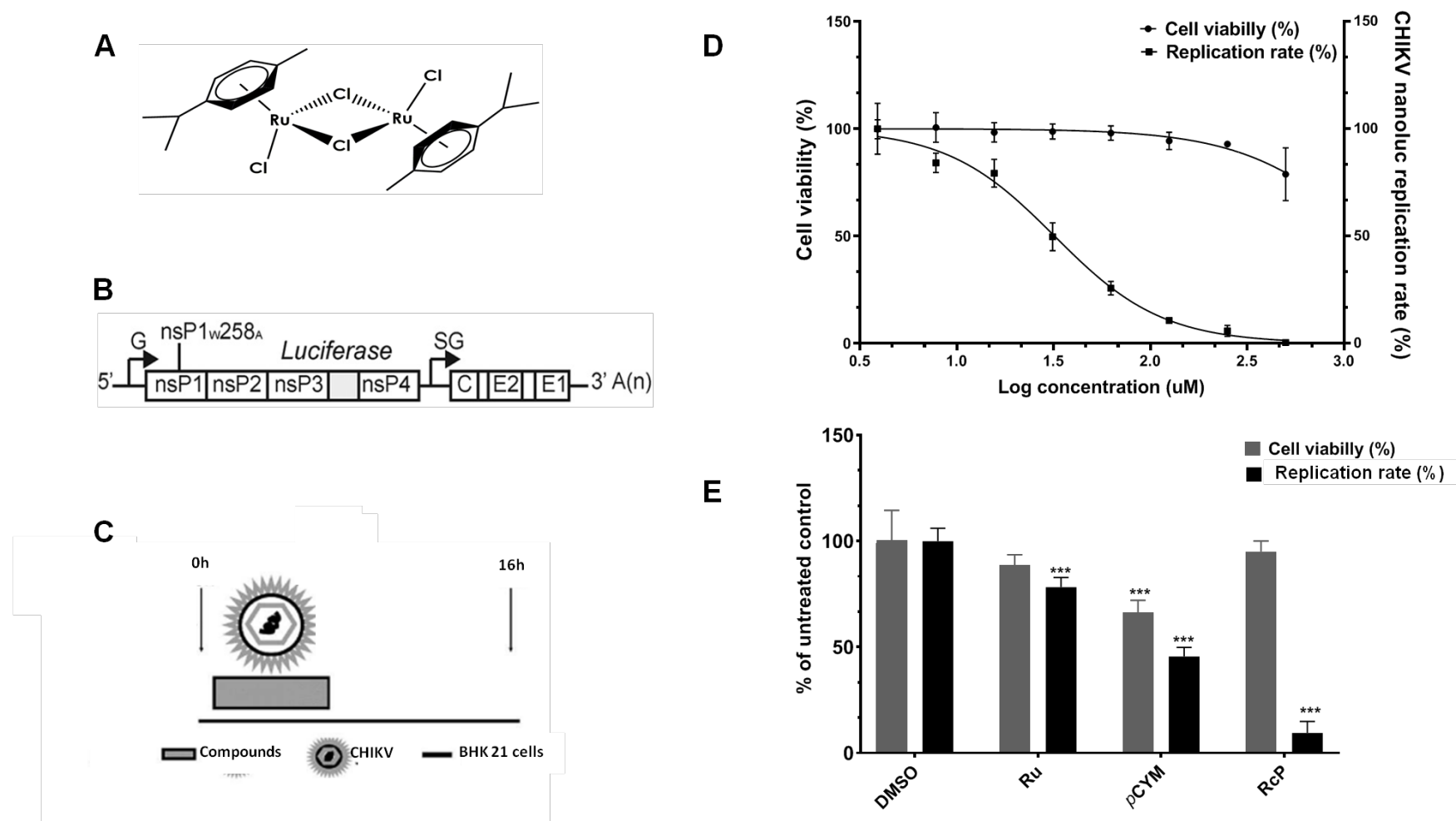
Figures and legends

Figure 1. CHIKV activity of ruthenium (Ru) and *para*-cymene(pCYM) complex (RcP). (A) RcP chemical structure (B) Schematic representation of CHIKV-*nanoluc* construction. (C) Schematic representation of infectivity assays. (D) BHK 21 cells were infected with

CHIKV-*nanoluc* at MOI 0.1 and treated with compounds at 125 μM for 16h. Infectivity and cell viability assays were performed. (E) Cells were treated with concentrations of RcP ranging from 500 a 3.9 μM and the effective concentration of 50% (EC$_{50}$) and cytotoxic concentration of 50% (CC$_{50}$) of RcP were determined. CHIKV replication was measured by luciferase assay (indicated by □) and cellular viability measured using an MTT assay (indicated by •). Mean values of three independent experiments each measured in quadruple including the standard deviation are shown.

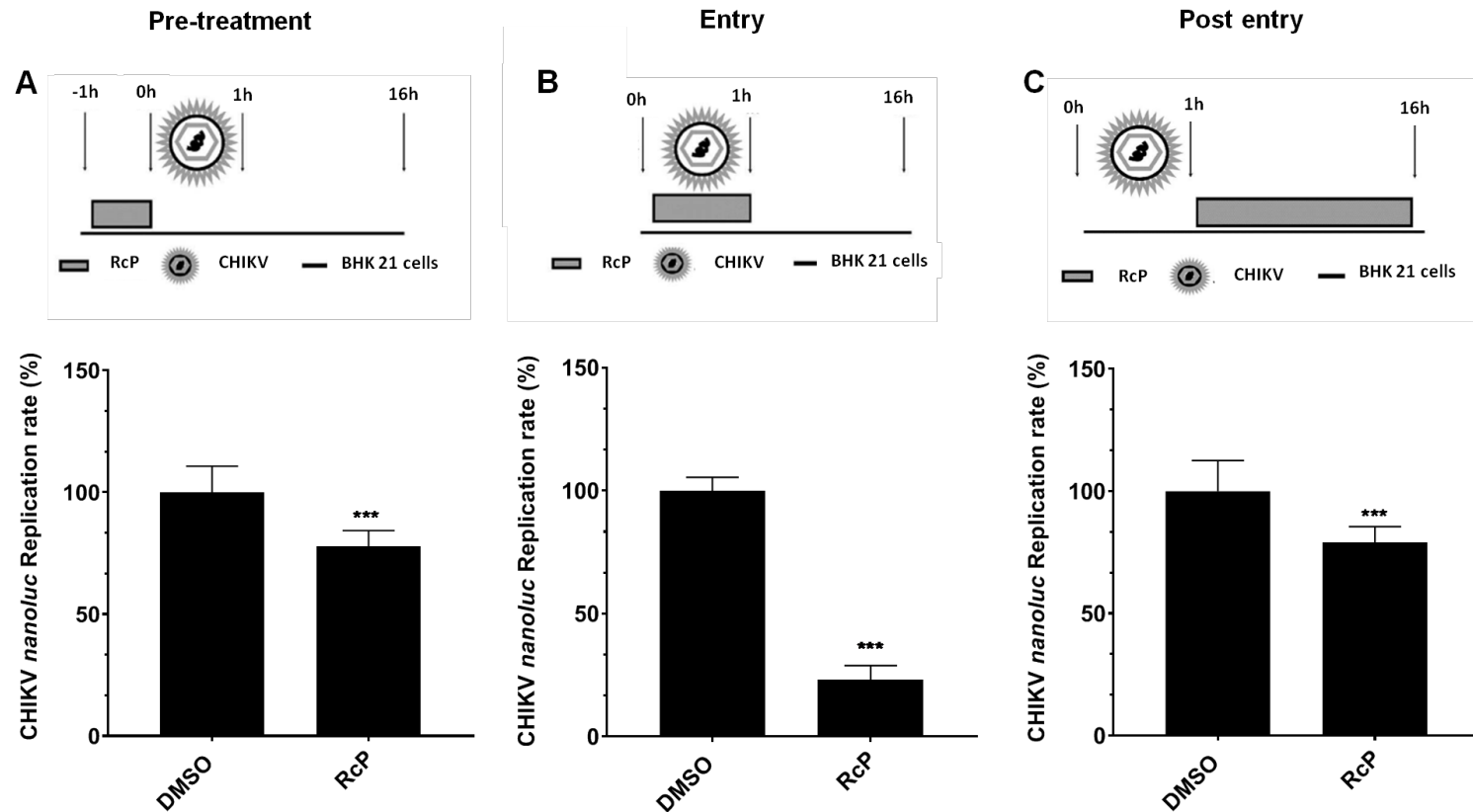**Figure   2.**
Antiviral effects of RcP at different stages of CHIKV replicative cycle. (A) BHK 21 cells were treated with RcP at125 μM for 1h. Then, cells were extensively washed and infected with CHIKV-*nanoluc* at a MOI 0.1 for 1h, compound containing media was removed and replaced by fresh media. (B) BHK 21 cells were infected with CHIKV-*nanoluc* (MOI 0.1) and simultaneously treated with RcPat125μM for 1 h. Cells

were washed and replaced with fresh media. (C) The cells were first infected with CHIKV-*nanoluc* (MOI 0.1) for 1h, washed to remove unbound virus and added of compound containing media. For all assays, CHIKV replication was measured by *nanoluc* activity at 16 h.p.i. Mean values of a minimum of three independent experiments each measured in triplicate. P<0.01 was considered significant.
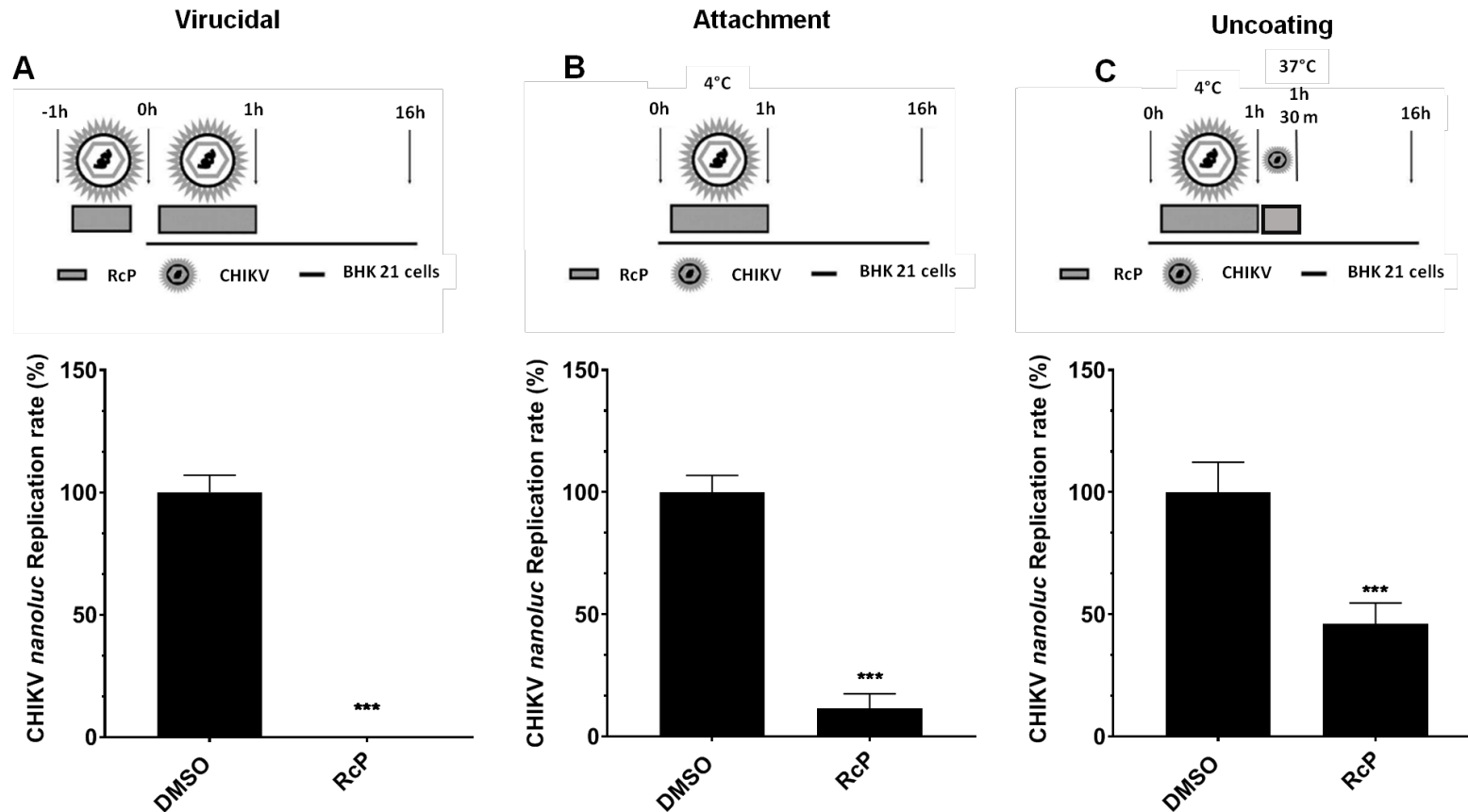
Figure 3. RcP activity on CHIKV entry to the host cells. (A) CHIKV-*nanoluc* and compound were incubated for 1 h and then for one additional hour in the cells. Then, the compound was removed and the cells added of media. (B) BHK 21 cells were infected with virus and simultaneously treated for 1 h at 4°C. The cells were washed to remove virus and compound and replaced with fresh media. (C) BHK 21

cells were infected with virus and simultaneously treated for 1 h at 4°C. Then, cells were incubated for a further 30 min with compound and virus at 37°C, were then washed to remove virus and compound and replaced with media. For all assays, CHIKV replication was measured by *nanoluc* activity at 16h.p.i.. Mean values of a minimum of three independent experiments each measured in triplicate P<0.01 was considered significant.
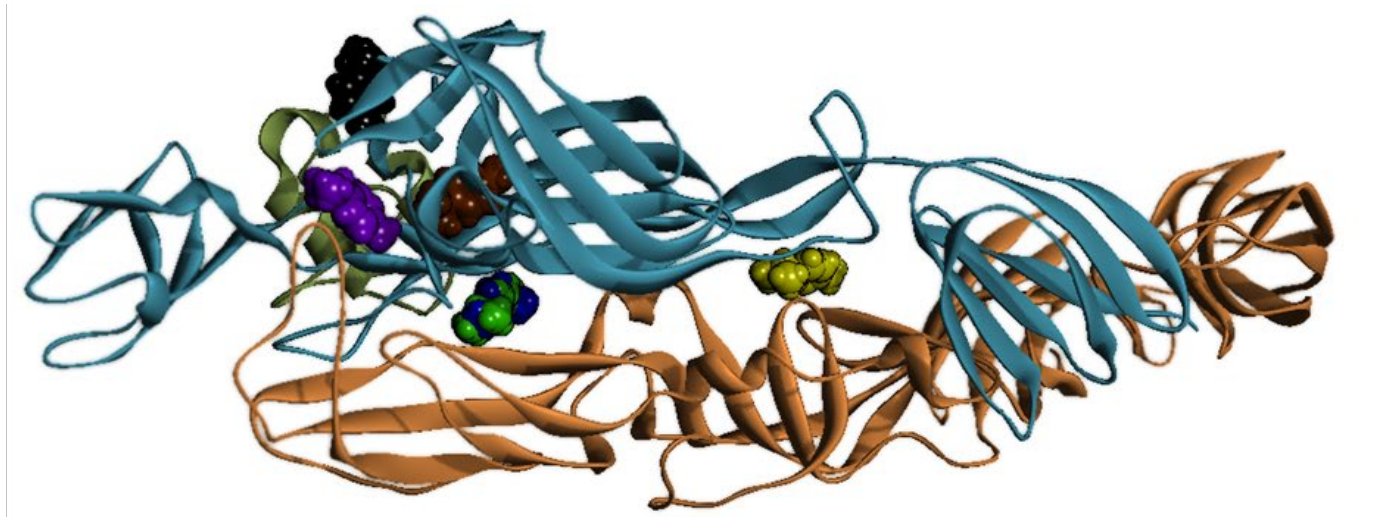

Figure 4. The CHIKV envelope glycoproteins E1 (Brown), E2 (Blue) and E3 (green), complexed with para-cymene, sites 1 (yellow), 2 (green), 3 (blue), 4 (purple), 5 (brown) and 7 (black).

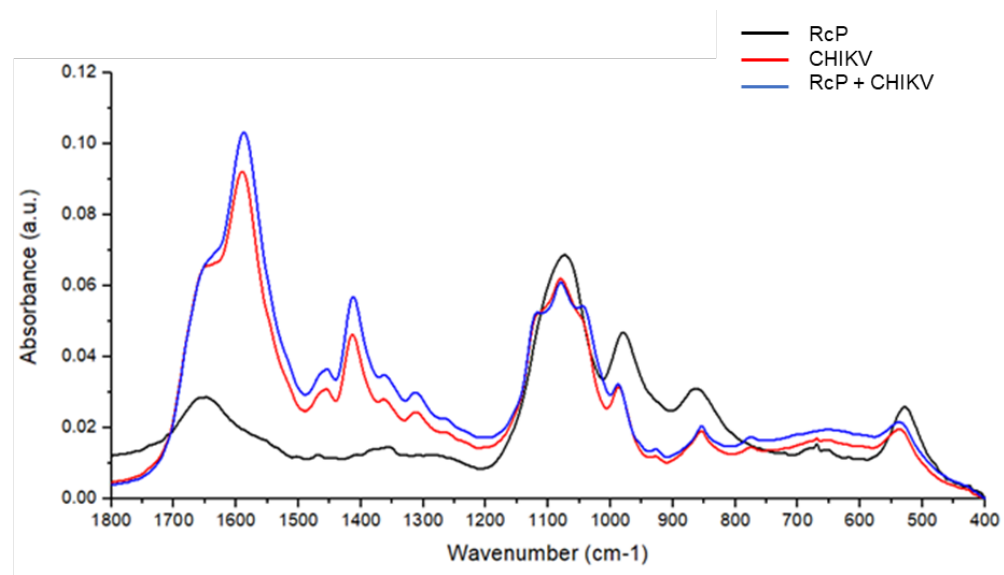**Figure 5.** Representative infrared average spectrum of RcP, CHIKV and RcP plus CHIKV, which contains different biochemical functional groups such as lipids, proteins, glycoproteins and nucleic acid.
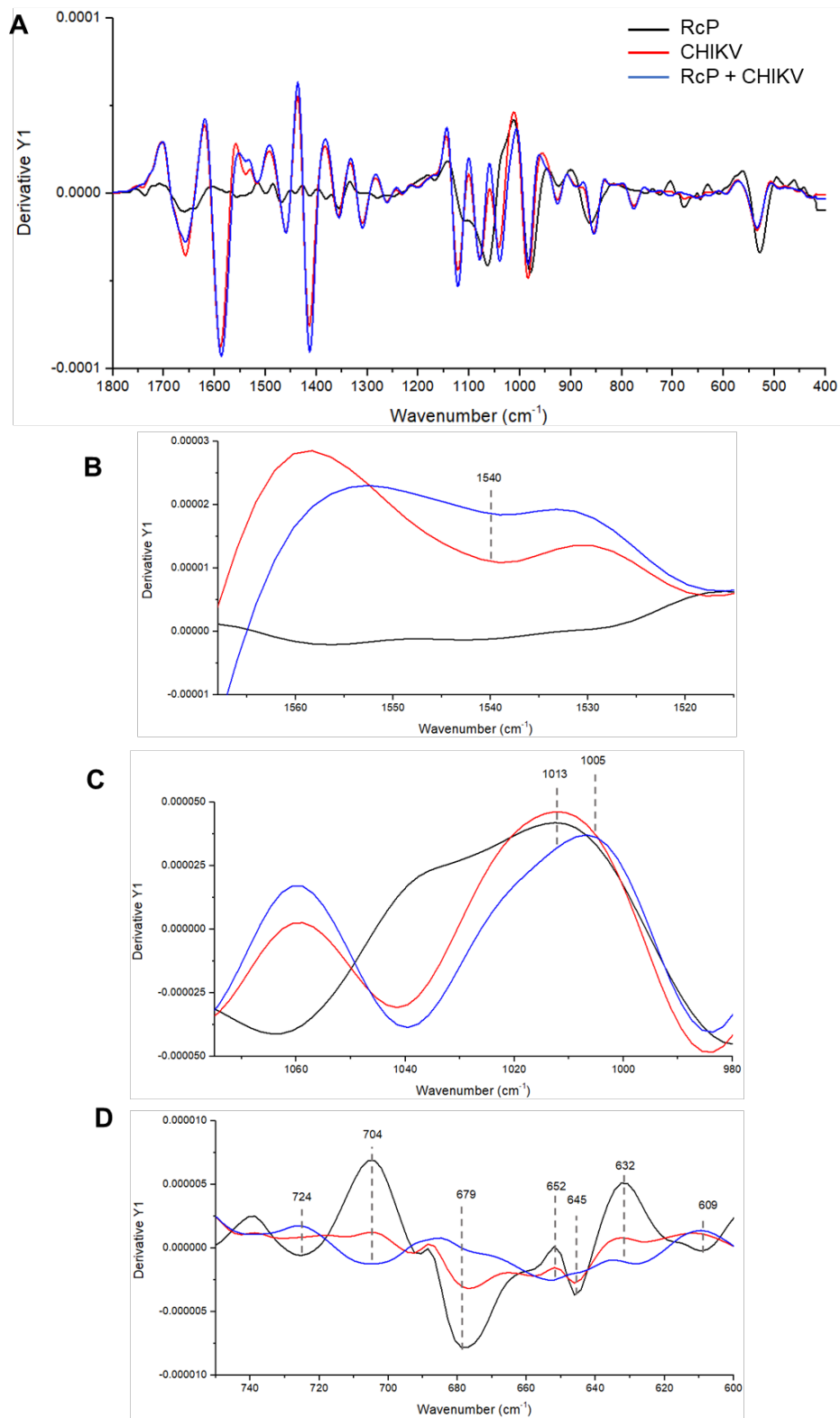
Figure 6. (A) Representative infrared average spectrum of second derivative analysis from RcP, CHIKV and RcP plus CHIKV. (B, C, D) Second derivative analysis, which the value heights indicate the intensity of each functional group.

viruses   MDPI

Antivirals Against Chikungunya Virus: Is the Solution in Nature?

**Daniel Oliveira Silva Martins [1,2,†], Igor de Andrade Santos [1,†] , Débora Moraes de Oliveira [1],
Victória Riquena Grosche [1] and Ana Carolina Gomes Jardim [1,2,*]**

[1] Laboratory of Virology, Institute of Biomedical Science, ICBIM, Federal University of Uberlândia,
    Uberlândia, MG 38408-100, Brazil; danielosmartins@gmail.com (D.O.S.M.); igoras244@gmail.com (I.d.A.S.);
    deboramoraes@hotmail.com (D.M.d.O.); victoriagrosche@live.com (V.R.G.)
[2] São Paulo State University, Institute of Biosciences, Letters and Exact Sciences (IBILCE), State University of
    São Paulo, São José do Rio Preto, SP 15054-000, Brazil
* Correspondence: jardim@ufu.br; Tel.: +55-(34)-3225-8679
† These authors contributed equally to this work.

check for updates

Abstract: The worldwide outbreaks of the chikungunya virus (CHIKV) in the last years demonstrated
the need for studies to screen antivirals against CHIKV. The virus was first isolated in Tanzania in
1952 and was responsible for outbreaks in Africa and Southwest Asia in subsequent years. Between
2007 and 2014, some cases were documented in Europe and America. The infection is associated with
low rates of death; however, it can progress to a chronic disease characterized by severe arthralgias in
infected patients. This infection is also associated with Guillain–Barré syndrome. There is no specific
antivirus against CHIKV. Treatment of infected patients is palliative and based on analgesics and
non-steroidal anti-inflammatory drugs to reduce arthralgias. Several natural molecules have been
described as antiviruses against viruses such as dengue, yellow fever, hepatitis C, and influenza.
This review aims to summarize the natural compounds that have demonstrated antiviral activity
against chikungunya virus in vitro.

Keywords: chikungunya virus; antiviral; natural compounds

---

1. Introduction

Chikungunya fever is a tropical disease caused by the chikungunya virus (CHIKV) which is
transmitted to humans by the bite of an infected mosquito of *Aedes* sp. The first case of chikungunya
fever was reported in 1952 in Tanzania [1]. In February 2005, a major outbreak of chikungunya
occurred on the islands of the Indian Ocean [2]. A large number of cases occurred in Europe and India
in 2006 and 2007, respectively [2]. Several other countries in Southeast Asia were also affected [3].
In December 2013, autochthonous cases were confirmed in the French part of the Caribbean island of
St Maarten [4]. Since then, local transmission has been confirmed in over 60 countries in Asia, Africa,
Europe, and the Americas. In 2014, more than 1 million suspected cases were reported in the Americas,
with 1,379,788 suspected cases and 191 deaths in the Caribbean islands, Latin American countries,
and the United States of America (USA) [5]. Canada, Mexico, and USA have also recorded imported
cases. The countries reporting the most cases were Brazil (265,000 suspected cases), and Bolivia and
Colombia (19,000 suspected cases each) [6]. The first autochthonous transmission of chikungunya
reported in Argentina occurred in 2016 following an outbreak of more than 1000 suspected cases [7].
In the African region, Kenya reported an outbreak of chikungunya resulting in more than 1700 suspected
cases. In 2017, Pakistan continues to respond to an outbreak which started in 2016 [8]. These virus
outbreaks have raised concerns on studies of CHIKV epidemiology and antiviral research [9].

CHIKV belongs to the Alphavirus genus and the *Togaviridae* family. It is a positive-sense, single-stranded RNA (12 kb in length) virus, with an enveloped icosahedral capsid [10]. The virus lifecycle starts via the attachment of the viral glycoproteins to the cell membrane receptors, mainly to MXRA8 [11,12] but also to prohibitin (PHB) [13], phosphatidylserine (PtdSer) [14], and glycosaminoglycans (GAGs) [15] receptors in mammalian and to ATP synthase β in mosquito cells [16], forming a pore. Then, a virus capsid is released into the cytoplasm, where the replication process takes place. Viral genome is uncoated and directly translated into nonstructural (NS) proteins nP1–4. The NS proteins form the viral replicase complex that catalyzes the synthesis of a negative strand, a template to synthesize the full-length positive sense genome, and the subgenomic mRNA. The subgenomic mRNA is translated in a polyprotein, which is cleaved to produce the structural proteins C, E3, E2, 6k, and E1, followed by the assembly of the viral components and virus release (Figure 1) [17,18].
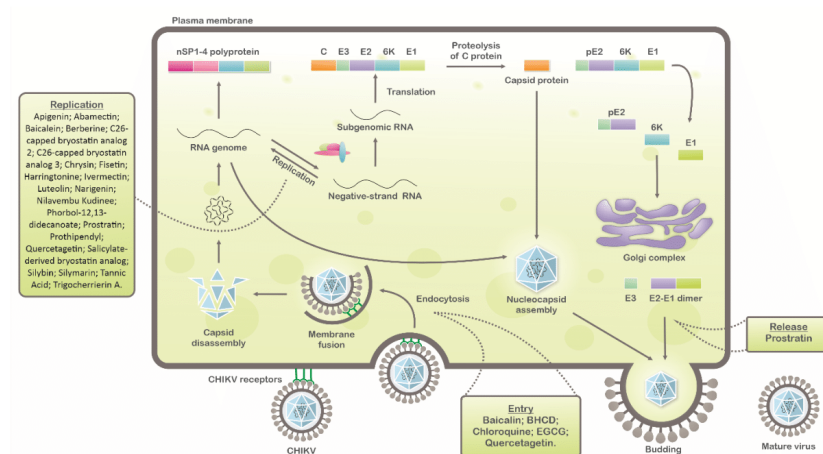

Figure 1. Schematic representation of chikungunya virus (CHIKV) replication cycle: Natural compounds with antiviral activity against CHIKV are indicated in each step of virus replication cycle (entry, replication, and release).

Chikungunya fever is characterized by strong fever, arthralgia, backache, headache, and fatigue. In some cases, cutaneous manifestation and neurological complications can occur [19,20]. There is no Food and Drug Administration (FDA) approved specific antiviral or vaccine against CHIKV. Therefore, the treatment of infected patients is based on palliative care, using analgesics for pain and non-steroidal anti-inflammatory drugs to reduce arthralgia in chronic infections [10].

Due to the lack of efficient anti-CHIKV therapy, researches have been developed to identify new drug candidates for the future treatment of chikungunya fever [21]. Among them, antiviral research based on natural molecules is a potential approach. Many natural compounds showed antiviral activity against a variety of human viruses such as dengue (DENV) [22–25], yellow fever (YFV) [25–27], hepatitis C (HCV) [28–32], influenza [33,34], and zika (ZIKV) [33,35,36]. Here, we aim to summarize the natural compounds previously described to possess anti-CHIKV activity (Table 1).

2. Inhibitors of CHIKV Replicative Cycle

2.1. Epigallocatechin Gallate (Green Tea)

Epigallocatechin gallate (EGCG) is the major catechin constituent in green tea that has shown antiviral activity against CHIKV in vitro [37]. HEK 293T cells (human kidney cells) were infected with the pseudo particles CHIKV-mCherry-490 with a multiplicity of infection of 1 (MOI = 1) in the presence or absence of EGCG at 10 μg/mL, which blocked up to 60% of CHIKV entry. Through lentiviral expression of CHIKV glycoprotein, the authors evaluated the antiviral activity of EGCG on entry steps and suggested that EGCG interferes with CHIKV entry due to their effect on CHIKV envelope protein [37].

2.2. Chloroquine

According to the studies of Khan and coworkers, a synthetic compound derived from the natural Chloroquine used to treat malaria infection has shown antiviral activity against CHIKV [38]. To do this, Vero cells were infected with the African East-Central-South (ECSA) CHIKV genotype, DRE-06 strain, and incubated with the compound at 5, 10, or 20 μM to evaluate its antiviral activity. Three treatment strategies were used for the plaque assay: (1) pretreatment of the cells 24 h before infection; (2) concurrent treatment by simultaneously adding virus and chloroquine; and (3) treatment of cells up to 6 h post-CHIKV infection of Vero cells. Chloroquine at 20 μM was nontoxic to the cells and inhibited CHIKV entry by approximately 94% when cells were pretreated, 70% in the concurrent treatment, and 65% in the post-infection treatment. The results suggested that this compound presents strong antiviral activity, mainly when administered 24 h prior to infection [38].

2.3. Apigenin, Chrysin, Luteonin, Narigerin, Silybin, and Prothipendyl

Pohjala and colleagues demonstrated the anti-CHIKV activity of five natural compounds by using either a replicon cell line expressing the nonstructural proteins of CHIKV and the *eGFP* and Renilla luciferase (*Rluc*) markers or the full-length virus genetically modified with the reporter *Rluc*. Firstly, BHK21 (baby hamster kidney) cells were infected with the full length CHIKV-*Rluc* (MOI = 0.001) and simultaneously treated with different concentrations of each compound ranging from 0.01 to 100 μM for 16 h. The compounds apigenin (inhibitory concentration (IC$_{50}$) = 70.8 μM), chrysin (IC$_{50}$ = 126.6 μM), narigenin (IC$_{50}$ = 118.4 μM), silybin (IC$_{50}$ = 92.3 μM), and prothipendyl (IC$_{50}$ = 97.3 μM) significantly inhibited CHIKV-*Rluc* replication [39].

In addition, Muralli and coworkers also tested the antiviral activity of apigenin and luteonin ethanolic fraction from *Cynodon dactylon* in Vero cells and found that the fractions inhibited 98% of CHIKV activity at concentration of 50 μg/mL through the cytopathic effect [40]. Using a reverse transcriptase polymerase chain-reaction (RT-PCR) the authors also demonstrated that virus RNA levels decreased under treatment. In another study, apigenin and luteonin were isolated from a fraction of the *Cynodon dactylon* plant, obtained from the National Institute of Virology of India, and were used to assess the cytotoxicity and antiviral activity in Vero cells. Results showed that concentrations ranging from 5 to 200 μg/mL were nontoxic as determined by 3-(4,5-dimethylthiazol-2-yl)-2,5-diphenyltetrazolium bromide cell proliferation assay (MTT assay). In addition, treatment of cells at 10, 25, and 50 μg/mL showed a reduction of viral activity by decreasing 68%, 88%, and 98% of the cytopathic effect of the virus, respectively [39,40].

2.4. Flavaglines

As CHIKV uses prohibitin as a receptor to entry into mammalian cells [13], Wintachai and colleagues investigated the anti-CHIKV activity of the plant-derived compounds sulfonyl amidines 1M and the flavaglines FL3 and FL23 [41], previously reported to interact with this receptor. These compounds demonstrated antiviral activity against the CHIKV strain E1:226V East-Central-South-Africa (ECSA) genotype of a Thai isolate. The cell line HEK-293T/17 was added to

each compound at specific concentrations (1, 5, 10, and 20 nM) for one hour and then infected with 10 pfu/cell of CHIKV. After 20 h, cell pellets were submitted to flow cytometry and the supernatant to a plaque assay to measure CHIKV titers. All three compounds significantly reduced the percentage of viral production in the infected cells at 10 and 20 nM concentrations. Sulfonyl amidine 1M and FL23 at 20 nM reduced viral cytopathic effect by approximately 40%, and FL3 at 20 nM reduced viral yield by 50% [41].

2.5. Compounds from Tectona grandis

The antiviral activity of three isolated and characterized compounds from *Tectona grandis* had its antiviral activity tested against the CHIKV strains ECSA KC 969208 and Asian KC969207 in Vero cells [42]. The authors determined IC_{50} of the compounds 2-(butoxycarbonyl) benzoic acid (BCB), 3,7,11,15-tetramethyl-1-hexadecanol (THD), and benzene-1-carboxylic acid-2-hexadeconate (BHCD). They demonstrated that the most potent anti-CHIKV activity was observed for BHCD with selectivity index (SI) of 116 for the Asian strain and 4.66 for ECSA. In silico analyses were performed and showed that the compound possessed strong interactions with CHIKV envelope protein 1 (E1) and poor interactions with nonstructural proteins (nSP) that may suggest that this compound could act on CHIKV entry [42].

2.6. Trigocherrierin A

The work of Bourjot and colleagues showed that compounds isolated from the *Trigonostemon cherrieri* presented inhibitory activity against CHIKV replication [43]. Vero cells were used in cell proliferation assay (MTS) to evaluate the anti-CHIKV activity of compounds by decreasing the cell death induced by the virus infection [43]. Among the isolated compounds, trigocherrierin A inhibited death of cells caused by the virus with a concentration that induced half of the maximum effect (EC_{50}) of 0.6 ± 0.1 μM, CC_{50} of 43 ± 16 μM, and the SI of 71.7. Thus, trigocherrierin A has been shown to be the most potent tested compound against CHIKV replication in this study [43].

2.7. Harringtonine

Harringtonine, a natural compound derived from the Japanese plant *Cephalotaxus harringtonia*, demonstrated antiviral activity against CHIKV replication [44]. The authors investigated the anti-CHIKV activity of this compound by using the cell lines BHK-21, C6/36 (embryonic tissue cells of the *Aedes albopictus* mosquito), and HSMM (human skeletal muscle myoblasts) and the virus strains CHIKV-0708 (Singapore 07/2008, lacking the A226V mutation in E1 protein) and CHIKV-122508 (SGEHICHD 122508, having the A226V mutation in the E1 protein) [44]. In BHK-21 cells, harringtonine at 1 and 10 μM showed potent anti-CHIKV action, inhibiting up to 90% of viral replication with cell viability higher than 80%. Aiming to investigate the harringtonine mechanism of action, the authors performed a time addition assay. Compounds were added at different concentrations, prior to infection (−2 h) and at 0, 2, 6, 12, and 16 h post infection (h.p.i.). Treatments showed inhibition of CHIKV replication at 2 h.p.i, indicating that harringtonine inhibits the early steps of the CHIKV replicative cycle. Additionally, cells were infected and treated for 6 h, and western blot and qRT-PCR assays were performed. The results showed that harringtonine reduced negative- and positive-sense RNAs of CHIKV and the production of nSP3 and E2 proteins [44].

2.8. Diterpene Ester (phorbol-12,13-didecanoate)

Twenty-nine diterpenoids isolated from *Euphorbiaceae* species had their antiviral activity tested against CHIKV (Indian Ocean strain 899) in vitro through MTS assay [45,46]. First, media with serial dilutions of each compound was added to empty 96-well microplate, and then, each well was added of media containing Vero cells (2.5×10^3 cells per well) and CHIKV for 6–7 days. Among the tested compounds, phorbol-12,13-didecanoate was shown to be the strongest candidate as an antivirus against CHIKV replication, with an EC_{50} 6.0 ± 0.9 nM [45,46].

2.9. Daphanane Diterpenoid Ortho Esters

A panel of diterpenoids or thioesters isolated from *Trigonostemon cherrieri* was used to evaluate the antiviral activity against CHIKV [47]. Vero cells were used to determine the cytotoxicity of compounds, and antiviral properties were accessed by plaque assay. Among the tested compounds, Trigoocherrins A, B, and F were shown to be potent inhibitors of CHIKV replication with SIs of 23, 36, and 8, respectively [45].

2.10. Aplysiatoxin-Related Compounds

Five bioactive compounds from the cyanobacteria *Trichodesmiumery thraeuma* had their antiviral activity evaluated [47]. Cell viability was measured and a dose-dependent anti-CHIKV assay was performed to access the antiviral activity of the compounds under pre- or post-treatment conditions. The Debromo analogues 2 and 5 showed significant antiviral activity in post-treatment of infected BHK 21 cells with EC_{50} of 1.3 and 2.7 μM and SI of 10.9 and 9.2, respectively. The authors suggested that the antiviral activity of these compounds blocks the replication step of the CHIKV replicative cycle [47].

2.11. Tannic Acid

Tannic acid (TA) is a compound found in different species of plants, but its structure varies according to their sources. It previously demonstrated antiviral activity against viruses as Herpes (HSV) and HCV [48,49]. The anti-CHIKV activity of TA was investigated by KONISHI and HOTTA by performing plaque reduction assay using BHK-21 cells [50]. TA reduced 50% of the virus infectivity in lower concentrations and demonstrated inhibition of virus post-entry steps in BHK-21 cells. To investigate which chemical group of TA is associated with its antiviral activity, the authors tested TA analogues on their virus-inhibiting capacities. The results demonstrated that phenolic hydroxyl groups may be related to the antiviral activity, since the displacement of these groups make the molecule ineffective [50].

2.12. Silymarin

Silymarin is a polyphenolic compound from flavonoids family, is extracted from *Silybum marianum*, and is described to possesses antiviral activity against HCV [51]. A study tested the activity of silymarin on CHIKV genotype ECSA with A226V mutation in E1 protein from a clinical strain isolated in an outbreak in 2008. BHK-21 and Vero cells were used to evaluate different steps of the viral replicative cycle, and silymarin showed inhibition of post-entry stages of CHIKV with an EC_{50} of 16.9 μg/mL and SI of 25.1. By using a stable cell line expressing CHIKV replicon and *EGFP* and *Rluc* markers [39], it was demonstrated that silymarin suppressed 93.4% of CHIKV replication. Western blot assay was performed, showing that silymarin treatment decreased the amounts of nSP1, nSP3, and E2 proteins [52].

2.13. Baicalein, Fisetin, and Quercetagetin

Baicalein, fisetin, and quercetagetin are compounds from the flavonoids family that exhibited antiviral activity against DENV [22] and enterovirus A71 [53]. Lani and colleagues infected Vero cells with the CHIKV genotype ECSA strain from the outbreak of 2008 and evaluated their effects in reducing the cytopathic effect resulting from viral infection [54]. All three compounds were found to inhibit CHIKV replication in a dose-dependent manner and reduced E2, nSP1, and nSP3 protein synthesis, as showed by Western blot analysis. Baicalein and quercetagetin showed anti-CHIKV activity by inactivating the virus, preventing the attachment of the virus to the host cells and blocking post-entry stages, with EC_{50} of 1.891 μg/mL and 13.85 μg/mL, respectively. Fisetin only inhibited post-entry steps with EC_{50} of 8.44 μg/mL [54].

2.14. Bryostatin

Bryostatin is a macrolide lactone derived from a marine animal named Bugula neritina [55]. It was described by the antineoplastic activity [56], affects Alzheimer's disease [57], and has been related to the eradication of human immunodeficiency virus reservoirs [58]. The anti-CHIKV activities of the Bryostatin analogs salicylate-derived analog 1, C26-capped analog 2, and C26-capped analog 3 were assessed by evaluating the cytopathic effect (CPE) caused by CHIKV Indian Ocean lineage strain 899 replication under treatment with these three compounds [59]. All of the Bryostatin analogs inhibited the CHIKV replicative cycle, decreasing infectious progeny and viral RNA copies, confirmed by supernatant titration and RT-PCR. A time-addition assay showed that these compounds inhibited late stages of CHIKV replication, with EC_{50} rates of 4 μM, 8 μM, and 7.5 μM, respectively. Additionally, salicylate-derived analog 1 but not the other compounds blocked entry of CHIKV pseudoparticles into Buffalo green monkey kidney cells (BGM) [59].

2.15. Prostatin

Bourjot and coworkers described the effect of prostratin, a compound derived from *Trigonostemon howii*, on CHIKV infection in Vero cells by a CPE assay (EC_{50} = 2.6 μM) [60]. Another work used CHIKV lineage Indian Ocean 899 to infected Vero, BGM, or Human embryonic lung fibroblasts (HEL) cells at MOI of 0.001 under the treatment with prostratin and obtained EC_{50} of 8 μM, 7.6 μM, and 7.1 μM, respectively. Using a delay treatment associated with a RT-PCR or CHIKV pseudoparticle techniques, it was demonstrated that prostratin decreased both the number of CHIKV genome copies and the production of infectious progeny virus particles. A western blot assay was used to detect CHIKV proteins and showed that prostratin also reduced the accumulation of nSP1 and capsid proteins [60].

2.16. Berberine

Berberine is a compound found in plants from the *Berberis* genus, family *Berberidaceae*, that previously demonstrated antiviral activity against other viruses [61]. Varghese and colleagues analyzed the antiviral effect of berberine on the CHIKV replication cycle using the CHIKV lineage LR2006 OPY1 with the *Rluc* marker to infect HEK-293T, HOS (humam bone osteosarcoma), and CRL-2522 cells. The berberine EC_{50} for each cell line were 4.5, 12.2, and 35.3 μM, respectively. This compound was also active against the different CHIKV strains LR2006 OPY1, SGP11, and CNR20235, showing EC_{50} of 37.6, 44.2, and 50.9 μM, respectively. Berberine showed no inhibition on CHIKV entry or replication but decreased viral RNA and viral protein synthesis, suggesting that berberine is indirectly perturbing CHIKV replication by affecting host components [61].

2.17. Avermectin Derivates

Avermectin is naturally produced in *Streptomyces avermitilis* bacteria and showed different biological properties including antiparasitic [62], antiviral [63], and antibacterial [64,65] activities. Ivermectin (IVN) and abamectin (ABN) are chemically modified derivatives of avermectin. The activity of these derivatives on the CHIKV replication cycle was described in a study that used BHK-21 with CHIKV containing the *Rluc* gene [66]. IVN and ABN demonstrated EC_{50} of 0.6 μM and 1.5 μM, respectively, and strongly reduced nSP1 and nSP3 even in high MOIs. A time-of-addition assay demonstrated that IVN and ABN interfered in earlier stages of CHIKV cycle but not when cells were pretreated. Alternatively, the activity of these compounds was decreased in the later stages of the CHIKV replicative cycle [66].

Table 1. Natural compounds with antiviral activity against CHIKV.
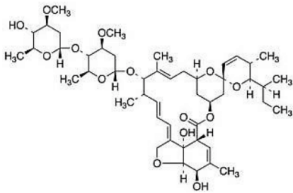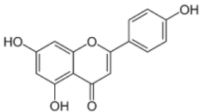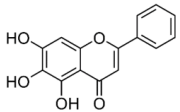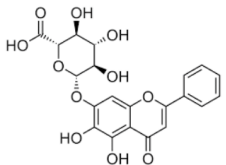
Compound	Structure	Inhibition	SI or EC$_{50}$	Cell Line
Abamectin [66]		Replication	1.5 μM	BHK-21
Apigenin [39,40]		Infection/Replication	70.8 μM	BHK 21
Baicalein [54]		Infection and replication	1.891 μg/mL	BHK-21
Baicalein [54]		Entry, binding	6.997 μM	Vero

Table 1. *Cont.*
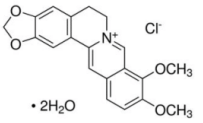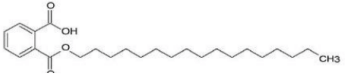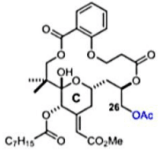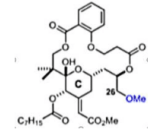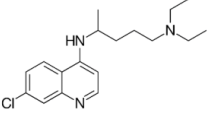
Compound	Structure	Inhibition	SI or EC$_{50}$	Cell Line
Berberine [61]		Replication (interfering in host components)	≤35.3 μM	CRL-2522, HEK-293T, and HOS
BHCD [42]		Entry	116 (Asian strain) and 4.66 (ECSA)	Vero and in silico
C26-capped bryostatin analog 2 [59]		Replication	8 μM	Vero
C26-capped bryostatin analog 3 [59]		Replication	7.5 μM	Vero
Chloroquine [38]		Entry	37.14	Vero

Table 1. *Cont.*
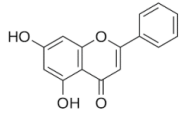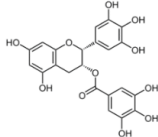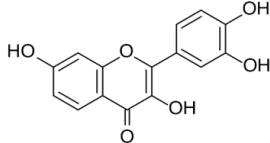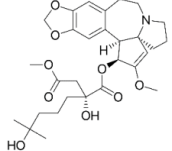
Compound	Structure	Inhibition	SI or EC$_{50}$	Cell Line
Chrysin [39]		Infection	126.6 μM	BHK 21
EGCG [37]		Entry steps; cell attachment	6.54 μg/mL	HEK 293T
Fisetin [54]		Replication	8.44 μg/mL	BHK-21
Harringtonine [44]		Early stages of replication	0.24 μM	BHK 21

107
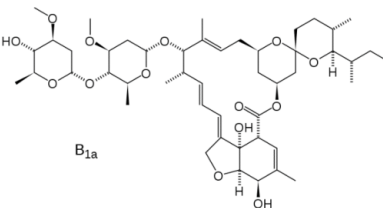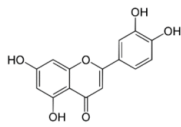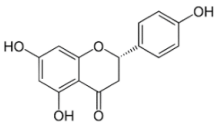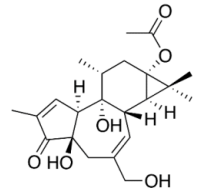
Table 1. *Cont.*

Compound	Structure	Inhibition	SI or EC$_{50}$	Cell Line
Ivermectin [66]	B$_{1a}$	Replication	0.6 µM	BHK-21
Luteolin [40]		Replication	NS	Vero
Narigenin [39]		Infection	118.4 µM	BHK 21
Prostratin [60]		Replication and release	2,6 µM and ± 8 µM	Vero, BGM, and HEL

Table 1. *Cont.*
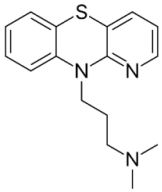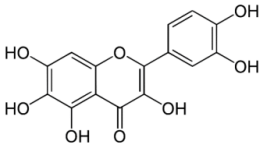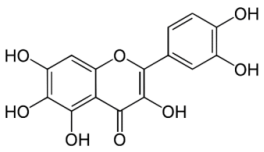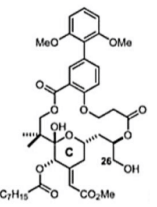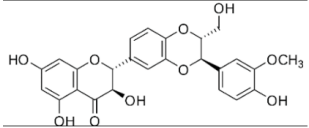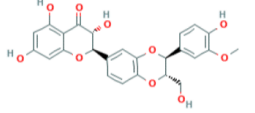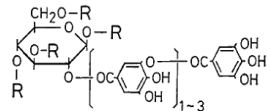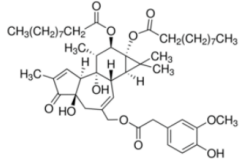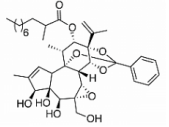
Compound	Structure	Inhibition	SI or EC$_{50}$	Cell Line
Prothipendyl [39]		Replication	97.3 μM	BHK 21
Quercetagetin [54]		Entry and binding	43.52 μM	Vero
Quercetagetin [54]		Entry and replication	13.85 μg/mL	BHK-21
Salicylate-derived bryostatin analog [59]		Entry and replication	4 μM	Vero

Table 1. *Cont.*

Compound	Structure	Inhibition	SI or EC$_{50}$	Cell Line
Silybin [39]		Infection	92.3 μM	BHK 21
Silymarin [52]		Replication	16.9 μg/mL	BHK-21 and Vero
Tannic Acid [50]		Replication	NS	BHK-21
Phorbol-12,13-dideca-noate [46]		Replication	6 ± 0.9 nM	Vero
Trigocherrierin [43]		Replication	0.6 ± 0.1 μM	Vero

NS = Not shown, data not shown.

3. Prospects

The aim of this review was to summarize data from literature concerning the natural compounds described to possess anti-CHIKV activity. Altogether, data is heterogeneous since authors developed a variety of assays using different cell lines and CHIKV strains or replicons. Some studies did not elucidate the mechanism of action (MOA) of the compound, retaining their information as EC_{50}, CC_{50}, and/or SI. For most of the compounds presented in this review, it would be desirable to demonstrate the MOA in order to elucidate the biochemical and molecular basis of the compound–virus or compound–cell interactions and to be able to predict and promote strategies for pharmacological outcomes in further studies [67]. Also, the investigation of the effects of each compound in different cell lines would provide important information concerning the effects of these compounds on the host cells [68,69]. Besides that, all data summarized here represent a relevant source of knowledge concerning the antiviral potential of molecules isolated from nature.

From the natural compounds cited in this review, chloroquine was the only compound tested in vivo, in non-human primates, and in human clinical trials. Chloroquine is already used for the treatment of malaria [70]. However, despite the in vitro results, chloroquine demonstrated no relevant results in vivo in decreasing viremia or in reducing clinical manifestations during acute stage of CHIKV infection [71]. Therefore, the results demonstrated by in vitro analysis were not correlated with the in vivo analysis that showed that chloroquine was not suitable for patients with CHIKV. Additionally, the remaining compounds described here have not been tested in vivo yet, representing a delay in anti-CHIKV drug development.

Apart from the chloroquine case, all compounds that demonstrated antiviral activity have the potential to be further investigated by their therapeutically properties against chikungunya fever. Furthermore, natural compounds may present as a source of molecules with potent biological activities that could be used as templates to the development of novel antivirals.

4. Conclusions

The spread of CHIKV in the last years demonstrated the need to develop effective antiviruses to treat chikungunya fever and to prevent future outbreaks. In this context, natural compounds have shown potent antiviral activity against a range of viruses. This review summarized the natural compounds described to possess anti-CHIKV activity by blocking early and/or late stages of virus replication in vitro. Apart from the great antiviral activity of the described compounds, further research is needed for the development of future treatments.

Conflicts of Interest: The authors declare no conflict of interest.

References

1. Ross, R.W. The virus: Isolation, Pathogenic properties and relationship to the epidemic. *Newala Epidemic* **1956**, 177–191.
2. Panning, M.; Grywna, K.; van Esbroeck, M.; Emmerich, P.; Drosten, C. Chikungunya Fever in Travelers Returning to Europe from the Indian Ocean Region, 2006. *Emerg. Infect. Dis.* **2008**, *14*, 416–422. [CrossRef] [PubMed]
3. Schuffenecker, I.; Frangeul, L.; Vaney, M.; Iteman, I.; Michault, A.; Lavenir, R.; Pardigon, N.; Reynes, J.; Biscornet, L.; Diancourt, L. Genome Microevolution of Chikungunya Viruses Causing the Indian Ocean Outbreak. *PLoS Med.* **2006**, *3*, 1058–1070. [CrossRef]
4. Henry, M.; Francis, L.; Asin, V.; Polson-Edwards, K.; Olowokure, B. Chikungunya virus outbreak in Sint Maarten, 2013-2014. *Rev. Panam. Salud Publica Pan Am. J. Public Health* **2017**, *41*, e61. [CrossRef]

5. Morens, D.M.; Fauci, A.S. Chikungunya at the Door — Déjà Vu All Over Again? *N. Engl. J. Med.* **2014**, *371*, 885–887. [CrossRef] [PubMed]

6. PAHO PAHO WHO. Chikungunya. Data, Maps and Statistics. Available online: https://www.paho.org/hq/index.php%3Foption%3Dcom_topics%26view%3Drdmore%26cid%3D5927%26item%3Dchikungunya%26type%3Dstatistics%26Itemid%3D40931%26lang%3Den (accessed on 28 December 2019).

7. Carbajo, A.E.; Vezzani, D. Waiting for chikungunya fever in Argentina: Spatio-temporal risk maps. *Mem. Inst. Oswaldo Cruz* **2015**, *110*, 259–262. [CrossRef] [PubMed]

8. Badar, N.; Salman, M.; Ansari, J.; Ikram, A.; Qazi, J.; Alam, M.M. Epidemiological trend of chikungunya outbreak in Pakistan: 2016–2018. *PLoS Negl. Trop. Dis.* **2019**, *13*, 2018–2019. [CrossRef] [PubMed]

9. Renault, P.; Solet, J.; Sissoko, D.; Balleydier, E.; Larrieu, S.; Filleul, L.; Lassalle, C.; Thiria, J.; Rachou, E.; De Valk, H.; et al. A Major Epidemic of Chikungunya Virus Infection on Réunion Island. *Am. Soc. Trop. Med. Hyg.* **2007**, *77*, 727–731. [CrossRef]

10. Thiberville, S.D.; Moyen, N.; Dupuis-Maguiraga, L.; Nougairede, A.; Gould, E.A.; Roques, P.; de Lamballerie, X. Chikungunya fever: Epidemiology, clinical syndrome, pathogenesis and therapy. *Antivir. Res.* **2013**, *99*, 345–370. [CrossRef]

11. Song, H.; Zhao, Z.; Chai, Y.; Jin, X.; Li, C.; Yuan, F.; Liu, S.; Gao, Z.; Wang, H.; Song, J.; et al. Molecular Basis of Arthritogenic Alphavirus Receptor MXRA8 Binding to Chikungunya Virus Envelope Protein. *Cell* **2019**, *177*, 1714–1724.e12. [CrossRef]

12. Zhang, R.; Earnest, J.T.; Kim, A.S.; Winkler, E.S.; Desai, P.; Adams, L.J.; Hu, G.; Bullock, C.; Gold, B.; Cherry, S.; et al. Expression of the Mxra8 Receptor Promotes Alphavirus Infection and Pathogenesis in Mice and Drosophila. *Cell Rep.* **2019**, *28*, 2647–2658.e5. [CrossRef] [PubMed]

13. Wintachai, P.; Wikan, N.; Kuadkitkan, A.; Jaimipuk, T.; Ubol, S.; Pulmanausakakil, R.; Auewarakul, P.; Kasinrerk, W.; Weng, W.-Y.; Panyasrivanit, M.; et al. Identification of Prohibitin as a Chikungunya Virus Receptor Protein. *J. Med. Virol.* **2012**, *84*, 1757–1770. [CrossRef] [PubMed]

14. Moller-Tank, S.; Kondratowicz, A.S.; Davey, R.A.; Rennert, P.D.; Maury, W. Role of the Phosphatidylserine Receptor TIM-1 in Enveloped-Virus Entry. *J. Virol.* **2013**, *87*, 8327–8341. [CrossRef] [PubMed]

15. Silva, L.A.; Khomandiak, S.; Ashbrook, A.W.; Weller, R.; Heise, M.T.; Morrison, T.E.; Dermody, T.S.; Lyles, D.S. A Single-Amino-Acid Polymorphism in Chikungunya Virus E2 Glycoprotein Influences Glycosaminoglycan Utilization. *J. Virol.* **2014**, *88*, 2385–2397. [CrossRef] [PubMed]

16. Fongsaran, C.; Jirakanwisal, K.; Kuadkitkan, A.; Wikan, N.; Wintachai, P.; Thepparit, C.; Ubol, S.; Phaonakrop, N.; Roytrakul, S.; Smith, D.R. Involvement of ATP synthase β subunit in chikungunya virus entry into insect cells. *Arch. Virol.* **2014**, *159*, 3353–3364. [CrossRef]

17. Abdelnabi, R.; Neyts, J.; Delang, L. Towards antivirals against chikungunya virus. *Antivir. Res.* **2015**, *121*, 59–68. [CrossRef]

18. Gould, E.A.; Coutard, B.; Malet, H.; Morin, B.; Jamal, S.; Weaver, S.; Gorbalenya, A.; Moureau, G.; Baronti, C.; Delogu, I.; et al. Understanding the alphaviruses: Recent research on important emerging pathogens and progress towards their control. *Antivir. Res.* **2010**, *87*, 111–124. [CrossRef]

19. De Lima, M.E.S.; Bachur, T.P.R.; Aragão, G.F. Guillain-Barre syndrome and its correlation with dengue, Zika and chikungunya viruses infection based on a literature review of reported cases in Brazil. *Acta Trop.* **2019**, *197*, 105064. [CrossRef]

20. W.H.O. Chikungunya. Available online: https://www.who.int/news-room/fact-sheets/detail/chikungunya (accessed on 28 December 2019).

21. Yactayo, S.; Staples, J.E.; Millot, V.; Cibrelus, L.; Ramon-Pardo, P. Epidemiology of Chikungunya in the Americas. *J. Infect. Dis.* **2016**, *214*, S441–S445. [CrossRef]

22. Zandi, K.; Teoh, B.-T.; Sam, S.-S.; Wong, P.-F.; Mustafa, M.R.; AbuBakar, S. Novel antiviral activity of baicalein against dengue virus. *BMC Complement. Altern. Med.* **2012**, *12*, 1185. [CrossRef]

23. Jain, J.; Kumar, A.; Narayanan, V.; Ramaswamy, R.S.; Sathiyarajeswaran, P.; Shree Devi, M.S.; Kannan, M.; Sunil, S. Antiviral activity of ethanolic extract of Nilavembu Kudineer against dengue and chikungunya virus through in vitro evaluation. *J. Ayurveda Integr. Med.* **2019**. [CrossRef] [PubMed]

24. Gómez-Calderón, C.; Mesa-Castro, C.; Robledo, S.; Gómez, S.; Bolivar-Avila, S.; Diaz-Castillo, F.; Martínez-Gutierrez, M. Antiviral effect of compounds derived from the seeds of Mammea americana and Tabernaemontana cymosa on Dengue and Chikungunya virus infections. *BMC Complement. Altern. Med.* **2017**, *17*, 57. [CrossRef] [PubMed]

25. Mastrangelo, E.; Pezzullo, M.; De burghgraeve, T.; Kaptein, S.; Pastorino, B.; Dallmeier, K.; De lamballerie, X.; Neyts, J.; Hanson, A.M.; Frick, D.N.; et al. Ivermectin is a potent inhibitor of flavivirus replication specifically targeting NS3 helicase activity: New prospects for an old drug. *J. Antimicrob. Chemother.* **2012**, *67*, 1884–1894. [CrossRef] [PubMed]

26. Julander, J.G. Experimental therapies for yellow fever. *Antivir. Res.* **2013**, *97*, 169–179. [CrossRef] [PubMed]

27. Danielle, V.; Muller, M.; Rinaldi, R.; Cristina, A.; Cintra, O.; Aurélio, M.; Alves-paiva, R.D.M.; Tadeu, L.; Figueiredo, M.; Vilela, S.; et al. Toxicon Crotoxin and phospholipases A 2 from Crotalus durissus terri fi cus showed antiviral activity against dengue and yellow fever viruses. *Toxicon* **2012**, *59*, 507–515.

28. Calland, N.; Dubuisson, J.; Rouillé, Y.; Séron, K. Hepatitis C virus and natural compounds: A new antiviral approach? *Viruses* **2012**, *4*, 2197–2217. [CrossRef]

29. Campos, G.R.F.; Bittar, C.; Jardim, A.C.G.; Shimizu, J.F.; Batista, M.N.; Paganini, E.R.; de Assis, L.R.; Bartlett, C.; Harris, M.; da Bolzani, V.S.; et al. Hepatitis C virus in vitro replication is efficiently inhibited by acridone Fac4. *J. Gen. Virol.* **2017**, *98*, 1693–1701. [CrossRef]

30. Stankiewicz-drogon, A.; Palchykovska, L.G.; Kostina, V.G.; Alexeeva, I.V.; Shved, A.D.; Boguszewska-chachulska, A.M. New acridone-4-carboxylic acid derivatives as potential inhibitors of Hepatitis C virus infection. *Bioorg. Med. Chem.* **2008**, *16*, 8846–8852. [CrossRef]

31. Jardim, A.C.G.; Igloi, Z.; Shimizu, J.F.; Santos, V.A.F.F.M.; Felippe, L.G.; Mazzeu, B.F.; Amako, Y.; Furlan, M.; Harris, M.; Rahal, P. Natural compounds isolated from Brazilian plants are potent inhibitors of hepatitis C virus replication in vitro. *Antivir. Res.* **2015**, *115*, 39–47. [CrossRef]

32. Shimizu, J.F.; Lima, C.S.; Pereira, C.M.; Bittar, C.; Batista, M.N.; Nazaré, A.C.; Polaquini, C.R.; Zothner, C.; Harris, M.; Rahal, P.; et al. Flavonoids from Pterogyne nitens Inhibit Hepatitis C Virus Entry. *Sci. Rep.* **2017**, *7*, 16127. [CrossRef]

33. Varghese, F.S.; Rausalu, K.; Hakanen, M.; Saul, S.; Kümmerer, B.M.; Susi, P.; Merits, A.; Ahola, T. Obatoclax Inhibits Alphavirus Membrane Fusion by Neutralizing the Acidic Environment of Endocytic Compartments. *Antimicrob. Agents Chemother.* **2017**, *61*, 1–17. [CrossRef] [PubMed]

34. Song, J.M.; Lee, K.H.; Seong, B.L. Antiviral effect of catechins in green tea on influenza virus. *Antivir. Res.* **2005**, *68*, 66–74. [CrossRef] [PubMed]

35. Li, C.; Deng, Y.; Wang, S.; Ma, F.; Aliyari, R.; Huang, X.-Y.; Zhang, N.-N.; Watanabe, M.; Dong, H.-L.; Liu, P.; et al. 25-Hydroxycholesterol Protects Host against Zika Virus Infection and Its Associated Microcephaly in a Mouse Model. *Immunity* **2017**, *46*, 446–456. [CrossRef] [PubMed]

36. Carneiro, B.M.; Batista, M.N.; Braga, A.C.S.; Nogueira, M.L.; Rahal, P. The green tea molecule EGCG inhibits Zika virus entry. *Virology* **2016**, *496*, 215–218. [CrossRef] [PubMed]

37. Weber, C.; Sliva, K.; Von Rhein, C.; Kümmerer, B.M.; Schnierle, B.S. The green tea catechin, epigallocatechin gallate inhibits chikungunya virus infection. *Antivir. Res.* **2015**, *113*, 1–3. [CrossRef]

38. Khan, M.; Santhosh, S.R.; Tiwari, M.; Rao, P.V.L.; Parida, M. Assessment of In Vitro Prophylactic and Therapeutic Efficacy of Chloroquine Against Chikungunya Virus in Vero Cells. *J. Med. Virol.* **2010**, *824*, 817–824. [CrossRef]

39. Pohjala, L.; Utt, A.; Varjak, M.; Lulla, A.; Merits, A.; Ahola, T.; Tammela, P. Inhibitors of Alphavirus Entry and Replication Identified with a Stable Chikungunya Replicon Cell Line and Virus-Based Assays. *PLoS ONE* **2011**, *6*, e28923. [CrossRef]

40. Murali, K.S.; Sivasubramanian, S.; Vincent, S.; Murugan, S.B.; Giridaran, B.; Dinesh, S.; Gunasekaran, P.; Krishnasamy, K.; Sathishkumar, R. Anti—chikungunya activity of luteolin and apigenin rich fraction from Cynodon dactylon. *Asian Pac. J. Trop. Med.* **2015**, *8*, 352–358. [CrossRef]

41. Wintachai, P.; Thuaud, F.; Basmadjian, C.; Roytrakul, S.; Ubol, S.; Désaubry, L.; Smith, D.R. Assessment of flavaglines as potential chikungunya virus entry inhibitors. *Microbiol. Immunol.* **2015**, *59*, 129–141. [CrossRef]

42. Sangeetha, K.; Purushothaman, I.; Rajarajan, S. Spectral characterisation, antiviral activities, in silico ADMET and molecular docking of the compounds isolated from Tectona grandis to chikungunya virus. *Biomed. Pharmacother.* **2017**, *87*, 302–310.

43. Bourjot, M.; Leyssen, P.; Neyts, J.; Dumontet, V.; Litaudon, M. Trigocherrierin A, a potent inhibitor of chikungunya virus replication. *Molecules* **2014**, *19*, 3617–3627. [CrossRef] [PubMed]

44. Kaur, P.; Thiruchelvan, M.; Lee, R.C.H.; Chen, H.; Chen, K.C.; Ng, M.L.; Chu, J.J.H. Inhibition of Chikungunya virus replication by harringtonine, a novel antiviral that suppresses viral protein expression. *Antimicrob. Agents Chemother.* **2013**, *57*, 155–167. [CrossRef] [PubMed]

45. Allard, P.M.; Leyssen, P.; Martin, M.T.; Bourjot, M.; Dumontet, V.; Eydoux, C.; Guillemot, J.C.; Canard, B.; Poullain, C.; Guéritte, F.; et al. Antiviral chlorinated daphnane diterpenoid orthoesters from the bark and wood of Trigonostemon cherrieri. *Phytochemistry* **2012**, *84*, 160–168. [CrossRef]

46. Nothias-Scaglia, L.-F.; Pannecouque, C.; Renucci, F.; Delang, L.; Neyts, J.; Roussi, F.; Costa, J.; Leyssen, P.; Litaudon, M.; Paolini, J. Antiviral Activity of Diterpene Esters on Chikungunya Virus and HIV Replication. *J. Nat. Prod.* **2015**, *78*, 1277–1283. [CrossRef]

47. Gupta, D.K.; Kaur, P.; Leong, S.T.; Tan, L.T.; Prinsep, M.R.; Chu, J.J.H. Anti-Chikungunya viral activities of aplysiatoxin-related compounds from the marine cyanobacterium Trichodesmium erythraeum. *Mar. Drugs* **2014**, *12*, 115–127. [CrossRef] [PubMed]

48. Liu, S.; Chen, R.; Hagedorn, C.H. Tannic Acid Inhibits Hepatitis C Virus Entry into Huh7.5 Cells. *PLoS ONE* **2015**, *10*, e0131358. [CrossRef]

49. Orłowski, P.; Kowalczyk, A.; Tomaszewska, E.; Ranoszek-Soliwoda, K.; Węgrzyn, A.; Grzesiak, J.; Celichowski, G.; Grobelny, J.; Eriksson, K.; Krzyzowska, M. Antiviral Activity of Tannic Acid Modified Silver Nanoparticles: Potential to Activate Immune Response in Herpes Genitalis. *Viruses* **2018**, *10*, 524. [CrossRef]

50. Konishi, E.; Hotta, S. Effects of Tannic Acid and Its Related Compounds upon Chikungunya Virus. *Microbiol. Immunol.* **1979**, *23*, 659–667. [CrossRef]

51. Wagoner, J.; Negash, A.; Kane, O.J.; Martinez, L.E.; Nahmias, Y.; Bourne, N.; Owen, D.M.; Grove, J.; Brimacombe, C.; McKeating, J.A.; et al. Multiple effects of silymarin on the hepatitis C virus lifecycle. *Hepatol. Baltim. Md* **2010**, *51*, 1912–1921. [CrossRef]

52. Lani, R.; Hassandarvish, P.; Chiam, C.W.; Moghaddam, E.; Chu, J.J.H.; Rausalu, K.; Merits, A.; Higgs, S.; Vanlandingham, D.; Abu Bakar, S.; et al. Antiviral activity of silymarin against chikungunya virus. *Sci. Rep.* **2015**, *5*, 11421. [CrossRef]

53. Li, X.; Liu, Y.; Wu, T.; Jin, Y.; Cheng, J.; Wan, C.; Qian, W.; Xing, F.; Shi, W. The Antiviral Effect of Baicalin on Enterovirus 71 In Vitro. *Viruses* **2015**, *7*, 4756–4771. [CrossRef] [PubMed]

54. Lani, R.; Hassandarvish, P.; Shu, M.-H.; Phoon, W.H.; Chu, J.J.H.; Higgs, S.; Vanlandingham, D.; Abu Bakar, S.; Zandi, K. Antiviral activity of selected flavonoids against Chikungunya virus. *Antivir. Res.* **2016**, *133*, 50–61. [CrossRef] [PubMed]

55. Halford, B. THE BRYOSTATINS' TALE. *Chem. Eng. News Arch.* **2011**, *89*, 10–17. [CrossRef]

56. Plimack, E.R.; Tan, T.; Wong, Y.-N.; von Mehren, M.M.; Malizzia, L.; Roethke, S.K.; Litwin, S.; Li, T.; Hudes, G.R.; Haas, N.B. A Phase I Study of Temsirolimus and Bryostatin-1 in Patients With Metastatic Renal Cell Carcinoma and Soft Tissue Sarcoma. *Oncologist* **2014**, *19*, 354–355. [CrossRef]

57. Schrott, L.M.; Jackson, K.; Yi, P.; Dietz, F.; Johnson, G.S.; Basting, T.F.; Purdum, G.; Tyler, T.; Rios, J.D.; Castor, T.P.; et al. Acute oral Bryostatin-1 administration improves learning deficits in the APP/PS1 transgenic mouse model of Alzheimer's disease. *Curr. Alzheimer Res.* **2015**, *12*, 22–31. [CrossRef]

58. Mehla, R.; Bivalkar-Mehla, S.; Zhang, R.; Handy, I.; Albrecht, H.; Giri, S.; Nagarkatti, P.; Nagarkatti, M.; Chauhan, A. Bryostatin Modulates Latent HIV-1 Infection via PKC and AMPK Signaling but Inhibits Acute Infection in a Receptor Independent Manner. *PLoS ONE* **2010**, *5*, e11160. [CrossRef]

59. Abdelnabi, R.; Staveness, D.; Near, K.E.; Wender, P.A.; Delang, L.; Neyts, J.; Leyssen, P. Comparative analysis of the anti-chikungunya virus activity of novel bryostatin analogs confirms the existence of a PKC-independent mechanism. *Biochem. Pharmacol.* **2016**, *120*, 15–21. [CrossRef]

60. Bourjot, M.; Delang, L.; Nguyen, V.H.; Neyts, J.; Guéritte, F.; Leyssen, P.; Litaudon, M. Prostratin and 12- O -Tetradecanoylphorbol 13-Acetate Are Potent and Selective Inhibitors of Chikungunya Virus Replication. *J. Nat. Prod.* **2012**, *75*, 2183–2187. [CrossRef]

61. Varghese, F.S.; Thaa, B.; Amrun, S.N.; Simarmata, D.; Rausalu, K.; Nyman, T.A.; Merits, A.; McInerney, G.M.; Ng, L.F.P.; Ahola, T. The Antiviral Alkaloid Berberine Reduces Chikungunya Virus-Induced Mitogen-Activated Protein Kinase Signaling. *J. Virol.* **2016**, *90*, 9743–9757. [CrossRef]

62. Campbell, W.C.; Fisher, M.H.; Stapley, E.O.; Albers-Schönberg, G.; Jacob, T.A. Ivermectin: A potent new antiparasitic agent. *Science* **1983**, *221*, 823–828. [CrossRef]

63. Wagstaff, K.M.; Sivakumaran, H.; Heaton, S.M.; Harrich, D.; Jans, D.A. Ivermectin is a specific inhibitor of importin α/β-mediated nuclear import able to inhibit replication of HIV-1 and dengue virus. *Biochem. J.* **2012**, *443*, 851–856. [CrossRef] [PubMed]

64. Muhammed Ameen, S.; Drancourt, M. Ivermectin lacks antituberculous activity. *J. Antimicrob. Chemother.* **2013**, *68*, 1936–1937. [CrossRef]

65. Laing, R.; Gillan, V.; Devaney, E. Ivermectin – Old Drug, New Tricks? *Trends Parasitol.* **2017**, *33*, 463–472. [CrossRef] [PubMed]

66. Varghese, F.S.; Kaukinen, P.; Gläsker, S.; Bespalov, M.; Hanski, L.; Wennerberg, K.; Kümmerer, B.M.; Ahola, T. Discovery of berberine, abamectin and ivermectin as antivirals against chikungunya and other alphaviruses. *Antivir. Res.* **2016**, 117–124. [CrossRef] [PubMed]

67. National Research Council (US) Committee on Applications of Toxicogenomic Technologies to Predictive Toxicology. *Application to the Study of Mechanisms of Action*; National Academies Press: Washington, DC, USA, 2007.

68. Kaur, G.; Dufour, J.M. Cell lines. *Spermatogenesis* **2012**, *2*, 1–5. [CrossRef] [PubMed]

69. Ulrich, A.B.; Pour, P.M. Cell Lines. In *Encyclopedia of Genetics*; Brenner, S., Miller, J.H., Eds.; Academic Press: New York, NY, USA, 2001; pp. 310–311.

70. Slater, A.F. Chloroquine: Mechanism of drug action and resistance in Plasmodium falciparum. *Pharmacol. Ther.* **1993**, *57*, 203–235. [CrossRef]

71. Roques, P.; Thiberville, S.-D.; Dupuis-Maguiraga, L.; Lum, F.-M.; Labadie, K.; Martinon, F.; Gras, G.; Lebon, P.; Ng, L.F.P.; de Lamballerie, X.; et al. Paradoxical Effect of Chloroquine Treatment in Enhancing Chikungunya Virus Infection. *Viruses* **2018**, *10*, 268. [CrossRef]

ANEXO III: Restoration of Cyclo-Gly-Pro-induced salivary hyposecretion and submandibular composition by naloxone in mice

PLOS ONE

Restoration of Cyclo-Gly-Pro-induced salivary hyposecretion and submandibular composition by naloxone in mice

Igor Santana Melo[1], Návylla Candeia-Medeiros[1], Jamylle Nunes Souza Ferro[1], Polliane Maria Cavalcante-Araújo[1], Tales Lyra Oliveira[1], Cassio Eráclito Alves Santos[2], Leia Cardoso-Sousa[3], Emilia Maria Gomes Aguiar[3], Stephanie Wutke Oliveira[3,4], Olagide Wagner Castro[1], Renata Pereira Alves-Balvedi[5], Luciano Pereira Rodrigues[5,6], Jandir M. Hickmann[2], Douglas Alexsander Alves[4], Igor Andrade Santos[3], Ana Carolina Gomes Jardim[3], Walter Luiz Siqueira[4], Angelo Ricardo Fávaro Pipi[7], Luiz Ricardo Goulart[5,8], Emiliano de Oliveira Barreto[1], Robinson Sabino-Silva[3,4]*

1 Institute of Biological Sciences and Health, Federal University of Alagoas, Maceio, Alagoas, Brazil, 2 Optics and Materials Group, Optma, Federal University of Alagoas, Maceio, Alagoas, Brazil, 3 Institute of Biomedical Sciences, Federal University of Uberlandia, Uberlandia, Minas Gerais, Brazil, 4 College of Dentistry, University of Saskatchewan, Saskatoon, Saskatchewan, Canada, 5 Institute of Genetics and Biochemistry, Federal University of Uberlandia, Uberlandia, Minas Gerais, Brazil, 6 Institute of Engineering, Science and Technology, Federal University of Jequitinhonha and Mucuri's Valley, Janaúba, Minas Gerais, Brazil, 7 National Centre for Sensor Research, School of Chemical Sciences, Dublin City University, Dublin, Ireland, 8 Department of Medical Microbiology and Immunology, University of California Davis, California, LA, United States of America

* robinsonsabino@gmail.com

Abstract

Cyclo-Gly-Pro (CGP) attenuates nociception, however its effects on salivary glands remain unclear. In this study, we investigated the acute effects of CGP on salivary flow and composition, and on the submandibular gland composition, compared with morphine. Besides, we characterized the effects of naloxone (a non-selective opioid receptor antagonist) on CGP- and morphine-induced salivary and glandular alterations in mice. After that, in silico analyses were performed to predict the interaction between CGP and opioid receptors. Morphine and CGP significantly reduced salivary flow and total protein concentration of saliva and naloxone restored them to the physiological levels. Morphine and CGP also reduced several infrared vibrational modes (Amide I, 1687-1594cm^{-1}; Amide II, 1594-1494cm^{-1}; CH_2/CH_3, 1488-1433cm^{-1}; C = O, 1432-1365cm^{-1}; PO_2 asymmetric, 1290-1185cm^{-1}; PO_2 symmetric, 1135-999cm^{-1}) and naloxone reverted these alterations. The in silico docking analysis demonstrated the interaction of polar contacts between the CGP and opioid receptor Cys219 residue. Altogether, we showed that salivary hypofunction and glandular changes elicited by CGP may occur through opioid receptor suggesting that the blockage of opioid receptors in superior cervical and submandibular ganglions may be a possible strategy to restore salivary secretion while maintaining antinociceptive action due its effects on the central nervous system.

116

Introduction

Saliva exerts multiple functions in the oral cavity such as protection against microorganisms, contribution to the taste and digestion and maintenance of oral health [1–3]. Salivary function is controlled by sympathetic and parasympathetic nervous system, which innervate acinar, ductal, myoepithelial and vascular cells in salivary glands [4,5]. The activation of muscarinic receptors in the acinar cells is the most important control of salivary flow rates [6]. Electrical stimulation of sympathetic efferent branch to the salivary glands results in a low flow of saliva which is rich in proteins [7]. Paradoxically, sympathectomy also generates decrease in salivary flow [8]. These findings demonstrate the complexity of the sympathetic regulation on salivary flow and salivary composition [9]. The activation of central pathways develops a great part in salivatory effects of intraperitoneal pilocarpine in rats [10].

Several substances with pharmacological properties can promote changes in salivary function. Morphine is an opioid receptor agonist that plays intense and long-lasting analgesia [11,12]. It was demonstrated that morphine increase lactate levels in serum, however its effects on salivary lactate concentration are unknown [13]. In humans and rats, the morphine administration was correlated to hyposalivation, and associated with changes in the ionic composition [14–15]. Bearing in mind that amylase is the most abundant protein in saliva [16], salivary amylase concentration decreased after morphine treatment [17]. It has been clearly demonstrated that morphine promotes reduction in the sympathetic activity to salivary glands by its action on the superior cervical ganglion and by inhibiting the release of neurotransmitter from postganglionic nerve endings [17]. Additionally, kappa-, delta-, and mu-opioid-receptor agonists are able to inhibit L-, N- and P/Q-types of calcium channels in submandibular ganglion neurons, indicating a reduction in parasympathetic activity to salivary glands [18]. The reduction on the parasympathetic nerve-induced salivary secretion generated by the morphine was partially reversed by naloxone, a non-selective opioid receptor antagonist. However, salivary secretion stimulated by intravenous infusion of acetylcholine was not reduced by morphine [19].

Cyclic dipeptides are among the smallest peptide derivatives frequently found in nature [20]. Cyclo-Gly-Pro (CGP) is an endogenous diketopiperazine derived from N-terminal tri-peptide, glycine-proline-glutamate which is naturally cleaved from the insulin-like growth factor 1 (IGF-1) [21,22]. Previous studies have shown that CGP induces neuroprotective effects after ischemic brain injury [22]. CGP 35348 has an adjuvant role to produce a dose-dependent antagonism of antinociception [23]. Recently, our group demonstrated that the antinociceptive effect of CGP seemed to be mediated by the interaction with the opioid system, also reducing the hyper nociception and paw inflammation induced by carrageenan [24]. This might indicate the potential of CGP as a candidate for antinociceptive role with fewer side effects on salivary glands. It is important to emphasize that several effects of CGP in oral territories remain unknown.

Despite the knowledge about the effect of pharmacological agents on salivary glands, and consequently on salivary secretion, the CGP capacity to modulate submandibular and salivary components has never been investigated. Besides, it is important to highlight that the interaction between CGP and opioid receptors has also not been demonstrated. Thus, the aims of the present study were to investigate the CGP acute effects on salivary flow and composition, and on submandibular gland composition compared with morphine. Besides, we characterized the naloxone (a non-selective opioid receptor antagonist) effect on CGP- and morphine-induced salivary and glandular alterations in mice. After that, *in silico* analyses were performed to predict the 3D-interaction between the CGP and opioid receptors.

117

Materials and methods

This study was carried out in strict accordance with the recommendations in the Guide for the Care and Use of Laboratory Animals of the Brazilian Society of Laboratory Animals Science (SBCAL). Experimental procedures were approved by the Ethical Committee of the Federal University of Alagoas (UFAL) (License 065/2011), according to Ethical Principles adopted by the Brazilian College of Animal Experimentation (COBEA). Animal studies are reported in compliance with the approved guidelines. To minimize the number of animals used and their suffering all effort were taken. Male Swiss mice (*Mus musculus*, 2 months) weighing 25–36 g were obtained from the breeding colonies of the UFAL and maintained at the Institute of Biological Sciences and Health rodent housing facility. Mice were randomly assigned to standard cages with five animals per cage. Animals were allowed free access to water and standard rodent chow diet and kept at $22 \pm 2°C$ with a 12 h light/dark cycle, light on at 07:00h. To minimize circadian effects, all experimental procedures were conducted during the light phase. Power analysis was used as a basis to set the number of animals per experiment [25]. The number of samples was insert in each legend.

Materials

All used reagents were of analytical grade and used without further purification. The following reagents were used: cyclo-Gly-Pro (CGP, $\geq$ 98% purity; Catalog number: 3705-27-9), morphine solution, naloxone and phosphate-buffered saline (Sigma Chemical Co., St. Louis, MO, USA).

Experimental procedures

Animals were treated with vehicle (NaCl, 0.9%), morphine or CGP (CGP, $\geq$ 98% purity) (Fig 1, Protocol 1). Morphine was applied at dose of 17.5 µmol kg^{-1} (0.1 ml/10g, i.p.) and CGP 1 µmol kg^{-1} (0.1 ml/10g, i.p.), considering the similar antinociceptive effects observed in the hot plate test [24]. For randomization, vehicle was injected in the control group, while the other mice received morphine or CGP. Blinding was implemented as follows: the operator was blinded to the group identity, but not to animals of the same group. Thus, for i.p. drug injection, different solutions were prepared: vehicle, morphine and CGP. In order to analyze the opioid receptors involvement in salivary secretion and changes in submandibular composition, similar analysis was performed in another set of animals under naloxone administration (pre-treatment)(15.3 µmol kg^{-1}, i.p.), an opioid receptor antagonist, 15 minutes before treatment with vehicle, morphine or CGP (Fig 1, Protocol 2).

Saliva and salivary glands collection

One hour after treatment with vehicle, morphine or CGP, the animals were intraperitoneally anesthetized (xylazine 5 mg kg^{-1}body weight; ketamine 35 mg kg^{-1}) and then parasympathetic stimulation was performed for salivary secretion through pilocarpine injection (2 mg kg^{-1}, i. p.). Total saliva was collected for 10 min from the oral cavity [26]. After that, submandibular and parotid glands were collected and weighted [27]. Salivary secretion was calculated based on volume of saliva acquired in 10 minutes collection divided by the weight of the salivary gland tissues (µl/g tissue) (Fig 1).

Total protein concentration of saliva

Total protein concentration was measured using Bradford Protein assay. Values were expressed in mg/ml using serum albumin as standard protein. [28].

118
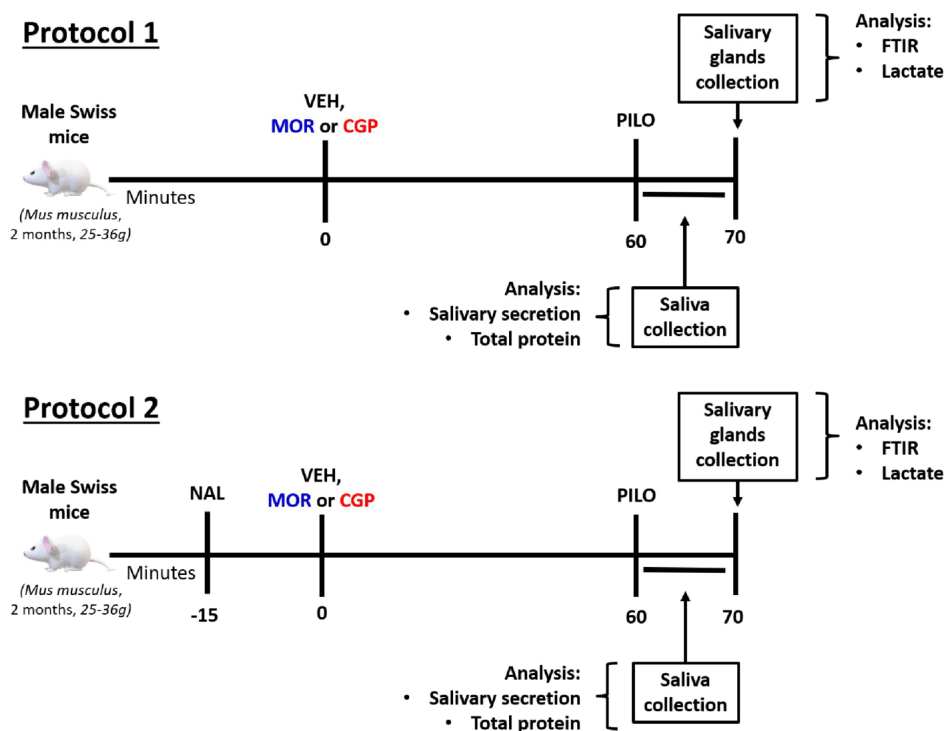
Fig 1. Experimental design of the acute treatment with vehicle, morphine or CGP in male Swiss mice in two protocols with or without the previous administration of naloxone. In protocol 1, mice were treated acutely with vehicle (VEH, NaCl, 0.9%), morphine (MOR, 17.5 µmol kg⁻¹, ip) or CGP (1 µmol kg⁻¹, ip). After one hour of treatment, a parasympathetic stimulus with pilocarpine (PILO, 2 mg kg⁻¹, ip) was performed during 10 min for salivary secretion and salivary composition analysis. Immediately after saliva collection, submandibular glands were removed and storage at −80˚C. The CGP and morphine effects on submandibular gland molecular composition were observed by Attenuated total reflectance Fourier transform infrared (ATR-FTIR) spectroscopy and lactate level analysis. In protocol 2, naloxone (15.3 µmol kg⁻¹, ip) was administered 15 minutes prior to acute treatment with vehicle, morphine and CGP in order to evaluate the opioid receptors involvement in saliva and submandibular gland.

Saliva analysis by dispersive x-ray analysis system (EDX)

Pilocarpine-stimulated saliva from Protocol 1 animals was used to assess the inorganic elements by EDX (Fig 1). In each experiment,15 µL of saliva were used to measure the ionic composition. EDX mode was set up as 180 seconds per sample ion detection using Si (Li) semiconductor detector (Shimadzu, Fukuoka, Japan) at 30 kV in a vacuum chamber. Ions quantification was taken from the excitement of their electrons.

Lactate concentration of submandibular glands

Submandibular gland specimens were tested using an enzymatic system for lactate quantitative determination (Labtest, Brazil). Experiment was done according to the manufacturer's

119

instruction. The submandibular tissue was removed, washed using physiological saline (NaCl 0.9%), and immediately frozen at—80˚C. Frozen gland tissue was homogenized in a phosphate buffer (1 : 10 w/v, pH 7.4). To measure the lactate concentration, the homogenate (25 μg) was incubated in a solution with 4- aminoantipyrine (50 mmol/L), peroxidase, L-lactate oxidase (1,000 U/L) e N-ethyl-N-(2-hydroxy-3-sulfopropyl)-3-methylaniline (1.5 mmol/L) and sodium azide (0.09%) at 37˚C for 5 minutes using a spectrophotometer at 340 nm.

Histology

The histological analysis in submandibular glands were performed only in animals described in protocol 1 (Fig 1). Submandibular glands were fixed in 10% buffered formalin. Subsequently, these glands were dehydrated in alcohol (80, 90 and 100%), cleared in xylene and embedded in paraffin. Histological sections with a thickness of 5 μm were acquired using a microtome (Leica RM2125). Then these sections were placed on slides and stained with hematoxylin and eosin. Histological slides were examined and micrograph pictures were obtained using an optical microscope (Olympus BX41).

Acetylcholinesterase activity of submandibular glands

The acetylcholinesterase (AChE) activity quantification in submandibular glands were performed only in animals described in protocol 1 (Fig 1) using a acetylcholine as substrate (Ach, Sigma Chemical, St. Louis, Mo, USA) at room temperature. The submandibular glands were homogenized in saline (1:10, 0.9%), through a tissue shredder (Polytron®). In a 96-well plate, acetylcholine (50μL) was added, and then color reagent was added and taken to incubator for 3 minutes at 37˚C. Subsequently, sample (20μL) was added [the first well received deionized water (20μL) and the second the standard solution (20μL)] and then taken back to the water bath for 2.5 minutes at 37˚C. Finally, a blocked solution (150μL) was added for subsequent reading at the spectrophotometer (at absorbance 410nm). The AChE activity was determined by the sample value product. Enzyme activity values were calculated after normalization by a total protein concentration measured using Bradford assay.

Molecular profile in submandibular glands by ATR-FTIR spectroscopy

Submandibular glands spectra were recorded in 4000–400 cm-1 region using FTIR spectrophotometer Vertex 70 (Bruker Optik) using a micro-attenuated total reflectance (ATR) accessory. The fingerprint region was chosen to be displayed due to the interest region. All spectra were recorded at room temperature (23±1˚C). The crystal material unit in ATR unit was a diamond disc as internal-reflection element. The sample penetration depth ranges between 0.1 and 2 μm and depends on the wavelength and the refractive index of the ATR-crystal material. In the ATR-crystal the infrared beam is reflected at the interface toward the sample. Twenty mg of submandibular were lyophilized using a rotary evaporator (Thermo Savant, San Jose, CA) to obtain sample spectra. The air spectrum was used as a background in ATR-FTIR analysis. Samples spectrum were taken with 4 cm^{-1} of resolution and 32 scans were performed to each analysis. The ATR-FTIR spectra were also baseline corrected using OPUS software [29]. Table 1 shows the frequencies and assignments of the vibrational modes identified in submandibular glands. Briefly, the vibrational mode between 1687–1594 cm^{-1} is identified as υ_NH (Amide I) bending vibrations [29–31]. The δ_NH (Amide II) bending vibration is usually represented between 1594-1494cm^{-1}[29,32]. The vibrational modes between 1488–1433 cm^{-1} are attributed to CH_2/CH_3 vibrations. The band between 1432–1365 cm^{-1} demonstrates CO groups (ester) stretching vibrations. Besides, spectral area between 1290–1185 cm^{-1} indicates PO_2 asymmetric [29]. The 1135–999 cm^{-1} spectral area corresponds PO_2 symmetric [29].

120

Table 1. ATR-FTIR wavenumber with respective vibrational modes and related chemical component in submandibular glands of vehicle-, morphine- and CGP-treated mice in the presence or absence of naloxone.

Wavenumber (cm^{-1})	Vibrational modes	Chemical component
1635 (1687–1594)	υ_NH (Amide I)	Proteins
1550 (1594–1494)	δ_NH (Amide II)	Proteins
1450 (1488–1433)	CH_2/CH_3	Lipids/proteins
1400 (1432–1365)	CO groups (ester)	Proteins
1232 (1290–1185)	PO_2 asymmetric	Phospholipids
1031 (1135–999)	PO_2 symmetric	Glycogen

The vibrational mode assignments were obtained from references [29–33].

https://doi.org/10.1371/journal.pone.0229761.t001

Cyclo-Gly-Pro (CGP) and opioid receptor (OR) structure assembly and interaction

The human Opioid Receptor protein FASTA sequence (Homo sapiens, access number in Gene Bank: AAA73958.1) was submitted online in I-TASSER server to predict and generate high-quality 3D predictions of this protein. The best model was verified using RAMPAGE: Assessment of the Ramachandran Plot, and Verify3D web tools to determine the spatial coherence and compatibility of the atomic model (3D) with its own amino acid sequence (1D). The CGP 3D structure was obtained from Pubchem (PubChem CID: 193540). After that, *in silico* analyses were performed to predict the interaction of both structures. Auto-DOCK Vina [34] was used do predict the molecular docking using the Root-mean-square deviation of atomic positions (RMSd) and free energy calculations. PyMOL Molecular Graphics System, Version 2.0 Schrödinger, LLC, was used to visualize the CGP-OP interactions and export image files.

Statistical analysis

In this study, data and statistical analysis comply with the recommendations on experimental design and analysis in pharmacology [35]. Values are presented as mean ± SEM. The heat map and analyses were performed using GraphPad Prism 5.0 (GraphPad Software, San Diego, CA, USA). Kolmorogov-Smirnov test was used to determine the normality of the sample distributions. Comparisons of results were performed by ANOVA, followed by Turkey's or Dunnett's post-test at P value <0.05.

Results

Effects of opioid receptors (OR) in salivary secretion and salivary composition

Salivary secretion was significantly reduced in morphine compared to vehicle (~15%; *p* <0.05). Similarly, CGP significantly decreased salivary secretion compared to vehicle (~20%, *p* <0.05). Differences in salivary secretion were not significant between morphine- and CGP-treated mice (Fig 2A). To confirm the effects of the opioid receptors, naloxone was administered before the treatment with vehicle, morphine or CGP. The pilocarpine-stimulated salivary secretion remained unchanged after naloxone administration in vehicle mice (*p* >0.05; Fig 2A). On the other hand, naloxone significantly increased the salivary secretion in mice treated with CGP and morphine (~20% and 30%, respectively; *p* <0.01) (Fig 2A).

121
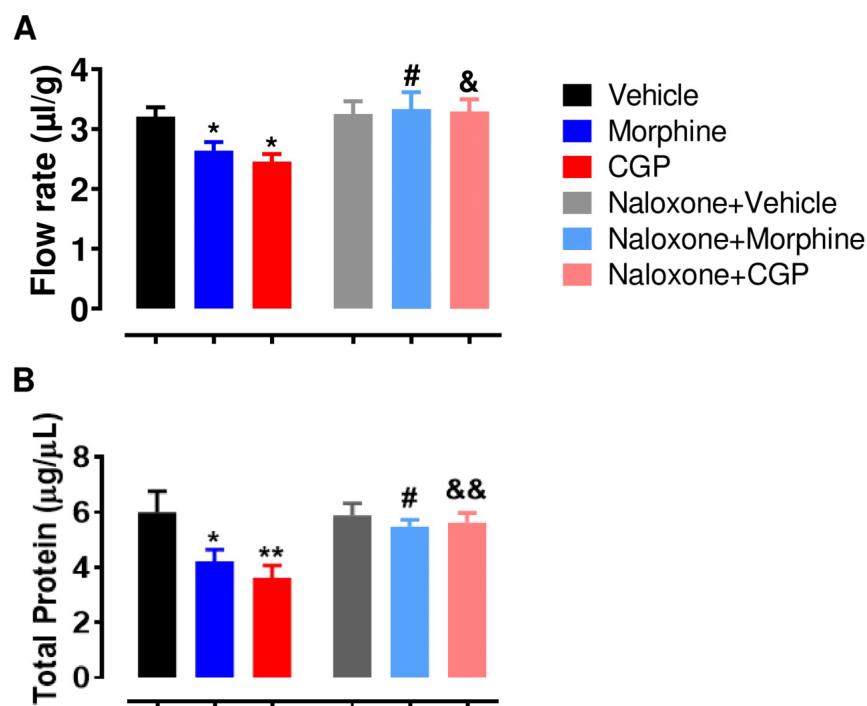
Fig 2. Salivary flow of Swiss mice and salivary total protein concentration after acute treatment with vehicle, morphine or CGP in the presence or absence of naloxone. CGP, Cyclo-Gly-Pro. Naloxone (15.3 μmol kg^{-1}, i.p.), an opioid receptor antagonist, was administered 15 minutes before treatment with vehicle, morphine or CGP. One hour after treatment, parasympathetic stimulation was performed for salivary secretion through pilocarpine injection (2 mg kg^{-1}, i.p.) and total saliva was collected for 10 minutes from the oral cavity. (A) Salivary flow was expressed as salivary secretion per gram of glandular tissue (μl/g tissue), equivalent to the ratio of the volume of salivary secretion and the weight sum of glandular parotid and submandibular. (B) Salivary total protein concentration was expressed as μg/μL. Results are represented as mean ± SEM of 6–9 animals; $^{*}P < 0.05$ vs. vehicle; #$P < 0.05$ vs. morphine; &$P < 0.05$ vs CGP. One-way ANOVA, Turkey as post hoc test.

In order to analyze the effects of CGP and morphine, total protein concentration in saliva was measure using Bradford assay. Total protein concentration in saliva significantly decreased ($p < 0.01$) when CGP (~45%) and morphine (~35%) was administrated and compared to vehicle (Fig 2B). Total protein concentration in saliva was similar ($p > 0.05$) in morphine and CGP-treated mice. The administration of naloxone in vehicle mice kept the total protein concentration stable ($p > 0.05$; Fig 2B). On the other hand, naloxone significantly increased the total protein concentration in saliva of mice treated with CGP and morphine (~40%; $p < 0.001$; Fig 2B).

Dispersive X-ray analysis was performed to analyze the CGP and morphine effects on the ionic composition in saliva. The composition of potassium, chloride, sodium and sulfur ions in saliva remained unchanged after acute treatment with morphine or CGP compared to vehicle (S1 Fig).

122

Maintenance of salivary glands weight under opioid receptors (OR) blockade

In order to investigate the CGP or morphine effects in salivary glands, the parotid and submandibular glands were properly weighed. The results demonstrated that the glands weight remained unchanged after acute treatment with morphine or CGP (Table 2). As expected, the salivary glands weight also did not change with the naloxone pre-treatment (Table 2).

Histological changes of submandibular gland under opioid receptors (OR) blockade

To determine whether CGP promoted morphological and structural changes in salivary gland compared to the morphine treatment, we stained the submandibular sections with hematoxylin-eosin. The acinar cells, ductal cells and connective tissue remained unaltered (S2A Fig). However, submandibular glands histological analysis showed of evacuated spaces increased between serous and mucous acini in glandular parenchyma after one-hour treatment with morphine or CGP compared to the vehicle (S2B and S2C Fig).

Effects of opioid receptors (OR) blockade on lactate levels of submandibular glands

Morphine (~15%) and CGP (~15%) increased ($p<0.001$) lactate levels in submandibular gland compared to vehicle (Fig 3). Lactate levels in submandibular glands were similar ($p>0.05$) in morphine and CGP-treated mice. The lactate levels in submandibular gland remained unchanged after naloxone administration in vehicle mice ($p>0.05$; Fig 3). On the other hand, naloxone significantly decreased this parameter in mice treated with CGP and morphine (~20%; $p<0.001$) (Fig 3).

Effects of opioid receptors (OR) blockade on acetylcholinesterase activity in of submandibular glands

The acetylcholinesterase activity in submandibular gland was unaffected after acute treatment with morphine (0.16 UA/μg ± 0.02, $p>0.05$) or CGP (0.15 UA/μg ± 0.02, $p>0.05$) compared to vehicle (0.15 UA/μg ± 0.03). Besides, acetylcholinesterase activity in submandibular gland was similar ($p>0.05$) in morphine and CGP-treated mice (S3 Fig).

Table 2. Parotid and submandibular weights from vehicle-, morphine- or CGP-treated mice in the presence or absence of naloxone.

Treatment	Submandibular weight (mg)	Parotid weight (mg)
Vehicle	51,21 ± 2,81 (9)	28,42 ± 1,55 (9)
Morphine	50,50 ± 3,05 (10)	34,44 ± 4,35 (10)
CGP	49,01 ± 2,62 (10)	31,56 ± 3,11 (10)
Naloxone+ Vehicle	50,20 ± 3,44 (6)	30,03 ± 5,38 (6)
Naloxone+Morphine	50,98 ± 4,12 (6)	32,77 ± 5,69 (6)
Naloxone+CGP	52,67 ± 5,39 (6)	31,22 ± 3,80 (6)

CGP, cyclo-Gly-Pro. $P>0.05$ vs. vehicle. One-way ANOVA, Student-Newman-Keuls as post hoc test.

https://doi.org/10.1371/journal.pone.0229761.t002

123
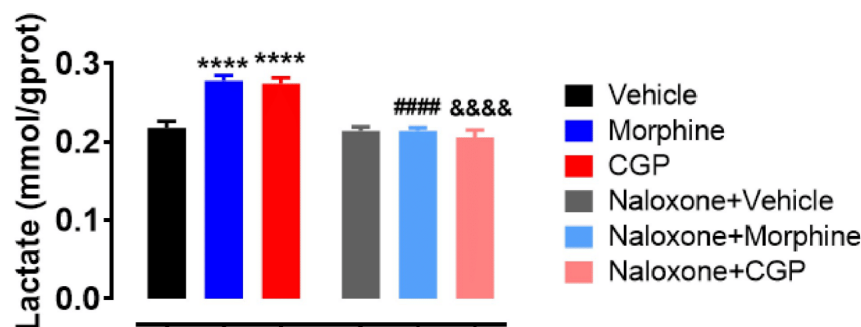
Fig 3. Lactate levels in submandibular gland of Swiss mice after acute treatment with vehicle, morphine or CGP in the presence or absence of naloxone. Morphine and CGP increased lactate levels in submandibular gland, but naloxone restored this parameter to the baseline. CGP, Cyclo-Gly-Pro. Results are represented as mean ± SEM of 6 animals; *$P < 0.05$ vs. vehicle. One-way ANOVA, Dunnett as post hoc test.

Effects of opioid receptors (OR) blockade on chemical profile in submandibular by ATR-FTIR spectroscopy

The submandibular gland infrared spectrum is a superposition of several compounds and the absorption bands in ATR-FTIR spectrum intensities are directly proportional to the components concentration. The submandibular gland spectra of vehicle-, CGP- or morphine-treated animals in presence or absence of naloxone are represented in Fig 4A.

To understand better the response of proteins, phospholipids and lipids in submandibular gland under opioid receptors (OR) blockade, we analyzed the area of molecular components using ATR-FTIR spectroscopy. There are six major vibrational modes highlighted at 1635 cm^{-1} (1687–1594 cm^{-1}), 1550 cm^{-1} (1594–1494 cm^{-1}), 1450 cm^{-1} (1488–1433 cm^{-1}), 1400 cm^{-1} (1432–1365 cm^{-1}), 1232 cm^{-1} (1290–1185 cm^{-1}) and 1031 cm^{-1} (1135–999 cm^{-1}), confirming the presence of proteins, lipids, phospholipids and glycogen, according to the details showed for each peak, corresponding to the specific vibration molecules (Fig 4A). The vibrational modes between 1687–1594 cm^{-1} and 1594–1494 cm^{-1}, representing amide I and amide II, respectively, were reduced in morphine- or CGP-treated mice. These changes were reversed by the pre-treatment with naloxone (Fig 4B and 4C). The vibrational modes between 1488–1433 cm^{-1} and 1432–1365 cm^{-1}, representing CH$_2$/CH$_3$ and C = O, respectively, were also reduced in morphine- or CGP-treated mice. These changes were also reversed by the pre-treatment with naloxone (Fig 4D and 4E). Besides, two vibrational modes at 1290–1185 and 1135–999 cm^{-1} were also reduced in morphine- or CGP-treated mice compare to the vehicle. These vibrational modes represent PO$_2$ asymmetric and PO$_2$ symmetric, respectively, and the naloxone pre-treatment reversed the changes in both submandibular glands components (Fig 4F and 4G). A heat map with the mean relative changes clearly demonstrates the expression in these vibrational modes (Fig 4H).

Assembly and interaction of the OR and CGP structure

In silico modeling of OR and molecular docking of OR and CGP were performed by I-TASSER server. Fig 5A shows the full cartoon structure of OP (green) interacting with CGP (red). The extended view of the interaction site from docking analysis demonstrated the polar contacts (yellow dashes) between the CGP (red) and the OR Cys219 residue (Fig 5B). Fig 5C shows the

125
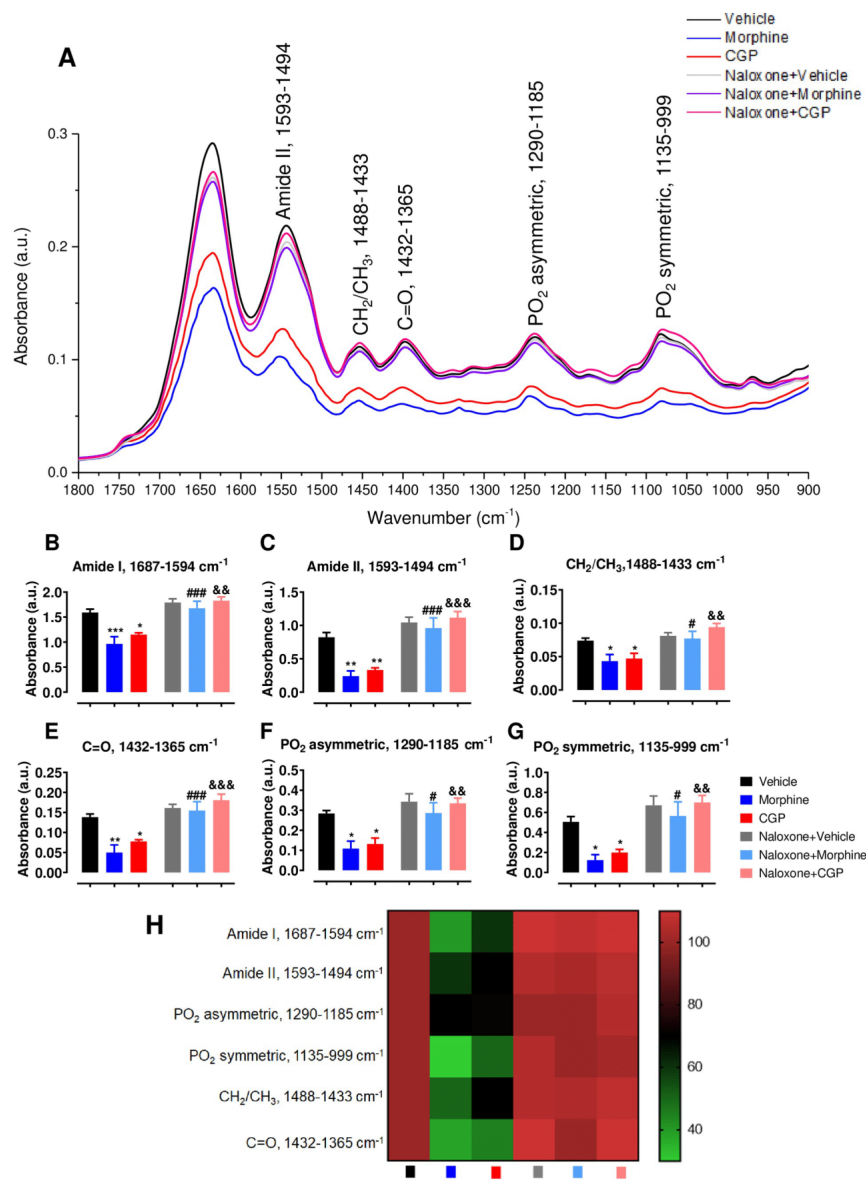
Fig 4. Chemical compounds profile in submandibular gland represented by means of ATR-FTIR spectra of Swiss mice after acute treatment with vehicle, morphine or CGP in the presence or absence of naloxone. (A) ATR-FTIR spectra displayed in 1800–800 cm^{-1} region. The major vibrational modes are represented, indicating changes under the acute treatment with CGP or morphine on the various chemical compounds present in the submandibular gland. These changes were reversed by naloxone pre-treatment. (B) Amide I (1687–1594 cm-1), (C) Amide II (1594–1494 cm^{-1}), (D) CH2/CH3 (1488–1433 cm^{-1}), (E) C = O (1432–1365 cm^{-1}), (F) PO$_2$ asymmetric (1290–1185 cm^{-1}) and (G) PO$_2$ asymmetric (1135–999 cm^{-1}). (H) Heat map with the relative expression of each vibrational mode (Vehicle expression was set as 100%). Results are represented as mean ± SEM of 6 animals.

full surface of the structure of OP (green) coupled with CGP (red) and Fig 5D presents the OP framework and conformational interaction site.

Discussion

The opioid agonist depressant mechanisms on salivary secretion and salivary glandular tissue effects remain unclear. Additionally, the potential effects of therapeutic agents in secondary target organs as salivary glands still need to be carefully investigated. Given the ongoing attempts to describe opioid side effects on salivary function, it is clearly important to understand and characterize the CGP effects in saliva and salivary glands composition compared with morphine. We showed that either CGP or morphine promoted the reduction in flow rates and in salivary protein concentration, increased lactate levels in glandular tissue and resulted in severe changes in chemical components in submandibular glands. Conversely, the naloxone (a non-selective opioid receptor antagonist) reversed this alteration in saliva and submandibular glands.

Human salivary secretion was decreased from 1 to 4 hours after administration of morphine intravenously [36]. Besides, the treatment with morphine (6 mg/kg) also inhibited the
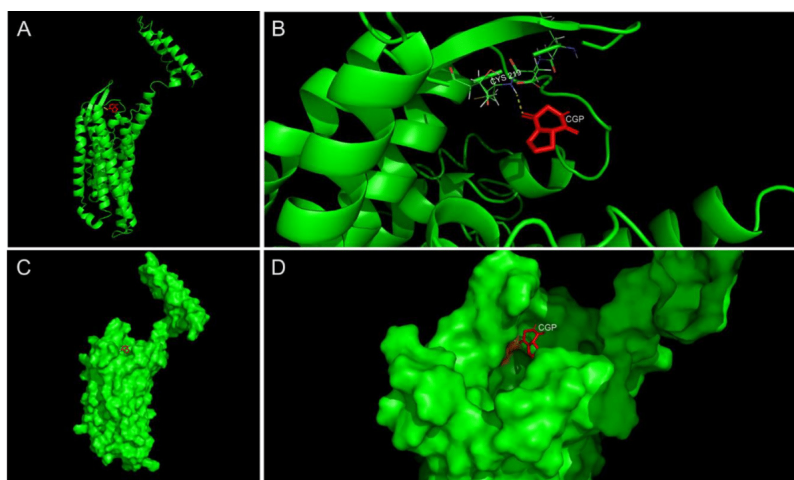
Fig 5. Assembly and interaction of the OR and CGP structure. (A) Full cartoon structure of OP (green) coupled with CGP (red). (B) Expanded image of binding site from docking analysis. Polar contacts are shown by yellow dashes between the CGP (red) and the OR Cys219 residue. (C) Full surface structure of OP (green) coupled with CGP (red). (D) OP framework and conformational interaction site (green). The binding spot to CGP (red) is presented in orange.

126

salivary flow in rats [14]. As expect, in this present study the acute treatment with morphine promoted salivary secretion reduction. Furthermore, for the first time, we showed that CGP also reduces salivary secretion in mice.

Previous studies have demonstrated that naloxone partially restores pilocarpine-stimulated and parasympathetic nerve stimulated-salivary secretion under morphine treatment [14,19]. As expected, our data corroborates previous studies demonstrating that naloxone reversed the morphine depressant effects in salivary flow. We further investigated whether the salivary flow changes elicited by CGP were also reversed by naloxone, due to its nonspecific antagonistic action on mu, kappa and delta opioid receptors [37]. It is important to point out that the opioid receptors blockage by naloxone was also able to reverse the inhibitory effect caused by CGP and to restore the salivary flow, indicating the CGP effect in opioid receptors as described to morphine treatment. So, these data suggest similar side effects on salivary glands by CGP or morphine.

Salivary ionic composition remained unchanged after acute treatment with CGP or morphine (5 mg kg^{-1}). In previous research, morphine at a dose of 25 mg kg^{-1}did not alter the sodium and calcium concentrations in parotid saliva of rats; on the other hand, led to an increase in salivary potassium concentration [19]. Interestingly, morphine at a dose of 6 mg kg^{-1} did not alter the presence of salivary potassium concentration, however it was able to reduce the salivary calcium and increase salivary sodium concentration [14]. It is possible that samples collected using different methods contributed to these different results. Despite the contradictory reports evaluating morphine effects on ions composition under lower and higher doses, our data on CGP showing no changes in salivary ionic composition has never been reported and suggests that CGP may not be involved in the regulation of several channels that regulate ionic composition in salivary glands.

We have also shown that CGP, as well as morphine, decreased salivary protein concentration in mice, which is corroborated elsewhere by the demonstration that an acute treatment with morphine (6 mg kg^{-1}) decreased protein concentration in saliva from the rat submandibular gland [14]. Considering that sympathetic activity on salivary glands is the most important control of salivary protein secretion and pointing out that the presence of opioid receptors in submandibular and parotid glands was never demonstrated, the CGP or morphine effects to reduce protein concentration in saliva could be due a direct interference of cAMP in cells that express opioid receptors. Moreover, the tolerance to opioid receptors changes the pathway signal transduction by the cAMP-dependent protein kinase [38,39]. Thus, if opioid receptors are expressed in salivary glands, probably morphine and CGP reduces the cAMP directly in these glands, which is a key mechanism that may be involved in reduced protein secretion in saliva. However, another explanation for morphine and CGP inhibitory effects on salivary protein concentration may be due to the opioid receptors presence that might have inhibited preganglionic or ganglionic sympathetic nerve projecting to salivary gland [40–42]. In both hypotheses, it seems clear that our study indicates inhibition of effects promoted by CGP and morphine by interaction with opioid receptors.

The reduction in salivary protein concentration and in Amide I/Amide II of submandibular promoted by opioid agonists is a characteristic of tissues that have low sympathetic activity and/or low glucose utilization, likely because they need to have a low energy status [43]. Besides, we also showed that both treatments are able to reduce glycogen, indicating influence of opioid system in glycogen metabolism on submandibular glands [44]. Specifically, the present study describes evacuated spaces (previously occupied by secretory acini) between acinar and ductal cells in glandular parenchyma of submandibular glands under morphine- and CGP-treatment. The fast (1h) effect of morphine and CGP suggests that it is not solely a consequence of reduction of parasympathetic/sympathetic activity. This is in agreement with

127

morphine-induced apoptosis of murine J774 cells mediated through TGF-beta [45]. Notably, this change is reinforced in morphine-treated mice. Considering the acute morphological changes with morphine and CGP, we can still propose induction of more profound morphological changes during chronic treatment. However, these effects could be promoted by the activation of kappa-, delta-, and/or mu-opioid-receptor by morphine and CGP in submandibular ganglion [18,24,46].

The CH_2 reduction in lipids [47] after morphine and CGP treatments suggests a decrease in lipid rafts that translocate proteins from intracellular structures to the plasma membrane [48], as well as decreasing energy status. Opioid agonists reduced PO_2 asymmetric of phospholipids, indicating damage in plasma membrane, which is also an apoptotic characteristic [49].

Considering the similar changes in salivary secretion and submandibular composition promoted by both therapeutic agents, we can consider that CGP have similar inhibitory effect on autonomic activity to salivary glands as described to morphine [18]. The CGP antinociceptive effect was antagonized by naloxone, a non-selective opioid receptor antagonist, suggesting that CGP effect may also occur through opioid receptor at the supraspinal level [24,50]. CGP increased neuronal activity in midbrain periaqueductal gray (PAG), a key relay station in the processing of nociceptive information in central nervous system [24,51] and that is interconnected with the hypothalamus [52]. Opioid receptors are spread in the hypothalamus [53] and these hypothalamic neurons may have inhibitory projections to superior salivary nucleus, from where ganglionic fibers of parasympathetic nervous system spread to submandibular glands [54–56]. Morphine also activates PAG [57], which suggest similar repercussion of CGP.

The muscarinic receptors sensitivity s in salivary glands was not reduced by morphine [19]. Therefore, we evaluated whether the salivary secretion reduction after treatment with CGP and morphine could be explained by acetylcholine decreased levels in the extracellular fluid, which could be demonstrated by acetylcholinesterase enzyme increased activity. Previous studies have shown an increase in brain acetylcholinesterase expression, 30 minutes after morphine injection (10 mg kg^{-1} of morphine), indicating a higher enzyme activity and further acetylcholine degradation.[58]. However, another study showed that morphine chronic administration decreases acetylcholinesterase activity in the midbrain [59]. It is noteworthy that the acute effect of morphine and CGP on acetylcholinesterase activity in salivary gland has never been reported. Bearing in mind that the expected reduction of acetylcholine in synaptic cleft due to lower parasympathetic activity [18] is associated with similar acetylcholinesterase activity in submandibular glands after morphine and CGP treatment, it is expected that the acetylcholine presence in synaptic cleft can be further reduced due to the acetylcholine/acetylcholinesterase ratio. Furthermore, these data emphasize that the reduction of pilocarpine–induced salivary secretion by morphine and CGP is likely to be prejunctional. Considering the present results and previous reports, we suggest a central and autonomic-pathway leading to changes in submandibular gland and hyposalivation by morphine and CGP (Fig 6).

To the best of our knowledge, this is the first report that demonstrates the salivary hyposecretion elicited by CGP, which is mediated by the opioid receptors' system and such effect was reversed by naloxone. The present study also provides new evidence for an inhibitory morphine effect in pilocarpine-salivary secretion mediated by the opioid system in mice. Morphine and CGP also reduced salivary protein concentration and increased the lactate in submandibular gland and naloxone reverted both alterations. Morphine and CGP also reduced several infrared vibrational modes representing Amide I, Amide II, CH_2/CH_3, C = O, PO_2 asymmetric and PO_2 symmetric, which was blocked by pre-treatment with naloxone. To confirm the pathway to CGP effects, the *in silico* docking analysis demonstrate the polar contacts interaction between the CGP and opioid receptor Cys219 residue. Altogether, we showed that salivary hypofunction and glandular changes elicited by CGP may occur through opioid receptor

128
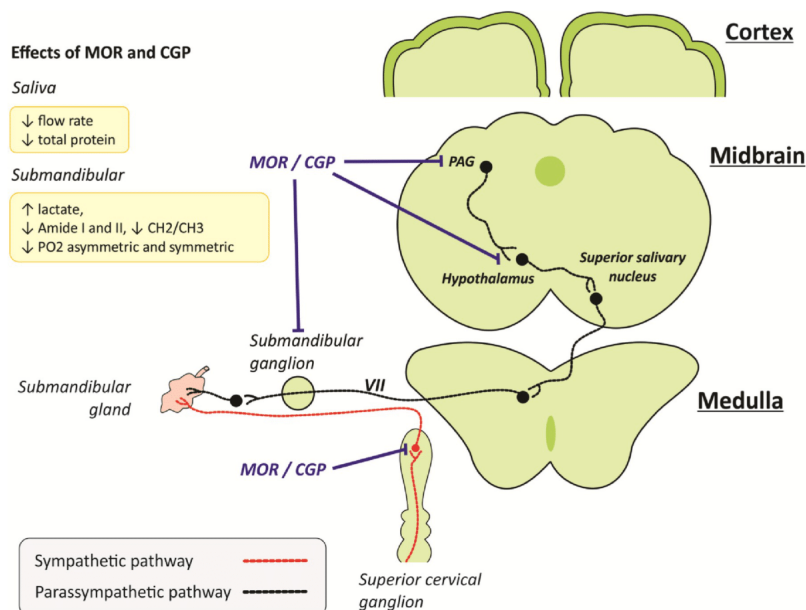
Fig 6. Schematic draw of a proposed pathway for morphine- and CGP-induced regulation of midbrain and autonomic ganglions.
Arrows indicate the salivary and submandibular gland contents regulations (↑increase, ↓decrease) under morphine or CGP treatments.
Blue line indicates the inhibitory effect of morphine and CGP to autonomic pathway to submandibular glands. Red and black lines
indicate the sympathetic and parasympathetic pathway to submandibular gland. Opioid receptors are expressed in PAG [51],
hypothalamus [52,53], submandibular ganglia [18,46] and superior cervical [41,42] ganglia. CGP, cyclo-Gly-Pro.

https://doi.org/10.1371/journal.pone.0229761.g006

suggesting that opioid receptors blockage in superior cervical ganglion and submandibular
ganglion may be a possible strategy to restore salivary secretion while maintaining antinoci-
ceptive effects due its effects in central nervous system.

Supporting information

**S1 Fig. Effect of acute treatment with CGP and morphine on ionic composition present in
stimulated saliva.** (A-D) Inorganic elements of pilocarpine-stimulated saliva were evaluated
the by fluorescent X-ray method. Concentrations of potassium (A), sulfur (B), chloride (C)
and sodium (D) ions in the stimulated saliva remained unchanged after acute treatment with
CGP and morphine. CGP, cyclo-Gly-Pro. Results are mean ± SEM of 6 animals; $P>0.05$ vs.
vehicle. One-way ANOVA, Dunnett as post hoc test.
(PPT)

**S2 Fig. Photomicrograph of submandibular gland from Swiss mice after 1h-treatment
with vehicle, morphine and CGP.** (A) The submandibular gland morphology is intact in vehi-
cle-treated mice. (B) The acute treatment with morphine was able to increase the evacuated
spaces (arrows) between the mucosal and serous acini in the submandibular gland

129

parenchyma. (C) This change was not markedly evident after one hour of CGP treatment. Images are representative of 8 animals in each group. CGP, cyclo-Gly-Pro. Magnification, x400; scale bar, 20 μm.
(PPT)

S3 Fig. Activity of AChE enzyme in submandibular glands from Swiss mice after acute treatment with vehicle, morphine and CGP. CGP, cyclo-Gly-Pro. Results are mean ± SEM of 5 animals; $p > 0.05$ vs. vehicle. One-way ANOVA, Dunnett as post hoc test.
(PPT)

Acknowledgments

Author Contributions

Conceptualization: Igor Santana Melo, Douglas Alexsander Alves, Emiliano de Oliveira Barreto, Robinson Sabino-Silva.

Data curation: Igor Santana Melo, Návylla Candeia-Medeiros, Jamylle Nunes Souza Ferro, Robinson Sabino-Silva.

Formal analysis: Igor Santana Melo, Jamylle Nunes Souza Ferro, Stephanie Wutke Oliveira, Douglas Alexsander Alves, Igor Andrade Santos, Ana Carolina Gomes Jardim, Walter Luiz Siqueira, Robinson Sabino-Silva.

Funding acquisition: Emiliano de Oliveira Barreto, Robinson Sabino-Silva.

Investigation: Igor Santana Melo, Návylla Candeia-Medeiros, Jamylle Nunes Souza Ferro, Polliane Maria Cavalcante-Araújo, Tales Lyra Oliveira, Cassio Eráclito Alves Santos, Leia Cardoso-Sousa, Emilia Maria Gomes Aguiar, Stephanie Wutke Oliveira, Renata Pereira Alves-Balvedi, Luciano Pereira Rodrigues, Douglas Alexsander Alves, Igor Andrade Santos, Ana Carolina Gomes Jardim, Walter Luiz Siqueira, Angelo Ricardo Fávaro Pipi, Robinson Sabino-Silva.

Methodology: Igor Santana Melo, Návylla Candeia-Medeiros, Jamylle Nunes Souza Ferro, Polliane Maria Cavalcante-Araújo, Tales Lyra Oliveira, Cassio Eráclito Alves Santos, Leia Cardoso-Sousa, Emilia Maria Gomes Aguiar, Stephanie Wutke Oliveira, Renata Pereira Alves-Balvedi, Luciano Pereira Rodrigues, Jandir M. Hickmann, Douglas Alexsander Alves, Igor Andrade Santos, Ana Carolina Gomes Jardim, Angelo Ricardo Fávaro Pipi, Luiz Ricardo Goulart, Emiliano de Oliveira Barreto, Robinson Sabino-Silva.

Project administration: Robinson Sabino-Silva.

Resources: Jandir M. Hickmann, Luiz Ricardo Goulart, Emiliano de Oliveira Barreto, Robinson Sabino-Silva.

Supervision: Ana Carolina Gomes Jardim, Walter Luiz Siqueira, Robinson Sabino-Silva.

Validation: Igor Santana Melo, Stephanie Wutke Oliveira, Robinson Sabino-Silva.

Visualization: Igor Santana Melo, Stephanie Wutke Oliveira, Olagide Wagner Castro, Douglas Alexsander Alves, Igor Andrade Santos, Ana Carolina Gomes Jardim, Walter Luiz Siqueira, Robinson Sabino-Silva.

130

References

1. Humphrey SP, Williamson RT. A review of saliva: Normal composition, flow, and function. J Prosthet Dent. 2001; 85: 162–169. https://doi.org/10.1067/mpr.2001.113778 PMID: 11208206

2. Aps JKM, Martens LC. Review: The physiology of saliva and transfer of drugs into saliva. Forensic Sci Int. 2005; 150: 119–131. https://doi.org/10.1016/j.forsciint.2004.10.026 PMID: 15944052

3. Ruhl S. The scientific exploration of saliva in the post-proteomic era: from database back to basic function. Expert Rev Proteomics. 2012; 9: 85–96. https://doi.org/10.1586/epr.11.80 PMID: 22292826

4. Emmelin N. Nerve interactions in salivary glands. J Dent Res. 1987; 66: 509–517. https://doi.org/10.1177/00220345870660022101 PMID: 3305629

5. Sabino-Silva R, Ceroni A, Koganezawa T, Michelini LC, Machado UF, Antunes VR. Baroreceptor-mediated activation of sympathetic nerve activity to salivary glands. Physiol Behav. 2012; 107: 390–6. https://doi.org/10.1016/j.physbeh.2012.09.012 PMID: 23022472

6. Proctor GB, Carpenter GH. Regulation of salivary gland function by autonomic nerves. Auton Neurosci Basic Clin. 2007; 133: 3–18. https://doi.org/10.1016/j.autneu.2006.10.006

7. Carpenter GH, Garrett JR, Hartley RH, Proctor GB. The influence of nerves on the secretion of immunoglobulin A into submandibular saliva in rats. J Physiol. 1998; 512 (Pt 2: 567–73. https://doi.org/10.1111/j.1469-7793.1998.567be.x

8. Garrett JR. The proper role of nerves in salivary secretion: a review. J Dent Res. 1987; 66: 387–397. https://doi.org/10.1177/00220345870660020201 PMID: 3305622

9. Sabino-Silva R, Alves-Wagner ABT, Burgi K, Okamoto MM, Alves AS, Lima G a, et al. SGLT1 protein expression in plasma membrane of acinar cells correlates with the sympathetic outflow to salivary glands in diabetic and hypertensive rats. Am J Physiol Endocrinol Metab. 2010; 299: E1028–37. https://doi.org/10.1152/ajpendo.00395.2010 PMID: 20841505

10. Renzi A, Colombari E, Mattos Filho TR, Silveira JE, Saad WA, Camargo LA, et al. Involvement of the central nervous system in the salivary secretion induced by pilocarpine in rats. J Dent Res. 1993; 72: 1481–4. https://doi.org/10.1177/00220345930720110401 PMID: 8227698

11. Meert TF, Vermeirsch H a. A preclinical comparison between different opioids: Antinociceptive versus adverse effects. Pharmacol Biochem Behav. 2005; 80: 309–326. https://doi.org/10.1016/j.pbb.2004.12.002 PMID: 15680184

12. Rougeot C, Robert F, Menz L, Bisson J-F, Messaoudi M. Systemically active human opiorphin is a potent yet non-addictive analgesic without drug tolerance effects. J Physiol Pharmacol. 2010; 61: 483–90. Available: http://www.ncbi.nlm.nih.gov/pubmed/20814077 PMID: 20814077

13. COSMO A. DiFAZIO;CHEN PIN-YANG. The Influence of Morphine on Excess Lactate Production. Anesth Analg. 1971; 50: 211–216. Available: https://insights.ovid.com/pubmed?pmid=5102636 PMID: 5102636

14. Abdollahi M, Safarhamidi H. Protection by nitric oxide of morphine-induced inhibition of rat submandibular gland function. Pharmacol Res. 2002; 45: 87–92. https://doi.org/10.1006/phrs.2001.0910 PMID: 11846618

15. Hashemi N, Mohammadirad A, Bayrami Z, Khorasani R, Vosough S, Aliahmadi A, et al. Restoration of morphine-induced alterations in rat submandibular gland function by N-methyl-D-aspartate agonist. Acta Biol Hung. 2006; 57: 283–294. https://doi.org/10.1556/ABiol.57.2006.3.2 PMID: 17048692

16. Crosara KTB, Zuanazzi D, Moffa EB, Xiao Y, Machado MA de AM, Siqueira WL. Revealing the Amylase Interactome in Whole Saliva Using Proteomic Approaches. Biomed Res Int. Hindawi; 2018; 2018: 1–15. https://doi.org/10.1155/2018/6346954

17. Miwa Y, Saeki M, Yamaji A, Maeda S, Saito K. Effect of morphine on secretion of amylase from isolated parotid acini. Life Sci. 1996; 59: 1809–19. Available: http://www.ncbi.nlm.nih.gov/pubmed/8937508 doi: 10.1016/0024-3205(96)00524-3 PMID: 8937508

131

18. Endoh T, Suzuki T. The regulating manner of opioid receptors on distinct types of calcium channels in hamster submandibular ganglion cells. Arch Oral Biol. 1998; 43: 221–33. Available: http://www.ncbi. nlm.nih.gov/pubmed/9631175 doi: 10.1016/s0003-9969(98)00002-8 PMID: 9631175

19. Bowen SR, Carpenter FG. Morphine depression and tolerance of nerve-induced parotid secretion. Br J Pharmacol. 1979; 65: 7–13. Available: http://www.ncbi.nlm.nih.gov/pubmed/760892 doi: 10.1111/j. 1476-5381.1979.tb17327.x PMID: 760892

20. Prasad C. Bioactive cyclic dipeptides. Peptides. 1995; 16: 151–64. Available: http://www.ncbi.nlm.nih. gov/pubmed/7716068 doi: 10.1016/0196-9781(94)00017-z PMID: 7716068

21. Burgos-Ramos E, Martos-Moreno G a, López MG, Herranz R, Aguado-Llera D, Egea J, et al. The N-terminal tripeptide of insulin-like growth factor-I protects against beta-amyloid-induced somatostatin depletion by calcium and glycogen synthase kinase 3 beta modulation. J Neurochem. 2009; 109: 360–370. doi:JNC5980 [pii]\r10.1111/j.1471-4159.2009.05980.x https://doi.org/10.1111/j.1471-4159.2009. 05980.x PMID: 19220704

22. Guan J, Gluckman PD. IGF-1 derived small neuropeptides and analogues: A novel strategy for the development of pharmaceuticals for neurological conditions. Br J Pharmacol. 2009; 157: 881–891. https://doi.org/10.1111/j.1476-5381.2009.00256.x PMID: 19438508

23. Hammond DL, Washington JD. Antagonism of L-baclofen-induced antinociception by CGP 35348 in the spinal cord of the rat. Eur J Pharmacol. 1993; 234: 255–62. Available: http://www.ncbi.nlm.nih.gov/ pubmed/8387011 doi: 10.1016/0014-2999(93)90961-g PMID: 8387011

24. Ferro JN de S, de Aquino FLT, de Brito RG, Dos Santos PL, Quintans J de SS, de Souza LC, et al. Cyclo-Gly-Pro, a cyclic dipeptide, attenuates nociceptive behaviour and inflammatory response in mice. Clin Exp Pharmacol Physiol. 2015; 42: 1287–95. https://doi.org/10.1111/1440-1681.12480 PMID: 26277051

25. Charan J, Kantharia N. How to calculate sample size in animal studies? J Pharmacol Pharmacother. 2013; 4: 303. https://doi.org/10.4103/0976-500X.119726 PMID: 24250214

26. Zoukhri D, Kublin CL. Impaired Neurotransmitter Release from Lacrimal and Salivary Gland Nerves of a Murine Model of Sjogren's Syndrome. Invest Ophthalmol Vis Sci. 2001; 42: 925–932. https://doi.org/10. 1016/j.biotechadv.2011.08.021.Secreted PMID: 11274068

27. Sabino-Silva R, Okamoto MM, David-Silva A, Mori RC, Freitas HS, Machado UF. Increased SGLT1 expression in salivary gland ductal cells correlates with hyposalivation in diabetic and hypertensive rats. Diabetol Metab Syndr. 2013; 5: 64. https://doi.org/10.1186/1758-5996-5-64 PMID: 24499577

28. Bradford MM. A rapid and sensitive method for the quantitation of microgram quantities of protein utilizing the principle of protein-dye binding. Anal Biochem. 1976; 72: 248–54. Available: http://www.ncbi. nlm.nih.gov/pubmed/942051 doi: 10.1006/abio.1976.9999 PMID: 942051

29. Khaustova S, Shkurnikov M, Tonevitsky E, Artyushenko V, Tonevitsky A. Noninvasive biochemical monitoring of physiological stress by Fourier transform infrared saliva spectroscopy. Analyst. 2010; 135: 3183–92. https://doi.org/10.1039/c0an00529k PMID: 20953513

30. Schultz CP, Ahmed MK, Dawes C, Mantsch HH. Thiocyanate levels in human saliva: quantitation by Fourier transform infrared spectroscopy. Anal Biochem. 1996; 240: 7–12. https://doi.org/10.1006/abio. 1996.0323 PMID: 8811872

31. Christersson CE, Lindh L, Arnebrant T. Film-forming properties and viscosities of saliva substitutes and human whole saliva. Eur J Oral Sci. 2000; 108: 418–25. Available: http://www.ncbi.nlm.nih.gov/ pubmed/11037758 doi: 10.1034/j.1600-0722.2000.108005418.x PMID: 11037758

32. Júnior PCC, Strixino JF, Raniero L. Analysis of saliva by Fourier transform infrared spectroscopy for diagnosis of physiological stress in athletes. Res Biomed Eng. 2015; 31: 116–124. https://doi.org/10. 1590/2446-4740.0664

33. Zohdi V, Whelan DR, Wood BR, Pearson JT, Bambery KR, Black MJ. Importance of Tissue Preparation Methods in FTIR Micro-Spectroscopical Analysis of Biological Tissues: 'Traps for New Users.' Tajmir-Riahi H-A, editor. PLoS One. Public Library of Science; 2015; 10: e0116491. https://doi.org/10.1371/ journal.pone.0116491 PMID: 25710811

34. Trott O, Olson AJ. AutoDock Vina: improving the speed and accuracy of docking with a new scoring function, efficient optimization, and multithreading. J Comput Chem. NIH Public Access; 2010; 31: 455–61. https://doi.org/10.1002/jcc.21334 PMID: 19499576

35. Curtis MJ, Bond RA, Spina D, Ahluwalia A, Alexander SPA, Giembycz MA, et al. Experimental design and analysis and their reporting: new guidance for publication in BJP. Br J Pharmacol. 2015; 172: 3461–71. https://doi.org/10.1111/bph.12856 PMID: 26114403

36. Westerling D, Höglund P, Lundin S, Svedman P. Transdermal administration of morphine to healthy subjects. Br J Clin Pharmacol. 1994; 37: 571–576. https://doi.org/10.1111/j.1365-2125.1994.tb04306.x PMID: 7917776

132

37. Peres e Serra A, Ashmawi HA. Influence of naloxone and methysergide on the analgesic effects of low-level laser in an experimental pain model. Rev Bras Anestesiol. 2010; 60: 302–10. https://doi.org/10.1016/S0034-7094(10)70037-4 PMID: 20682161

38. Fundytus ME, Coderre TJ. Chronic inhibition of intracellular Ca2+ release or protein kinase C activation significantly reduces the development of morphine dependence. Eur J Pharmacol. 1996; 300: 173–181. doi:0014299995008713 [pii] https://doi.org/10.1016/0014-2999(95)00871-3 PMID: 8739205

39. Smith FL, Lohmann AB, Dewey WL. Involvement of phospholipid signal transduction pathways in morphine tolerance in mice. Br J Pharmacol. 1999; 128: 220–6. https://doi.org/10.1038/sj.bjp.0702771 PMID: 10498855

40. TRENDELENBURG U. The action of morphine on the superior cervical ganglion and on the nictitating membrane of the cat. Br J Pharmacol Chemother. 1957; 12: 79–85. Available: http://www.ncbi.nlm.nih.gov/pubmed/13413156 doi: 10.1111/j.1476-5381.1957.tb01366.x PMID: 13413156

41. Zhang C, Bachoo M, Polosa C. The receptors activated by exogenous and endogenous opioids in the superior cervical ganglion of the cat. Brain Res. 1993; 622: 211–214. https://doi.org/10.1016/0006-8993(93)90821-4 PMID: 8242358

42. Zhang C, Bachoo M, Morales M, Collier B, Polosa C. The site of inhibitory action of endogenous opioids in the superior cervical ganglion of the cat. Brain Res. Elsevier; 1995; 683: 59–64. https://doi.org/10.1016/0006-8993(95)00360-3

43. Isabella R, Raffone E. Does ovary need D-chiro-inositol? J Ovarian Res. 2012; 5: 14. https://doi.org/10.1186/1757-2215-5-14 PMID: 22587479

44. Gill A, Gao N, Lehrman MA. Rapid activation of glycogen phosphorylase by the endoplasmic reticulum unfolded protein response. J Biol Chem. 2002; 277: 44747–53. https://doi.org/10.1074/jbc.M205001200 PMID: 12223475

45. Singhal PC, Kapasi AA, Franki N, Reddy K. Morphine-induced macrophage apoptosis: the role of transforming growth factor-beta. Immunology. 2000; 100: 57–62. Available: http://www.ncbi.nlm.nih.gov/pubmed/10809959 doi: 10.1046/j.1365-2567.2000.00007.x PMID: 10809959

46. Endoh T, Suzuki T. The effects of delta-opioid receptor agonists on synaptic transmission in hamster submandibular ganglion. Bull Tokyo Dent Coll. 1995; 36: 87–90. Available: http://www.ncbi.nlm.nih.gov/pubmed/8689748 PMID: 8689748

47. Huang N, Short M, Zhao J, Wang H, Lui H, Korbelik M, et al. Full range characterization of the Raman spectra of organs in a murine model. Opt Express. 2011; 19: 22892–909. Available: http://www.ncbi.nlm.nih.gov/pubmed/22109167 doi: 10.1364/OE.19.022892 PMID: 22109167

48. Feng S, Huang S, Lin D, Chen G, Xu Y, Li Y, et al. Surface-enhanced Raman spectroscopy of saliva proteins for the noninvasive differentiation of benign and malignant breast tumors. Int J Nanomedicine. 2015; 10: 537–47. https://doi.org/10.2147/IJN.S71811 PMID: 25609959

49. Tegeder I, Geisslinger G. Opioids as modulators of cell death and survival—unraveling mechanisms and revealing new indications. Pharmacol Rev. 2004; 56: 351–69. https://doi.org/10.1124/pr.56.3.2 PMID: 15317908

50. Heinricher MM, Tavares I, Leith JL, Lumb BM. Descending control of nociception: Specificity, recruitment and plasticity. Brain Res Rev. 2009; 60: 214–25. https://doi.org/10.1016/j.brainresrev.2008.12.009 PMID: 19146877

51. Bandler R, Shipley MT. Columnar organization in the midbrain periaqueductal gray: modules for emotional expression? Trends Neurosci. 1994; 17: 379–89. Available: http://www.ncbi.nlm.nih.gov/pubmed/7817403 doi: 10.1016/0166-2236(94)90047-7 PMID: 7817403

52. Yaksh TL, Yeung JC, Rudy TA. Systematic examination in the rat of brain sites sensitive to the direct application of morphine: observation of differential effects within the periaqueductal gray. Brain Res. 1976; 114: 83–103. Available: http://www.ncbi.nlm.nih.gov/pubmed/963546 doi: 10.1016/0006-8993(76)91009-x PMID: 963546

53. Yaksh TL. Spinal systems and pain processing: Development of novel analgesic drugs with mechanistically defined models. Trends Pharmacol Sci. 1999; 20: 329–337. https://doi.org/10.1016/s0165-6147(99)01370-x PMID: 10431212

54. Segal K, Lisnyansky I, Nageris B, Feinmesser R. Parasympathetic innervation of the salivary glands. Oper Tech Otolaryngol Neck Surg. Elsevier; 1996; 7: 333–338. https://doi.org/10.1016/S1043-1810(96)80005-4

55. Lin LH, Agassandian K, Fujiyama F, Kaneko T, Talman WT. Evidence for a glutamatergic input to pontine preganglionic neurons of the superior salivatory nucleus in rat. J Chem Neuroanat. 2003; 25: 261–268. doi:S0891061803000334 [pii] https://doi.org/10.1016/s0891-0618(03)00033-4 PMID: 12842271

56. Mitoh Y, Funahashi M, Kobashi M, Matsuo R. Excitatory and inhibitory postsynaptic currents of the superior salivatory nucleus innervating the salivary glands and tongue in the rat. Brain Res. 2004; 999: 62–72. https://doi.org/10.1016/j.brainres.2003.11.053 PMID: 14746922

133

PLOS ONE

Restoration of cyclo-Gly-Pro-induced salivary hyposecretion

57. Hao S, Liu S, Zheng X, Zheng W, Ouyang H, Mata M, et al. The role of TNFα in the periaqueductal gray during naloxone-precipitated morphine withdrawal in rats. Neuropsychopharmacology. 2011; 36: 664–76. https://doi.org/10.1038/npp.2010.197 PMID: 21068718

58. Mohanakumar KP, Sood PP. Acetylcholinesterase changes in the central nervous system of mice during the development of morphine tolerance addiction and withdrawal. Brain Res Bull. 1983; 10: 589–96. Available: http://www.ncbi.nlm.nih.gov/pubmed/6683583 doi: 10.1016/0361-9230(83)90026-6 PMID: 6683583

59. Neugebauer NM, Einstein EB, Lopez MB, McClure-Begley TD, Mineur YS, Picciotto MR. Morphine dependence and withdrawal induced changes in cholinergic signaling. Pharmacol Biochem Behav. 2013; 109: 77–83. https://doi.org/10.1016/j.pbb.2013.04.015 PMID: 23651795

134

ANEXO IV: Antivirals against Coronaviruses: candidate drugs for the SARS-CoV-2 treatment?

Antivirals against Coronaviruses: candidate drugs for the SARS-CoV-2 treatment?

Igor d. Santos[1], Victória R. Grosche[1], Robinson Sabino-Silva[2, 3], Ana C. Jardim[1, 4*]

[1]Laboratory of Virology, Institute of Biomedical Sciences, Federal University of Uberlândia, Brazil, [2]Department of Physiology, Institute of Biomedical Sciences, Federal University of Uberlandia, Brazil, [3]College of Dentistry, University of Saskatchewan, Canada, [4]Institute of Biosciences, Humanities and Exact Sciences, São Paulo State University, Brazil

In review

135

Author contribution statement

IA: Drafting the manuscript and literature review. VR: Drafting the manuscript and illustration. AC and RS: critical revision and editing, and final approval of the final version. All the authors read and approved the final manuscript.

Keywords

antivirals, Coronaviruses, COVID-19, SARS-CoV-2, Treatment

Abstract

Word count: 120

Coronaviruses (CoVs) is a group of viruses from family Coronaviridae which can infect human and animals, causing mild to severe diseases. The ongoing pandemic of the severe acute respiratory syndrome coronavirus 2 (SARS-CoV-2) represents a global threat, urging into the development of new therapeutic strategies. Here we presented a selection of relevant compounds, from 2005 up to now, with in vitro and/or in vivo antiviral activities against human and/or animal CoVs. We also presented compounds that have reached clinical trials, as well as further discuss the potentiality of other molecules towards their application in (re)emergent CoVs outbreaks. Finally, through the rationalization of the data herein presented, we wish to encourage further research encompassing these compounds as potential SARS-CoV-2 drug candidates.

Contribution to the field

Coronaviruses (CoVs) is a group of viruses from Coronaviridae family. These viruses are able to infect vertebrate animals causing acute and chronic disease in respiratory, cardiac, enteric and central nervous systems, both in humans and animals. There are seven human CoVs which can induce mild to severe symptoms as dyspnea, severe acute respiratory disease (SARS) and even death. CoVs are classified as a zoonotic disease and are linked to host jumps as were seen in severe acute respiratory disease CoV (SARS-CoV), middle east respiratory syndrome CoV (MERS-CoV) and, more recently, in SARS-CoV-2. The spread of SARS-CoV-2 worldwide is classified as a pandemic disease and represent a threat to global public health. Associated with the high transmissibility, the lack of vaccine and antivirals drugs demonstrates the need to develop novel therapies to treat infected patients. This review aims to summarize compounds from 2005 up to now with already described antiviral activity in vitro and in vivo to human and animal CoVs. These compounds may present as a source of molecules with potent biological activities which could be further investigated for their use as novel approaches against SARS-CoV-2.

Antivirals against Coronaviruses: candidate drugs for the SARS-CoV-2 treatment?

Igor de Andrade Santos[1], Victória Riquena Grosche[1,2], Fernando Rodrigues Goulart Bergamini[3], Robinson Sabino-Silva[4] and Ana Carolina Gomes Jardim[1,2*].

[1]Laboratory of Virology, Institute of Biomedical Science, Federal University of Uberlândia, Uberlândia, MG, Brazil

[2]Institute of Biosciences, Language and Exact Sciences, São Paulo State University, São José do Rio Preto, SP, Brazil

[3]Laboratory of Synthesis of Bioinspired Molecules, Institute do Chemistry, Federal University of Uberlândia, Uberlândia, MG, Brazil;[4]Department of Physiology, Institute of Biomedical Sciences, Federal University of Uberlândia, Uberlândia, MG, Brazil

* Correspondence:

Corresponding author**:** Professor Ana Carolina Gomes Jardim

E-mail: jardim@ufu.br

Institute of Biomedical Science, ICBIM/UFU, Avenida Amazonas, 4C- Room 216, Umuarama, Uberlândia, Minas Gerais, Brazil, CEP: 38405-302

Tel: +55 (34) 3225‑8682

Words: 9983   Figures: 2   Tables:2

ABSTRACT

Coronaviruses (CoVs) is a group of viruses from family *Coronaviridae* which can infect human and animals, causing mild to severe diseases. The ongoing pandemic of the severe acute respiratory syndrome coronavirus 2 (SARS-CoV-2) represents a global threat, urging into the development of new therapeutic strategies. Here we presented a selection of relevant compounds, from 2005 up to now, with *in vitro* and/or *in vivo* antiviral activities against human and/or animal CoVs. We also presented compounds that have reached clinical trials, as well as further discuss the potentiality of other

30   molecules towards their application in (re)emergent CoVs outbreaks. Finally, through the

31   rationalization of the data herein presented, we wish to encourage further research encompassing these

32   compounds as potential SARS-CoV-2 drug candidates.

33

34   **INTRODUCTION**

35   Coronaviruses (CoVs) were first identified in 1960 (Kahn and McIntosh, 2005) and were

36   classified as members of the family *Coronaviridae*. CoVs are enveloped, single-stranded RNA viruses

37   with a genome varying from 25 to 32 kb (Payne, 2017). The viral structure is primarily formed by the

38   structural proteins such as spike (S), membrane (M), envelope (E), and nucleocapsid (N) proteins. The

39   S, M, and E proteins are embedded in the viral envelope, a lipid bilayer derived from the host cell

40   membrane. The N protein, on other hand, interacts with the viral RNA into the core of the virion (Figure

41   1) (Fehr and Perlman, 2015).

42   These viruses can infect vertebrate animals causing acute to chronic diseases in respiratory,

43   cardiac, enteric and central nervous systems, both in animals and humans (Weiss and Navas-Martin,

44   2005). In animals, the most common CoVs are infectious bronchitis virus (IBV), feline CoV (FeCoV),

45   and mouse hepatitis virus (MHV), which infects chickens, felines and rodents, respectively (Cui et al.,

46   2019). To date, there are seven known CoVs that cause diseases in humans: HCoV-229E, HCoV-

47   NL63, HCoV-OC43, HCoV-HKU1, severe acute respiratory syndrome coronavirus (SARS-CoV),

48   middle east respiratory syndrome coronavirus (MERS-CoV) and, most recently, SARS-CoV-2

49   (Graham et al., 2013; CDC, 2020). The CoVs HCoV-229E, HCoV-NL63, HCoV-OC43 and HCoV-

50   HKU1 cause mild symptoms, similar to a common cold (Payne, 2017). However, SARS-CoV, MERS-

51   CoV and SARS-CoV-2 can cause mild to severe symptoms related to upper respiratory infection as

52   fever, cough, dyspnea, pneumonia, acute respiratory distress syndrome (ARDS), ultimately leading to

53   death (Lai et al., 2020). The severe clinical condition generated specially by SARS-CoV-2 have been

54   burdening the public health system worldwide (Hsu et al., 2020), evidencing the mandatory need for

55   further research encompassing this somehow and, until recently, relatively ignored topic by broad

56   pharmaceutical and medicinal fields (Lu et al., 2015; Cui et al., 2019).

57   CoVs are linked to a zoonotic transmission for their ability to infect different species. It can

58   lead to host jumps, allowing the emergence of a new coronaviruses such as SARS-CoV, MERS-CoV

59   and SARS-CoV-2 (Lu et al., 2015; Reusken et al., 2016; Andersen et al., 2020). The transmission of

2

60   CoVs is based on fecal-oral route in animals (Kipar et al., 2010). In humans, CoVs transmission occurs

61   by direct contact with droplets when infected and recipient individuals are in close contact (about one

62   meter). These infectious oral and respiratory droplets produced by talking, coughing, sneezing need to

63   contact the mucosae (mouth and nose) or conjunctiva (eyes) of the recipient person. Additionally,

64   indirect transmission can occur by touching a surface with viable CoV and subsequent contact with

65   mouth, nose or eyes (Doremalen et al., 2020). Viral particles may remain viable on surfaces for several

66   days, increasing the probability of infection by third parts (Doremalen et al., 2020).

67   Recently, SARS-CoV-2 emergence was related to zoonotic transmission, but it is still not clear

68   how this virus was first transmitted to humans (Andersen et al., 2020; Gorbalenya et al., 2020b). By

69   phylogenetic analysis, the SARS-CoV-2 was grouped within bat SARS-related coronaviruses,

70   suggesting that a host jump have occurred (Cao et al., 2020a; Lai et al., 2020). Aggravatingly, the high

71   transmissibility of this new CoV allowed the rapid and efficient spread of the virus across the world,

72   becoming a pandemic disease in just a few months (CDC, 2020; Wu et al., 2020).

73   Due to the novelty of such disease, there is a lack of understanding of SARS-CoV-2 replication

74   process in host cells. The general mechanisms of entry into host cell, replication and release follow

75   characteristics described to other CoVs and that have partially been confirmed to SARS-CoV-2. To

76   date, it is known that the SARS-CoV-2 virion entries the host cells by the attachment of the S protein

77   with the angiotensin-converting enzyme 2 receptor (ACE2), defining SARS-CoV-2 tropism for cells

78   that express this receptor, as pulmonary, hepatic, gastrointestinal and renal human cells (Chu et al.,

79   2020; Hoffmann et al., 2020; Tai et al., 2020). The interaction of ACE2 with the receptor binding

80   domain (RBD) of the S protein triggers the virion endocytoses and formation of an endosome (Rabi et

81   al., 2020). The S protein possess two subunits, S1 and S2 (Walls et al., 2020). During endocytoses, an

82   acid-dependent proteolytic cleavage of the S1 protein by cellular proteases, like cathepsin, TMPRRS2

83   and trypsin, exposes the S2 subunit, a fusion peptide that allows the fusion of the viral envelope with

84   the endosome membrane, and consequently, release the capsid into the cell cytoplasm (Belouzard et

85   al., 2009; Matsuyama et al., 2020). In the cytoplasm, the CoV viral genome is uncoated and the viral

86   RNA is released. The positive-sense RNA viral genome is translated to produce nonstructural proteins

87   (nsps) from two open reading frames (ORFs), ORF1a and ORF1b. The ORF1a encodes the polyprotein

88   pp1a that is cleaved in 11 nsps, while the ORF1b encodes the polyprotein pp1ab which is cleaved into

89   15 nsps. The proteolytic cleavage is performed by viral proteases nsp3 and nsp5 (Yogo et al., 1977;

90   Lai and Stohlman, 1981; Kim et al., 2020). The nsps assemble to form a replicase-transcriptase

91   complex (RTC) responsible for RNA synthesis, replication and transcription of nine subgenomic RNAs

3

92   (sgRNAs) (Chen et al., 2020; Kim et al, 2020; Fehr and Perlman, 2015). The sgRNAs act as mRNAs

93   for structural and accessory genes localized downstream of the replicase polyproteins. SARS-CoV-2

94   has 6 accessory proteins: 3a, 6, 7a, 7b, 8 and 10 (Kim et al., 2020). The structural proteins S, E and M

95   are translated from the sgRNAs and forwarded to the endoplasmic reticulum (ER), and, subsequently,

96   inserted in an intermediate compartment of ER with Golgi (ERGIC). There, viral genomes are

97   encapsulated by N proteins and assembled with the structural proteins to form virions (Fehr and

98   Perlman, 2015; Li et al., 2020; Siu et al., 2008). The M proteins bind to E protein and nucleocapsid,

99   and then, the S protein is incorporated, forming a complete virion. Finally, the virions are transported

100 to the cell surface in vesicles and released in a pathway mediated by exocytosis (Figure 2) (Fehr and

101 Perlman, 2015; Kim et al, 2020; Li et al., 2020).

102   It is important to emphasize that SARS-CoV-2 shows different epidemiological and clinical

103 features from the epidemics of SARS-CoV and MERS-CoV (Ceccarelli et al., 2020; Gorbalenya et al.,

104 2020b, 2020a). The high transmissibility of SARS-CoV-2 may be related to its entry on host cells (Sun

105 et al., 2020). Although both the SARS-CoV and SARS-CoV-2 glycoprotein S attaches to the ACE2 to

106 enter the host cells, the binding affinity of SARS-CoV-2 is higher, thus enhancing its infectivity (Sun

107 et al., 2020; Yan et al., 2020). Despite the relative homology between S1 and S2 amino acid sequences,

108 a 1.2 Å root-mean-square deviation at 417 position (Lusvarghi and Bewley, 2016) of S2 protein in

109 SARS-CoV-2 may be related to its higher infectiveness, contributing to a 10- to 20-fold higher kinetics

110 affinity of SARS-CoV-2 ectodomain, as evidenced by Wrapp and co-workers, employing surface

111 plasmon resonance measurements (Wrapp et al., 2020).

112   Considering the particularities of SARS-CoV-2 and the emergency caused by its outbreak,

113 several strategies have been adopted to develop therapeutics and prophylactic measures against this

114 virus. The strategies approached in these development include: i) utilization of bioinformatics onto

115 prediction and investigation of potential ligands towards target molecules in the viral structure and/or

116 replication (Ahmed et al., 2020, 2; Jeon et al., 2020, 2); ii) employment of cell culture systems,

117 permissive to CoVs (Caly et al., 2020; Liu et al., 2020), associated with pseudo particles, subgenomic

118 replicons and/or full-length CoVs, seeking to assess cellular response or effects of the compounds on

119 viral replicative cycle (Roberts et al., 2006; Hoffmann et al., 2020); iii) animal models as mice, mouse,

120 guinea pig, hamster and non-human primates for evaluating therapeutic options or antibody production

121 in immunization (Natoli et al., 2020; Sheahan et al., 2020) and iv) clinical trials, assessing

122 administration, distribution, metabolism and toxicity profiles (ADMeTox) of potential the therapeutics

123 as well as immunization effects in humans (Clark et al., 2019).

4

124   Based in previous results in vaccine development for MERS-CoV and SARS-CoV, and their

125 similarity with SARS-CoV-2 (Dhama et al., 2020), the current vaccine candidates are more focused in

126 S protein, since is a major inducer of neutralizing antibodies in infected patients (Walls et al., 2020).

127 For this reason, the efforts are concentrated in using approaches as mRNA, DNA, viral vectors or virus-

128 like particles vaccines with a full-length S protein or S1 receptor-binding domain (RBD) to stimulates

129 immune response and immunization (Ahmed et al., 2020; Chen et al., 2020). The most promising

130 vaccines are: i) adenovirus-vectored (AZD1222) produced by Oxford University (Thomas, 2020), a

131 vaccine which is currently in clinical phase 3, being tested in several countries, including the United

132 States, Brazil, and countries in Asia and Africa; ii) mRNA-1273 associated with a lipidic nanoparticle

133 (NCT04283461), currently in clinical phase 2; and iii) inactivated virus vaccine, currently in clinical

134 phase 1 (Mullard, 2020; Tu et al., 2020).

135   The high transmissibility and viral variability of the novel SARS-CoV-2, associated with the

136 lack of vaccine or drugs to treat the infected patients, threaten the global health system. In this context,

137 the development of effective antivirals is critical to bring short-term therapies able to reduce the

138 severity of clinical outcomes of the coronavirus disease 2019 (COVID-19) and to reduce the spread of

139 SARS-CoV-2. Here, we summarized compounds described to possess antiviral activity *in vitro* and/or

140 *in vivo* against CoVs, from 2005 up to now, and critically compared molecules that could be further

141 investigated by their clinical applicability (Table 1). We also discussed the compounds that have

142 reached clinical trials (Table 2) as well as the potentiality of other molecules towards their application

143 in (re)emergent CoVs outbreaks. Finally, we aimed to encourage further research encompassing these

144 compounds as potential SARS-CoV-2 drug candidates.

145

INHIBITORS OF CoVs REPLICATIVE CYCLE

Inhibitors of CoVs entry into host cells

148   The entry of human CoVs into the host cells is mainly related to the binding of viral S protein

149 to the ACE2 receptor (Prabakaran et al., 2004; Sun et al., 2020). Therefore, it is reasonable to

150 hypothesize that compounds affecting this interaction could be potential antivirals (Prabakaran et al.,

151 2004).

152   In this context, a survey encompassing *in silico* studies of more than 140 thousand potential S-

153 Protein-inhibiting drugs indicated that the molecule N-(2-aminoethyl)-1 aziridineethanamine (NAAE)

5

154   showed the highest docking grade (-23,7 kcal/mol) (Huentelman, et al., 2004). The activity of NAAE

155   was further confirmed employing an *in vitro* enzymatic inhibitory assay, using a human recombinant

156   ACE2. In this assay, ACE2 removes the C-terminal dinitrophenyl moiety that quenches the inherent

157   fluorescence of the 7-methoxycoumain group, increasing the fluorescence when ACE2 is active

158   (Huentelman et al., 2004). The results showed that NAAE inhibited the ACE2 enzymatic activity with

159   an IC_{50} of 57 µmol/L (Huentelman, et al., 2004). In addition, 293T cells expressing ACE2 receptor

160   were incubated with the NAAE, and then with S glycoprotein-expressing 293T cells, and measurement

161   of β-galactosidase activity (reported gene in cell-cell fusion) were performed. NAAE at 0.5 µM

162   inhibited 50% of SARS-CoVs spike protein-mediated cell fusion and suggested that NAAE might be

163   a candidate for treating SARS-infection, by impairing the viral attachment via the interference with

164   ACE2. (Huentelman, et al., 2004). However, detailed explanation on how NAAE is a more efficient

165   ligand to ACE2 than other compounds was not approached by the authors.

166   Ramos-Tovar and Muriel reported the antiviral activity of Glycyrrhizin (GL), a major

167   constituent from licorice root (Ramos-Tovar and Muriel, 2019), that was able to inhibit SARS-CoV

168   entry into Vero cells with an effective concentration of 50% (EC_{50}) of 300 mg·L^{-1} and cytotoxicity

169   concentration of (CC_{50}) of > 20.000 mg·L^{-1}. GL was less effective when the administration occurred

170   during the viral adsorption period than when it was administered after entry into host cells. Cumulative

171   effects were observed when this compound was administrated both during and post entry in host cells,

172   which indicates a significantly potent inhibitor against the virus, under the tested conditions (Cinatl et

173   al., 2003). Additionally, the antiviral activity of 15 GL derivates against SARS-CoV was assessed

174   (Hoever et al., 2005). Conjugation on both acidic moieties of GL disaccharide group with 2-acetamido-

175   α-D-glucopyranosylamine, benzylcysteine and Gly-Leu peptide generated compounds with an increase

176   of 10 to 70-folds anti-SARS-CoV activity when compared to GL itself (Hoever et al., 2005). For the

177   case of 2-acetamido-α-D-glucopyranosylamine derivative, it was speculated that viral entry was

178   inhibited through N-acetylglycosamine binding onto S-protein carbohydrates. Other derivatives such

179   as the introduction of heterocyclic amides such as 6-amine-thiouracil induced a higher cytotoxicity

180   profile.

181   The endossomal cathepsins are essential enzymes in viral entry into host cells (Huang et al.,

182   2006) and cathepsin L has been pointed with a crucial role in membrane fusion with the endosomes

183   (Belouzard et al., 2009; Matsuyama et al., 2020). In this context, Shah and coworkers demonstrated

184   the effective activity of the tetrahydroquinoline oxocarbazate (CID 23631927), an oxocarbazate

185   inhibitor of cathepsin L against SARS-CoV. Employing a pseudovirus system with a luciferase reporter

6

186   to infect 293T cells, the compound inhibited viral entry with an EC_{50} of 273 ηM and $CC_{50} > 100$ µM

187   (Shah et al., 2010). The authors also showed that the compound CID 23631927 seems to bind with a

188   lower inhibition constant (K_i) to cathepsin L, improving the compound/cathepsin L interaction. This

189   might be related to the optimized structure with stronger hydrophobic interactions and better hydrogen

190   bonds between the compound and cathepsin L (Shah et al., 2010).

191   An extensive work screened a library of compounds following the Lipinski's rule (Lipinski et

192   al., 2001) and identified 3 noncytotoxic compounds capable of inhibiting SARS-CoV pseudoparticle

193   entry into 293T cells (Adedeji et al., 2013). N-(9,10-dioxo-9,10-dihydroanthracen-2-yl)benzamide

194   (SSAA09E1) blocked early interactions of SARS-CoV S protein with ACE2 (EC_{50} of 6.7 µM and CC_{50}

195   > 100 µM), whereas N-[[4-(4-methylpiperazin-1-yl)phenyl]methyl]-1,2-oxazole-5-carboxamide

196   (SSAA09E2) affected cathepsin L activity (EC_{50} of 3.1 µM and $CC_{50} > 100$ µM). Conversely, [(Z)-1-

197   thiophen-2-ylethylideneamino]thiourea (SSAA09E3) prevented the fusion of the viral envelope with

198   host membrane cells by a direct interaction with spike protein (EC_{50} of 9.7 µM and $CC_{50} > 20$ µM)

199   (Adedeji et al., 2013). The compound SSAA09E3 presented the highest cytotoxic, probably due the

200   interactions with host proteins. The authors suggested that since these three compounds are derived

201   from molecules with antiviral activities, presented a good oral bioavailability and rapid systemic

202   distribution in animal models, they might exhibit interesting pharmacokinetics (Adedeji et al., 2013).

203   Other compounds also demonstrated to inhibit CoVs entry as presented for emodin (6-methyl-

204   1,3,8-trihydroxyanthraquinone), a component from *Rheum officinale* roots, which at 50 µM inhibited

205   about 80% the infectivity of S protein-pseudotype retrovirus from SARS-CoV in Vero cells (Ho et al.,

206   2007). Besides the entry activity, emodin was described with an additional post-entry antiviral action.

207   The authors suggested that emodin might be impairing virus release by affecting 3a viral protein which

208   is related to ion channels in infected Vero cells (Schwarz et al., 2011). This effect may play an

209   important role in immune response.

210   The exploitation of other natural compounds such as proteins seeking potential anti-CoV drugs

211   was also performed. Griffithsin (GRFT) is a protein isolated from the red alga *Griffithsia* sp. which

212   have shown a powerful viral entry inhibition against several enveloped viruses, such as the human

213   immunodeficiency virus (HIV). GRFT is capable to bind to terminal mannoses of oligosaccharides and

214   also to glycans localized on the viral envelope glycoproteins (Lusvarghi and Bewley, 2016). GFRT did

215   not present cytotoxicity in Vero cells, human ileocecal colorectal adenocarcinoma cells, human diploid

216   fibroblast cells and rhesus monkey kidney cells. Its broad-spectrum antiviral activity *in vitro* was

7

217   demonstrated against several CoVs such as SARS-CoV (EC_{50} of 0.61 µg/mL), bovine coronavirus

218   (BCoV) (EC_{50} of 0.057 µg·mL^{-1}), MHV (EC_{50} of 0.23 µg·mL^{-1}), HCoV-OC43 (EC_{50} of 0.16 µg·mL^{-1}),

219   HCoV-229E (EC_{50} of 0.18 µg·mL^{-1}) and HCoV-NL63 (EC_{50} < 0.032 µg·mL^{-1}) (O'Keefe et al., 2010).

220   In another study, GRFT inhibited early stages of MERS-CoV infection in HEK-293T cells (Millet et

221   al., 2016). Furthermore, GRFT improved surviving in SARS-CoV infected mice and protected the

222   Balb/c female mice against infection by binding with S protein (O'Keefe et al., 2010). Altogether,

223   GRFT could be considered as a potential SARS-CoV-2 entry inhibitor with activity against S proteins.

224   Antiviral activity by entry inhibition was also evaluated employing antibacterial

225   chemotherapeutics. Vancomycin, eremomycin and teicoplanin, glycopeptide compounds used to treat

226   infections caused by Gram-positive bacteria (Preobrazhenskaya and Olsufyeva, 2004), as well as

227   hydrophobic derivatives of these drugs, were described to possess antiviral activity against HIV

228   (Printsevskaya et al., 2005). A study showed that vancomycin, eremomycin, and teicoplanin were not

229   toxic to Vero and T lymphoblast (CEM) cells. Nonetheless, these compounds were not able to inhibit

230   the feline CoV (FIPV) and SARS-CoV in assays employing such cell lines. Conversely, the

231   eremomycin derivatives molecules labeled 27 and 39 showed the best inhibition profile against FIPV

232   (EC_{50} of 5.4 µM and 12 µM, respectively) and SARS-CoV (EC_{50} of 14 µM and 22 µM, respectively)

233   (Balzarini et al., 2006).

234   Cationic antimicrobial peptides (AMPs) are another type of peptides which have been

235   considered as potential broad-spectrum antiviral agents. For instance, mucroporin is an AMP found in

236   *Lychas mucronatus* scorpions venom (Dai et al., 2008). Mucroporin was then optimized synthetically

237   generating mucroporin-M1, that was able to inhibit measles virus (MeV), SARS-CoV and influenza

238   H5N1. Specifically, mucroporin M-1 affected SARS-CoV pseudovirus entry with EC_{50} of 14.46

239   µg·mL^{-1} and CC_{50} of 61.58 µg·mL^{-1}, by a virucidal activity in HeLa-ACE2 cells (Li et al., 2011). The

240   activity of this synthetic peptide seems to be related to positive charges of the hydrophilic site that can

241   enhance the interaction with viral surface, inactivating the viral particle.

242   Other potential antiviral peptides were selected by Struck and colleges. Through the

243   exploitation of bioinformatics tools, the authors were able to predict sixteen peptides with effective

244   binding onto the receptor binding domain (RDB) present in S proteins of CoVs. These compounds

245   were then synthesized, and the hexapeptide Tyr-Lys-Tyr-Arg-Tyr-Leu at 14 mM inhibited the SARS-

246   CoV and HCoV-NL63 infection in Vero cells, without triggering cytotoxicity (Struck et al., 2012).

247   This peptide was designed specifically to bind to the site of interaction with S protein, and does not

8

248   interfere with the ACE2 receptor activity, so it might be a good candidate to block SARS-CoV-2 entry

249   without impairing host metabolism. Taking into consideration that cellular factors such as the Tumor

250   Necrosis Factor-alpha (TNF-α) converting enzyme (TACE) facilitates the SARS-CoV entry (Haga et

251   al., 2008), it is reasonable to suggest that TACE inhibitors could hinder SARS-CoV infection. In this

252   context, TAPI-2, a compound able to inhibit TACE, has shown a potent antiviral activity promoting

253   65% blockade of the SARS-CoV entry in HEK-293T cells. However, the compound did not affect the

254   virus titer in *in vivo* assays (Haga et al., 2010). The authors suggested that since SARS-CoV attaches

255   to additional receptors such as DC-SIGN and L-SIGN (Sa et al., 2004; Han et al., 2007), viral entry

256   might be not impaired by this molecule.

257   In addition to amino acid-based inhibitors, monoclonal antibodies (mAbs) have attracted

258   attention due to their use in infectious and chronic diseases treatments (Green et al., 2000; Haynes et

259   al., 2009; Pettitt et al., 2013; D'Amato et al., 2014), overcoming drawbacks caused in polyclonal Abs

260   therapy, as those related to donor compatibility (Marasco and Sui, 2007). Human neutralizing Abs

261   against human CoVs have been generated targeting S glycoproteins to impair viral entry (Belouzard et

262   al., 2012; Reguera et al., 2012). Notably, several mAbs were identified as inhibitors of MERS-CoV

263   and SARS-CoV infections both *in vitro* and *in vivo,* protecting cells and animals when administered

264   24h prior or post-infection (Agnihothram et al., 2014; Lip et al., 2006; Zhu et al., 2007; Shanmugaraj

265   et al., 2020). The mAbs are developed by merging B lymphocytes and myeloma cells, producing

266   hybridomas capable of recognizing antigens and produce a single Abs class to bind specific epitopes

267   (Lipman et al., 2005). For that reason, mAbs cross-reactivity among different coronaviruses seems to

268   be ineffective (Totura and Bavari, 2019). In the particular case of SARS-CoV-2, Wang and coworkers

269   produced mAbs using 51 lineages of SARS-S hybridoma cells and identified the 47D11 H2L2

270   neutralizing Abs through ELISA assays. This antibody was produced using mice cells; therefore, it

271   was further modified to produce a fully human immunoglobulin IgG1, producing the human

272   monoclonal antibody 47D11. The results showed that 47D11 binds to the RBD region and inhibited

273   SARS-CoV-2 entry in Vero cells with EC$_{50}$ of 0.57 µg/mL (Wang et al., 2020a). In this context, this

274   mAbs can be used alone or in association with other compounds to treat COVID-19 infections.

275   **Inhibitors of post-entry stages of CoVs replicative cycle**

276   Among the proteins that are pivotal for CoVs viral replication are the main proteases (Mpro)

277   such as the chymotrypsin-like protease (3CLpro) and the papain-like proteases (PPL). These enzymes

278   process viral polyproteins and control replicase complex activity (Anand et al., 2003), figuring as very

9

279 attractive targets for drug development against CoVs. Several natural products and synthetic peptides
280 have been reported to inhibit Mpro (Cinatl et al., 2005; Vuong et al., 2020).

281   Gan and coworkers used molecular docking methods to select the octapeptide Ala-Val-Leu-
282 Gln-Ser-Gly-Phe-Arg as Mpro inhibitor of SARS-CoV and evaluated its antiviral activity in infected
283 Vero cells. The octapeptide presented an EC_{50} of 2.7 x 10^{-2} mg·mL^{-1} and a CC_{50} > 100 mg·mL^{-1},
284 resulting on a selectivity index of over 3704 (Gan et al., 2006). Moreover, five Phe-Phe dipeptide
285 inhibitors (A-E) were designed and selected *in silico* to interact with 3CLpro, and showed to be able
286 to protect Vero cells from cytopathic effect (CPE) caused by SARS-CoV. The C analogue (JMF1521)
287 was obtained by the condensation of Phe-Phe dipeptide unsaturated ester with cinnamic acid and
288 exhibited the highest activity with EC_{50} of 0.18 µM and CC_{50} > 200 µM (Shie et al., 2005). The authors
289 also performed enzymatic assay to evaluate the activity of JMF1521 on 3CLpro and showed that the
290 peptide inhibited the 3CLpro activity with an inhibition constant of 0.52 µM. The results suggested
291 that this analogue disposes a rather rigid coplanar structure in the N-terminal motif that results in more
292 effective hydrogen bonds with the enzymes residues (Shie et al., 2005).

293   Another example of dipeptide-based compound as protease inhibitor is dipeptidyl EP128533
294 (Zhang et al., 2006) that showed antiviral activity against SARS-CoV in Vero cells, with an EC_{50} and
295 CC_{50} of 3.6 µM and > 100 µM, respectively (Zhang et al., 2006). In accordance with this study, it was
296 also demonstrated that EP128533 inhibited SARS-CoV with an EC_{50} of 1.4 µg/mL and CC_{50} > 100
297 µg/mL (Day et al., 2009). However, the compound was not efficient in reducing the effects of viral
298 replication in BALB/c mice (Day et al., 2009). The authors proposed that EP128533 is relatively
299 insoluble and its lack of activity might be related to a low bioavailability in the animal models.

300   The dipeptides GC373 (dipeptidyl aldehyde) and GC376 (dipeptidyl bisulfite adduct salt from
301 GC373) were also designed and synthesized as protease inhibitors of the 3CLpro enzyme (Kim et al.,
302 2012). Their activity was assessed *in vitro* and results showed that GC373 inhibited HCoV-229E (EC_{50}
303 of 0.2 µM), feline infectious peritonitis virus (FIPV, EC_{50} of 0.3 µM), MHV (EC_{50} of 2 µM),
304 transmissible gastroenteritis virus (TGEV, EC_{50} of 0.3 µM) and the bovine coronavirus (BCV, EC_{50} of
305 0.7 µM) (Kim et al., 2012). GC376 also inhibited HCoV-229E (EC_{50} of 0.15 µM), FIPV (EC_{50} of 0.2
306 µM), MHV (EC_{50} of 1.1 µM), TGEV (EC_{50} of 0.15 µM) and BCV (EC_{50} of 0.6 µM). The 3CLpro
307 activity of these compounds against the SARS-CoV was also analyzed. The GC373 and GC376
308 inhibited enzymatic activity of SARS-CoV 3CLpro with an inhibition constant of 50% of 3.48 µM and
309 4.35 µM, respectively (Kim et al., 2012). However, the activity of these compounds was not evaluated

10

310 using infected cells or animal models. Additionally, the effects of GC373 and GC376 were assessed

311 against feline coronavirus WSU (FCoV-WSU) (EC$_{50}$ values for GC373 and GC376 were 0.15 µM and

312 0.40 µM, respectively) (Kim et al., 2013). Moreover, the authors described that the concomitant

313 treatment with these compounds can improve the antiviral effect against feline coronaviruses, and since

314 the 3CLpro is conserved among CoVs, it might present broad-spectrum activity (Kim et al., 2013).

315 RNA-dependent RNA polymerase (RdRp) also figures as a promising target for antivirals. In

316 viral replication, RdRp is responsible for catalyzing the replication of the viral RNA using a

317 complementary RNA as template. Therefore, compounds that interfere in this process are excellent

318 drug candidates for treating viral infections (Ganeshpurkar et al., 2019). Nucleoside analogues of

319 pyrimidine interfere in uridine triphosphate (UTP) metabolism, directly affecting viral replication

320 (Murphy and Middleton, 2012), as demonstrated by β-D-N^4-hydroxycytidine (NHC) which inhibited

321 SARS-CoV (EC$_{50}$ of 10 µM and CC$_{50}$ > 100 µM) and HCoV-NL63 (EC$_{50}$ of 400 nM and CC$_{50}$ > 100

322 µM) (Barnard et al., 2004). NHC presented a potent antiviral activity against SARS-CoV-2 in infected

323 Vero (IC$_{50}$ of 0.3 µM and CC$_{50}$ of >10 µM) and Calu-3 cells (IC$_{50}$ of 0.08 µM and CC$_{50}$ > 100 µM)

324 (Sheahan et al., 2020). The authors assessed the broad-spectrum antiviral activity of NHC against

325 MERS-CoV (IC$_{50}$ 0.024 µM) and SARS-CoV (IC$_{50}$ 0.14 µM) (Sheahan et al., 2020), and also evaluated

326 the NHC effect in SARS-CoV and MERS-CoV infected mice. NHC improved pulmonary function and

327 decreased viral load in lungs and the authors proposed that NHC might be useful in emerging CoVs.

328 Other pyrimidine analogue with potential antiviral activity is 6-azauridine, that inhibited HCoV-NL63

329 replication in LLC-MK2 cells with an EC$_{50}$ of 32 nM and CC$_{50}$ of 80 µM (Pyrc et al., 2006).

330 Ribavirin is a synthetic nucleoside analogue of guanosine used for the treatment of patients

331 chronically infected by the hepatitis C virus (PubChem, 2005c). Ribavirin antiviral activities have been

332 described against several RNA viruses, also presenting broad-spectrum antiviral for CoVs (Chan et al.,

333 2013; Shen et al., 2016). Its activities were described for SARS-CoV *in vitro* (EC$_{50}$ of 20 µg/mL and

334 CC$_{50}$ > 200 µg/mL) (Saijo et al., 2005). Nevertheless, no viral load reduction was observed *in vivo*

335 employing BALB/c mice (Barnard et al., 2006). The *in vitro* decrease of ribavirin efficacy was

336 demonstrated to be associated with the excision of its nucleoside analogues by conserved coronavirus

337 proofreading mechanisms (Ferron et al., 2017). Moreover, ribavirin showed good results for the

338 treatment of critically MERS-CoV patients (Al-Tawfiq et al., 2014), and the combined treatment of

339 ribavirin with type I Interferons (IFN-I) in primate models improved MERS disease symptoms

340 (Falzarano et al., 2013). Although ribavirin has been given as part of treatment regimens for SARS and

11

341 MERS patients, meta-analyses of cases of study have found limited efficacy of its activities in treating

342 patients with highly pathogenic coronavirus respiratory syndromes (Morra et al., 2018).

343 What is more, a nucleoside analogue based on the acyclic sugar scaffold of acyclovir showed

344 antiviral potential against coronaviruses (Tan et al., 2004). Peters and contributors demonstrated that

345 this compound has a powerful antiviral activity against MERS-CoV (EC_{50} and CC_{50} of 23 µM and 71

346 µM, respectively) and HCoV-NL63 (EC_{50} and CC_{50} of 8.8 µM and 120 µM, respectively) (Peters et

347 al., 2015). However, the mechanisms of which this analogue impairs viral replication are not suggested

348 by the author, leading to questioning whether it acts as its precursor acyclovir, impairing viral

349 replication, or by alternative mechanism of action.

350 As of others drug options in post-entry stages of viral replicative cycle it is possible to report

351 the activities of Niclosamide, a drug used in antihelminthic treatment (Katz, 1977). Niclosamide

352 presented antiviral activity on post-entry steps of SARS-CoV infection in Vero cells, with an EC_{50} of

353 1-3 µM and CC_{50} of 250 µM (Wu et al., 2004). Similarly, this compound suppressed the cytopathic

354 effect of SARS-CoV at a concentration < 1 µM and inhibited viral replication with an EC_{50} value of

355 less than 0.1 µM in Vero E6 cells (Wen et al., 2007). Both authors suggested that Niclosamide impairs

356 post-entry steps. However, this effect seems to not be related to an interaction with 3CLpro.

357 An additional potential compound is mycophenolic acid (MPA), an antibiotic derived from

358 penicillium fungal species (PubChem, 2005b), which inhibited MERS-CoV replication in Vero cells

359 with EC_{50} of 2.87 µM (Hart et al., 2014). However, MPA was not active against SARS-CoV both in

360 *in vitro* and *in vivo* assays (Barnard et al., 2006). Data suggested that MPA inhibits the enzyme IMP

361 dehydrogenase, inducing apoptosis on alveolar macrophages, and consequently, inhibiting or

362 suppressing cellular immune responses, important to prevent or limit viral infection (Barnard et al.,

363 2006).

364 Bananins, on the other hand, are a class of adamantane-based compounds conjugated with

365 pyridoxal moiety (vitamin B6) (Kesel, 2003). These molecules showed effective inhibition of SARS-

366 CoV in FRhK-4 cells, with EC_{50} < 10 µM and CC_{50} of 390 µM. By both time addition and ATPase

367 assays, authors proposed that the action of bananin is mainly on the post-entry step of virus replication,

368 and may be related to an effect on the helicase function and/or on components of cellular pathways

369 (Tanner et al., 2005).

12

370   Finally, the nonstructural protein 10 (nsp10) of CoVs was described as responsible for a
371   stimulatory effect on nsp16, a classical S-adenosylmethionine-dependent (nucleoside-2′-O)-
372   methyltransferase that acts in RNA binding or catalysis. The peptide TP29 was designed as a ligand to
373   MHV nsp10 and presented broad-spectrum activity, inhibiting SARS-CoV (EC_{50} of 200 µM) and
374   MHV (EC_{50} of 60 µM) replication in infected cell lines (Wang et al., 2015). The authors also assessed
375   TP29 activity in MHV infected mice, and demonstrated that treatment improved survival, decreased
376   viral load in liver and induced type 1 IFN. Based on this data, it was suggested that the TP29 impaired
377   nsp10/nsp16 2'-O-MTase activity, dysregulating the genome replication process.

378

379   **Looking towards host machinery: A different approach to CoVs treatment**

380   Targeting the host process during viral infection figures as a promising alternative for drug
381   development and can play an important role onto abrogating viral replication (Sayce et al., 2010; Ullah
382   et al., 2019). Nitazoxanide is a broad-spectrum antiviral agent exploited onto treatment of, for instance,
383   influenza A and B viruses, as well as Ebola virus (EBOV) (Rossignol, 2014; Jasenosky et al., 2019),
384   with its activity related to the interference in host-regulated pathways during viral replication
385   (Rossignol, 2016). *In vitro* studies demonstrated that Nitazoxanide was able to inhibit MERS-CoV in
386   LLC-MK2 cells, with an EC_{50} of 0.92 µg·mL^{-1}. The authors suggested that nitazoxanide affects pro-
387   inflammatory cytokines and suppresses its overproduction (Rossignol, 2016).

388   Another host-target compound is Saracatinib (AZD0530), a tyrosine kinase (SFK) inhibitor.
389   This compound suppressed early stages of the MERS-CoV replicative cycle in Huh7 cells (EC_{50} of 2.9
390   µM and CC_{50} > 50 µM), possibly by affecting the SFKs pathways (Shin et al., 2018). SFK possesses
391   central function in signaling pathways such as ERK/MAPK and PI3K/AKT (Thomas and Brugge,
392   1997), which are strictly related to CoVs infection. Therefore, the SFKs inhibition might promote viral
393   clearance, and can be used in association with other drugs (Shin et al., 2018).

394   Moreover, Cyclosporin A (CsA), a peptide with activity on the cyclophilin family of host
395   enzymes (isomerases that act as chaperones) (PubChem, 2005a; Davis et al., 2010), inhibited SARS-
396   CoV (100% inhibition at 16 µM), HCoV-229E (75% inhibition at 16 µM) and MHV (100% inhibition
397   at 16 µM) in human and animals infected cell culture. CsA presented broad-spectrum antiviral activity
398   against CoVs and it seems to interfere to the genome replication/transcription during CoVs infections
399   (de Wilde et al., 2011, 2013; Pfefferle et al., 2011). Alisporivir, a non-immunosuppressive cyclosporin

13

400   A analogue, inhibited the replication of SARS-CoV in Vero E6 infected cells at low-micromolar

401   concentrations (EC$_{50}$ of 8.3 µM; CC$_{50}$ > 50 µM). This compound also showed broad-spectrum anti-

402   CoVs activity, inhibiting MERS-CoV EMC/2012 (EC$_{50}$ of 3.6 µM), MERS-CoV N3/Jordan (EC$_{50}$ of

403   3 µM) and SARS-CoV MA-15 (EC$_{50}$ of 1.3 µM) *in vitro* (de Wilde et al., 2017). However, the authors

404   demonstrated that Alisporivir did not enhance survival in CoV infected mice (de Wilde et al., 2017).

405   Other promising biomolecules as drug antivirals are interference RNAs (iRNAs). These

406   macromolecules are small non-coding RNAs associated with controlling the expression of genetic

407   information (Wilson and Doudna, 2013), and have been described as promising candidates for the

408   treatment of hepatitis B virus (HBV), hepacivirus (HCV), HIV and human T-cell lymphotropic virus

409   (HTLV) infections (Y et al., 2007; Shah and Schaffer, 2011; Sanan-Mishra et al., 2017). The short

410   interference RNAs (siRNAs) were described effective for *in vitro* antiviral treatment of FIPV, a type

411   of FCoV (McDonagh et al., 2011, 2015). Most recently, Li and colleagues designed and synthesized

412   siRNAs that targeted the M and N genes of swine and porcine coronaviruses (SECoV and PDCoV,

413   respectively). These siRNAs inhibited up to 99% of the expression of these proteins in both Vero and

414   LLC-PK1 infected cells (Li et al., 2019). Additionally, synthetic siRNAs targeting the structural

415   proteins E, M and N of SARS-CoV have also been developed, showing reduction of the referred genes

416   expression in Vero cells (Shi et al., 2005). Moreover, siRNAs targeting the structural proteins 7a, 7b,

417   3a, 3b, and S reduced approximately 70% of SARS-CoV progeny in Vero cells (Åkerström et al.,

418   2007). The different authors propose that treatment with siRNAs can improve treatment-resistance

419   among viruses, and that these molecules can be designed to target multiple proteins aiming a broad-

420   spectrum activity.

421

422   **Ongoing clinical evaluations with candidate drugs against SARS-CoV-2**

423   The current situation of the pandemic of COVID-19 accentuated the mandatory and immediate

424   demand for effective treatments. Based on previous data concerning the activities against other viruses

425   and the empirical knowledge from treatments used in case reports, several drugs entered clinical trials

426   phases to access their therapeutic potential against SARS-CoV-2. In this section, we discussed the

427   current knowledge on the most promising candidates for the treatment of COVID-19. Data from these

428   drugs are summarized on the Table 2.

14

429   The nucleoside analogue Remdesivir (GS-5734) is a monophosphoramidate prodrug, which has

430   antiviral activity described against the EBOV in non-human primates (Warren et al., 2016, 57). Its

431   activity was assessed in human airways epithelial (HAE) cells infected with SARS-CoV (EC$_{50}$ of 0.069

432   µM and CC$_{50}$ > 10 µM) and MERS-CoV (EC$_{50}$ of 0.074 µM and CC$_{50}$ > 10 µM), and demonstrated to

433   inhibit these virus RdRp. Also, GS-5734 reduced infectious virus production of bat CoV by 1.5 to 2.0

434   log$_{10}$ in HAE cells and reduced virus titers and virus-induced lung pathologies in a SARS-CoV assay

435   *in vivo* (Sheahan et al., 2017). This compound also reduced the severity of MERS-CoV disease, virus

436   replication and damage in the lungs of rhesus macaques (Wit et al., 2020). The clinical efficacy of GS-

437   5734 has been assessed by several clinical trials in different countries like France (NCT04365725),

438   Canada (NCT04330690), USA (NCT04292899) among others, which have been conducted based on

439   the first reported COVID-19 case treated with Remdesivir in Washington, USA (Holshue et al., 2020).

440   In the first findings from Wang and coworkers encompassing a randomized, double-blind, multicenter

441   and placebo-controlled trial with 255 patients, Remdesivir did not present significant antiviral effects

442   against SARS-CoV-2, nor did it improve clinical outcomes (Wang et al., 2020c). To date, there are

443   several active clinical trials registered in the PubMed database involving such compound. However,

444   most of them presented no conclusive outcomes.

445   As other candidates, Lopinavir and Ritonavir are protease inhibitors used in association to treat

446   HIV infections (Mills et al., 2009). Lopinavir demonstrated antiviral activities protecting cells of

447   MERS-CoV infection (EC$_{50}$ of 8 µM) and reducing viral loads in animal assays (Wilde et al., 2014;

448   Kim et al., 2015). Ritonavir also demonstrated anti-MERS-CoV activities with EC$_{50}$ of 24.9 µM

449   (Sheahan et al., 2020). It is important to point out that these results do not agree with another work that

450   was unable to demonstrate *in vitro* antiviral activity of Lopinavir against MERS-CoV (Chan et al.,

451   2013). In clinical assays for MERS-CoV, the association of Lopinavir with Ritonavir reduced clinical

452   outcomes and viral load in infected patients (Sheahan et al., 2020; Yao et al., 2020a). In particular to

453   SARS-CoV, Lopinavir and Ritonavir presented a low to medium antiviral activity *in vitro*, and *in vivo*

454   assays have not been performed yet (Yao et al., 2020a). In addition, Lopinavir and Ritonavir played an

455   important role in the clinical outcome of SARS-CoV infected patients by reducing symptoms and the

456   period of hospitalization, representing a possibility for the treatment of SARS-CoV-2 (Chu et al.,

457   2004). Cao and collaborators conducted a randomized clinical trial with 199 patients with severe

458   COVID-19 (Cao et al., 2020b). The patients treated with the association Lopinavir/Ritonavir did not

459   improve symptoms, nor impaired detectable viral RNA when compared to standard-care (supplemental

460   oxygen, noninvasive and invasive ventilation, antibiotic agents, vasopressor support, renal-

15

461   replacement therapy and extracorporeal membrane oxygenation). Additionally, the treatment generated
462   relevant adverse effects to some of the patients (Cao et al., 2020b). The authors proposed that the low
463   efficacy of Lopinavir with Ritonavir might be associated with the time of administration, since
464   individuals that were treated on the onset of the disease, had improved clinical results (Cao et al.,
465   2020b). Later, it was shown that the association of lopinavir and ritonavir with interferon-β1 and
466   ribavirin to treat mild to moderate COVID-19 patients alleviated symptoms and decreased duration of
467   viral infection and hospital stay (Hung et al., 2020). This might be related to the inducing cellular
468   immune response, impairing virus replication.

469   The type 1 interferons (IFN-I) were also employed in clinical trials. These proteins belong to
470   the cytokines family and are associated to the immune response in viral infections, thus, playing major
471   roles in antiviral immunity due to its immunomodulatory properties (Samuel, 2001). Therefore, they
472   are commonly employed on the treatment of several diseases such as Hepatitis C (Kobayashi et al.,
473   1993). There are two subtypes of IFN-I, alpha (IFN-α) and beta (IFN-β) (Samuel, 2001). IFN-β is
474   associated with a more potent activity (Chan et al., 2015), and therefore is capitalized as treatment for
475   multiple sclerosis patients (Axtell et al., 2010). Due to its more potent inhibition profile, it was
476   associated with potent antiviral effects against SARS-CoV, MERS-CoV, MHV and HCoV-229E *in*
477   *vitro* and *in vivo* (Sperber and Hayden, 1989; Vassão et al., 2000; Hensley et al., 2004; Falzarano et
478   al., 2013; Chan et al., 2015). IFN-β, in particular, has a protective effect in endothelial cells, up-
479   regulating CD73, consequently, stimulating the anti-inflammatory molecules and maintenance of
480   endothelial barrier (Bellingan et al., 2014; Sallard et al., 2020). However, a clinical trial with 301
481   patients showed that this effect was not sufficient to decrease mortality in SARS patients (Ranieri et
482   al., 2020). Therefore, in SARS-CoV-2, IFN-β has been associated with other drugs in clinical trials,
483   improving outcomes in COVID-19 patients as in lopinavir or ribavirin (Hung et al., 2020).

484   COVID-19 patients with mild to severe symptoms can develop an hyperinflammation and
485   hypercytokinaemia that can lead to multiple organs failure and death (Mehta et al., 2020). The
486   employment of corticosteroids has shown to be an alternative to overcome the cytokine storm and
487   hyperinflammation, due to its activities on immune cells (Wilkinson et al., 1991). Such capitalization
488   was previously reported in SARS-CoV patients, during 2002-2003 epidemic (Chihrin and Loutfy,
489   2005). For SARS-CoV-2, corticosteroids can improve the clinical condition of patients, reducing
490   hyperinflammation and the development of ARDS, with faster improvement of symptoms (Wang et
491   al., 2020; Zha et al., 2020). However, contrasting data concerning these drugs efficacy was recently
492   described, showing that corticosteroids did not improve symptoms in COVID-19 patients (Zha et al.,

16

493   2020). Moreover, dexamethasone emerged as a potential drug to treat COVID-19 patients as showed

494   by results of a randomized, controlled, open-lab and multicenter trial which assessed the effects of

495   dexamethasone in 454 patients, described to date in pre-prints findings (Horby et al., 2020). Data

496   suggested that dexamethasone reduced death in one-third of patients in invasive mechanical ventilation

497   and one-fifth of patients in non-invasive oxygen mechanical ventilation. However, it did not impair

498   mortality in patients with no respiratory support (Horby et al., 2020). Others trials have been conducted

499   such as NCT043274011, but considering the preliminary results, WHO suggested that the treatment

500   with dexamethasone may be applied during the third phase of COVID-19, when the hyperinflammation

501   is determined and respiratory support is needed.

502   Another antiviral drug assayed towards SARS-CoV-2 is Umifenovir, a licensed antiviral

503   exploited upon the prophylaxis and treatment of influenza viruses (Arbidol®) which demonstrated

504   good pharmacokinetics when absorbed by the organism (Proskurnina et al., 2020). This drug has

505   antiviral effect against SARS-CoV *in vitro* at 50 µg·mL^{-1} (Khamitov et al., 2008). Lian and coworkers

506   coordinated an observational study with 81 patients with moderate to severe SARS-CoV-2 infection

507   (Lian et al., 2020) which demonstrated that Umifenovir did not shorten the hospitalization period

508   neither improved prognosis in infected patients (Lian et al., 2020).

509   Broad-spectrum drugs used against parasitic infections as Ivermectin (Campbell, 2012; Laing

510   et al., 2017) have also been investigated by their antiviral activity as showed for Dengue virus (DENV),

511   Influenza A viruses, Chikungunya virus (CHIKV) and HIV (Tay et al., 2013; Götz et al., 2016;

512   Varghese et al., 2016; Caly et al., 2020). Its activity is based on impairing several stages of viral

513   replication, for instance, interfering with nonstructural proteins (Varghese et al., 2016). Caly and

514   collaborators assessed the effect of Ivermectin on SARS-CoV-2 replication in Vero cells, showing that

515   the compound at 5 µM presented no toxicity to cells and inhibited up to 99% of viral replication by a

516   possible antiviral effect on viral release, which is consistent with previous data against other RNA

517   viruses (Tay et al., 2013; Caly et al., 2020). Clinical trials have been conducted in different medical

518   centers in Argentina (NCT04381884), Mexico (NCT04391127), Spain (NCT04390022) and USA

519   (NCT04374279) to access the clinical implications of the use of Ivermectin for COVID-19. However,

520   to the best of our knowledge, there are no published results in this topic. The NCT04343092 is a phase

521   1 clinical trial in Iraq conducted to its completion that has evaluated the efficacy of Ivermectin on

522   COVID-19 patients, so the results might be published soon.

17

523   According to Guan and colleagues, approximately 15.7% of Chinese patients with COVID-19

524   developed severe pneumonia, and cytokine release syndrome (CRS), an important factor leading to

525   rapid progression of the disease (Chousterman et al., 2017; Guan et al., 2020). In this context, one of

526   the key cytokines involved in infection-induced cytokine storm is the interleukin 6 (IL-6) (Scheller and

527   Rose-John, 2006; Zhang et al., 2020a). Tocilizumab is an IL-6 receptor antagonist approved by the US

528   FDA for the treatment of severe CRS (Grupp et al., 2013) and figures as an interesting drug to treat

529   cytokine storm caused by SARS-CoV-2 (Zhang et al., 2020b). The treatment of patients with severe

530   COVID-19 with Tocilizumab presented no complications in the 21 assisted patients, with an average

531   age of 56.8 ± 16.5 and no history of illness deterioration or death. Thus, it immediately improved the

532   clinical outcome and appeared to be an effective treatment to reduce mortality (Xu et al., 2020). A

533   study reinforced such observations, employing the treatment of COVID-19 patients with Tocilizumab

534   for 14 days in which it was observed an effective decrease in inflammatory markers, radiological

535   improvement and ventilatory support requirements for these patients (Alattar et al., 2020).

536   Additionally, Toniati and collaborators administrated Tocilizumab in 100 patients in Italy (average age

537   of 62 years old), diagnosed with COVID-19 pneumonia and ARDS, and requiring ventilatory support.

538   Overall, at 10 days of follow-up, the respiratory condition was improved or stabilized in 77% of the

539   patients, and, based on their data, the response of this drug in patients with severe COVID-19 was

540   rapid, sustained and associated with significant clinical improvement (Toniati et al., 2020).

541   Chloroquine is a 9-aminoquinole that increases the pH in acidic vesicles (Mauthe et al., 2018) and

542   possesses antiviral activities against HIV and other viruses (Jacobson et al., 2016; Al-Bari, 2017).

543   Chloroquine was described as an entry inhibitor of SARS-CoV infection in Vero cells and prevented

544   cell-to-cell spread of the virus (Vincent et al., 2005). Furthermore, it affected the entry and post-entry

545   stages of the replicative cycle of FCoV in *Felis catus* cells and monocytes. Additionally, an *in vivo*

546   study in cats demonstrated that the treatment with chloroquine improved the clinical score of treated-

547   groups when compared to the untreated-group (Takano et al., 2013). Chloroquine also had its anti-CoV

548   activities tested in Vero cells (EC_{50} of 5.47 µM) (Wang et al., 2020; Yao et al., 2020b). Despite the

549   performance of chloroquine *in vitro*, clinical studies conducted in China and France showed

550   contradictory clinical data (Chen et al., 2020, 2020; Gao et al., 2020; Molina et al., 2020). Gao and

551   collaborators defined that chloroquine phosphate was recommended to treat COVID-19 associated

552   pneumonia only during the urgent clinical demand, because of its antiviral and anti-inflammatory

553   activities (Gao et al., 2020). Hydroxychloroquine is an analogue of chloroquine which was described

554   to have antiviral activity inhibiting SARS-CoV-2 *in vitro* with EC_{50} of 0.72 µM (Liu et al., 2020; Yao

555   et al., 2020b). In clinical trials, an open-label non-randomized study by Gautret and colleagues affirmed

18

556 that hydroxychloroquine reduced symptoms from SARS-CoV-2 patients, and the association with

557 azithromycin could reinforce its effects (Gautret et al., 2020). However, these results have been

558 questioned. The study had a small sample size and there were limitations in the methodologies

559 (Juurlink, 2020).

560 Recent studies have been contradicting the safety used of chloroquine and hydroxychloroquine

561 since these drugs presented severe side effects that interfered in their use in clinical use, even during

562 short course therapies (Liu et al., 2020; Juurlink, 2020). Apart from the mild adverse effects, such as

563 pruritus, nausea and headache, these drugs can predispose patients to life-threatening arrhythmias, an

564 effect that may be enhanced by concomitant use of azithromycin (Chorin et al., 2020). Both

565 chloroquine and hydroxychloroquine interfere with ventricular repolarization, leading to prolongation

566 of the cardiac QT interval and an increased risk of torsades de pointes (TdP), which is a risk especially

567 for patients with cardiac disease, for children or those taking other drugs that delay repolarization

568 (Juurlink, 2020; Mzayek et al., 2007; Pukrittayakamee et al., 2014; Ursing et al., 2020). Others possible

569 damages are hypoglycemia, even in non-diabetic patients (Unübol et al., 2011; El-Solia et al., 2018);

570 neuropsychiatric effects, including agitation, insomnia, confusion, paranoia, depression, psychosis and

571 suicidal ideation (Mohan et al., 1981); hypersensitivity reactions, as severe cutaneous adverse reactions

572 (Cameron et al., 2014; Girijala et al., 2019); and drug–drug interactions, which are improved by the

573 genetic variability (genetic polymorphisms of hepatic cytochrome P450 enzyme 2D6 (CYP2D6),

574 responsible for chloroquine metabolization) (Kirchheiner et al., 2008; Lee et al., 2016). There is a lack

575 of reliable information on target concentrations or doses for COVID-19, and so doses that proved

576 effective and safe in malaria for both adults and children are considered onto the treatment (Smit et al.,

577 2020). Recently, WHO stopped the hydroxychloroquine arm of Solidarity trial to treat COVID-19

578 based on absence of effectiveness to reduce mortality of hospitalized COVID-19 patients (WHO,

579 2020). Besides, FDA also cautioned against the administration of hydroxychloroquine or chloroquine

580 in COVID-19 patients mainly due to risk of heart rhythm issues (FDA, 2020). From these results, it is

581 evident that the use of these drugs for COVID-19 requires further investigation.

582 An alternative treatment for COVID-19 is the utilization of convalescent plasma (CP) (Chen et al.,

583 2020). This treatment refers to plasma therapy based on plasma or plasma derivatives, obtained from

584 donors who were previously infected and have developed antibodies. These plasma/derivative are, in

585 their turn, transfused into individuals with SARS-CoV-2 acute infection (Garraud, 2017; Cao and Shi,

586 2020). Even though the mechanism of action of convalescent plasma therapy is not fully understood,

587 it presented great results in the treatment of patients with the SARS, during the SARS-CoV outbreak

19

588 in Hong Kong in early 2000s (Cheng et al., 2005). It is possible that the efficacy of CP therapy is due

589 to the fact that the antibodies from convalescent plasma might suppress viremia (Chen et al., 2020).

590 Duan and colleagues reported the CP transfusion to rescue ten severe cases of SARS-CoV-2 adult

591 patients. The study showed that one dose (200 mL) of CP significantly increased or maintained the

592 neutralizing antibodies at a high level, leading to the disappearance of viremia in 7 days. Clinical

593 symptoms rapidly improved within 3 days and radiological examination showed varying degrees of

594 absorption of lung lesions within 7 days. According to these results, CP can also provide a promising

595 rescue option for severe COVID-19 (Duan et al., 2020). However, the author suggested key points to

596 guarantee the effectiveness of CP therapy: Abs titers and the treatment time point. Firstly, taking into

597 consideration previous knowledge from MERS-CoV CP therapy, Abs in plasma donor must have a

598 titer equal or higher of 1:80 (Ko et al., 2018). This titer is only found in recently recovered patients,

599 since antibody levels decrease 4 months after the disease. Secondly, patients receiving CP treatment

600 prior to 14 days post-infection responded better than patients treated after 14 days (Duan et al., 2020).

601

602 **PERSPECTIVES**

603 This review aimed to summarize and discuss data from the literature regarding compounds that

604 possess anti-CoVs activities and that could be further exploited for the treatment of human and animal

605 CoVs. Furthermore, we described ongoing clinical trials for SARS-CoV-2 in order to elucidate the

606 current findings and discussed the relevant features concerning candidate drugs against SARS-CoV-2.

607 As previously mentioned, most of human-related CoVs emerged by a zoonotic transmission from

608 animals (Huynh et al., 2012; Coleman and Frieman, 2014; Reusken et al., 2016). Since *Coronaviridae*

609 seem to have a very well conserved genome and structures among their viruses (Huentelman Matthew

610 J. et al., 2004; Guan et al., 2012; Yang and Leibowitz, 2015; Madhugiri et al., 2018), it is possible to

611 hypothesize that compounds with antiviral activities against different human and/or animal CoVs

612 (broad-spectrum activity) could be potential candidates for the SARS-CoV-2 treatment. In a less

613 optimistic scenario, the chemical structures of such compounds and their pharmacological outcomes

614 have potential to set some light onto drug design of possible anti-SARS-CoV-2 drugs.

615 Among the strategies for drug design, targeting host-immune factors or using iRNAs figure as

616 promising alternatives towards antiviral drug development. Also, the exploitation of *in silico* studies

617 for drug screening seeking specific targets, as well as for a better comprehension of their interactions

20

618   headed for viral biomolecules have been shown as promising tools to expedite drug development. By
619   narrowing down the number of drug candidates, *in silico* studies have the potential to avoid some of
620   the laborious and generally costly synthesis of many of these compounds (Lengauer and Sing, 2006;
621   Villegas-Rosales et al., 2012). Nevertheless, there are several predicted compounds in the literature
622   that were only screened by *in silico* and/or interaction assays (Arya et al., 2020; Balasubramaniam and
623   Reis, 2020; Chen et al., 2005; Kaeppler et al., 2005; Lee et al., 2005; Kim et al., 2012), which ultimately
624   hinders the proper assessment of the compounds antiviral activities. Therefore, it is imperative the
625   association of these studies with *in vitro* and *in vivo* assays in order to confirm the predicted activities
626   in biological models, as well as to evaluate pharmacological outcomes (Toxicology, 2007). So, this
627   review encompassed only compounds that have been evaluated by, at least, *in vitro* models (Table 1).

628   In this context, from the molecules and drugs described with *in vitro* activity, we highlighted the
629   most promising to suggest further evaluation using *in vivo* systems of CoVs infection, specially, SARS-
630   CoV-2. The compounds were: NAAE, Glycyrrhizin, 2-acetamido-α-D-Glucopyranosylamine
631   derivative, Tetrahydroquinoline oxocarbazate (CID 23631927), SSAA09E1, 2 and 3, Emodin,
632   Eremomycin 27 and 29, Mucroporin-M1, Monoclonal antibody 47D11, AVLQSGFR, Phe-Phe
633   dipeptide inhibitor C (JMF1521), GC373 and 376, 6-azauridine, Acyclic sugar scaffold of acyclovir
634   and Bananins. As described above, these compounds were capable to significantly impair CoVs
635   infection in cell cultures and might offer important progress into the treatment of described CoVs, as
636   well as viruses which might be responsible for future viral outbreaks.

637   Here, we also described compounds that were evaluated *in vivo* to elucidate their role in the
638   pathogenesis of CoVs, as well as to assess possible adverse effects. It is important to emphasize that
639   there is a lack of *in vivo* model assays, representing a delay in anti-CoVs drugs development, which
640   directly impact in SARS-CoV-2 pandemic. Here we identified some studies that employed animal
641   models, as in Balb/c mice and C57BL/6, to evaluate the antiviral effect of compounds in CoVs infection
642   (Barnard et al., 2006; Cinatl et al., 2003; Day et al., 2009; Hart et al., 2014; Saijo et al., 2005; Zhang
643   et al., 2006). The *in vivo* assays allow the gathering of knowledge regarding the ADMeTox profile of
644   these compounds in complex biologic systems, the viral titers in different organs, host immune
645   responses to the infection, as well as potential tissue damage caused by the viruses in the presence or
646   absence of candidate drugs, which represents an advance in understanding pathologies caused by viral
647   infections (Adachi and Miura, 2014). It is also important to emphasize that protocols used in studies of
648   animal-related viruses are not easily translated onto human CoVs, since these viruses are classified in
649   different biological safety levels, representing a risk of infection to scientists (Bayot and King, 2020;

21

650   CDC, 2020). Additionally, the pathologies induced by animal CoVs are mostly related to

651   gastrointestinal symptoms, differently to what is observed for human-related CoVs that affect mostly

652   the upper respiratory symptoms (Pedersen et al., 1984; Coleman and Frieman, 2014). The development

653   of refined and secure protocols to study SARS-CoV-2 infection and its treatment options are required.

654   Bearing in mind the obstacles cited above, the assessment of the effect in animal models and further

655   translate to humans remains one of the main challenges.

656   However, some of the studies were able to assess antiviral effects of some compounds *in vivo*. The

657   most relevant compounds we propose that may represent immediate candidates to clinical trials,

658   considering the urgency of COVID-19, are Griffithsin (GRFT), β-D-N^4-hydroxycytidine (NHC),

659   TP29, Cyclosporin A (CsA), Alisporivir, iRNAs, Saracatinib, Tizoxanide, Nitazoxanide, Niclosamide

660   and Ribavirin. These compounds abrogated CoVs infection *in vitro* and *in vivo*, and improved

661   symptoms and survival of animals. In addition, Saracatinib, Tizoxanide, Nitazoxanide, Niclosamide

662   and Ribavirin are molecules licensed to treat diseases such as those from viral and helminthic

663   infections, or Alzheimer's disease, representing possibilities for clinical trials as repurposing drugs.

664   Regarding the clinical trials, most drugs discussed in this review presented adverse effects as

665   nausea, headache, diarrhea, urticaria, pathologies related to the gastrointestinal system and interference

666   with liver enzymes (Ruiz-Irastorza et al., 2010; Takano et al., 2013; Roques et al., 2018; Yao et al.,

667   2020a). Remdesivir, Lopinavir and Ritonavir, and Umifenovir are drugs employed for the treatment of

668   other viral infections as EBOV and SARS-CoV, but, in the clinical trials with COVID-19 patients,

669   these treatments did not reduce symptoms and/or decrease viral load. Tocilizumab, Chloroquine and

670   Hydroxychloroquine demonstrated to inhibit SARS-CoV-2 *in vitro* and in some clinical trials reduced

671   COVID-19 symptoms, period of hospitalization and viral load in patients, despite the strong adverse

672   effects of Chloroquine (Table 2). Even so, recent studies are contradicting the safety profiles of

673   Chloroquine and Hydroxychloroquine, since it might cause arrhythmia in patients, representing risk

674   for a considerable number of patients (Juurlink, 2020).

675   Ongoing studies have been evaluating IFN-β and Ivermectin as treatments against COVID-19.

676   IFN- β can be associated with other drugs, collaborating to control immune response against the viral

677   infection (Table 2). On the other hand, corticosteroids, such as dexamethasone, sound promising, but

678   there are some issues related to its use. These compounds induce immunosuppression and when

679   administered during initial phases (viral replication) might dysregulate T cells production and

680   activation of B cells for antibody secretion, that are essential to viral clearance (Cohn, 1991; Giles et

22

681   al., 2018). Furthermore, convalescent plasma therapy is an alternative approach, which presented

682   positive effects in studies on SARS-CoV-2/COVID-19 patients. Though, its safety is not well defined,

683   due to the donor-dependent variability and compatibility (antibody titers and other factors vary among

684   donors), which might cause severe adverse effects in lung, cardiovascular system, and, in some cases,

685   even transmit diseases (Roback and Guarner, 2020).

686   Despite the finds encompassing these drugs, it is important to take some aspects in consideration:

687   i) the trials were generally conducted with a significant number of patients in each study, but it might

688   not be enough to expand the results to a public health care; ii) some of the studies were observational,

689   which means they were based on public data, that can be not well documented, leaving information

690   gaps about particular health issues; additionally, the outcomes in patients are defined by their own

691   circumstances, and not by an investigator; iii) some studies were not placebo-controlled and double-

692   blind, so the placebo effect cannot be discarded (Kernan et al., 1999; Hess and Abd-Elsayed, 2019);

693   iv) the trials were conducted selecting a group of COVID-19 patients, considering mild, moderate or

694   severe cases, and different outcomes can be expected in each situation since there are factors in viral

695   load, the progression of the disease and immune response (Kernan et al., 1999; Hess and Abd-Elsayed,

696   2019). Therefore, drugs with no effect in severe cases cannot be rejected as a possible treatment in mild

697   to severe cases. When these aspects are not considered, the investigators might be open to commit error

698   type I or II in trials (Kernan et al., 1999; Hess and Abd-Elsayed, 2019). For that matter, it is also

699   important to consider that SARS-CoV-2 is a new virus and we have currently limited knowledge about

700   its physiopathology. Finally, the development of new treatment options is critical and efforts have been

701   focused on targeting therapies which aim to improve patient outcome by increasing antiviral activity

702   associated with minimal toxicity.

703   Another point to be considered in CoVs treatment is that RNA viruses are known by the high levels

704   of mutations (error rate) in the replication process (Ganeshpurkar et al., 2019). It can result in resistance

705   to antiviral treatment, as observed for HIV, HCV, and Influenza viruses (Laplante and St George, 2014;

706   Li and Chung, 2019; Olearo et al., 2019; Takashita, 2020). A recent study in pre-print raised the

707   genomic variability of SARS-CoV-2 and the intra-patient capacity of polymorphic quasispecies, which

708   may offer resistance to antiviral drugs (Karamitros et al., 2020). In addition, previous studies

709   demonstrated that the use of Chloroquine analogues for decades against malaria has established

710   chloroquine-resistant Plasmodium strains (Stocks et al., 2002; Al-Bari, 2017; Aguiar et al., 2018). Due

711   to the beneficial immunomodulatory effects of analogues with severe inflammatory complications of

712   several viral diseases, such as HIV and SARS-CoV infections, these drugs have been tested

23

713   indiscriminately (Jacobson et al., 2016; Al-Bari, 2017). However, it is a possibility that prophylactic

714   exposure to pro-apoptotic chloroquine drugs caused natural selection for strains of viruses and other

715   parasites that have enhanced anti-apoptotic abilities (Parris, 2004). Despite the side effects, the wide

716   use of some drugs during the SARS-CoV-2 pandemic might raise concerns on the emergence of

717   resistant viral strains in the future, and we emphasize the lack of information on resistance-associated

718   to these drugs in the treatment of viral infections.

719

720   **CONCLUSIONS**

721   The spread of SARS-CoV-2 worldwide is classified as a pandemic disease and represents a

722   threat to global public health. By 04th July 2020, SARS-CoV-2 infected 10 922 324 people and had

723   caused 523 011 deaths around the world (WHO, 2020). In this context, compounds described to possess

724   antiviral activity against human and/or animal coronaviruses could provide relevant information for

725   the development of novel SARS-CoV-2 treatments. Herein, we presented and discussed the most

726   promising compounds that can figure as possible candidates for clinical trials. Moreover, the ongoing

727   clinical trials evaluating possible COVID-19 therapies were also highlighted.

728   From what was presented in this review, a plethora of different potential compounds can be

729   capitalized as possible drugs or even set points for further drug development, seeking to narrow down

730   the SARS-CoV-2/COVID-19 outbreak. However, time, resources and new experimental protocols are

731   essential to advance an efficacious treatment. In addition, and despite the urgency of treatment

732   protocols, it is important to point out the striking need for the establishment of fail-proof regulatory

733   initiatives that could prevent impacts on health care of patients which could, otherwise, be avoided by

734   a more stringent control.

735   In this context, this review describes drugs that might be overlooked, for future analysis and

736   could possibly become effective antiviral treatments. As a final remark, we can conclude that, to date,

737   there is no "one hundred percent" effective antiviral therapy against SARS-CoV-2/COVID-19 and

738   further research is needed to achieve the best therapeutic protocol, that may not be based on an unique

739   drug, but rather in a combination of active antivirals.

740   **Conflicts of Interest:** The authors declare no conflict of interest.

741

24

742 **Author Contributions**

743   IS: Drafting the manuscript and literature review. VG: Drafting the manuscript and illustration.
744 FB, RS and AJ: critical revision and editing, and approval of the final version. All the authors read and
745 approved the final manuscript.

746

760

761 **REFERENCES**

762 Adachi, A., and Miura, T. (2014). Animal model studies on viral infections. *Front. Microbiol.* 5.
763   doi:10.3389/fmicb.2014.00672.

764 Adedeji, A. O., Severson, W., Jonsson, C., Singh, K., Weiss, S. R., and Sarafianos, S. G. (2013). Novel
765   Inhibitors of Severe Acute Respiratory Syndrome Coronavirus Entry That Act by Three
766   Distinct Mechanisms. *J. Virol.* 87, 8017–8028. doi:10.1128/JVI.00998-13.

767 Aguiar, A. C. C., Murce, E., Cortopassi, W. A., Pimentel, A. S., Almeida, M. M. F. S., Barros, D. C.
768   S., et al. (2018). Chloroquine analogs as antimalarial candidates with potent in vitro and in vivo
769   activity. *Int. J. Parasitol. Drugs Drug Resist.* 8, 459–464. doi:10.1016/j.ijpddr.2018.10.002.

770 Agnihothram, S., Gopal, R., Yount, B. L., Donaldson, E. F., Menachery, V. D., Graham, R. L., et al.
771   (2014). Evaluation of Serologic and Antigenic Relationships Between Middle Eastern

25

Respiratory Syndrome Coronavirus and Other Coronaviruses to Develop Vaccine Platforms for the Rapid Response to Emerging Coronaviruses. *J. Infect. Dis.* 209, 995–1006. doi:10.1093/infdis/jit609.

Ahmed, S. F., Quadeer, A. A., and McKay, M. R. (2020). Preliminary Identification of Potential Vaccine Targets for the COVID-19 Coronavirus (SARS-CoV-2) Based on SARS-CoV Immunological Studies. *Viruses* 12. doi:10.3390/v12030254.

Åkerström, S., Mirazimi, A., and Tan, Y.-J. (2007). Inhibition of SARS-CoV replication cycle by small interference RNAs silencing specific SARS proteins, 7a/7b, 3a/3b and S. *Antiviral Res.* 73, 219–227. doi:10.1016/j.antiviral.2006.10.008.

Alattar, R., Ibrahim, T. B. H., Shaar, S. H., Abdalla, S., Shukri, K., Daghfal, J. N., et al. (2020). Tocilizumab for the treatment of severe coronavirus disease 2019. J. Med. Virol. doi:10.1002/jmv.25964.

Al-Bari, M. A. A. (2017). Targeting endosomal acidification by chloroquine analogs as a promising strategy for the treatment of emerging viral diseases. *Pharmacol. Res. Perspect.* 5, 1–13. doi:10.1002/prp2.293.

Al-Tawfiq, J. A., Momattin, H., Dib, J., and Memish, Z. A. (2014). Ribavirin and interferon therapy in patients infected with the Middle East respiratory syndrome coronavirus: an observational study. *Int. J. Infect. Dis.* 20, 42–46. doi:10.1016/j.ijid.2013.12.003.

Anand, K., Ziebuhr, J., Wadhwani, P., Mesters, J. R., and Hilgenfeld, R. (2003). Coronavirus Main Proteinase (3CLpro) Structure: Basis for Design of Anti-SARS Drugs. *Science* 300, 1763–1767. doi:10.1126/science.1085658.

Andersen, K. G., Rambaut, A., Lipkin, W. I., Holmes, E. C., and Garry, R. F. (2020). The proximal origin of SARS-CoV-2. *Nat. Med.*, 1–3. doi:10.1038/s41591-020-0820-9.

Anson, B. J., Chapman, M. E., Lendy, E. K., Pshenychnyi, S., D'Aquila, R. T., Satchell, K. J. F., et al. (2020). Broad-spectrum inhibition of coronavirus main and papain-like proteases by HCV drugs. doi:10.21203/rs.3.rs-26344/v1.

Arya, R., Das, A., Prashar, V., and Kumar, M. (2020). Potential inhibitors against papain-like protease of novel coronavirus (SARS-CoV-2) from FDA approved drugs. *ChemRxiv* [Preprint]. Available at: 10.26434/chemrxiv.11860011.v2 (Acessed June 13, 2020).

Axtell, R. C., de Jong, B. A., Boniface, K., van der Voort, L. F., Bhat, R., De Sarno, P., et al. (2010). T helper type 1 and 17 cells determine efficacy of interferon-β in multiple sclerosis and experimental encephalomyelitis. *Nat. Med.* 16, 406–412. doi:10.1038/nm.2110.

Balasubramaniam, M., and Reis, R. J. S. (2020). Computational target-based drug repurposing of elbasvir, an antiviral drug predicted to bind multiple SARS-CoV-2 proteins. *ChemRxiv* [Preprint]. Available at: 10.26434/chemrxiv.12084822 (Acessed June 13, 2020).

26

807   Balzarini, J., Keyaerts, E., Vijgen, L., Egberink, H., De Clercq, E., Van Ranst, M., et al. (2006).
808   Inhibition of feline (FIPV) and human (SARS) coronavirus by semisynthetic derivatives of
809   glycopeptide antibiotics. *Antiviral Res.* 72, 20–33. doi:10.1016/j.antiviral.2006.03.005.

810   Barnard, D. L., Day, C. W., Bailey, K., Heiner, M., Montgomery, R., Lauridsen, L., et al. (2006).
811   Enhancement of the infectivity of SARS-CoV in BALB/c mice by IMP dehydrogenase
812   inhibitors, including ribavirin. *Antiviral Res.* 71, 53–63. doi:10.1016/j.antiviral.2006.03.001.

813   Barnard, D. L., Hubbard, V. D., Burton, J., Smee, D. F., Morrey, J. D., Otto, M. J., et al. (2004).
814   Inhibition of severe acute respiratory syndrome-associated coronavirus (SARSCoV) by calpain
815   inhibitors and beta-D-N4-hydroxycytidine. *Antivir. Chem. Chemother.* 15, 15–22.
816   doi:10.1177/095632020401500102.

817   Bayot, M. L., and King, K. C. (2020). "Biohazard Levels," in *StatPearls* (Treasure Island (FL):
818   StatPearls Publishing). Available at: http://www.ncbi.nlm.nih.gov/books/NBK535351/
819   [Accessed June 12, 2020].

820   Bellingan, G., Maksimow, M., Howell, D. C., Stotz, M., Beale, R., Beatty, M., et al. (2014). The effect
821   of intravenous interferon-beta-1a (FP-1201) on lung CD73 expression and on acute respiratory
822   distress syndrome mortality: an open-label study. *Lancet Respir. Med.* 2, 98–107.
823   doi:10.1016/S2213-2600(13)70259-5.

824   Belouzard, S., Chu, V. C., and Whittaker, G. R. (2009). Activation of the SARS coronavirus spike
825   protein via sequential proteolytic cleavage at two distinct sites. *Proc. Natl. Acad. Sci. U. S. A.*
826   106, 5871–5876. doi:10.1073/pnas.0809524106.

827   Belouzard, S., Millet, J. K., Licitra, B. N., and Whittaker, G. R. (2012). Mechanisms of coronavirus
828   cell entry mediated by the viral spike protein. *Viruses* 4, 1011–1033. doi:10.3390/v4061011.

829   Caly, L., Druce, J. D., Catton, M. G., Jans, D. A., and Wagstaff, K. M. (2020). The FDA-approved
830   drug ivermectin inhibits the replication of SARS-CoV-2 in vitro. *Antiviral Res.* 178, 104787.
831   doi:10.1016/j.antiviral.2020.104787.

832   Cameron, M. C., Word, A. P., and Dominguez, A. (2014). Hydroxychloroquine-induced fatal toxic
833   epidermal necrolysis complicated by angioinvasive rhizopus. *Dermatol. Online J.* 20.

834   Campbell, W. C. (2012). *Ivermectin and Abamectin*. Springer Science & Business Media.

835   Cao, H., and Shi, Y. (2020c). Convalescent plasma: possible therapy for novel coronavirus disease
836   2019. Transfusion 60. doi:10.1111/trf.15797.

837   Cao, Y., Li, L., Feng, Z., Wan, S., Huang, P., Sun, X., et al. (2020a). Comparative genetic analysis of
838   the novel coronavirus (2019-nCoV/SARS-CoV-2) receptor ACE2 in different populations. *Cell*
839   *Discov.* 6, 11. doi:10.1038/s41421-020-0147-1.

27

840   Cao, B., Wang, Y., Wen, D., Liu, W., Wang, J., Fan, G., et al. (2020b). A Trial of Lopinavir–Ritonavir
841   in Adults Hospitalized with Severe Covid-19. *N. Engl. J. Med.* 382, 1787–1799.
842   doi:10.1056/NEJMoa2001282.

843   Carbajo-Lozoya, J., Ma-Lauer, Y., Malešević, M., Theuerkorn, M., Kahlert, V., Prell, E., et al. (2014).
844   Human coronavirus NL63 replication is cyclophilin A-dependent and inhibited by non-
845   immunosuppressive cyclosporine A-derivatives including Alisporivir. *Virus Res.* 184, 44–53.
846   doi:10.1016/j.virusres.2014.02.010.

847   CDC   (2020).   Coronavirus | Human   Coronavirus   Types | CDC.   Available   at:
848   https://www.cdc.gov/coronavirus/types.html [Accessed March 31, 2020].

849   CDC (2020). Information for Laboratories about Coronavirus (COVID-19). *Cent. Dis. Control Prev.*
850   Available   at: https://www.cdc.gov/coronavirus/2019-ncov/lab/lab-biosafety-guidelines.html
851   [Accessed June 12, 2020].

852   Ceccarelli, M., Berretta, M., Rullo, E. V., Nunnari, G., and Cacopardo, B. (2020). Differences and
853   similarities between Severe Acute Respiratory Syndrome (SARS)-CoronaVirus (CoV) and
854   SARS-CoV-2. Would a rose by another name smell as sweet? 3.

855   Chan, J. F. W., Chan, K.-H., Kao, R. Y. T., To, K. K. W., Zheng, B.-J., Li, C. P. Y., et al. (2013).
856   Broad-spectrum antivirals for the emerging Middle East respiratory syndrome coronavirus. *J.
857   Infect.* 67, 606–616. doi:10.1016/j.jinf.2013.09.029.

858   Chan, J. F.-W., Yao, Y., Yeung, M.-L., Deng, W., Bao, L., Jia, L., et al. (2015). Treatment With
859   Lopinavir/Ritonavir or Interferon-β1b Improves Outcome of MERS-CoV Infection in a
860   Nonhuman Primate Model of Common Marmoset. *J. Infect. Dis.* 212, 1904–1913.
861   doi:10.1093/infdis/jiv392.

862   Chen, J., Liu, D., Liu, L., Liu, P., Xu, Q., Xia, L., et al. (2020). [A pilot study of hydroxychloroquine
863   in treatment of patients with moderate COVID-19]. *Zhejiang Xue Xue Bao Yi Xue Ban J.
864   Zhejiang Univ. Med. Sci.* 49, 215–219.

865   Chen, Y., Liu, Q., and Guo, D. (2020b). Emerging coronaviruses: Genome structure, replication, and
866   pathogenesis. *J. Med. Virol.* 92, 418–423. doi:10.1002/jmv.25681.

867   Chen, L.-R., Wang, Y.-C., Lin, Y. W., Chou, S.-Y., Chen, S.-F., Liu, L. T., et al. (2005). Synthesis and
868   evaluation of isatin derivatives as effective SARS coronavirus 3CL protease inhibitors. *Bioorg.
869   Med. Chem. Lett.* 15, 3058–3062. doi:10.1016/j.bmcl.2005.04.027.

870   Chen, L., Xiong, J., Bao, L., and Shi, Y. (2020). Convalescent plasma as a potential therapy for
871   COVID-19. Lancet Infect. Dis. 20, 398–400. doi:10.1016/S1473-3099(20)30141-9.

872   Chen, W.-H., Strych, U., Hotez, P. J., and Bottazzi, M. E. (2020). The SARS-CoV-2 Vaccine Pipeline:
873   an Overview. *Curr. Trop. Med. Rep.*, 1–4. doi:10.1007/s40475-020-00201-6.

874   Cheng, Y., Wong, R., Soo, Y. O. Y., Wong, W. S., Lee, C. K., Ng, M. H. L., et al. (2005). Use of
875   convalescent plasma therapy in SARS patients in Hong Kong. Eur. J. Clin. Microbiol. Infect.
876   Dis. 24, 44–46. doi:10.1007/s10096-004-1271-9.

877   Chen, Z., Hu, J., Zhang, Z., Jiang, S., Han, S., Yan, D., et al. (2020). Efficacy of hydroxychloroquine
878   in patients with COVID-19: results of a randomized clinical trial. *medRxiv* [Preprint]. Available
879   at: https://doi.org/10.1101/2020.03.22.20040758 (Accessed June 13, 2020)

880   Chihrin, S., and Loutfy, M. R. (2005). Overview of antiviral and anti-inflammatory treatment for
881   severe acute respi ratory syndrome. *Expert Rev. Anti Infect. Ther.* 3, 251–262.
882   doi:10.1586/14787210.3.2.251.

883   Chorin, E., Dai, M., Shulman, E., Wadhwani, L., Cohen, R. B., Barbhaiya, C., et al. (2020). The QT
884   Interval   in   Patients   with   SARS-CoV-2   Infection   Treated   with
885   Hydroxychloroquine/Azithromycin.   *medRxiv*   [Preprint].   Available   at:
886   https://doi.org/10.1101/2020.04.02.20047050 (Accessed July 04, 2020)

887   Chousterman, B. G., Swirski, F. K., and Weber, G. F. (2017). Cytokine storm and sepsis disease
888   pathogenesis. Semin. Immunopathol. 39, 517–528. doi:10.1007/s00281-017-0639-8.

889   Chu, C. M., Cheng, V. C. C., Hung, I. F. N., Wong, M. M. L., Chan, K. H., Chan, K. S., et al. (2004).
890   Role of lopinavir/ritonavir in the treatment of SARS: initial virological and clinical findings.
891   *Thorax* 59, 252–256. doi:10.1136/thorax.2003.012658.

892   Chu, H., Chan, J. F.-W., Yuen, T. T.-T., Shuai, H., Yuan, S., Wang, Y., et al. (2020). Comparative
893   tropism, replication kinetics, and cell damage profiling of SARS-CoV-2 and SARS-CoV with
894   implications for clinical manifestations, transmissibility, and laboratory studies of COVID-19:
895   an observational study. *Lancet Microbe* 1, e14–e23. doi:10.1016/S2666-5247(20)30004-5.

896   Cinatl, J., Michaelis, M., Hoever, G., Preiser, W., and Doerr, H. W. (2005). Development of antiviral
897   therapy   for   severe   acute   respiratory   syndrome.   *Antiviral   Res.*   66,   81–97.
898   doi:10.1016/j.antiviral.2005.03.002.

899   Cinatl, J., Morgenstern, B., Bauer, G., Chandra, P., Rabenau, H., and Doerr, H. W. (2003).
900   Glycyrrhizin, an active component of liquorice roots, and replication of SARS-associated
901   coronavirus. *The Lancet* 361, 2045–2046. doi:10.1016/S0140-6736(03)13615-X.

902   Clark, L. T., Watkins, L., Piña, I. L., Elmer, M., Akinboboye, O., Gorham, M., et al. (2019). Increasing
903   Diversity in Clinical Trials: Overcoming Critical Barriers. *Curr. Probl. Cardiol.* 44, 148–172.
904   doi:10.1016/j.cpcardiol.2018.11.002.

905   Cohn, L. A. (1991). The influence of corticosteroids on host defense mechanisms. *J. Vet. Intern.*
906   *Med.* 5, 95–104. doi:10.1111/j.1939-1676.1991.tb00939.x.

907   Coleman, C. M., and Frieman, M. B. (2014). Coronaviruses: Important Emerging Human Pathogens.
908   *J. Virol.* 88, 5209–5212. doi:10.1128/JVI.03488-13.

29

909   Cui, J., Li, F., and Shi, Z.-L. (2019). Origin and evolution of pathogenic coronaviruses. *Nat. Rev.*
910   *Microbiol.* 17, 181–192. doi:10.1038/s41579-018-0118-9.

911   Cvetkovic, R. S., and Goa, K. L. (2003). Lopinavir/Ritonavir. *Drugs* 63, 769–802.
912   doi:10.2165/00003495-200363080-00004.

913   D'Amato, G., Stanziola, A., Sanduzzi, A., Liccardi, G., Salzillo, A., Vitale, C., et al. (2014). Treating
914   severe allergic asthma with anti-IgE monoclonal antibody (omalizumab): a review. *Multidiscip.*
915   *Respir. Med.* 9, 23. doi:10.1186/2049-6958-9-23.

916   Dai, C., Ma, Y., Zhao, Z., Zhao, R., Wang, Q., Wu, Y., et al. (2008). Mucroporin, the First Cationic
917   Host Defense Peptide from the Venom of Lychas mucronatus. *Antimicrob. Agents Chemother.*
918   52, 3967–3972. doi:10.1128/AAC.00542-08.

919   Davis, T. L., Walker, J. R., Campagna-Slater, V., Finerty, P. J., Paramanathan, R., Bernstein, G., et al.
920   (2010). Structural and biochemical characterization of the human cyclophilin family of
921   peptidyl-prolyl isomerases. *PLoS Biol.* 8, e1000439. doi:10.1371/journal.pbio.1000439.

922   Day, C. W., Baric, R., Cai, S. X., Frieman, M., Kumaki, Y., Morrey, J. D., et al. (2009). A new mouse-
923   adapted strain of SARS-CoV as a lethal model for evaluating antiviral agents in vitro and in
924   vivo. *Virology* 395, 210–222. doi:10.1016/j.virol.2009.09.023.

925   de Olano, J., Howland, M. A., Su, M. K., Hoffman, R. S., and Biary, R. (2019). Toxicokinetics of
926   hydroxychloroquine following a massive overdose. *Am. J. Emerg. Med.* 37, 2264.e5-2264.e8.
927   doi:10.1016/j.ajem.2019.158387.

928   de Wilde, A. H., Falzarano, D., Zevenhoven-Dobbe, J. C., Beugeling, C., Fett, C., Martellaro, C., et al.
929   (2017). Alisporivir inhibits MERS- and SARS-coronavirus replication in cell culture, but not
930   SARS-coronavirus infection in a mouse model. Virus Res. 228, 7–13.
931   doi:10.1016/j.virusres.2016.11.011.

932   de Wilde, A. H., Raj, V. S., Oudshoorn, D., Bestebroer, T. M., van Nieuwkoop, S., Limpens, R. W. A.
933   L., et al. (2013). MERS-coronavirus replication induces severe in vitro cytopathology and is
934   strongly inhibited by cyclosporin A or interferon-α treatment. *J. Gen. Virol.* 94, 1749–1760.
935   doi:10.1099/vir.0.052910-0.

936   de Wilde, A. H., Zevenhoven-Dobbe, J. C., van der Meer, Y., Thiel, V., Narayanan, K., Makino, S., et
937   al. (2011). Cyclosporin A inhibits the replication of diverse coronaviruses. *J. Gen. Virol.* 92,
938   2542–2548. doi:10.1099/vir.0.034983-0.

939   Devaux, C. A., Rolain, J.-M., Colson, P., and Raoult, D. (2020). New insights on the antiviral effects
940   of chloroquine against coronavirus: what to expect for COVID-19? *Int. J. Antimicrob. Agents*
941   55, 105938. doi:10.1016/j.ijantimicag.2020.105938.

942   Dhama, K., Sharun, K., Tiwari, R., Dadar, M., Malik, Y. S., Singh, K. P., et al. (2020). COVID-19, an
943   emerging coronavirus infection: advances and prospects in designing and developing vaccines,

30

944   immunotherapeutics, and therapeutics. *Hum. Vaccines Immunother.*, 1–7.
945   doi:10.1080/21645515.2020.1735227.

946   Duan, K., Liu, B., Li, C., Zhang, H., Yu, T., Qu, J., et al. (2020). Effectiveness of convalescent plasma
947   therapy in severe COVID-19 patients. Proc. Natl. Acad. Sci. U. S. A. 117, 9490–9496.
948   doi:10.1073/pnas.2004168117.

949   El-Solia, A., Al-Otaibi, K., and Ai-Hwiesh, A. K. (2018). Hydroxychloroquine-induced
950   hypoglycaemia in non-diabetic renal patient on peritoneal dialysis. *BMJ Case Rep.* 2018.
951   doi:10.1136/bcr-2017-223639.

952   Falzarano, D., de Wit, E., Martellaro, C., Callison, J., Munster, V. J., and Feldmann, H. (2013).
953   Inhibition of novel β coronavirus replication by a combination of interferon-α2b and ribavirin.
954   *Sci. Rep.* 3, 1686. doi:10.1038/srep01686.

955   Falzarano, D., de Wit, E., Rasmussen, A. L., Feldmann, F., Okumura, A., Scott, D. P., et al. (2013).
956   Treatment with interferon-α2b and ribavirin improves outcome in MERS-CoV–infected rhesus
957   macaques. Nat. Med. 19, 1313–1317. doi:10.1038/nm.3362.

958   FDA (2020). FDA cautions against use of hydroxychloroquine or chloroquine for COVID-19 outside
959   of the hospital setting or a clinical trial due to risk of heart rhythm problems. *FDA*. Available
960   at: https://www.fda.gov/drugs/drug-safety-and-availability/fda-cautions-against-use-
961   hydroxychloroquine-or-chloroquine-covid-19-outside-hospital-setting-or [Accessed July 5,
962   2020].

963   Fehr, A. R., and Perlman, S. (2015). Coronaviruses: An Overview of Their Replication and
964   Pathogenesis. *Methods Mol. Biol. Clifton NJ* 1282, 1–23. doi:10.1007/978-1-4939-2438-7_1.

965   Ferron, F., Subissi, L., De Morais, A. T. S., Le, N. T. T., Sevajol, M., Gluais, L., et al. (2017). Structural
966   and molecular basis of mismatch correction and ribavirin excision from coronavirus RNA.
967   Proc. Natl. Acad. Sci. U. S. A. 115, E162–E171. doi:10.1073/pnas.1718806115.

968   Gan, Y.-R., Huang, H., Huang, Y.-D., Rao, C.-M., Zhao, Y., Liu, J.-S., et al. (2006). Synthesis and
969   activity of an octapeptide inhibitor designed for SARS coronavirus main proteinase. *Peptides*
970   27, 622–625. doi:10.1016/j.peptides.2005.09.006.

971   Ganeshpurkar, A., Gutti, G., and Singh, S. K. (2019). "Chapter 1 - RNA-Dependent RNA Polymerases
972   and Their Emerging Roles in Antiviral Therapy," in *Viral Polymerases*, ed. S. P. Gupta
973   (Academic Press), 1–42. doi:10.1016/B978-0-12-815422-9.00001-2.

974   Gao, J., Tian, Z., and Yang, X. (2020). Breakthrough: Chloroquine phosphate has shown apparent
975   efficacy in treatment of COVID-19 associated pneumonia in clinical studies. Biosci. Trends 14,
976   72–73. doi:10.5582/BST.2020.01047.

977   Garraud, O. (2017). Use of convalescent plasma in Ebola virus infection. Transfus. Apher. Sci. 56, 31–
978   34. doi:10.1016/j.transci.2016.12.014.

31

979 Gautret, P., Lagier, J.-C., Parola, P., Hoang, V. T., Meddeb, L., Mailhe, M., et al. (2020).
980   Hydroxychloroquine and azithromycin as a treatment of COVID-19: results of an open-label
981   non-randomized   clinical   trial.   *Int.   J.   Antimicrob.   Agents*,   105949.
982   doi:10.1016/j.ijantimicag.2020.105949.

983 Giles, A. J., Hutchinson, M.-K. N. D., Sonnemann, H. M., Jung, J., Fecci, P. E., Ratnam, N. M., et al.
984   (2018). Dexamethasone-induced immunosuppression: mechanisms and implications for
985   immunotherapy. *J. Immunother. Cancer* 6, 51. doi:10.1186/s40425-018-0371-5.

986 Girijala, R. L., Siddiqi, I., Kwak, Y., Wright, D., Patel, D. B., and Goldberg, L. H. (2019). Pustular
987   DRESS Syndrome Secondary to Hydroxychloroquine With EBV Reactivation. *J. Drugs
988   Dermatol. JDD* 18, 207–209.

989 Gorbalenya, A. E., Baker, S. C., Baric, R. S., de Groot, R. J., Drosten, C., Gulyaeva, A. A., et al.
990   (2020a). *Severe acute respiratory syndrome-related coronavirus* : The species and its viruses –
991   a statement of the Coronavirus Study Group. Microbiology doi:10.1101/2020.02.07.937862.

992 Gorbalenya, A. E., Baker, S. C., Baric, R. S., de Groot, R. J., Drosten, C., Gulyaeva, A. A., et al.
993   (2020b). The species Severe acute respiratory syndrome-related coronavirus : classifying 2019-
994   nCoV and naming it SARS-CoV-2. *Nat. Microbiol.* 5, 536–544. doi:10.1038/s41564-020-
995   0695-z.

996 Götz, V., Magar, L., Dornfeld, D., Giese, S., Pohlmann, A., Höper, D., et al. (2016). Influenza A viruses
997   escape from MxA restriction at the expense of efficient nuclear vRNP import. *Sci. Rep.* 6,
998   23138. doi:10.1038/srep23138.

999 Graham, R. L., Donaldson, E. F., and Baric, R. S. (2013). A decade after SARS: strategies for
1000   controlling   emerging   coronaviruses.   *Nat.   Rev.   Microbiol.*   11,   836–848.
1001   doi:10.1038/nrmicro3143.

1002 Green, M. C., Murray, J. L., and Hortobagyi, G. N. (2000). Monoclonal antibody therapy for solid
1003   tumors. *Cancer Treat. Rev.* 26, 269–286. doi:10.1053/ctrv.2000.0176.

1004 Grupp, S. A., Kalos, M., Barrett, D., Aplenc, R., Porter, D. L., Rheingold, S. R., et al. (2013). Chimeric
1005   Antigen Receptor–Modified T Cells for Acute Lymphoid Leukemia. N. Engl. J. Med. 368,
1006   1509–1518. doi:10.1056/NEJMoa1215134.

1007 Guan, B.-J., Su, Y.-P., Wu, H.-Y., and Brian, D. A. (2012). Genetic Evidence of a Long-Range RNA-
1008   RNA Interaction between the Genomic 5′ Untranslated Region and the Nonstructural Protein 1
1009   Coding Region in Murine and Bovine Coronaviruses. *J. Virol.* 86, 4631–4643.
1010   doi:10.1128/JVI.06265-11.

1011 Guan, W., Ni, Z., Hu, Y., Liang, W., Ou, C., He, J., et al. (2020). Clinical Characteristics of
1012   Coronavirus   Disease   2019   in   China.   N.   Engl.   J.   Med.   382,   1708–1720.
1013   doi:10.1056/NEJMoa2002032.

32

1014 Haga, S., Nagata, N., Okamura, T., Yamamoto, N., Sata, T., Yamamoto, N., et al. (2010). TACE
1015   antagonists blocking ACE2 shedding caused by the spike protein of SARS-CoV are candidate
1016   antiviral compounds. *Antiviral Res.* 85, 551–555. doi:10.1016/j.antiviral.2009.12.001.

1017 Haga, S., Yamamoto, N., Nakai-Murakami, C., Osawa, Y., Tokunaga, K., Sata, T., et al. (2008).
1018   Modulation of TNF- -converting enzyme by the spike protein of SARS-CoV and ACE2 induces
1019   TNF- production and facilitates viral entry. *Proc. Natl. Acad. Sci.* 105, 7809–7814.
1020   doi:10.1073/pnas.0711241105.

1021 Han, D. P., Lohani, M., and Cho, M. W. (2007). Specific Asparagine-Linked Glycosylation Sites Are
1022   Critical for DC-SIGN- and L-SIGN-Mediated Severe Acute Respiratory Syndrome
1023   Coronavirus Entry. *J. Virol.* 81, 12029–12039. doi:10.1128/JVI.00315-07.

1024 Hart, B. J., Dyall, J., Postnikova, E., Zhou, H., Kindrachuk, J., Johnson, R. F., et al. (2014). Interferon-
1025   β and mycophenolic acid are potent inhibitors of middle east respiratory syndrome coronavirus
1026   in cell-based assays. J. Gen. Virol. 95, 571–577. doi:10.1099/vir.0.061911-0.

1027 Haynes, L. M., Caidi, H., Radu, G. U., Miao, C., Harcourt, J. L., Tripp, R. A., et al. (2009). Therapeutic
1028   Monoclonal Antibody Treatment Targeting Respiratory Syncytial Virus (RSV) G Protein
1029   Mediates Viral Clearance and Reduces the Pathogenesis of RSV Infection in BALB/c Mice. *J.*
1030   *Infect. Dis.* 200, 439–447. doi:10.1086/600108.

1031 Hensley, L. E., Fritz, E. A., Jahrling, P. B., Karp, C., Huggins, J. W., and Geisbert, T. W. (2004).
1032   Interferon-β 1a and SARS Coronavirus Replication. *Emerg. Infect. Dis.* 10, 317–319.
1033   doi:10.3201/eid1002.030482.

1034 Hess, A. S., and Abd-Elsayed, A. (2019). "Observational Studies: Uses and Limitations," in *Pain: A*
1035   *Review Guide*, ed. A. Abd-Elsayed (Cham: Springer International Publishing), 123–125.
1036   doi:10.1007/978-3-319-99124-5_31.

1037 Ho, T.-Y., Wu, S.-L., Chen, J.-C., Li, C.-C., and Hsiang, C.-Y. (2007). Emodin blocks the SARS
1038   coronavirus spike protein and angiotensin-converting enzyme 2 interaction. *Antiviral Res.* 74,
1039   92–101. doi:10.1016/j.antiviral.2006.04.014.

1040 Hoever, G., Baltina, L., Michaelis, M., Kondratenko, R., Baltina, L., Tolstikov, G. A., et al. (2005).
1041   Antiviral Activity of Glycyrrhizic Acid Derivatives against SARS−Coronavirus. *J. Med. Chem.*
1042   48, 1256–1259. doi:10.1021/jm0493008.

1043 Hoffmann, M., Kleine-Weber, H., Schroeder, S., Krüger, N., Herrler, T., Erichsen, S., et al. (2020).
1044   SARS-CoV-2 Cell Entry Depends on ACE2 and TMPRSS2 and Is Blocked by a Clinically
1045   Proven Protease Inhibitor. *Cell*, S0092867420302294. doi:10.1016/j.cell.2020.02.052.

1046 Holshue, M. L., DeBolt, C., Lindquist, S., Lofy, K. H., Wiesman, J., Bruce, H., et al. (2020). First Case
1047   of 2019 Novel Coronavirus in the United States. *N. Engl. J. Med.* 382, 929–936.
1048   doi:10.1056/NEJMoa2001191.

1049 Horby, P., Lim, W. S., Emberson, J., Mafham, M., Bell, J., Linsell, L., et al. (2020). Effect of
1050   Dexamethasone in Hospitalized Patients with COVID-19: Preliminary Report. *medRxiv*
1051   [Preprint]. Available at: https://doi.org/10.1101/2020.06.22.20137273 (Accessed July 01,
1052   2020).

1053 Huentelman Matthew J., Zubcevic Jasenka, Hernández Prada Jose A., Xiao Xiaodong, Dimitrov
1054   Dimiter S., Raizada Mohan K., et al. (2004). Structure-Based Discovery of a Novel
1055   Angiotensin-Converting Enzyme 2 Inhibitor. *Hypertension* 44, 903–906.
1056   doi:10.1161/01.HYP.0000146120.29648.36.

1057 Hsu, L. Y., Chia, P. Y., and Lim, J. F. (2020). The Novel Coronavirus (SARS-CoV-2) Epidemic.
1058   *Ann. Acad. Med. Singapore* 49, 1–3.

1059 Huang, I.-C., Bosch, B. J., Li, F., Li, W., Lee, K. H., Ghiran, S., et al. (2006). SARS coronavirus, but
1060   not human coronavirus NL63, utilizes cathepsin L to infect ACE2-expressing cells. *J. Biol.*
1061   *Chem.* 281, 3198–3203. doi:10.1074/jbc.M508381200.

1062 Huentelman, M. J., Zubcevic, J., Katovich, M. J., and Raizada, M. K. (2004). Cloning and
1063   characterization of a secreted form of angiotensin-converting enzyme 2. *Regul. Pept.* 122, 61–
1064   67. doi:10.1016/j.regpep.2004.05.003.

1065 Hung, I. F.-N., Lung, K.-C., Tso, E. Y.-K., Liu, R., Chung, T. W.-H., Chu, M.-Y., et al. (2020). Triple
1066   combination of interferon beta-1b, lopinavir-ritonavir, and ribavirin in the treatment of patients
1067   admitted to hospital with COVID-19: an open-label, randomised, phase 2 trial. *Lancet Lond.*
1068   *Engl.* 395, 1695–1704. doi:10.1016/S0140-6736(20)31042-4.

1069 Huynh, J., Li, S., Yount, B., Smith, A., Sturges, L., Olsen, J. C., et al. (2012). Evidence Supporting a
1070   Zoonotic Origin of Human Coronavirus Strain NL63. *J. Virol.* 86, 12816–12825.
1071   doi:10.1128/JVI.00906-12.

1072 Jacobson, J. M., Bosinger, S. E., Kang, M., Belaunzaran-Zamudio, P., Matining, R. M., Wilson, C. C.,
1073   et al. (2016). The Effect of Chloroquine on Immune Activation and Interferon Signatures
1074   Associated with HIV-1. *AIDS Res. Hum. Retroviruses* 32, 636–647.
1075   doi:10.1089/aid.2015.0336.

1076 Jasenosky, L. D., Cadena, C., Mire, C. E., Borisevich, V., Haridas, V., Ranjbar, S., et al. (2019). The
1077   FDA-Approved Oral Drug Nitazoxanide Amplifies Host Antiviral Responses and Inhibits
1078   Ebola Virus. *iScience* 19, 1279–1290. doi:10.1016/j.isci.2019.07.003.

1079 Jeon, S., Ko, M., Lee, J., Choi, I., Byun, S. Y., Park, S., et al. (2020). Identification of antiviral drug
1080   candidates against SARS-CoV-2 from FDA-approved drugs. *Antimicrob. Agents Chemother.*
1081   doi:10.1128/AAC.00819-20.

1082 Julião, A. (2020). No mundo todo, 153 fármacos são testados em pacientes com COVID-19. *AGÊNCIA*
1083   *FAPESP*. Available at: http://agencia.fapesp.br/no-mundo-todo-153-farmacos-sao-testados-
1084   em-pacientes-com-covid-19/33335/ [Accessed June 9, 2020].

1085   Juurlink, D. N. (2020). Safety considerations with chloroquine, hydroxychloroquine and azithromycin
1086   in   the   management   of   SARS-CoV-2   infection.   *CMAJ*   192,   E450–E453.
1087   doi:10.1503/cmaj.200528.

1088   Kaeppler, U., Stiefl, N., Schiller, M., Vicik, R., Breuning, A., Schmitz, W., et al. (2005). A New Lead
1089   for Nonpeptidic Active-Site-Directed Inhibitors of the Severe Acute Respiratory Syndrome
1090   Coronavirus Main Protease Discovered by a Combination of Screening and Docking Methods.
1091   *J. Med. Chem.* 48, 6832–6842. doi:10.1021/jm0501782.

1092   Kahn, J. S., and McIntosh, K. (2005). History and Recent Advances in Coronavirus Discovery. *(Riou
1093   et al., 1988; de Olano et al., 2019; Smit et al., 2020)*

1094   Karamitros, T., Papadopoulou, G., Bousali, M., Mexias, A., Tsiodras, S., and Mentis, A. (2020). SARS-
1095   CoV-2 exhibits intra-host genomic plasticity and low-frequency polymorphic quasispecies.
1096   *bioRxiv* [Preprint]. Available at: https://doi.org/10.1101/2020.03.27.009480 (Accessed July 03,
1097   2020).

1098   Katz, M. (1977). Anthelmintics. *Drugs* 13, 124–136. doi:10.2165/00003495-197713020-00002.

1099   Kernan, W. N., Viscoli, C. M., Makuch, R. W., Brass, L. M., and Horwitz, R. I. (1999). Stratified
1100   Randomization   for   Clinical   Trials.   *J.   Clin.   Epidemiol.*   52,   19–26.   doi:10.1016/S0895-
1101   4356(98)00138-3.

1102   Kesel, A. J. (2003). A system of protein target sequences for anti-RNA-viral chemotherapy by a
1103   vitamin B6-Derived zinc-Chelating trioxa-adamantane-triol. *Bioorg. Med. Chem.* 11, 4599–
1104   4613. doi:10.1016/S0968-0896(03)00500-5.

1105   Kirchheiner, J., Keulen, J.-T. H. A., Bauer, S., Roots, I., and Brockmöller, J. (2008). Effects of the
1106   CYP2D6 gene duplication on the pharmacokinetics and pharmacodynamics of tramadol. *J.
1107   Clin. Psychopharmacol.* 28, 78–83. doi:10.1097/JCP.0b013e318160f827.

1108   Khamitov, R., Loginova, S., Borisevich, S., Maksimov, V., and Shuster, A. (2008). Antiviral activity
1109   of arbidol and its derivatives against the pathogen of severe acute respiratory syndrome in the
1110   cell cultures. 9–13. Available at: https://europepmc.org/article/med/18756809 [Accessed June
1111   10, 2020].

1112   Kim, D., Lee, J., Yang, J., Jw, K., Vn, K., and H, C. (2020). The Architecture of SARS-CoV-2
1113   Transcriptome. *Cell* 181, 914-921.e10. doi:10.1016/j.cell.2020.04.011.

1114   Kim, Y., Lovell, S., Tiew, K.-C., Mandadapu, S. R., Alliston, K. R., Battaile, K. P., et al. (2012). Broad-
1115   Spectrum Antivirals against 3C or 3C-Like Proteases of Picornaviruses, Noroviruses, and
1116   Coronaviruses. *J. Virol.* 86, 11754–11762. doi:10.1128/JVI.01348-12.

1117   Kim, Y., Mandadapu, S. R., Groutas, W. C., and Chang, K.-O. (2013). Potent inhibition of feline
1118   coronaviruses with peptidyl compounds targeting coronavirus 3C-like protease. *Antiviral Res.*
1119   97, 161–168. doi:10.1016/j.antiviral.2012.11.005.

1120 Kipar, A., Meli, M. L., Baptiste, K. E., Bowker, L. J., and Lutz, H. (2010). Sites of feline coronavirus
1121   persistence in healthy cats. *J. Gen. Virol.* 91, 1698–1707. doi:10.1099/vir.0.020214-0.

1122 Ko, J.-H., Seok, H., Cho, S. Y., Ha, Y. E., Baek, J. Y., Kim, S. H., et al. (2018). Challenges of
1123   convalescent plasma infusion therapy in Middle East respiratory coronavirus infection: a single
1124   centre experience. *Antivir. Ther.* 23, 617–622. doi:10.3851/IMP3243.

1125 Kobayashi, Y., Watanabe, S., Konishi, M., Yokoi, M., Kakehashi, R., Kaito, M., et al. (1993).
1126   Quantitation and typing of serum hepatitis C virus RNA in patients with chronic hepatitis C
1127   treated with interferon-β. *Hepatology* 18, 1319–1325. doi:10.1002/hep.1840180606.

1128 Lai, C.-C., Shih, T.-P., Ko, W.-C., Tang, H.-J., and Hsueh, P.-R. (2020). Severe acute respiratory
1129   syndrome coronavirus 2 (SARS-CoV-2) and coronavirus disease-2019 (COVID-19): The
1130   epidemic and the challenges. *Int. J. Antimicrob. Agents* 55, 105924.
1131   doi:10.1016/j.ijantimicag.2020.105924.

1132 Lai, M. M., and Stohlman, S. A. (1981). Comparative analysis of RNA genomes of mouse hepatitis
1133   viruses. *J. Virol.* 38, 661–670. Available at:
1134   https://www.ncbi.nlm.nih.gov/pmc/articles/PMC171196/ [Accessed March 31, 2020].

1135 Laing, R., Gillan, V., and Devaney, E. (2017). Ivermectin – Old Drug, New Tricks? *Trends Parasitol.*
1136   33, 463–472. doi:10.1016/j.pt.2017.02.004.

1137 Laplante, J., and St George, K. (2014). Antiviral resistance in influenza viruses: laboratory testing.
1138   *Clin. Lab. Med.* 34, 387–408. doi:10.1016/j.cll.2014.02.010.

1139 Lee, J. Y., Vinayagamoorthy, N., Han, K., Kwok, S. K., Ju, J. H., Park, K. S., et al. (2016). Association
1140   of Polymorphisms of Cytochrome P450 2D6 With Blood Hydroxychloroquine Levels in
1141   Patients With Systemic Lupus Erythematosus. *Arthritis Rheumatol.* 68, 184–190.
1142   doi:10.1002/art.39402.

1143 Lee, T.-W., Cherney, M. M., Huitema, C., Liu, J., James, K. E., Powers, J. C., et al. (2005). Crystal
1144   Structures of the Main Peptidase from the SARS Coronavirus Inhibited by a Substrate-like Aza-
1145   peptide Epoxide. *J. Mol. Biol.* 353, 1137–1151. doi:10.1016/j.jmb.2005.09.004.

1146 Lengauer, T., and Sing, T. (2006). Bioinformatics-assisted anti-HIV therapy. *Nat. Rev. Microbiol.* 4,
1147   790–797. doi:10.1038/nrmicro1477.

1148 Li, D. K., and Chung, R. T. (2019). Overview of Direct-Acting Antiviral Drugs and Drug Resistance
1149   of Hepatitis C Virus. *Methods Mol. Biol. Clifton NJ* 1911, 3–32. doi:10.1007/978-1-4939-8976-
1150   8_1.

1151 Li, K., Li, H., Bi, Z., Song, D., Zhang, F., Lei, D., et al. (2019). Significant inhibition of re-emerged
1152   and emerging swine enteric coronavirus in vitro using the multiple shRNA expression vector.
1153   *Antiviral Res.* 166, 11–18. doi:10.1016/j.antiviral.2019.03.010.

36

Li, Q., Zhao, Z., Zhou, D., Chen, Y., Hong, W., Cao, L., et al. (2011). Virucidal activity of a scorpion venom peptide variant mucroporin-M1 against measles, SARS-CoV and influenza H5N1 viruses. *Peptides* 32, 1518–1525. doi:10.1016/j.peptides.2011.05.015.

Li, X., Geng, M., Peng, Y., Meng, L., and Lu, S. (2020). Molecular immune pathogenesis and diagnosis of COVID-19. *J. Pharm. Anal.* 10, 102–108. doi:10.1016/j.jpha.2020.03.001.

Lian, N., Xie, H., Lin, S., Huang, J., Zhao, J., and Lin, Q. (2020). Umifenovir treatment is not associated with improved outcomes in patients with coronavirus disease 2019: a retrospective study. *Clin. Microbiol. Infect.* doi:10.1016/j.cmi.2020.04.026.

Lip, K.-M., Shen, S., Yang, X., Keng, C.-T., Zhang, A., Oh, H.-L. J., et al. (2006). Monoclonal antibodies targeting the HR2 domain and the region immediately upstream of the HR2 of the S protein neutralize in vitro infection of severe acute respiratory syndrome coronavirus. *J. Virol.* 80, 941–950. doi:10.1128/JVI.80.2.941-950.2006.

Lipinski, C. A., Lombardo, F., Dominy, B. W., and Feeney, P. J. (2001). Experimental and computational approaches to estimate solubility and permeability in drug discovery and development settings. *Adv. Drug Deliv. Rev.* 46, 3–26. doi:10.1016/s0169-409x(00)00129-0.

Lipman, N. S., Jackson, L. R., Trudel, L. J., and Weis-Garcia, F. (2005). Monoclonal Versus Polyclonal Antibodies: Distinguishing Characteristics, Applications, and Information Resources. *ILAR J.* 46, 258–268. doi:10.1093/ilar.46.3.258.

Liu, J., Cao, R., Xu, M., Wang, X., Zhang, H., Hu, H., et al. (2020). Hydroxychloroquine, a less toxic derivative of chloroquine, is effective in inhibiting SARS-CoV-2 infection in vitro. *Cell Discov.* 6, 1–4. doi:10.1038/s41421-020-0156-0.

Lu, G., Wang, Q., and Gao, G. F. (2015). Bat-to-human: spike features determining 'host jump' of coronaviruses SARS-CoV, MERS-CoV, and beyond. *Trends Microbiol.* 23, 468–478. doi:10.1016/j.tim.2015.06.003.

Lusvarghi, S., and Bewley, C. A. (2016). Griffithsin: An Antiviral Lectin with Outstanding Therapeutic Potential. *Viruses* 8. doi:10.3390/v8100296.

Madhugiri, R., Karl, N., Petersen, D., Lamkiewicz, K., Fricke, M., Wend, U., et al. (2018). Structural and functional conservation of cis-acting RNA elements in coronavirus 5'-terminal genome regions. *Virology* 517, 44–55. doi:10.1016/j.virol.2017.11.025.

Marasco, W. A., and Sui, J. (2007). The growth and potential of human antiviral monoclonal antibody therapeutics. *Nat. Biotechnol.* 25, 1421–1434. doi:10.1038/nbt1363.

Matsuyama, S., Nao, N., Shirato, K., Kawase, M., Saito, S., Takayama, I., et al. (2020). Enhanced isolation of SARS-CoV-2 by TMPRSS2-expressing cells. *Proc. Natl. Acad. Sci.* doi:10.1073/pnas.2002589117.

37

1188 Mauthe, M., Orhon, I., Rocchi, C., Zhou, X., Luhr, M., Hijlkema, K.-J., et al. (2018). Chloroquine
1189   inhibits autophagic flux by decreasing autophagosome-lysosome fusion. *Autophagy* 14, 1435–
1190   1455. doi:10.1080/15548627.2018.1474314.

1191 McDonagh, P., Sheehy, P. A., and Norris, J. M. (2011). In vitro inhibition of feline coronavirus
1192   replication by small interfering RNAs. *Vet. Microbiol.* 150, 220–229.
1193   doi:10.1016/j.vetmic.2011.01.023.

1194 McDonagh, P., Sheehy, P. A., and Norris, J. M. (2015). Combination siRNA therapy against feline
1195   coronavirus can delay the emergence of antiviral resistance in vitro. *Vet. Microbiol.* 176, 10–
1196   18. doi:10.1016/j.vetmic.2014.12.009.

1197 Medical, J. S.-03/02/2020 2 mins-, and News (2020). CureVac Bids to Develop First mRNA
1198   Coronavirus Vaccine. *Labiotech.eu*. Available at: https://www.labiotech.eu/medical/curevac-
1199   coronavirus-outbreak-cepi/ [Accessed June 8, 2020].

1200 Mehta, P., McAuley, D. F., Brown, M., Sanchez, E., Tattersall, R. S., and Manson, J. J. (2020).
1201   COVID-19: consider cytokine storm syndromes and immunosuppression. *Lancet Lond. Engl.*
1202   395, 1033–1034. doi:10.1016/S0140-6736(20)30628-0.

1203 Millet, J. K., Séron, K., Labitt, R. N., Danneels, A., Palmer, K. E., Whittaker, G. R., et al. (2016).
1204   Middle East respiratory syndrome coronavirus infection is inhibited by griffithsin. *Antiviral
1205   Res.* 133, 1–8. doi:10.1016/j.antiviral.2016.07.011.

1206 Mills, A. M., Nelson, M., Jayaweera, D., Ruxrungtham, K., Cassetti, I., Girard, P.-M., et al. (2009).
1207   Once-daily darunavir/ritonavir vs. lopinavir/ritonavir in treatment-naive, HIV-1-infected
1208   patients: 96-week analysis. *AIDS* 23, 1679–1688. doi:10.1097/QAD.0b013e32832d7350.

1209 Mohan, D., Mohandas, E., and Rajat, R. (1981). Chloroquine psychosis: a chemical psychosis? *J. Natl.
1210   Med. Assoc.* 73, 1073–1076.

1211 Molina, J. M., Delaugerre, C., Le Goff, J., Mela-Lima, B., Ponscarme, D., Goldwirt, L., et al. (2020).
1212   No evidence of rapid antiviral clearance or clinical benefit with the combination of
1213   hydroxychloroquine and azithromycin in patients with severe COVID-19 infection. *Med. Mal.
1214   Infect.* 50, 384. doi:10.1016/j.medmal.2020.03.006.

1215 Morra, M. E., Van Thanh, L., Kamel, M. G., Ghazy, A. A., Altibi, A. M. A., Dat, L. M., et al. (2018).
1216   Clinical outcomes of current medical approaches for Middle East respiratory syndrome: A
1217   systematic review and meta-analysis. Rev. Med. Virol. 28, e1977. doi:10.1002/rmv.1977.

1218 Mullard, A. (2020). COVID-19 vaccine development pipeline gears up. *The Lancet* 395, 1751–1752.
1219   doi:10.1016/S0140-6736(20)31252-6.

1220 Murphy, F., and Middleton, M. (2012). "45 - Cytostatic and cytotoxic drugs," in *Side Effects of Drugs
1221   Annual* A worldwide yearly survey of new data in adverse drug reactions and interactions., ed.
1222   J. K. Aronson (Elsevier), 731–747. doi:10.1016/B978-0-444-59499-0.00045-3.

38

1223   Mzayek, F., Deng, H., Mather, F. J., Wasilevich, E. C., Liu, H., Hadi, C. M., et al. (2007). Randomized
1224   Dose-Ranging Controlled Trial of AQ-13, a Candidate Antimalarial, and Chloroquine in
1225   Healthy Volunteers. *PLOS Clin. Trials* 2, e6. doi:10.1371/journal.pctr.0020006.

1226   Natoli, S., Oliveira, V., Calabresi, P., Maia, L. F., and Pisani, A. (2020). Does SARS-Cov-2 invade the
1227   brain? Translational lessons from animal models. *Eur. J. Neurol.* n/a. doi:10.1111/ene.14277.

1228   O'Keefe, B. R., Giomarelli, B., Barnard, D. L., Shenoy, S. R., Chan, P. K. S., McMahon, J. B., et al.
1229   (2010). Broad-Spectrum In Vitro Activity and In Vivo Efficacy of the Antiviral Protein
1230   Griffithsin against Emerging Viruses of the Family Coronaviridae. *J. Virol.* 84, 2511–2521.
1231   doi:10.1128/JVI.02322-09.

1232   Olearo, F., Nguyen, H., Bonnet, F., Yerly, S., Wandeler, G., Stoeckle, M., et al. (2019). Impact of the
1233   M184V/I Mutation on the Efficacy of Abacavir/Lamivudine/Dolutegravir Therapy in HIV
1234   Treatment-Experienced Patients. *Open Forum Infect. Dis.* 6, ofz330. doi:10.1093/ofid/ofz330.

1235   Parris, G. E. (2004). Hypothesis links emergence of chloroquine-resistant malaria and other
1236   intracellular pathogens and suggests a new strategy for treatment of diseases caused by
1237   intracellular parasites. *Med. Hypotheses* 62, 354–357. doi:10.1016/j.mehy.2003.12.004.

1238   Pastick, K. A., Okafor, E. C., Wang, F., Lofgren, S. M., Skipper, C. P., Nicol, M. R., et al. (2020).
1239   Review: Hydroxychloroquine and Chloroquine for Treatment of SARS-CoV-2 (COVID-19).
1240   *Open Forum Infect. Dis.* 7. doi:10.1093/ofid/ofaa130.

1241   Payne, S. (2017). "Chapter 17 - Family Coronaviridae," in *Viruses*, ed. S. Payne (Academic Press),
1242   149–158. doi:10.1016/B978-0-12-803109-4.00017-9.

1243   Peters, H. L., Jochmans, D., de Wilde, A. H., Posthuma, C. C., Snijder, E. J., Neyts, J., et al. (2015).
1244   Design, synthesis and evaluation of a series of acyclic fleximer nucleoside analogues with anti-
1245   coronavirus   activity.   *Bioorg.   Med.   Chem.   Lett.*   25,   2923–2926.
1246   doi:10.1016/j.bmcl.2015.05.039.

1247   Pettitt, J., Zeitlin, L., Kim, D. H., Working, C., Johnson, J. C., Bohorov, O., et al. (2013). Therapeutic
1248   Intervention of Ebola Virus Infection in Rhesus Macaques with the MB-003 Monoclonal
1249   Antibody   Cocktail.   *Sci.   Transl.   Med.*   5,   199ra113-199ra113.
1250   doi:10.1126/scitranslmed.3006608.

1251   Pedersen, N. C., Black, J. W., Boyle, J. F., Evermann, J. F., McKeirnan, A. J., and Ott, R. L. (1984).
1252   "Pathogenic Differences Between Various Feline Coronavirus Isolates," in *Molecular Biology*
1253   *and Pathogenesis of Coronaviruses* Advances in Experimental Medicine and Biology., eds. P.
1254   J. M. Rottier, B. A. M. van der Zeijst, W. J. M. Spaan, and M. C. Horzinek (Boston, MA:
1255   Springer US), 365–380. doi:10.1007/978-1-4615-9373-7_36.

1256   Pfefferle, S., Schöpf, J., Kögl, M., Friedel, C. C., Müller, M. A., Carbajo-Lozoya, J., et al. (2011). The
1257   SARS-Coronavirus-Host Interactome: Identification of Cyclophilins as Target for Pan-
1258   Coronavirus Inhibitors. *PLoS Pathog.* 7. doi:10.1371/journal.ppat.1002331.

39

1259 Prabakaran, P., Xiao, X., and Dimitrov, D. S. (2004). A model of the ACE2 structure and function as
1260   a SARS-CoV receptor. *Biochem. Biophys. Res. Commun.* 314, 235–241.
1261   doi:10.1016/j.bbrc.2003.12.081.

1262 Preobrazhenskaya, M. N., and Olsufyeva, E. N. (2004). Patents on glycopeptides of the vancomycin
1263   family and their derivatives as antimicrobials: January 1999 – June 2003. *Expert Opin. Ther.*
1264   *Pat.* 14, 141–173. doi:10.1517/13543776.14.2.141.

1265 Printsevskaya, S. S., Solovieva, S. E., Olsufyeva, E. N., Mirchink, E. P., Isakova, E. B., De Clercq, E.,
1266   et al. (2005). Structure−Activity Relationship Studies of a Series of Antiviral and Antibacterial
1267   Aglycon Derivatives of the Glycopeptide Antibiotics Vancomycin, Eremomycin, and
1268   Dechloroeremomycin. *J. Med. Chem.* 48, 3885–3890. doi:10.1021/jm0500774.

1269 Proskurnina, E. V., Izmailov, D. Y., Sozarukova, M. M., Zhuravleva, T. A., Leneva, I. A., and
1270   Poromov, A. A. (2020). Antioxidant Potential of Antiviral Drug Umifenovir. *Molecules* 25,
1271   1577. doi:10.3390/molecules25071577.

1272 PubChem (2005a). Cyclosporin A. Available at:
1273   https://pubchem.ncbi.nlm.nih.gov/compound/5284373 [Accessed April 1, 2020].

1274 PubChem (2005b). Mycophenolic acid. Available at:
1275   https://pubchem.ncbi.nlm.nih.gov/compound/446541 [Accessed April 1, 2020].

1276 PubChem (2005c). Ribavirin. Available at: https://pubchem.ncbi.nlm.nih.gov/compound/37542
1277   [Accessed April 1, 2020].

1278 Pukrittayakamee, S., Tarning, J., Jittamala, P., Charunwatthana, P., Lawpoolsri, S., Lee, S. J., et al.
1279   (2014). Pharmacokinetic Interactions between Primaquine and Chloroquine. *Antimicrob.*
1280   *Agents Chemother.* 58, 3354–3359. doi:10.1128/AAC.02794-13.

1281 Pyrc, K., Bosch, B. J., Berkhout, B., Jebbink, M. F., Dijkman, R., Rottier, P., et al. (2006). Inhibition
1282   of human coronavirus NL63 infection at early stages of the replication cycle. *Antimicrob.*
1283   *Agents Chemother.* 50, 2000–2008. doi:10.1128/AAC.01598-05.

1284 Rabi, F. A., Al Zoubi, M. S., Kasasbeh, G. A., Salameh, D. M., and Al-Nasser, A. D. (2020). SARS-
1285   CoV-2 and Coronavirus Disease 2019: What We Know So Far. *Pathog. Basel Switz.* 9.
1286   doi:10.3390/pathogens9030231.

1287 Ramajayam, R., Tan, K.-P., Liu, H.-G., and Liang, P.-H. (2010). Synthesis, docking studies, and
1288   evaluation of pyrimidines as inhibitors of SARS-CoV 3CL protease. *Bioorg. Med. Chem. Lett.*
1289   20, 3569–3572. doi:10.1016/j.bmcl.2010.04.118.

1290 Ramos-Tovar, E., and Muriel, P. (2019). "Chapter 9 - Phytotherapy for the Liver∗," in *Dietary*
1291   *Interventions in Liver Disease*, eds. R. R. Watson and V. R. Preedy (Academic Press), 101–
1292   121. doi:10.1016/B978-0-12-814466-4.00009-4.

40

Ranieri, V. M., Pettilä, V., Karvonen, M. K., Jalkanen, J., Nightingale, P., Brealey, D., et al. (2020). Effect of Intravenous Interferon β-1a on Death and Days Free From Mechanical Ventilation Among Patients With Moderate to Severe Acute Respiratory Distress Syndrome: A Randomized Clinical Trial. *JAMA* 323, 725–733. doi:10.1001/jama.2019.22525.

Reguera, J., Santiago, C., Mudgal, G., Ordoño, D., Enjuanes, L., and Casasnovas, J. M. (2012). Structural Bases of Coronavirus Attachment to Host Aminopeptidase N and Its Inhibition by Neutralizing Antibodies. *PLoS Pathog.* 8. doi:10.1371/journal.ppat.1002859.

Reusken, C. B., Raj, V. S., Koopmans, M. P., and Haagmans, B. L. (2016). Cross host transmission in the emergence of MERS coronavirus. *Curr. Opin. Virol.* 16, 55–62. doi:10.1016/j.coviro.2016.01.004.

Roback, J. D., and Guarner, J. (2020). Convalescent Plasma to Treat COVID-19: Possibilities and Challenges. *JAMA* 323, 1561–1562. doi:10.1001/jama.2020.4940.

Roberts, R. S., Yount, B. L., Sims, A. C., Baker, S., and Baric, R. S. (2006). "Renilla Luciferase as a Reporter to Assess SARS-CoV mRNA Transcription Regulation and Efficacy of ANTI-SARS-CoV Agents," in *The Nidoviruses* Advances in Experimental Medicine and Biology., eds. S. Perlman and K. V. Holmes (Boston, MA: Springer US), 597–600. doi:10.1007/978-0-387-33012-9_108.

Roques, P., Thiberville, S.-D., Dupuis-Maguiraga, L., Lum, F.-M., Labadie, K., Martinon, F., et al. (2018). Paradoxical Effect of Chloroquine Treatment in Enhancing Chikungunya Virus Infection. *Viruses* 10. doi:10.3390/v10050268.

Rossignol, J.-F. (2014). Nitazoxanide: A first-in-class broad-spectrum antiviral agent. *Antiviral Res.* 110, 94–103. doi:10.1016/j.antiviral.2014.07.014.

Rossignol, J.-F. (2016). Nitazoxanide, a new drug candidate for the treatment of Middle East respiratory syndrome coronavirus. *J. Infect. Public Health* 9, 227–230. doi:10.1016/j.jiph.2016.04.001.

Ruiz-Irastorza, G., Ramos-Casals, M., Brito-Zeron, P., and Khamashta, M. A. (2010). Clinical efficacy and side effects of antimalarials in systemic lupus erythematosus: a systematic review. *Ann. Rheum. Dis.* 69, 20–28. doi:10.1136/ard.2008.101766.

Sa, J., Sm, T., L, G.-R., Em, H., Je, A., Gj, B., et al. (2004). CD209L (L-SIGN) is a receptor for severe acute respiratory syndrome coronavirus. *Proc. Natl. Acad. Sci. U. S. A.* 101, 15748–15753. doi:10.1073/pnas.0403812101.

Saijo, M., Morikawa, S., Fukushi, S., Mizutani, T., Hasegawa, H., Nagata, N., et al. (2005). Inhibitory effect of mizoribine and ribavirin on the replication of severe acute respiratory syndrome (SARS)-associated coronavirus. *Antiviral Res.* 66, 159–163. doi:10.1016/j.antiviral.2005.01.003.

41

1328   Sallard, E., Lescure, F.-X., Yazdanpanah, Y., Mentre, F., and Peiffer-Smadja, N. (2020). Type 1
1329   interferons as a potential treatment against COVID-19. *Antiviral Res.* 178, 104791.
1330   doi:10.1016/j.antiviral.2020.104791.

1331   Samuel, C. E. (2001). Antiviral Actions of Interferons. *Clin. Microbiol. Rev.* 14, 778–809.
1332   doi:10.1128/CMR.14.4.778-809.2001.

1333   Sanan-Mishra, N., Chakraborty, S., Gupta, D., and Mukherjee, S. K. (2017). "RNAi Suppressors:
1334   Biology and Mechanisms," in *Plant Epigenetics* RNA Technologies., eds. N. Rajewsky, S.
1335   Jurga, and J. Barciszewski (Cham: Springer International Publishing), 199–230.
1336   doi:10.1007/978-3-319-55520-1_11.

1337   Santos, I. A., Grosche, V. R., Sabino-Silva, R., and Jardim, A. C. G. (2020). Antivirals against human
1338   and animal Coronaviruses: different approach in SARS-CoV-2 treatment. *Open Science
1339   Framework: OSF preprints*. doi:10.31219/osf.io/ycjgq.

1340   Sayce, A. C., Miller, J. L., and Zitzmann, N. (2010). Targeting a host process as an antiviral approach
1341   against dengue virus. *Trends Microbiol.* 18, 323–330. doi:10.1016/j.tim.2010.04.003.

1342   Scheller, J., and Rose-John, S. (2006). Interleukin-6 and its receptor: from bench to bedside. Med.
1343   Microbiol. Immunol. 195, 173–183. doi:10.1007/s00430-006-0019-9.

1344   Schwarz, S., Wang, K., Yu, W., Sun, B., and Schwarz, W. (2011). Emodin inhibits current through
1345   SARS-associated   coronavirus   3a   protein.   *Antiviral   Res.*   90,   64–69.
1346   doi:10.1016/j.antiviral.2011.02.008.

1347   Shah, P. P., Wang, T., Kaletsky, R. L., Myers, M. C., Purvis, J. E., Jing, H., et al. (2010). A Small-
1348   Molecule Oxocarbazate Inhibitor of Human Cathepsin L Blocks Severe Acute Respiratory
1349   Syndrome and Ebola Pseudotype Virus Infection into Human Embryonic Kidney 293T cells.
1350   *Mol. Pharmacol.* 78, 319–324. doi:10.1124/mol.110.064261.

1351   Shah, P. S., and Schaffer, D. V. (2011). Antiviral RNAi: Translating Science Towards Therapeutic
1352   Success. *Pharm. Res.* 28, 2966–2982. doi:10.1007/s11095-011-0549-8.

1353   Shanmugaraj, B., Siriwattananon, K., Wangkanont, K., and Phoolcharoen, W. (2020). Perspectives on
1354   monoclonal antibody therapy as potential therapeutic intervention for Coronavirus disease-19
1355   (COVID-19). *Asian Pac. J. Allergy Immunol.* doi:10.12932/AP-200220-0773.

1356   Sheahan, T. P., Sims, A. C., Graham, R. L., Menachery, V. D., Gralinski, L. E., Case, J. B., et al.
1357   (2017). Broad-spectrum antiviral GS-5734 inhibits both epidemic and zoonotic coronaviruses.
1358   *Sci. Transl. Med.* 9. doi:10.1126/scitranslmed.aal3653.

1359   Sheahan, T. P., Sims, A. C., Leist, S. R., Schäfer, A., Won, J., Brown, A. J., et al. (2020). Comparative
1360   therapeutic efficacy of remdesivir and combination lopinavir, ritonavir, and interferon beta
1361   against MERS-CoV. *Nat. Commun.* 11, 1–14. doi:10.1038/s41467-019-13940-6.

42

Sheahan, T. P., Sims, A. C., Zhou, S., Graham, R. L., Pruijssers, A. J., Agostini, M. L., et al. (2020). An orally bioavailable broad-spectrum antiviral inhibits SARS-CoV-2 in human airway epithelial cell cultures and multiple coronaviruses in mice. *Sci. Transl. Med.* 12. doi:10.1126/scitranslmed.abb5883.

Sheahan, T. P., Sims, A. C., Zhou, S., Graham, R. L., Pruijssers, A. J., Agostini, M. L., et al. (2020). An orally bioavailable broad-spectrum antiviral inhibits SARS-CoV-2 in human airway epithelial cell cultures and multiple coronaviruses in mice. Sci. Transl. Med. 12, 1–20. doi:10.1126/scitranslmed.abb5883.

Shen, L., Yang, Y., Ye, F., Liu, G., Desforges, M., Talbot, P. J., et al. (2016). Safe and Sensitive Antiviral Screening Platform Based on Recombinant Human Coronavirus OC43 Expressing the Luciferase Reporter Gene. Antimicrob. Agents Chemother. 60, 5492–5503. doi:10.1128/AAC.00814-16.

Shi, Y., Yang, D. H., Xiong, J., Jia, J., Huang, B., and Jin, Y. X. (2005). Inhibition of genes expression of SARS coronavirus by synthetic small interfering RNAs. *Cell Res.* 15, 193–200. doi:10.1038/sj.cr.7290286.

Shie, J.-J., Fang, J.-M., Kuo, T.-H., Kuo, C.-J., Liang, P.-H., Huang, H.-J., et al. (2005). Inhibition of the severe acute respiratory syndrome 3CL protease by peptidomimetic α,β-unsaturated esters. *Bioorg. Med. Chem.* 13, 5240–5252. doi:10.1016/j.bmc.2005.05.065.

Shin, J. S., Jung, E., Kim, M., Baric, R. S., and Go, Y. Y. (2018). Saracatinib Inhibits Middle East Respiratory Syndrome-Coronavirus Replication In Vitro. *Viruses* 10, 283. doi:10.3390/v10060283.

Siu, Y. L., Teoh, K. T., Lo, J., Chan, C. M., Kien, F., Escriou, N., et al. (2008). The M, E, and N structural proteins of the severe acute respiratory syndrome coronavirus are required for efficient assembly, trafficking, and release of virus-like particles. *J. Virol.* 82, 11318–11330. doi:10.1128/JVI.01052-08.

Softic, L., Brillet, R., Berry, F., Ahnou, N., Nevers, Q., Morin-Dewaele, M., et al. (2020). Inhibition of SARS-CoV-2 infection by the cyclophilin inhibitor Alisporivir (Debio 025). *Antimicrob. Agents Chemother.*, AAC.00876-20, aac;AAC.00876-20v1. doi:10.1128/AAC.00876-20.

Sperber, S. J., and Hayden, F. G. (1989). Comparative Susceptibility of Respiratory Viruses to Recombinant Interferons-α2b and -β. *J. Interferon Res.* 9, 285–293. doi:10.1089/jir.1989.9.285.

Stocks, P. A., Raynes, K. J., Bray, P. G., Park, B. K., O'Neill, P. M., and Ward, S. A. (2002). Novel Short Chain Chloroquine Analogues Retain Activity Against Chloroquine Resistant K1 Plasmodium falciparum. *J. Med. Chem.* 45, 4975–4983. doi:10.1021/jm0108707.

Struck, A.-W., Axmann, M., Pfefferle, S., Drosten, C., and Meyer, B. (2012). A hexapeptide of the receptor-binding domain of SARS corona virus spike protein blocks viral entry into host cells via the human receptor ACE2. *Antiviral Res.* 94, 288–296. doi:10.1016/j.antiviral.2011.12.012.

43

1398 Sun, C., Chen, L., Yang, J., Luo, C., Zhang, Y., Li, J., et al. (2020). SARS-CoV-2 and SARS-CoV
1399   Spike-RBD Structure and Receptor Binding Comparison and Potential Implications on
1400   Neutralizing Antibody and Vaccine Development. *bioRxiv* [Preprint]. Available at:
1401   https://doi.org/10.1101/2020.02.16.951723 (Accessed March 26, 2020).

1402 Tai, W., He, L., Zhang, X., Pu, J., Voronin, D., Jiang, S., et al. (2020). Characterization of the receptor-
1403   binding domain (RBD) of 2019 novel coronavirus: implication for development of RBD protein
1404   as a viral attachment inhibitor and vaccine. *Cell. Mol. Immunol.*, 1–8. doi:10.1038/s41423-020-
1405   0400-4.

1406 Takano, T., Katoh, Y., Doki, T., and Hohdatsu, T. (2013). Effect of chloroquine on feline infectious
1407   peritonitis virus infection in vitro and in vivo. *Antiviral Res.* 99, 100–107.
1408   doi:10.1016/j.antiviral.2013.04.016.

1409 Takashita, E. (2020). Influenza Polymerase Inhibitors: Mechanisms of Action and Resistance. *Cold
1410   Spring Harb. Perspect. Med.* doi:10.1101/cshperspect.a038687.

1411 Tan, E. L. C., Ooi, E. E., Lin, C.-Y., Tan, H. C., Ling, A. E., Lim, B., et al. (2004). Inhibition of SARS
1412   Coronavirus Infection In Vitro with Clinically Approved Antiviral Drugs. *Emerg. Infect. Dis.*
1413   10, 581–586. doi:10.3201/eid1004.030458.

1414 Tanner, J. A., Zheng, B.-J., Zhou, J., Watt, R. M., Jiang, J.-Q., Wong, K.-L., et al. (2005). The
1415   Adamantane-Derived Bananins Are Potent Inhibitors of the Helicase Activities and Replication
1416   of SARS Coronavirus. *Chem. Biol.* 12, 303–311. doi:10.1016/j.chembiol.2005.01.006.

1417 Tay, M. Y. F., Fraser, J. E., Chan, W. K. K., Moreland, N. J., Rathore, A. P., Wang, C., et al. (2013).
1418   Nuclear localization of dengue virus (DENV) 1–4 non-structural protein 5; protection against
1419   all 4 DENV serotypes by the inhibitor Ivermectin. *Antiviral Res.* 99, 301–306.
1420   doi:10.1016/j.antiviral.2013.06.002.

1421 Thomas, T. (2020). The Oxford Vaccine Centre COVID-19 Phase II/III Clinical Trial Explained.
1422   *COVID-19 Oxf. Vaccine Trial*. Available at: https://covid19vaccinetrial.co.uk/phase-iiiii-trial-
1423   explained [Accessed July 1, 2020].

1424 Thomas, S. M., and Brugge, J. S. (1997). Cellular functions regulated by Src family kinases. *Annu.
1425   Rev. Cell Dev. Biol.* 13, 513–609. doi:10.1146/annurev.cellbio.13.1.513.

1426 Toniati, P., Piva, S., Cattalini, M., Garrafa, E., Regola, F., Castelli, F., et al. (2020). Tocilizumab for
1427   the treatment of severe COVID-19 pneumonia with hyperinflammatory syndrome and acute
1428   respiratory failure: A single center study of 100 patients in Brescia, Italy. *Autoimmun. Rev.* 19,
1429   102568. doi:10.1016/j.autrev.2020.102568.

1430 Totura, A. L., and Bavari, S. (2019). Broad-spectrum coronavirus antiviral drug discovery. *Expert
1431   Opin. Drug Discov.* 14, 397–412. doi:10.1080/17460441.2019.1581171

1432   Toxicology, N. R. C. (US) C. on A. of T. T. to P. (2007). *Application to the Study of Mechanisms of*
1433   *Action*.   National   Academies   Press   (US)   Available   at:
1434   https://www.ncbi.nlm.nih.gov/books/NBK10203/ [Accessed December 28, 2019].

1435   Tu, Y.-F., Chien, C.-S., Yarmishyn, A. A., Lin, Y.-Y., Luo, Y.-H., Lin, Y.-T., et al. (2020). A Review
1436   of SARS-CoV-2 and the Ongoing Clinical Trials. *Int. J. Mol. Sci.* 21, 2657.
1437   doi:10.3390/ijms21072657.

1438   Ullah, H., Hou, W., Dakshanamurthy, S., and Tang, Q. (2019). Host targeted antiviral (HTA):
1439   functional inhibitor compounds of scaffold protein RACK1 inhibit herpes simplex virus
1440   proliferation. *Oncotarget* 10, 3209–3226. doi:10.18632/oncotarget.26907.

1441   Unübol, M., Ayhan, M., and Guney, E. (2011). Hypoglycemia induced by hydroxychloroquine in a
1442   patient treated for rheumatoid arthritis. *J. Clin. Rheumatol. Pract. Rep. Rheum. Musculoskelet.*
1443   *Dis.* 17, 46–47. doi:10.1097/RHU.0b013e3182098e1f.

1444   Ursing, J., Rombo, L., Eksborg, S., Larson, L., Bruvoll, A., Tarning, J., et al. (2020). High-Dose
1445   Chloroquine for Uncomplicated Plasmodium falciparum Malaria Is Well Tolerated and Causes
1446   Similar QT Interval Prolongation as Standard-Dose Chloroquine in Children. *Antimicrob.*
1447   *Agents Chemother.* 64. doi:10.1128/AAC.01846-19.

1448   van Doremalen, N., Bushmaker, T., Morris, D. H., Holbrook, M. G., Gamble, A., Williamson, B. N.,
1449   et al. (2020). Aerosol and Surface Stability of SARS-CoV-2 as Compared with SARS-CoV-1.
1450   *N. Engl. J. Med.* 0, null. doi:10.1056/NEJMc2004973.

1451   Varghese, F. S., Kaukinen, P., Gläsker, S., Bespalov, M., Hanski, L., Wennerberg, K., et al. (2016).
1452   Discovery of berberine, abamectin and ivermectin as antivirals against chikungunya and other
1453   alphaviruses. *Antiviral Res.* 126, 117–124. doi:10.1016/j.antiviral.2015.12.012.

1454   Vassão, R. C., de Franco, M. T., Hartz, D., Modolell, M., Sippel, A. E., and Pereira, C. A. (2000).
1455   Down-regulation of Bgp1a Viral Receptor by Interferon-γ Is Related to the Antiviral State and
1456   Resistance   to   Mouse   Hepatitis   Virus   3   Infection.   *Virology*   274,   278–283.
1457   doi:10.1006/viro.2000.0463.

1458   Villegas-Rosales, P. M., Méndez-Tenorio, A., Ortega-Soto, E., and Barrón, B. L. (2012).
1459   Bioinformatics prediction of siRNAs as potential antiviral agents against dengue viruses.
1460   *Bioinformation* 8, 519–522. doi:10.6026/97320630008519.

1461   Vincent, M. J., Bergeron, E., Benjannet, S., Erickson, B. R., Rollin, P. E., Ksiazek, T. G., et al. (2005).
1462   Chloroquine is a potent inhibitor of SARS coronavirus infection and spread. *Virol. J.* 2, 69.
1463   doi:10.1186/1743-422X-2-69.

1464   Vuong, W., Khan, M. B., Fischer, C., Arutyunova, E., Lamer, T., Shields, J., et al. (2020). Feline
1465   coronavirus drug inhibits the main protease of SARS-CoV-2 and blocks virus replication.
1466   *bioRxiv* [Preprint]. Available at: https://doi.org/10.1101/2020.05.03.073080 (Accessed June
1467   06, 2020).

45

1468 Walls, A. C., Park, Y.-J., Tortorici, M. A., Wall, A., McGuire, A. T., and Veesler, D. (2020). Structure,
1469   Function, and Antigenicity of the SARS-CoV-2 Spike Glycoprotein. *Cell*.
1470   doi:10.1016/j.cell.2020.02.058.

1471 Wang, C., Li, W., Drabek, D., Okba, N. M. A., van Haperen, R., Osterhaus, A. D. M. E., et al. (2020a).
1472   A human monoclonal antibody blocking SARS-CoV-2 infection. *Nat. Commun.* 11, 2251.
1473   doi:10.1038/s41467-020-16256-y.

1474 Wang, M., Cao, R., Zhang, L., Yang, X., Liu, J., Xu, M., et al. (2020b). Remdesivir and chloroquine
1475   effectively inhibit the recently emerged novel coronavirus (2019-nCoV) in vitro. *Cell Res.* 30,
1476   269–271. doi:10.1038/s41422-020-0282-0.

1477 Wang, Y., Jiang, W., He, Q., Wang, C., Wang, B., Zhou, P., et al. (2020). Early, low-dose and short-
1478   term application of corticosteroid treatment in patients with severe COVID-19 pneumonia:
1479   single-center experience from Wuhan, China. *medRxiv* [Preprint]. Available at:
1480   https://doi.org/10.1101/2020.03.06.20032342 (Accessed June 28, 2020).

1481 Wang, Y., Sun, Y., Wu, A., Xu, S., Pan, R., Zeng, C., et al. (2015). Coronavirus nsp10/nsp16
1482   Methyltransferase Can Be Targeted by nsp10-Derived Peptide In Vitro and In Vivo To Reduce
1483   Replication and Pathogenesis. *J. Virol.* 89, 8416–8427. doi:10.1128/JVI.00948-15.

1484 Wang, Y., Zhang, D., Du, G., Du, R., Zhao, J., Jin, Y., et al. (2020c). Remdesivir in adults with severe
1485   COVID-19: a randomised, double-blind, placebo-controlled, multicentre trial. *The Lancet* 395,
1486   1569–1578. doi:10.1016/S0140-6736(20)31022-9.

1487 Warren, T. K., Jordan, R., Lo, M. K., Ray, A. S., Mackman, R. L., Soloveva, V., et al. (2016).
1488   Therapeutic efficacy of the small molecule GS-5734 against Ebola virus in rhesus monkeys.
1489   *Nature* 531, 381–385. doi:10.1038/nature17180.

1490 Weiss, S. R., and Navas-Martin, S. (2005). Coronavirus Pathogenesis and the Emerging Pathogen
1491   Severe Acute Respiratory Syndrome Coronavirus. *Microbiol. Mol. Biol. Rev.* 69, 635–664.
1492   doi:10.1128/MMBR.69.4.635-664.2005.

1493 Wen, C. C., Kuo, Y. H., Jan, J. T., Liang, P. H., Wang, S. Y., Liu, H. G., et al. (2007). Specific plant
1494   terpenoids and lignoids possess potent antiviral activities against severe acute respiratory
1495   syndrome coronavirus. J. Med. Chem. 50, 4087–4095. doi:10.1021/jm070295s.

1496 Wilkinson, J. R., Lane, S. J., and Lee, T. H. (1991). Effects of Corticosteroids on Cytokine Generation
1497   and Expression of Activation Antigens by Monocytes in Bronchial Asthma. *Int. Arch. Allergy
1498   Immunol.* 94, 220–221. doi:10.1159/000235365.

1499 WHO (2020). Clinical management of COVID-19. *Clin. Manag. COVID-19*. Available at:
1500   https://www.who.int/publications-detail-redirect/clinical-management-of-covid-19 [Accessed
1501   June 8, 2020].

46

1502 WHO (2020). Q&A : Hydroxychloroquine and COVID-19. Available at: https://www.who.int/news-
1503 room/q-a-detail/q-a-hydroxychloroquine-and-covid-19 [Accessed July 5, 2020].

1504 WHO (2020). Novel Coronavirus (2019-nCoV) situation reports. Available at:
1505 https://www.who.int/emergencies/diseases/novel-coronavirus-2019/situation-reports
1506 [Accessed July 04, 2020].

1507 Wilde, A. H. de, Jochmans, D., Posthuma, C. C., Zevenhoven-Dobbe, J. C., Nieuwkoop, S. van,
1508 Bestebroer, T. M., et al. (2014). Screening of an FDA-Approved Compound Library Identifies
1509 Four Small-Molecule Inhibitors of Middle East Respiratory Syndrome Coronavirus Replication
1510 in Cell Culture. *Antimicrob. Agents Chemother.* 58, 4875–4884. doi:10.1128/AAC.03011-14.

1511 Wilson, R. C., and Doudna, J. A. (2013). Molecular Mechanisms of RNA Interference. *Annu. Rev.
1512 Biophys.* 42, 217–239. doi:10.1146/annurev-biophys-083012-130404.

1513 Wit, E. de, Feldmann, F., Cronin, J., Jordan, R., Okumura, A., Thomas, T., et al. (2020). Prophylactic
1514 and therapeutic remdesivir (GS-5734) treatment in the rhesus macaque model of MERS-CoV
1515 infection. *Proc. Natl. Acad. Sci.* 117, 6771–6776. doi:10.1073/pnas.1922083117.

1516 Wrapp, D., Wang, N., Corbett, K. S., Goldsmith, J. A., Hsieh, C.-L., Abiona, O., et al. (2020). Cryo-
1517 EM structure of the 2019-nCoV spike in the prefusion conformation. *Science* 367, 1260.
1518 doi:10.1126/science.abb2507.

1519 Wu, C.-J., Jan, J.-T., Chen, C.-M., Hsieh, H.-P., Hwang, D.-R., Liu, H.-W., et al. (2004). Inhibition of
1520 Severe Acute Respiratory Syndrome Coronavirus Replication by Niclosamide. *Antimicrob.
1521 Agents Chemother.* 48, 2693–2696. doi:10.1128/AAC.48.7.2693-2696.2004.

1522 Wu, D., Wu, T., Liu, Q., and Yang, Z. (2020). The SARS-CoV-2 outbreak: what we know. *Int. J.
1523 Infect. Dis.* 0. doi:10.1016/j.ijid.2020.03.004.

1524 Xu, X., Han, M., Li, T., Sun, W., Wang, D., Fu, B., et al. (2020). Effective treatment of severe COVID-
1525 19 patients with tocilizumab. Proc. Natl. Acad. Sci. 117, 202005615.
1526 doi:10.1073/pnas.2005615117.

1527 Y, M., Cy, C., and Ml, H. (2007). RNA interference and antiviral therapy. *World J. Gastroenterol.* 13,
1528 5169–5179. doi:10.3748/wjg.v13.i39.5169.

1529 Yan, R., Zhang, Y., Li, Y., Xia, L., Guo, Y., and Zhou, Q. (2020). Structural basis for the recognition
1530 of the SARS-CoV-2 by full-length human ACE2. *Science*, eabb2762.
1531 doi:10.1126/science.abb2762.

1532 Yang, D., and Leibowitz, J. L. (2015). The structure and functions of coronavirus genomic 3′ and 5′
1533 ends. *Virus Res.* 206, 120–133. doi:10.1016/j.virusres.2015.02.025.

1534 Yao, T.-T., Qian, J.-D., Zhu, W.-Y., Wang, Y., and Wang, G.-Q. (2020a). A systematic review of
1535 lopinavir therapy for SARS coronavirus and MERS coronavirus—A possible reference for
1536 coronavirus disease-19 treatment option. *J. Med. Virol.* n/a. doi:10.1002/jmv.25729.

1537 Yao, X., Ye, F., Zhang, M., Cui, C., Huang, B., Niu, P., et al. (2020b). In Vitro Antiviral Activity and
1538   Projection of Optimized Dosing Design of Hydroxychloroquine for the Treatment of Severe
1539   Acute Respiratory Syndrome Coronavirus 2 (SARS-CoV-2). *Clin. Infect. Dis.*
1540   doi:10.1093/cid/ciaa237.

1541 Yogo, Y., Hirano, N., Hino, S., Shibuta, H., and Matumoto, M. (1977). Polyadenylate in the Virion
1542   RNA of Mouse Hepatitis Virus. *J. Biochem. (Tokyo)* 82, 1103–1108.
1543   doi:10.1093/oxfordjournals.jbchem.a131782.

1544 Zha, L., Li, S., Pan, L., Tefsen, B., Li, Y., French, N., et al. (2020). Corticosteroid treatment of patients
1545   with coronavirus disease 2019 (COVID-19). *Med. J. Aust.* 212, 416–420.
1546   doi:10.5694/mja2.50577.

1547 Zhang, H.-Z., Zhang, H., Kemnitzer, W., Tseng, B., Cinatl, Jindrich, Michaelis, M., et al. (2006).
1548   Design and Synthesis of Dipeptidyl Glutaminyl Fluoromethyl Ketones as Potent Severe Acute
1549   Respiratory Syndrome Coronovirus (SARS-CoV) Inhibitors. *J. Med. Chem.* 49, 1198–1201.
1550   doi:10.1021/jm0507678.

1551 Zhang, C., Wu, Z., Li, J., Zhao, H., and Wang, G. (2020a). Cytokine release syndrome in severe
1552   COVID-19 : interleukin-6 receptor antagonist tocilizumab may be the key to reduce mortality.

1553 Zhang, S., Li, L., Shen, A., Chen, Y., and Qi, Z. (2020b). Rational Use of Tocilizumab in the Treatment
1554   of Novel Coronavirus Pneumonia. Clin. Drug Investig. doi:10.1007/s40261-020-00917-3.

1555 Zhu, Z., Chakraborti, S., He, Y., Roberts, A., Sheahan, T., Xiao, X., et al. (2007). Potent cross-reactive
1556   neutralization of SARS coronavirus isolates by human monoclonal antibodies. *Proc. Natl.
1557   Acad. Sci.* 104, 12123–12128. doi:10.1073/pnas.0701000104.

1558

1559

1560 **FIGURE CAPTIONS**

1561

1562 **Figure 1**: Schematic structure of SARS-CoV-2. The viral structure is primarily formed by the structural
1563 proteins such as spike (S), membrane (M), envelope (E), and nucleocapsid (N) proteins. The S, M, and
1564 E proteins are all embedded in the viral envelope, a lipid bilayer derived from the host cell membrane.
1565 The N protein interacts with the viral RNA in to the core of the virion.

1566

1567 **Figure 2:** Schematic representation of SARS-CoV-2 replication cycle in host cells. SARS-CoV-2
1568 attaches to the host cells by interaction between the ACE2 receptors and spike proteins. After entry,
1569 viral uncoating process results in the release of viral genome and replication stage occurs (translation
1570 and transcription). Structural proteins are produced in intermediate compartment of endoplasmic

48

1571   reticulum with Golgi complex and forwarded to assembly, packaging and virus release. Compounds
1572   with antiviral activity against SARS-CoV-2 are indicated in each step of virus replication cycle.

1573

49

1574 **Table 1:** Compounds with antiviral activity against human and animal coronaviruses.

Compound	Inhibition Step	EC50 or inhibition (%)	CoVs	Advantges and/or limitations	Reference
NAAE	Entry	0.5 µM	SARS-CoV	Synthetic molecule, evaluated *in silico*, easily produced but lacks of *in vivo* assays	Huentelman et al., 2004
Glycyrrhizin	Entry	300 mg·L⁻¹	SARS-CoV	Natural molecule, high tolerated but lacks of *in vivo* assays	Cinatl et al., 2003
2-acetamido-α-D-Glucopyranosylamine derivative	Entry	40 µM	SARS-CoV	Semi-synthetic molecule, high tolerated, and more potent inhibitor but lacks of *in vivo* assays	Hoever et al., 2005
Tetrahydroquinoline oxocarbazate (CID 23631927)	Entry (Cathepsin L)	273 nM	SARS-CoV	Synthetic molecule, highly tolerated, easily produced but lacks of *in vivo* assays	Shah et al., 2010
SSAA09E1	Entry	6.7 µM	SARS-CoV	Synthetic molecule, highly tolerated, easily produced but lacks of *in vivo* assays	Adedeji et al., 2013
SSAA09E2	Entry	3.1 µM	SARS-CoV	Synthetic molecule, highly tolerated, easily produced but lacks of *in vivo* assays	Adedeji et al., 2013
SSAA09E3	Entry	9.7 µM	SARS-CoV	Synthetic molecule, highly tolerated, easily produced but lacks of *in vivo* assays	Adedeji et al., 2013
Emodin	Entry And Post-Entry	50 µM	SARS-CoV	Natural molecule, high tolerated but lacks of *in vivo* assays	Ho et al., 2007; Schwarz et al., 2011
Griffithsin (GRFT)	Entry	0.16 µg·mL⁻¹	HCoV-OC43	Natural molecule, highly tolerated, with a broad-spectrum effect (human and animal CoVs) with animal assay (Balb/c) which protected against infection and improved surviving	O'Keefe et al., 2010
	Entry	0.18 µg·mL⁻¹	HCoV-229E		
	Entry	0.61 µg·mL⁻¹	SARS-CoV		
	Entry	< 0.032 µg·mL⁻¹	HCoV-NL63		
	Entry	0.057 µg·mL⁻¹	BCoV		
	Entry	0.23 µg·mL⁻¹	MHV		
Eremomycin derivate 27	Entry	5.4 µM	FIPV	The precursor molecules are used to treat bacterial infections, may facilitates clinical assays, lacks of knowledge of mechanism of action.	Balzarini et al., 2006
	Entry	14 µM	SARS-CoV		
Eremomycin derivate 39	Entry	12 µM	FIPV		
	Entry	22 µM	SARS-CoV		
Mucroporin-M1	Entry	14.46 µg·mL⁻¹	SARS-CoV	Synthetic molecule, moderately tolerated, easily produced but lacks of *in vivo* assays	Li et al., 2011

Antivirals against human-animal Coronaviruses

Tyr-Lys-Tyr-Arg-Tyr-Leu	Entry	14 mM	SARS-CoV	Synthetic molecule specifically designed to S protein of SARS-CoV, high tolerated, do not impair ACE2 activity but lacks of *in vivo* assays	Struck et al., 2012
	Entry	14 mM	HCoV-NL63		
TAPI-2	Entry	65%	SARS-CoV	Good effects in vitro assays but did not had effect on *in vivo* assays	Haga et al., 2010
Monoclonal antibody 47D11	Entry	0.57 µg·mL⁻¹	SARS-CoV-2	Are human antibody, specifically to SARS-CoV-2, highly tolerated and easily applicable	Wang et al., 2020a
AVLQSGFR	Replication	2.7 x 10⁻² mg·mL⁻¹	SARS-CoV	Synthetic molecule, highly tolerated, easily produced but lacks of *in vivo* assays	Gan et al., 2006
Phe-Phe dipeptide inhibitor C (JMF1521)	Replication	0.18 µM	SARS-CoV	Synthetic molecule, highly tolerated, easily produced but lacks of *in vivo* assays	Shie et al., 2005
Dipeptidyl EP128533	Replication	3.6 µM or 1.4µg·mL⁻¹	SARS-CoV	Synthetic molecule, highly tolerated, easily produced but has contrasting effects in literature, and did not inhibited the virus *in vivo* assays	Day et al., 2009; Zhang et al., 2006
GC373	Replication	0.2 µM	HCoV-229E	Synthetic molecule, highly tolerated, easily produced, seems to interact with SARS-CoV 3CLpro but there are not *in vivo* assays	Kim et al., 2012; Kim et al., 2013
		0.3 µM	FIPV		
		2 µM	MHV		
		0.3 µM	TGEV		
		0.7 µM	BCV		
		0.15 µM	FCoV-WSU		
GC376	Replication	0.15 µM	HCoV-229E	Synthetic molecule, highly tolerated, easily produced, seems to interact with SARS-CoV 3CLpro but there are not *in vivo* assays	Kim et al., 2012; Kim et al., 2013
		0.2 µM	FIPV		
		1.1 µM	MHV		
		0.15 µM	TGEV		
		0.6 µM	BCV		
		0.40 µM	FCoV-WSU		
6-azauridine	Replication	32 nM	HCoV-NL63	Synthetic molecule, highly tolerated, easily produced but there are not *in vivo* assays	Pyrc et al., 2006

51

2-(benzylthio)-6-oxo-4-phenyl-1,6-dihydropyrimidine	Replication	NE	SARS-CoV	Synthetic molecule, highly tolerated, easily produced but there are not in vivo assays	Ramajayam et al., 2010
β-D-N⁴-hydroxycytidine	Replication	10 µM	SARS-CoV	Synthetic molecule, highly tolerated, easily produced and improved pulmonary function and decreased viral load un lungs in infected mice	Barnard et al., 2004; Sheahan et al., 2020
	Replication	400 nM	HCoV-NL63		
	Replication	0.08 - 0.3 µM	SARS-CoV-2		
	Replication	0.024 µM	MERS-CoV		
Ribavirin	Replication	20 µg·mL⁻¹	SARS-CoV	Synthetic molecule, highly tolerated, easily produced, good results in MERS-CoV. However, has limited efficacy in meta-analyses study.	Saijo et al., 2005; Barnard et al., 2006
Acyclic sugar scaffold of acyclovir	Replication	23 µM	MERS-CoV	Synthetic molecule, highly tolerated, easily produced but there are not in vivo assays	Peters et al., 2015
		8.8 µM	HCoV-NL63	Synthetic molecule, highly tolerated, derivate from Acyclovir, easily produced but there are not in vivo assays	
Niclosamide	Replication	0.1 µM	SARS-CoV	Drug already in use to treat helminthic infections, good inhibition in vitro	Wu et al., 2004; Wen et al., 2007
Mycophenolic acid (MPA)	Replication	2.87 µM	MERS-CoV	Good effects in vitro with MERS-CoV but did not inhibited SARS-CoV in vitro and in vivo assays	Hart et al., 2014; Cinatl et al., 2003; Barnard et al., 2006
TP29 peptide	Replication	60 µM	MHV	Inhibited two species of CoV in mice, also improved survival and induced INF-I. Inhibited CoV in cell lines, synthetic compound designed for nonstructural proteins.	Wang et al., 2015
	Replication	200 µM	SARS-CoV		
Bananins	Replication	< 10 µM	SARS-CoV	Synthetic molecule, highly tolerated, easily produced but there are not in vivo assays	Tanner et al., 2005
Nitazoxanide	Host Enzymes	0.92 µg·mL⁻¹	MERS-CoV	Drug already in use to treat viral infections, good inhibition in vitro	Rossignol, 2016
Tizoxanide	Host Enzymes	0.83 µg·mL⁻¹	MERS-CoV	Drug derived from Nitazoxanide, good inhibition in vitro	Rossignol, 2016
Saracatinib	Tyrosine Kinases	2.9µM	MERS-CoV	Synthetic molecule, highly tolerated, used to treat Alzheimer's disease and easily produced but there are not in vivo assays	Shin et al., 2018
Cyclosporin A (CsA)	Hosts Cyclophilin Family Enzymes	9-32 µM	SARS-CoV, MERS-CoV and MHV	Drug already used to treat several chronic and infectious diseases, with broad spectrum activity among CoVs	de Wilde et al., 2011, 2013; Pfefferle et al., 2011

Alisporivir	Hosts Cyclophilin Family Enzymes	8.3 µM	SARS-CoV	Analogue from CsA and has a strong inhibition in vitro against SARS-CoV and other CoVs	de Wilde et al., 2017
Interference RNA (iRNAs)	Viral Proteins Translation	70%	SARS-CoV	Different approach, specific targeting viral proteins, can block replication steps and has no cytotoxicity	Åkerström et al., 2007
	Viral Proteins Translation	99%	SECoV	Different approach, specific targeting viral proteins, can block replication steps and has no cytotoxicity	Li et al., 2019

1575 EC50: effective concentration of 50%; NE: not evaluated

1576

1577 **Table 2:** Ongoing clinical trials with candidate drugs against SARS-CoV-2 in COVID-19 patients.

Drug	Cell culture assays	Inhibition Step in vitro	Animal assays	Clinical trials	Outcomes in Clinical Trials	Advantages and/or Limitations
Remdesivir	Inhibited SARS-CoV, MERS-CoV and SARS-CoV-2	Replication (RdRp)	Inhibited EBOV and SARS-CoV in both infected mice and monkeys	Clinical case and clinical trial against SARS-CoV-2	Did not provide antiviral effects or improved clinical outcomes	It is a multicentre, double-blind, placebo-controlled clinical trial, but might be needed more studies to confirm, since this was if 255 people, and has some adverse effects.
Lopinavir and Ritonavir	Inhibited SARS-CoV and MERS-CoV	Replication (protease inhibitor)	NE	Clinical trial with SARS-CoV-2	Did not provide antiviral effects or improved clinical outcomes in severe patients. However, in early infections clinical were improved.	It is used to other human CoVs but the study was not multicentre, double-blind, placebo-controlled. It is necessary more studies to confirm since it has only 199 people and showed some adverse effects.
IFN-β	Inhibited SARS-CoV, MERS-CoV, MHV, and HCoV-229E	Host Factors (inducing immune response)	Inhibited SARS-CoV, MERS-CoV, MHV, and HCoV-229E	Clinical trial with SARS-CoV-2 and is used to other diseases	Do not have effect alone	It is safe, little adverse effects but in clinical trials its used is affective only when associated with other drugs.
Umifenovir	Inhibited SARS-CoV	NE	NE	Observational study with 81 patients	Did not provide antiviral effects or improved clinical outcomes	Observational study, and might suffer bias from lack and/or loss of information and data. It is an applicable study, since demonstrates a tendency, and is drug already used to treat Influenza viruses.

Corsticosteroids (dexamethasone)	NE	Host factors (controlling immune response)	NE	Clinical trial with 454 treated patients	Reduced death in one-third in invasive mechanical ventilation patients and one-fifth in oxygen without invasive mechanical ventilation patients. However, it did not impaired mortality in patients without respiratory support	It is a multicentre, double-blind, placebo-controlled clinical trial. More studies are needed to understand better the effect on different phases of COVID-19. May be a good alternative for hyperinflammation and hypersecretion of cytokines.
Ivermectin	Inhibited SARS-CoV-2 and arboviruses (CHIKV and DENV)	Replication (nonstructural proteins)	NE	Clinical trials are begining	NE	Is safe to use in humans, since it is used to treat several parasitic infections.
Tocilizumab	NE	Inhibitor of IL-6	NE	Ongoing clinical trials with SARS-CoV-2 patients, and one with 100 patients concluded.	Positive effects, improved inflammatory markers and ventilatory support in patients	Is already used to treat viral infections controlling immune response, impairing cytokine storms, improving antiviral response and best clinical outcomes.
Chloroquine	Inhibited HIV, CHIKV, SARS-CoV and SARS-CoV-2	Entry	Improved outcomes in FCoV positive cats	Several clinical trials are being conducted	Impairs virus replication and has anti-inflammatory activities	Possess important side effects and indicated only in severe cases. However, there are some studies with contrasting results regarding its safety, since it can cause arrhythmias, hypoglycemia, neuropsychiatric effects and depression.
Hydroxychlo-roquine	Inhibited HIV, CHIKV, SARS-CoV and SARS-CoV-2	Entry	NE	Several clinical trials are being conducted	Less toxic option, impairs virus replication	Improved patients' outcomes, including when associated with azithromycin. Less toxic option to chloroquine treatment, but there are studies with contrasting results regarding its safety, since it can cause arrhythmias, hypoglycemia, neuropsychiatric effects and depression.
Convalescent Plasma	NE	Entry	NE	Cases report	Improved outcomes and suppressed viremia.	Risk to patients since it is related to donor-dependent variability and compatibility. Antibody titers may interfere in its activity. In addition, it might cause side effects in lung and cardiovascular system.

1578   EC50: effective concentration of 50%; NE: not evaluated

1579

54

188

Figure 1.JPEG

SARS-CoV-2
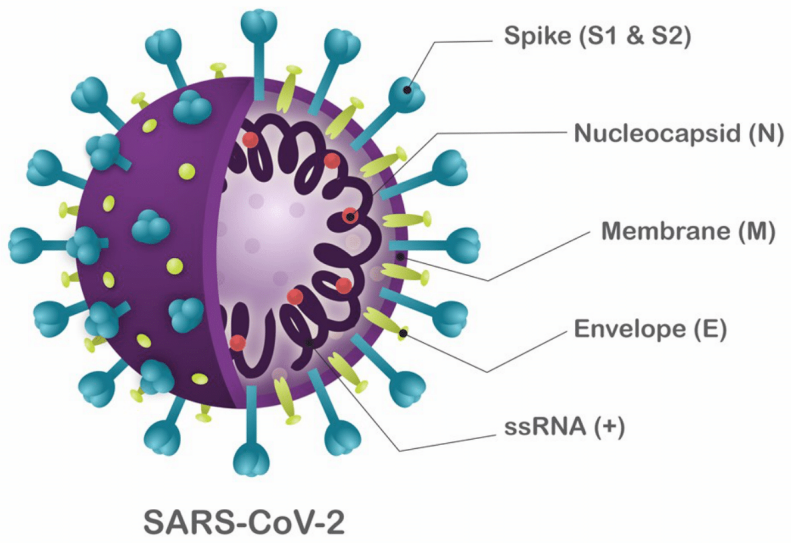
Figure 2.JPEG
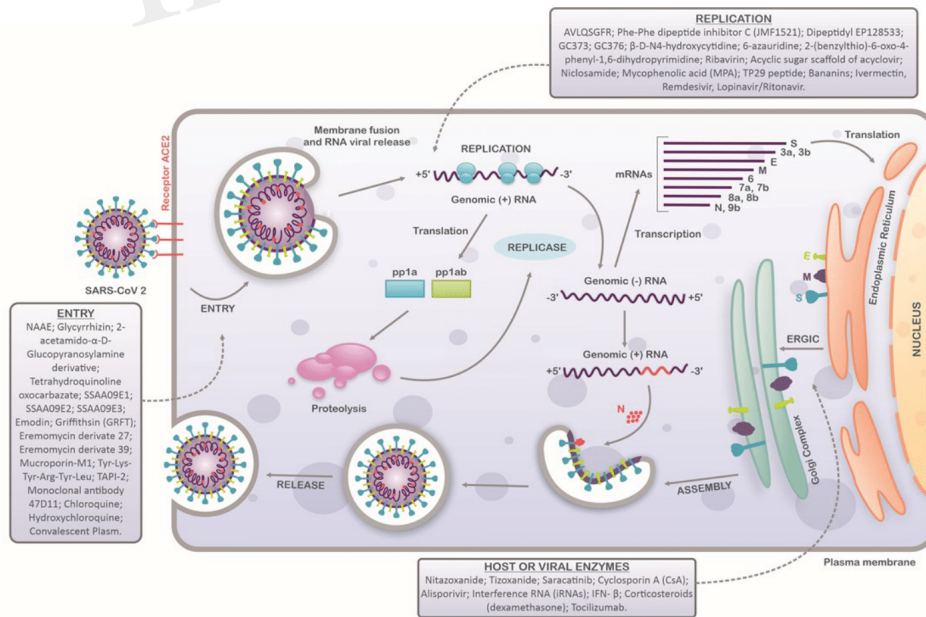
ANEXO V: Insights into the antiviral activity of phospholipases A₂ (PLA2s) from snake venoms

Review

Insights into the antiviral activity of phospholipases A$_2$ (PLA$_2$s) from snake venoms

S.C. Teixeira [a], B.C. Borges [a], V.Q. Oliveira [b], L.S. Carregosa [b], L.A. Bastos [b], I.A. Santos [c], A.C.G. Jardim [c], F.M. Freire [b], L. Martins [b], V.M. Rodrigues [d,*], D.S. Lopes [b,e,*]

[a] *Department of Immunology, Institute of Biomedical Science, Federal University of Uberlândia, Uberlândia, MG, Brazil*
[b] *Multidisciplinary Institute of Health, Anísio Teixeira Campus, Federal University of Bahia, Vitória da Conquista, BA, Brazil*
[c] *Laboratory of Virology, Institute of Biomedical Science, Federal University of Uberlândia, Uberlândia, MG, Brazil*
[d] *Laboratory of Biochemistry and Animal Toxins, Institute of Biotechnology, Federal University of Uberlândia, Uberlândia, MG, Brazil*
[e] *Institute of Health Sciences, Department of Bio-Function, Federal University of Bahia, Salvador, BA, Brazil*

ARTICLE INFO

ABSTRACT

Viruses are associated with several human diseases that infect a large number of individuals, hence directly affecting global health and economy. Owing to the lack of efficient vaccines, antiviral therapy and emerging resistance strains, many viruses are considered as a potential threat to public health. Therefore, researches have been developed to identify new drug candidates for future treatments. Among them, antiviral research based on natural molecules is a promising approach. Phospholipases A$_2$ (PLA$_2$s) isolated from snake venom have shown significant antiviral activity against some viruses such as Dengue virus, Human Immunodeficiency virus, Hepatitis C virus and Yellow fever virus, and have emerged as an attractive alternative strategy for the development of novel antiviral therapy. Thus, this review provides an overview of remarkable findings involving PLA$_2$s from snake venom that possess antiviral activity, and discusses the mechanisms of action mediated by PLA$_2$s against different stages of virus replication cycle. Additionally, molecular docking simulations were performed by interacting between phospholipids from Dengue virus envelope and PLA$_2$s from *Bothrops asper* snake venom. Studies on snake venom PLA$_2$s highlight the potential use of these proteins for the development of broad-spectrum antiviral drugs.

© 2020

1. Viral diseases: a public health problem

Viruses are associated to several endemic diseases, including Enterovirus [1], HPV (Human papillomavirus) [2], HIV (Human immunodeficiency virus) [3] and HSV (Herpes simplex virus) [4], as well as in outbreaks as Ebola virus, ZIKV (Zika virus), Influenza virus, YFV (Yellow Fever virus), DENV (Dengue virus) and, currently, the SARS-CoV-2 (Severe Acute Respiratory Coronavirus 2) [5–9]. Most of the reported outbreaks since 1980 were related to virus infections [10], which are still a global burden for public health and economy. In addition, due to their genetic diversity, viruses are able to infect a wide range of hosts that can result in host jumps after zoonotic contacts [11,12].

Pandemics caused by viruses are usually severe and can claim up to million lives, as shown during the pandemic of H1N1 in 1918 [13], H1N1 'swine flu' in 2009 [14] and Coronavirus Disease 2019 (COVID-19) [15], that infected 4,993,470 people and caused 327,738 deaths until May 22, 2020 in worldwide according to World Health Organiza-

tion. Furthermore, the global incidence of dengue has grown dramatically in recent decades. It is estimated that 100 to 400 million cases of dengue occur annually worldwide [16].

Viral infection depends on the successful replication into the host cells [17,18]. In general, the replicative cycle starts by the viral particle attaching to specific receptors in the surface of host cells that triggers the viral entry by endocytosis (non-enveloped or enveloped virus), membrane fusion (enveloped virus) and direct penetration [19–21]. After internalization, the capsid is released into the cytoplasm, allowing viral genome uncoating [22], which is replicated to produce copies of the genome and translated to viral proteins. In the endoplasmic reticulum (ER) and Golgi complex, the viral structure is assembled, matured and then forwarded to host cell membrane, where the progeny of virus particles is released [23].

Currently, specific antiviral drugs and vaccines are not sufficient to control emerging and reemerging viral diseases [24,25]. Thus, the discovery of novel antiviral drugs is mandatory. In general, antiviral therapy is the only approach to specifically treat viral infections, abrogating viral replicative cycle [26]. However, due to the high genetic variability, viruses can rapidly acquire resistance to antiviral treatment, especially RNA viruses [27–29]. Furthermore, antiviral therapy and the prolonged treatment can cause several adverse effects, including gastrointestinal effects, fatigue, headache, neuropathy and liver toxic-

ity [30–32]. In addition, there are no antivirals to all diseases and the only course is supportive therapy and, thereby, numerous innovative drugs have been developed from natural prototypes such as aspirin (anti-inflammatory) and morphine (analgesic) [33].

In this way, a diversity of compounds isolated from natural sources has set grounds for further advances in drug development against various diseases [34]. Among them, many drugs based on snake venoms were approved by the FDA or are involved in preclinical or clinical trials for a variety of therapeutic applications [35–39]. The development of snake venom-derived drugs gained a significant improve since the discovery of bradykinin-potentiating peptides (BPP) isolated from the Brazilian arrowhead viper (*Bothrops jararaca*) venom, which allowed the development of captopril, an inhibitor of the angiotensin-converting enzyme that is widely used against hypertension process [40,41]. Besides that, other snake venom-derived drugs have been found in clinical use, such as tirofiban and eptifibatide (antiplatelet agents) [42,43], batroxobin, moojenin and vivostat (anticoagulant agents) [44–47]. Other drugs which comprise molecules from snake venom as scaffolds are also being explored in preclinical studies [48].

Due to this therapeutic potential, snake venom toxins have been widely explored for the discovery of new bioactive compounds and stand out as an alternative source for therapeutics for a variety of diseases, including life-threatening viral illnesses [49–52].

2. Phospholipases A₂ from snake venom

Phospholipases (EC 3.1.) family is widely distributed in nature and includes hydrolase enzymes, which are essential for phospholipid metabolism and for the regulation of membrane lipids, membrane composition, signaling, digestion, and inflammation [53]. These proteins are classified into four major families (A, B, C and D) based on the site cleaved in the phospholipid molecule [54,55].

Among phospholipases family, the Phospholipases A₂ (PLA₂s) are the most studied group [53,54]. These enzymes hydrolyze 2-acyl ester bond to 2-sn phospholipids, releasing free fatty acid and lysophospholipids [56,57]. The free fatty acids (arachidonic acid) can be converted into eicosanoids (prostaglandins, thromboxanes, prostacyclins and leukotrienes), which are associated to a range of physiological and pathological effects, such as inflammation and platelet activation. In addition, the lysophospholipids are also related to a variety of physiological roles in cell signaling [53,58].

PLA₂s are classified into six groups: cytosolic (cPLA₂), Ca^{2+}-independent (iPLA₂), platelet-activating factor acetylhydrolase (PAF-AH), lysosomal PLA₂ (LyPLA₂), adipose specific PLA₂ (AdPLA₂) and secretory PLA2 (sPLA₂) [53]. In addition, the sPLA₂s are divided into the following groups: IA, IB, IIA, IIB, IIC, IID, IIE, IIF, III, V, IX, X, XIA, XIB, XII, XIII and XIV [53,54]. PLA₂s from snake venom belong to the group of secreted type of enzymes (sPLA₂s) and can be classified into the structural group IB (in Elapidae snake venoms), which exhibits homology to the mammalian pancreatic juice PLA₂, and also into the group IIA (in Viperidae snake venoms), that is homologous to the mammalian 'inflammatory' PLA₂ [59]. Although the PLA₂s family is more frequent in snake venom, recent proteome studies have demonstrated that Phospholipases B (PLB) can also be found in snake venom [60–62].

sPLA₂s are proteins with molecular mass of about 14 kDa, pH optimum at 7 and share a conserved catalytic mechanism based on a His/Asp dyad using Ca^{2+} as an essential cofactor for the catalytic activity. Group II of sPLA₂s presents an extended C-terminal segment (5–7 amino acids) [63,64] and is subdivided into two main subgroups, depending on the amino acid residue at position 49 in the protein primary structure. Aspartate (Asp49 or D49) sPLA₂s are enzymatically active, while lysine (Lys49 or K49) sPLA₂s present no enzymatic activity [65–67]. However, there are further variants, as the serine (Ser49), asparagine (Asn49) or arginine (Arg49) [68–70].

Lys49 PLA₂s are devoid of catalytic activity due to their inability to bind Ca^{2+}, a key cofactor for PLA₂ activity. Although the lack of enzymatic activity, the Lys49 PLA₂ homologues have shown to display toxicity, especially myotoxicity [67]. The toxicity of Lys49 proteins can be related to a cluster of cationic and hydrophobic/aromatic amino acid residues located at the C-terminal region of these toxins [71,72].

Therefore, the cytotoxicity of sPLA₂ is probably mediated by the interaction between the C-terminal region and the plasma membrane [73,74]. Moreover, the PLA₂ effects can be mediated through the integrins and other receptors, such as vascular endothelial growth factor receptor-2 (VEGFR-2), and M–Type receptors [75–77]. Recently, it was demonstrated that the cell surface nucleolin interacts with and internalizes the PLA₂-like *Bothrops asper* myotoxin-II, which is responsible to mediate its toxic activity [78].

sPLA₂s from snake venom can act on cell membranes of specific tissues inducing several pharmacological actions such as myotoxicity, neurotoxicity, cardiotoxicity, platelet aggregation activation or inhibition, hypotension, edema among others [57,79]. In this scenario, these proteins have emerged as a potential therapeutic model, since numerous studies have focused on their microbicidal [80], antitumor [81–83], antiangiogenesis [84], antiparasitic [85–87] and antiviral activities [51].

The development of efficient antiviral therapies has become a global health emergency. In this sense, several researches have demonstrated the antiviral activity of sPLA₂s from snake venom against human viruses, including DENV, YFV, HCV and others [88–92]. Hence, the present review aimed to summarize the sPLA₂s from snake venom that were previously described to possess antiviral activity, highlighting the mechanisms of action of sPLA₂s against different stages of virus replication cycle (Table 1).

3. sPLA₂s from snake venom with antiviral effects

3.1. Crotoxin, PLA₂-CB (basic chain of crotoxin) and PLA₂-IC from Crotalus durissus terrificus venom

The venom of *Crotalus durissus terrificus* (*C. d. terrificus*), a South American rattlesnake, is composed by a large number of molecules with biological activities, such as crotoxin, crotamin, PLA₂ "inter-cro" (PLA₂-IC), convulxin and gyroxin [93,94]. Crotoxin, which comprehends more than a half of the dry weight of *C. d. terrificus* venom, is a heterodimeric compound composed by the PLA₂-CB (a basic phospholipase component) and crotapotin (an acidic nontoxic catalytically inactive protein) [95,96]. Villarrubia and coworkers [97] reported that crotoxin has anti-HIV (HIV-1, 2) effect by a direct interaction with Gag p24 glycoprotein on the viral surface, which appears to abrogate the HIV anchoring to host cell.

Furthermore, Muller and colleagues [88] working with diverse sPLA₂s isolated from *C. d. terrificus* venom explored different approaches to unveil the potent antiviral activity mediated by crotoxin, PLA₂-CB and PLA₂-IC against DENV-2 and YFV (enveloped virus). The authors demonstrated that all investigated sPLA₂s promoted a significant inhibition of DENV-2 and YFV entry into VERO E6 cells by a direct action on the viral particles (virucidal activity), and by interfering in the adsorption and internalization steps (early stages of the viral replication cycle) [88]. Besides that, cell pretreatment with three sPLA₂s was able to protect host cell against flaviviruses infection after 7 days by the reduction in the number of plaque formation. Interestingly, sPLA₂s treatment after viral infection promoted an enhancement of load viral, indicating that antiviral effect occurs in the early stages of viral infection [88]. In addition, the researchers gained insights into the role of catalytic sites of the tested sPLA₂s, proposing the use of a sPLA₂ without catalytic activity (BthTX-I) isolated from *Bothrops jararacussu* [98].

Table 1
sPLA$_2$s from snake venom with antiviral effects.

Source/species	Protein name	EC50/used dosage	Virus	Proposed action mechanism (inhibition)	Reference
Bothrops asper	Mt–I	50 μg/mL	DENV-1, 2, 3	Entry (virucidal activity)	[92]
		50 μg/mL	YFV		
		1.5 ng/mL (EC50)	DENV-2		
	Mt–II	50 μg/mL	DENV-1, 2, 3		
		50 μg/mL	YFV		
		2768 ng/mL (EC50)	DENV-2		
Bothrops jararacussu	BthTX-I	4.8 ng/μL (EC50)	DENV-2	Entry (virucidal activity)	[88]
		7.063 ng/μL (EC50)	YFV		
		57.3 ng/μL (EC50)	DENV-2	Entry (interfering in adsorption)	
		25.0 ng/μL (EC50)	YFV		
		69.0 ng/μL (EC50)	DENV-2	Entry (interfering in internalization)	
		23.4 ng/μL (EC50)	YFV		
Bothrops leucurus	BlK-PLA$_2$	20 μg/mL	DENV-1, 2 3	Replication (interfering in host cell components)	[91]
	BlD-PLA$_2$	20 μg/mL			
Crotalus durissus terrificus	Crotoxin	0.001 ng/μL (EC50)	DENV-2	Entry (virucidal activity)	[88–90,97]
		0.00045 ng/μL (EC50)	YFV		
		0.0046 ng/μL (EC50)	ROCV		
		0.0036 ng/μL (EC50)	MAYV		
		0.0054 ng/μL (EC50)	OROV		
		–	HIV-1,2		
		10 μg/mL	HCV		
		0.018 ng/μL (EC50)	DENV-2	Entry (interfering in adsorption)	
		0.0365 ng/μL (EC50)	YFV		
		34.4 ng/μL (EC50)	DENV-2	Entry (interfering in internalization)	
		13.7 ng/μL (EC50)	YFV		
		0.05 ng/μL (EC50)	DENV-2	Replication (interfering in host cell components)	
		0.04 ng/μL (EC50)	YFV		
		10 μg/mL	HCV	Release	

193

Table 1 (*Continued*)

Source/species	Protein name	EC50/used dosage	Virus	Proposed action mechanism (inhibition)	Reference
	PLA$_2$-CB (subunit of crotoxin)	0.00003 ng/μL (EC50)	DENV-2	Entry (virucidal activity)	[88–90]
		0.0037 ng/μL (EC50)	YFV		
		0.021 ng/μL (EC50)	ROCV		
		0.066 ng/μL (EC50)	MAYV		
		0.0067 ng/μL (EC50)	OROV		
		10 μg/mL	HCV		
		0.044 ng/μL (EC50)	DENV-2	Entry (interfering in adsorption)	
		0.01647 ng/μL (EC50)	YFV		
		17.2 ng/μL (EC50)	DENV-2	Entry (interfering in internalization)	
		3.3 ng/μL (EC50)	YFV		
		10 μg/mL	HCV		
		10 μg/mL	HCV	Entry (interfering in host cell components)	
		0.06 ng/μL (EC50)	DENV-2	Replication (interfering in host cell components)	
		0.26 ng/μL (EC50)	YFV		
		6.08 μg/mL (EC50)	HCV		
	PLA$_2$-IC	0.0137 ng/μL (EC50)	DENV-2	Entry (virucidal activity)	[88]
		0.0054 ng/μL (EC50)	YFV		
		0.133 ng/μL (EC50)	DENV-2	Entry (interfering in adsorption)	
		0.268 ng/μL (EC50)	YFV		
		21.6 ng/μL (EC50)	DENV-2	Entry (interfering in internalization)	
		0.775 ng/μL (EC50)	DENV-2	Replication (interfering in host cell components)	
		1.30 ng/μL (EC50)	YFV		
Naja mossambica mossambica	CM-II-sPLA$_2$	0.036 ng/mL (EC50)	HCV	Entry (virucidal activity)	[114]
		0.031 ng/mL (EC50)	DENV		
		1.34 ng/mL (EC50)	JEV		
		10,000 ng/mL (EC50)	MERS-CoV		
		>10,000 ng/mL (EC50)	SINV		

Table 1 (*Continued*)

Source/species	Protein name	EC50/used dosage	Virus	Proposed action mechanism (inhibition)	Reference
		>10,000 ng/mL (EC50)	FLUAV		
		>10,000 ng/mL (EC50)	SeV		
		2300 ng/mL (EC50)	VSNJV		
		5.4 ng/mL (EC50)	HIV-1		
		>10,000 ng/mL (EC50)	HSV-1		
		>10,000 ng/mL (EC50)	CV-B3		
		>10,000 ng/mL (EC50)	EMCV		
	Nmm$_{CMIII}$	0.4 nM (EC50)	HIV-1 isolates	Entry (interfering in host cell components)	[107]
Naja nigricollis	Nigexine	0.4 nM (EC50)	HIV-1 isolates		
Oxyuranus scutellatus	Taipoxin	0.8 nM (EC50)	HIV-1 isolates		

CV-B3 (Coxsackievirus B3; Picornaviridae); DENV (Dengue virus); EMCV (Encephalomyocarditis virus; Picornaviridae); FLUAV (Influenza A virus); HCV (Hepatitis C virus); HIV (Human immunodeficiency virus); HSV (Herpes simplex virus); JEV (Japanese encephalitis virus); MAYV (Mayaro virus); MERS-CoV (Middle East respiratory syndrome coronavirus); OROV (Oropouche virus); ROCV (Rocio virus); SeV (Sendai virus); SINV (Sindbis virus); VSNJV (Vesicular stomatitis New Jersey virus); YFV (Yellow Fever virus).

BthTX-I revealed antiviral activity against YFV and DENV-2 in the virucidal, adsorption and internalization assays. Interestingly, as shown to other catalytically-active sPLA$_2$s at 100 ng/μL, BthTX-I at the same concentration was also able to inhibit YFV entry by virucidal activity (100%), interfering in adsorption (77%) and internalization (78%) [88]. Although BthTX-I showed antiviral activity, the effective concentration 50% (EC50) values obtained for this toxin were extremely higher when compared to the catalytically-active sPLA$_2$s. For example, for the half-maximum virucidal activity against YFV, this toxin required 7.063 ng/μL, while crotoxin, PLA$_2$-CB and PLA$_2$-IC demanded 0.00045, 0.0037 and 0.0054 ng/μL, respectively. In a similar way against DENV-2, BthTX-I acted at 4.8 ng/μL, in contrast to the crotoxin, PLA$_2$-CB and PLA$_2$-IC that required 0.001, 0.00003 and 0.0137 ng/μL, respectively. As shown, the huge differences of EC50 values between BthTX-I and enzymatically active proteins reflect that the enzymatic activity is an important factor for the antiviral activity of sPLA$_2$s [88].

In a further study, PLA$_2$-CB and crotoxin inhibited virus entry by virucidal activity against other enveloped viruses, such as Rocio virus (ROCV; Flaviviridae family), Oropouche virus (OROV; Bunyaviridae family), and Mayaro virus (MAYV; Togaviridae family). However, these compounds did not show virucidal effect against Coxsackie B5 virus (CV-B5; Picornaviridae family; non-enveloped virus), hence suggesting that the possible antiviral action occurs upon the lipid bilayer viral envelope [89]. To corroborate these findings, it was demonstrated that preincubating DENV-2 with PLA$_2$-CB or crotoxin resulted in an increase of exposure and degradation of viral RNA [89]. Also, Russo and collaborators [99] expressed two recombinant PLA$_2$-CB isoforms through a prokaryotic system and noted that both rPLA$_2$-CB1 and rPLA$_2$-CB2 maintained the viral inhibitory activity against CHIKV, DENV-2, YFV and ZIKV when compared to the native sPLA$_2$-CB. Additionally, Muller and colleagues [88,89] suggested that the mechanism of action of PLA$_2$-CB isolated from *C. t. terrificus* against DENV can occur through an interaction with components on the host cell surface or mainly due to the glycerophospholipid cleavage on the virus envelope, destabiliz-

ing viral E proteins and resulting in the viral envelope disruption and RNA viral exposure before the infection of host cells.

In order to gain insights into the antiviral mechanism of sPLA$_2$s obtained from *C. t. terrificus*, Shimizu and colleagues [90] showed that PLA$_2$-CB inhibited HCVcc JFH-1 virus strain entry and replication in Huh 7.5 cells, and crotoxin blocked virus entry and release, suggesting that these proteins possess multiple antiviral effects against HCV. Moreover, the authors also reported that PLA$_2$-CB significantly decrease the levels of lipid droplets, which are essential for the HCV replication complex, and reduced the levels of HCV NS5A protein due to the replication inhibition, evidencing that besides the action on virus entry, PLA$_2$-CB is able to disrupt HCV replication probably by an interference in lipid metabolism of host cell [90,100,101].

3.2. BlK-PLA$_2$ and BlD-PLA$_2$ from Bothrops leucurus venom

Both BlK-PLA$_2$ (Lys49 sPLA$_2$s) and BlD-PLA$_2$ (Asp49 sPLA$_2$s) are two basic sPLA$_2$s isolated from *Bothrops leucurus* venom, a pit viper (white-tailed-jararaca) commonly found in the northeast of Brazil [102]. Cecilio and coworkers [91] showed that the pretreatment of LLC-MK2 cells (Rhesus Monkey Kidney Epithelial cells) with each isoform of Bl-PLA$_2$ followed by viral infection was able to inhibit DENV infectivity (serotypes 1, 2 and 3), measured by qRT-PCR quantification of the DENV viral load in the cell supernatants after virus infection. On the other hand, Bl-PLA$_2$s treatment after viral entry was not capable of inhibiting viral replication, then suggesting that the antiviral effect occurs upon components on the surface of the host cell membrane. The authors did not assess the potential virucidal mechanism of Bl-PLA$_2$s against DENV. However, they suggested that the possible mechanism of action of Bl-PLA$_2$s does not depend exclusively on their catalytic site. The Lys49-BlK-PLA$_2$ treatment was able to interfere in the viral load, indicating that the functional effect mediated by Bl-PLA$_2$s also may occur due to the presence of pharmacological domains on the enzyme surface that would allow the interaction with host cell proteins, as well as the enzymatic activity [91]. The authors hypothesized that

the DENV RNA level reduction is mediated by the intracellular action of Bl-PLA$_2$s due to the higher penetrability capacity of basic sPLA$_2$s, in comparison to neutral and acidic enzymes [91,103].

3.3. Mt-I and Mt-II from Bothrops asper venom

Bothrops asper is a viperid specie found in Central America and its venom contains significant concentrations of acid and basic sPLA$_2$ enzymes [104]. The *B. asper* venom has both the basic enzymatically-active sPLA$_2$ (Mt-I) and the catalytically-inactive sPLA$_2$-like protein (Mt-II) [74].

Brenes and collaborators [92] investigated the antiviral potential triggered by both Mt-I and Mt-II isoforms isolated from *B. asper* venom. The authors showed that these sPLA$_2$s at concentration of 50 μg/mL completely blocked virus entry by a virucidal action against members of Flaviviridae family, such as DENV and YFV, while exhibited moderate to negligible effects against other enveloped viruses (HSV-1, HSV-2, Influenza A H3N2 and Vesicular stomatitis VSV) or non-enveloped viruses (Sabin Poliovirus 1, 2 and 3). Interestingly, for the half-maximum virucidal activity against DENV-2, Mt-I required 1.5 ng/mL, while Mt-II acted at 2768 ng/mL, revealing that Mt-I is extremely more potent than Mt-II [92]. Investigating the role of the enzymatic activity in the inhibitory effect upon DENV-2, it was promoted the inactivation of the catalytic activity of Mt-I with *p*-bromophenacyl bromide (*p*BPB). The data showed that the chemical inactivation of Mt-I resulted in a reduction of the virucidal potency, indicating the relevant role of the enzymatic action against viral infection [92]. Even without enzymatic activity, the C-terminal region of Mt-II, which encompasses the amino acid residues 115–129, is responsible for the membrane-permeabilizing effect caused in many cellular types [67], as well as its bactericidal activity [105]. Notwithstanding that, the authors demonstrated that, even at high concentrations, the synthetic peptide "p115" corresponding to the C- terminal region of Mt-II (amino acid residues 115–129) did not inhibit DENV-2 [92]. Thus, the authors speculate that the weak virucidal effect of Mt-II may be intrinsic or more possible related to a trace contamination with Mt-I, where the total chromatographic separation for these toxins is hardly achieved [92].

In addition, it was suggested that Mt-I acts by a direct virucidal mechanism that depends on its enzymatic activity, which may hydrolyze viral envelope phospholipids and disrupt the viral envelope of flaviviruses leading to the impairment of the infection. Also, the mode of action of Mt-I and Mt-II is not related to an effect on host cell, since cell treatment after infection did not interfere in viral replication [92]. Furthermore, in a pretreatment assay, it was demonstrated a partial reduction of viral plaques, that may be explained by a slight cytotoxic action of Mt-I on cells [92]. Finally, the higher antiviral activity of Mt-I against Flaviviridae viruses in comparison to other enveloped virus families may be related to the specific structural organization, physicochemical composition, curvature and fluidity of viral envelope from flaviviruses, which may positively affect the catalytic activity of Mt-I against this family [106].

3.4. Taipoxin (Oxyuranus scutellatus), nigexine (Naja nigricollis) and Nmm$_{CMIII}$ (Naja mossambica mossambica)

In a previous study, Fenard and colleagues [107] demonstrated anti-HIV-1 effects of different sPLA$_2$s from snake venom, such as taipoxin (*Oxyuranus scutellatus* venom), Nmm$_{CMIII}$ (*Naja mossambica mossambica* venom) [108,109] and nigexine (*Naja nigricollis* venom) [110]. Investigating the possible mode of action of some of these sPLA$_2$s, it was observed that despite their enzymatic activity, Nmm$_{CMIII}$ and taipoxin did not show virucidal effects against HIV-1, but promoted an efficient inhibition of HIV-1 entry by preventing the intracellular release of HIV-1 Gap p24 proteins from the viral capsid [107].

The blockage of HIV entry appears to not depend exclusively on sPLA$_2$s catalytically active, which was confirmed through two manners: i) the use of inhibitors of sPLA$_2$s activity, such as phenacyl bromide, aristolochic acid or oleoyloxyethylphosphocholine, that were not able to interfere in the blockage of virus entry mediated by sPLA$_2$s; ii) the use of cleavage products of sPLA$_2$s, such as arachidonic acid, lysophosphatidylethanolamine, lysophosphatidic acid, oleoyl-lysophosphatidylcholine and palmitoyl-lysophosphatidylcholine, which were also not able to inhibit virus entry [107]. In addition, competition binding assays between sPLA$_2$s and host cells showed extremely low dissociation constant (K) values for Nmm$_{CMIII}$, taipoxin and nigexine, suggesting that the inhibition of HIV-1 entry triggered by sPLA$_2$s is more probably linked to sPLA$_2$s binding membrane receptors of host cells than their enzymatic activity [107,111].

3.5. CM-II-sPLA$_2$ from Naja mossambica mossambica venom

CM-II-sPLA$_2$ is a secreted PLA$_2$ isoform isolated from *Naja mossambica mossambica* venom [112,113]. Recently, Chen and coworkers [114] reported that this sPLA$_2$ possesses a potent dose-dependent virucidal activity that impairs the entry of enveloped viruses from budding through the endoplasmic reticulum, such as HCV, DENV and JEV (Japanese encephalitis virus) belonging to the Flaviviridae family. In contrast, CM-II-sPLA$_2$ demonstrated a low antiviral activity against other enveloped viruses by: i) budding through the plasma membrane, as observed for SINV (Sindbis virus; Togaviridae), SeV (Sendai virus; Paramyxoviridae), FLUAV (Influenza A virus; Orthomyxoviridae), VS-NJV (Vesicular stomatitis New Jersey virus; Rhabdoviridae) and HIV-1 (Retroviridae); ii) budding through the trans-Golgi network, as seen for HSV- 1 (Herpes simplex virus type 1; Herpesviridae); iii) budding through the ER-Golgi intermediate compartment, as for MERS-CoV (Middle East respiratory syndrome coronavirus; Coronaviridae). Additionally, the slight effect was also observed against non-enveloped viruses, such as EMCV (Encephalomyocarditis virus; Picornaviridae) and CV-B3 (Coxsackievirus B3; Picornaviridae) [114].

The disruption of viral envelope by CM-II-sPLA$_2$ appears to be directly related to its enzymatic activity, which was confirmed by the use of manoalide (a specific sPLA$_2$ inhibitor) that inhibited the virucidal activity of CM-II-sPLA$_2$ against HCV and DENV [114]. Moreover, the selectivity of CM-II-sPLA$_2$ for virus buds through endoplasmic reticulum may be related to the differences in the phospholipid contents and physicochemical characteristics (thickness and sturdiness) that can differ among the different routes of viral budding, which would enhance the sensitivity to CM-II-sPLA$_2$ mediated by hydrolysis against HCV, DENV and JEV [114–117].

4. Proposed antiviral mechanism of sPLA$_2$s from snake venom

Findings from the current literature about the antiviral activity of toxins (Table 1) are heterogeneous, since authors developed a variety of assays/models using different sPLA$_2$s and viruses. The virucidal model corresponds to the strategy in which the toxins act directly on the virus particles before infecting the cell monolayer; in the pre-infection model, the uninfected monolayers are previously treated with toxins before viral infection; and in the post-infection model, cell monolayers are adsorbed with the virus followed by toxin treatment. In this sense, many studies raised the following questions: in which stages of virus replication are the sPLA$_2$s able to interfere? Does the antiviral action of sPLA$_2$s depend on their catalytic activity? Based on this, we summarize a possible model of antiviral action mediated by sPLA$_2$s from snake venom.

As discussed above, sPLA$_2$s have demonstrated to be potent antiviral inhibitors by interfering in different stages of virus replicative cycle as entry steps, replication and release (Fig. 1). Current studies have reported that the antiviral action of sPLA$_2$s on steps of viral cycle can oc-
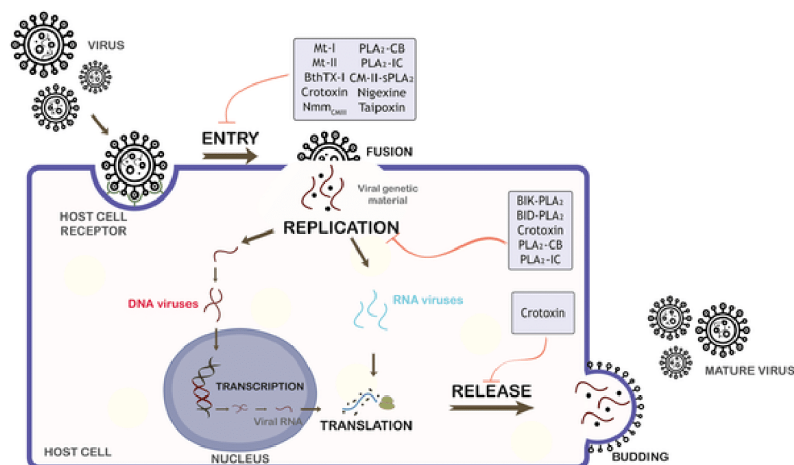
Fig. 1. Schematic representation of the mechanisms of action of sPLA$_2$s from snake venom on viral replicative cycle. sPLA$_2$s, which possess antiviral activity, are indicated in early and/or late stages of the viral life cycle: entry, replication and release. Mt-I and Mt-II (*Bothrops asper*), BthTX-I (*Bothrops jararacussu*), crotoxin, PLA$_2$-CB and PLA$_2$-IC (*Crotalus durissus terrificus*), CM-II-sPLA$_2$ and Nmm$_{CMIII}$ (*Naja mossambica mossambica*), nigexine (*Naja nigricollis*), taipoxin (*Oxyuranus scutellatus*), BlK-PLA$_2$ and BlD-PLA$_2$ (*Bothrops leucurus*) are demonstrated.

cur through a direct action upon viral particle and/or by an interaction with virus or host cell components.

Regarding the virucidal activity, studies have shown that both catalytically-active sPLA$_2$s (crotoxin, PLA$_2$-IC, PLA$_2$-CB, Mt-I and CM-II-PLA$_2$) and catalytically-inactive sPLA$_2$s (Mt-II and BthTX-I) indicated virucidal activity preferentially against enveloped viruses, such as DENV (serotypes 1, 2 and 3), YFV, ROCV, OROV, MAYV, HCV, JEV, MERS-CoV, SINV, FLUAV, SeV, VSNJV, HIV-1 and HSV-1 [88–90,92,114].

It is proposed that the potent virucidal activity of sPLA$_2$s against enveloped viruses is likely associated with the ability that catalytically-active sPLA$_2$s have to cleave glycerophospholipids in the virus lipid envelope, and it is reasonable to propose that sPLA$_2$s also present domains that are capable to interact with viral envelope components, which could lead to viral envelope disruption, hence resulting in exposure of the viral content (viral inactivation) and compromising the early stages of viral replication. Additionally, Muller and colleagues [88,89], through a steric and electrostatic analysis of the interaction of PLA$_2$-CB with the DENV envelope lipid bilayer, showed that PLA$_2$-CB probably accesses the DENV lipid bilayer through the pore found on each of the twenty 3-fold vertices in the E protein shell on the DENV surface, which would allow the glycerophospholipid cleavage on the virus envelope and destabilization of the E proteins. Interestingly, it has been demonstrated that the structural organization and lipid composition of viral envelope may influence the antiviral efficiency of some sPLA$_2$s, suggesting that the virucidal mechanism mediated by sPLA$_2$s is specific [92].

Independent studies have revealed that sPLA$_2$s such as crotoxin, PLA$_2$-IC, PLA$_2$-CB, Bl-PLA$_2$ and BthTX-I are also able to dramatically impact the entry, replication and release of viruses by targeting host cell components [88–91]. To gain insights into these viral cycle stages, it was demonstrated that Nmm$_{CMIII}$, taipoxin and nigexine prevented the intracellular release of HIV-1 Gap p24 proteins from the viral capsid (inhibition virus entry) by a direct binding to membrane receptors of host cells [107]. In addition, PLA$_2$-CB was able to disrupt HCV replication probably by an interference in lipid metabolism of host cell [90].

It was demonstrated through the use of both specific sPLA$_2$ inhibitors and the catalytically-inactive sPLA$_2$s that the antiviral effect of the major tested catalytically-active sPLA$_2$s, such as crotoxin, PLA$_2$-IC, PLA$_2$-CB, BlD-PLA$_2$, Mt-I and CM-II-sPLA$_2$ is significantly higher when presented their functional catalytic site to sPLA$_2$s with no enzymatic activity (BthTX-I, BlK-PLA$_2$ and Mt-II) [88,91,92,114].

In order to corroborate with the data from the current literature, we performed docking simulations between the sPLA$_2$s from *Bothrops asper* venom and three phospholipids found in the DENV envelope, which are 1-Palmitoyl-2-oleoylphosphatidylcholine (POPC), 1-palmitoyl-2-oleoylphosphatidylethanolamine (POPE) and 1-Palmitoyl-2-oleoylphosphatidylserine (POPS) [118]. The molecular docking simulations were done by using the 3D crystal structure of Mt-I (PDB: 5TFV) and Mt-II (PDB ID 4YV5) retrieved from Protein Database (https://www.rcsb.org/).

We simulated the interaction in the enzymatic site of sPLA$_2$s with palmitoyl phospholipids (head or complete structure) using AutoDock Vina software [119]. The predicted affinity between sPLA$_2$s and palmitoyl phospholipids (head or complete) was similar (Table 2). Concerning to the interaction with the phospholipids head, Mt-I showed a higher affinity to POPC, POPE and POPS (-5.1, -4.7 and -5.0 kcal/mol, respectively) related to Mt-II (Table 2). When we simulated

Table 2
Docking simulations between Mt-I and Mt-II with palmitoyl phospholipids (head or complete structure) from DENV envelope.

PLA$_2$s affinity (kcal/mol)	Phospholipids					
	POPC		POPE		POPS	
	Head	Complete	Head	Complete	Head	Complete
Mt-I	-5.1	-5.4	-4.7	-5.1	-5.0	-5.4
Mt-II	-4.3	-4.5	-4.3	-4.7	-4.3	-4.8

POPC - 1-palmitoyl-2-oleoylphosphatidylcholine; POPE - 1-palmitoyl-2-oleoylphosphatidylethanolamine; POPS - 1-palmitoyl-2-oleoylphosphatidylserine.

the docking with the complete palmitoyl phospholipid molecule, Mt-I also has a higher affinity than Mt-II (Table 2).

Although we do not observe a strong difference in the affinity between Mt-I and Mt-II for palmitoyl phospholipids, it is possible to note structural variation in the enzymatic site of these two toxins. Compared to Mt-II, the enzymatic site of Mt-I (Fig. 2A) is more suitable due to a smaller aspartic acid radical group. The van der Waals radii volume of aspartic acid is 91 and hence it is more prominent, while the lysine has a volume of 135, and this results in less space in enzymatic site entrance in Mt-II (Fig. 2B). This difference could create an enzymatic site more restricted to palmitoyl phospholipid entrance/binding and be partially responsible for the absence of enzymatic activity in Mt-II [120]. In addition, the enzymatic activity of Mt-I can be attributed to highly conserved catalytic site formed by the amino acid residues His48, Asp49, Tyr52 and Asp99. Asp49 coordinates the hydrolysis reaction of phospholipids together with the residues of the Ca2+ binding loop, essential in the catalytic activity of PLA$_2$s. The substitution of lysine residue at the same position affects the ability of this protein to bind to $Ca^{2+,}$ resulting in the absence of catalytic activity [92].

Despite the stronger antiviral activity is associated with the enzymatic activity, the antiviral mechanism of sPLA$_2$s does not depend exclusively on their catalytic site, since Lys49 sPLA$_2$s and inhibited catalytically-active sPLA$_2$s were also able to show antiviral effects, suggesting that sPLA$_2$s may possess different mechanisms of action. How-

Fig. 2. Docking simulations between sPLA$_2$s and 1-palmitoyl-2-oleoylphosphatidylcholine (POPC). Mt-I (A) and Mt-II (B) are showed as surface and the enzymatic site is colored. The amino acids from the enzymatic site are H48 in red, D49 (Mt-I) or K49 (Mt-II) in blue, and Y52 in green. The POPC is showed as wire structure. The aspartic acid has a smaller volume than lysine, which may result in a less open entrance in Mt-II (panel B) compared with Mt-I (panel A). H: histidine; D: aspartate; K: lysine; Y: tyrosine. (For interpretation of the references to color in this figure legend, the reader is referred to the web version of this article.)

ever, additional studies with different Lys49 from snake venom are required to better characterize the antiviral potential of this protein class.

Functional and structural studies have described that the activity of Lys49 PLA$_2$s from snake venom toward cell membranes in myotoxic mechanism involves an allosteric transition, and the participation of two independent interaction sites with the target membrane [67,72,121–123]. The action of Lys49 PLA$_2$s is related to a cluster of cationic and hydrophobic/aromatic amino acid residues located at the C-terminal region of this toxin. These two conserved regions in most Lys49-PLA$_2$s are designed by "cationic membrane-docking site" (MDoS), which are formed by the strictly conserved C-terminal residues (Lys115 and Arg118), eventually aided by other cationic and exposed residues such as Lys20, Lys80, Lys122 and Lys127; and the "hydrophobic membrane-disruption site" (MDiS) formed by residues of Leu121 and Phe125. The key step for protein activation is the binding of a fatty acid at the hydrophobic channel, which leads to allosteric transition and structure stabilization exposing MDoS and MDiS to the membrane, following by the insertion of the MDiS region from both monomers into the target membrane. This penetration disrupts the lipid bilayer, causing alterations in the membrane permeability, highlighted by a prominent influx of ions (*i.e.*, Ca^{2+} and Na^{+}), and eventually, irreversible intracellular alterations and cell death [123].

According to myotoxic mechanism of Lys49 PLA$_2$s from viperid snake venoms, it is proposed that the fatty acids which are important to protein activation may come from membrane phospholipid hydrolysis by catalytic PLA$_2$s (Asp49), highlighting the synergism between Asp49 PLA$_2$s and Lys49 PLA$_2$ in snake envenomation [124]. In this way, the antiviral effects of the Lys49 PLA$_2$s from snake venom, showed in this review, may be associated to fatty acids from the catalytic activity of cytosolic PLA$_2$ (cPLA$_2$) from virus lipid envelope, once it was demonstrated that enzymatic activity of the cPLA$_2$ is required for replication of various virus [125–127]. Muller and colleagues [126] showed that the pharmacological inhibition of a cellular phospholipase, cPLA$_2$, using a specific small-molecule inhibitor, drastically reduces coronavirus RNA synthesis and, as a consequence, protein accumulation and the production of infectious virus progeny. In addition, cPLA$_2$ activity was shown to be critically involved in the production of infectious progeny of HCV and DENV [128].

5. Concluding remarks: sPLA$_2$s as a possible useful tool for the development of antiviral compounds

The present review highlighted that PLA$_2$s from snake venom have become valuable as pharmacological tools and/or therapeutic approaches due to their extremely high specificity and potent activity against microbial infection. Regarding to antiviral properties, we highlighted the following remarks: (i) the antiviral effects of sPLA$_2$s can be mediated by either a dependent or independent catalytic mechanism; (ii) sPLA$_2$s-antiviral effects are more evident against enveloped virus; (iii) sPLA$_2$s promoted the blockage of viral entry into host cells by the direct action on the viral particle, resulting in glycerophospholipids cleavage and destabilization of viral envelope proteins; (iv) the structural organization, physicochemical composition, and the curvature and fluidity of viral envelope may influence in the antiviral efficiency of some sPLA$_2$s; (v) sPLA$_2$s promoted the blockage of entry, replication and release of virus probably by the interference on the host cell components.

The structure and function of sPLA$_2$s from snake venom have been widely explored. Homology studies with sPLA$_2$s have demonstrated highly conserved regions in these proteins capable of disrupting the integrity of membranes and provoking many pharmacological effects. Despite extensive studies on sPLA$_2$s in over decades, there is few of them focusing on mechanistic aspects of the antiviral activities and to date are limited to *in vitro* and *in silico* models. It is important to note that these sPLA$_2$s showed damage effects *in vivo*, such as myotoxicity
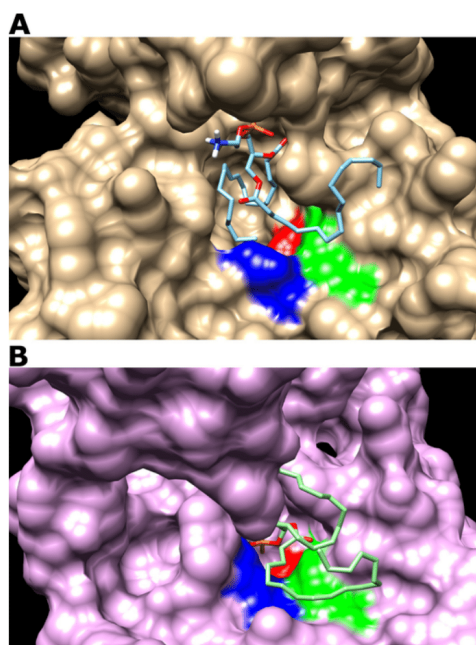
and inflammation. Thus, further *in vivo* studies for attesting antiviral effects of sPLA$_2$s need to be addressed to investigate their safety, toxicity and pharmacokinetics. Taken together, new structural and functional studies with sPLA$_2$s are essential to discover new relevant motifs responsible for the antiviral activities that would allow the future use of these proteins or peptides for the design of antiviral drugs, capable of ensuring more stability and targeting the specific site of action.

Acknowledgements

References

[1] D Lugo, P Krogstad, Enteroviruses in the early 21st century: new manifestations and challenges, Curr. Opin. Pediatr. 28 (1) (2016) 107–113.

[2] K P Braaten, M R Laufer, Human papillomavirus (HPV), HPV-related disease, and the HPV vaccine, Rev. Obstet. Gynecol. 1 (1) (2008) 2–10.

[3] P J Dodd, G P Garnett, T B Hallett, Examining the promise of HIV elimination by 'test and treat' in hyperendemic settings, AIDS (London, England) 24 (5) (2010) 729–735.

[4] D M Koelle, L Corey, Herpes simplex: insights on pathogenesis and possible vaccines, Annu. Rev. Med. 59 (2008) 381–395.

[5] M W Carroll, D A Matthews, J A Hiscox, M J Elmore, G Pollakis, A Rambaut, R Hewson, I Garcia-Dorival, J A Bore, R Koundouno, S Abdellati, B Afrough, J Aiyepada, P Akhilomen, D Asogun, B Atkinson, M Badusche, A Bah, S Bate, J P Baumann, D Becker, B Becker-Ziaja, A Bocquin, B Borremans, A Bosworth, J P Boettcher, A Cannas, F Carletti, C Castilletti, S Clark, F Colavita, S Diederich, A Donatus, S Duraffour, D Ehichioya, H Ellerbrok, M D Fernandez-Garcia, A Fizet, E Fleischmann, S Gryseels, A Hermelink, J Hinzmann, U Hopf-Guevara, Y Ighodalo, L Jameson, A Kelterbaum, Z Kis, S Kloth, C Kohl, M Korva, A Kraus, E Kuisma, A Kurth, B Liedigk, C H Logue, A Ludtke, P Maes, J McCowen, S Mely, M Mertens, S Meschi, B Meyer, J Michel, P Molkenthin, C Munoz-Fontela, D Muth, E N Newman, D Ngabo, L Oestereich, J Okosun, T Olokor, R Omiunu, E Omomoh, E Pallasch, B Palyi, J Portmann, T Pottage, C Pratt, S Priesnitz, S Quartu, J Rappe, J Repits, M Richter, M Rudolf, A Sachse, K M Schmidt, G Schudt, T Strecker, R Thom, S Thomas, E Tobin, H Tolley, J Trautner, T Vermoesen, I Vitoriano, M Wagner, S Wolff, C Yue, M R Capobianchi, B Kretschmer, Y Hall, J G Kenny, N Y Rickett, G Dudas, C E Coltart, R Kerber, D Steer, C Wright, F Senyah, S Keita, P Drury, B Diallo, H de Clerck, M Van Herp, A Sprecher, A Traore, M Diakite, M K Konde, L Koivogui, N Magassouba, T Avsic-Zupanc, A Nitsche, M Strasser, G Ippolito, S Becker, K Stoecker, M Gabriel, H Raoul, A Di Caro, R Wolfel, P Formenty, S Gunther, Temporal and spatial analysis of the 2014–2015 Ebola virus outbreak in West Africa, Nature 524 (7563) (2015) 97–101.

[6] J Heukelbach, C H Alencar, A A Kelvin, W K de Oliveira, L Pamplona de Goes Cavalcanti, Zika virus outbreak in Brazil, Journal of infection in developing countries 10 (2) (2016) 116–120.

[7] G Neumann, T Noda, Y Kawaoka, Emergence and pandemic potential of swine-origin H1N1 influenza virus, Nature 459 (7249) (2009) 931–939.

[8] N D Collins, A D Barrett, Live attenuated yellow fever 17D vaccine: a legacy vaccine still controlling outbreaks in modern day, Curr. Infect. Dis. Rep. 19 (3) (2017) 14.

[9] D Wu, T Wu, Q Liu, Z Yang, The SARS-CoV-2 outbreak: what we know, Int. J. Infect. Dis. 94 (2020) 44–48.

[10] K F Smith, M Goldberg, S Rosenthal, L Carlson, J Chen, C Chen, S Ramachandran, Global rise in human infectious disease outbreaks, J. R. Soc. Interface 11 (101) (2014) 20140950.

[11] J R Pulliam, Viral host jumps: moving toward a predictive framework, EcoHealth 5 (1) (2008) 80–91.

[12] M Shi, X D Lin, X Chen, J H Tian, L J Chen, K Li, W Wang, J S Eden, J J Shen, L Liu, E C Holmes, Y Z Zhang, The evolutionary history of vertebrate RNA viruses, Nature 556 (7700) (2018) 197–202.

[13] P Palese, Influenza: old and new threats, Nat. Med. 10 (12 Suppl) (2004) S82–S87.

[14] F Krammer, Emerging influenza viruses and the prospect of a universal influenza virus vaccine, Biotechnol. J. 10 (5) (2015) 690–701.

[15] L Qin, Q Sun, Y Wang, K F Wu, M Chen, B C Shia, S Y Wu, Prediction of Number of Cases of 2019 Novel Coronavirus (COVID-19) Using Social Media Search Index, 17, 2020 (7).

[16] S Bhatt, P W Gething, O J Brady, J P Messina, A W Farlow, C L Moyes, J M Drake, J S Brownstein, A G Hoen, O Sankoh, M F Myers, D B George, T Jaenisch, G R Wint, C P Simmons, T W Scott, J J Farrar, S I Hay, The global distribution and burden of dengue, Nature 496 (7446) (2013) 504–507.

[17] D M Haig, Subversion and piracy: DNA viruses and immune evasion, Res. Vet. Sci. 70 (3) (2001) 205–219.

[18] W-S Ryu, Antivir. Ther. (2017) 367–381.

[19] A Nanbo, M Imai, S Watanabe, T Noda, K Takahashi, G Neumann, P Halfmann, Y Kawaoka, Ebolavirus is internalized into host cells via macropinocytosis in a viral glycoprotein-dependent manner, PLoS Pathog. 6 (9) (2010) e1001121.

[20] J A Thorley, J A McKeating, J Z Rappoport, Mechanisms of viral entry: sneaking in the front door, Protoplasma 244 (1–4) (2010) 15–24.

[21] P Aleksandrowicz, A Marzi, N Biedenkopf, N Beimforde, S Becker, T Hoenen, H Feldmann, H J Schnittler, Ebola virus enters host cells by macropinocytosis and clathrin-mediated endocytosis, J. Infect. Dis. 204 (Suppl. 3) (2011) S957–S967.

[22] B Marintcheva, Introduction to Viral Structure, Diversity and Biology (Parts of this chapter were originally published in Marintcheva B. A box of paradoxes: the fascinating world of viruses. Bridgew Rev 2013;32(2):25–8. http://vc.bridgew.edu/br_rev/vol32/iss2/8 and are reproduced here with the permission of the editor) 2018, pp. 1–26.

[23] I A Rodenhuis-Zybert, J Wilschut, J M Smit, Dengue virus life cycle: viral and host factors modulating infectivity, Cell. Mol. Life Sci. 67 (16) (2010) 2773–2786.

[24] S H Kaufmann, M J McElrath, D J Lewis, G Del Giudice, Challenges and responses in human vaccine development, Curr. Opin. Immunol. 28 (2014) 18–26.

[25] J N Maslow, The cost and challenge of vaccine development for emerging and emergent infectious diseases, Lancet Glob. Health 6 (12) (2018) e1266–e1267.

[26] P Mohammadi Pour, S Fakhri, S Asgary, M H Farzaei, J Echeverria, The signaling pathways, and therapeutic targets of antiviral agents: focusing on the antiviral approaches and clinical perspectives of anthocyanins in the management of viral diseases, Front. Pharmacol. 10 (2019) 1207.

[27] S Duffy, Why are RNA virus mutation rates so damn high?, PLoS Biol. 16 (8) (2018) e3000003.

[28] D K Li, R T Chung, Overview of direct-acting antiviral drugs and drug resistance of hepatitis C virus, Methods in molecular biology (Clifton, N.J.) 1911 (2019) 3–32.

[29] E Takashita, Influenza polymerase inhibitors: mechanisms of action and resistance, Cold Spring Harbor perspectives in medicine (2020).

[30] A Carr, D A Cooper, Adverse effects of antiretroviral therapy, Lancet (London, England) 356 (9239) (2000) 1423–1430.

[31] K K Lai, D L Gang, J K Zawacki, T P Cooley, Fulminant hepatic failure associated with 2′,3′-dideoxyinosine (ddI), Ann. Intern. Med. 115 (4) (1991) 283–284.

[32] V Montessori, N Press, M Harris, L Akagi, J S Montaner, Adverse effects of antiretroviral therapy for HIV infection, Can. Med. Assoc. J. 170 (2) (2004) 229–238.

[33] D A Dias, S Urban, U Roessner, A historical overview of natural products in drug discovery, Metabolites 2 (2) (2012) 303–336.

[34] G Brahmachari, Natural Products in Drug Discovery: Impacts and Opportunities — An Assessment, 2011, pp. 1–199.

[35] T Mohamed Abd El-Aziz, A Garcia Soares, J D Stockand, Snake venoms in drug discovery: valuable therapeutic tools for life saving, Toxins 11 (10) (2019).

[36] R Schoni, The use of snake venom-derived compounds for new functional diagnostic test kits in the field of haemostasis, Pathophysiol. Haemost. Thromb. 34 (4–5) (2005) 234–240.

[37] M Millard, S Odde, N Neamati, Integrin targeted therapeutics, Theranostics 1 (2011) 154–188.

[38] C Y Koh, R M Kini, From snake venom toxins to therapeutics—cardiovascular examples, Toxicon 59 (4) (2012) 497–506.

[39] L A Calderon, J C Sobrinho, K D Zaqueo, A A de Moura, A N Grabner, M V Mazzi, S Marcussi, A Nomizo, Antitumoral Activity of Snake Venom Proteins: New Trends in Cancer Therapy, 2014, 2014, p. 203639.

[40] M A Ondetti, N J Williams, E F Sabo, J Pluscec, E R Weaver, O Kocy, Angiotensin-converting enzyme inhibitors from the venom of Bothrops jararaca. Isolation, elucidation of structure, and synthesis, Biochemistry 10 (22) (1971) 4033–4039.

[41] D W Cushman, M A Ondetti, History of the design of captopril and related inhibitors of angiotensin converting enzyme, Hypertension (Dallas, Tex.: 1979) 17 (4) (1991) 589–592.

[42] R M Scarborough, J W Rose, M A Hsu, D R Phillips, V A Fried, A M Campbell, L Nannizzi, I F Charo, Barbourin. A GPIIb-IIIa-specific integrin antagonist from the venom of Sistrurus m. barbouri, J. Biol. Chem. 266 (15) (1991) 9359–9362.

[43] Z R Gan, R J Gould, J W Jacobs, P A Friedman, M A Polokoff, Echistatin. A potent platelet aggregation inhibitor from the venom of the viper, Echis carinatus, J. Biol. Chem. 263 (36) (1988) 19827–19832.

[44] C Funk, J Gmur, R Herold, P W Straub, Reptilase-R—a new reagent in blood coagulation, Br. J. Haematol. 21 (1) (1971) 43–52.

[45] D S Wang, M Hanamoto, F Fang, M Ohba, M Ishii, F Kimura, E Higaki, H Senga, Defibrinogenating effect of batroxobin (Defibrase) in rats and inhibition of migration of human vascular smooth muscle cells by the plasma of batroxobin-treated rats in vitro, Atherosclerosis 156 (1) (2001) 73–80.

[46] N C de Morais, C C Neves Mamede, K C Fonseca, M R de Queiroz, S A Gomes-Filho, N A Santos-Filho, C Bordon Kde, M E Beletti, S V Sampaio, E C Arantes, F de Oliveira, Isolation and characterization of moojenin, an acid-active, anticoagulant metalloproteinase from Bothrops moojeni venom, Toxicon 60 (7) (2012) 1251–1258.

[47] F Graziano, R Maugeri, L Basile, F Meccio, D G Iacopino, Aulogous fibrin sealant (Vivostat((R))) in the neurosurgical practice: part II: vertebro-spinal procedures, Surg. Neurol. Int. 7 (Suppl. 3) (2016) S77–S82.

[48] H Waheed, S F Moin, M I Choudhary, Snake venom: from deadly toxins to life-saving therapeutics, Curr. Med. Chem. 24 (17) (2017) 1874–1891.

[49] P Bailey, J Wilce, Venom as a source of useful biologically active molecules, Emergency medicine (Fremantle, W.A.) 13 (1) (2001) 28–36.

[50] A M Soares, J P Zuliani, Toxins of animal venoms and inhibitors: molecular and biotechnological tools useful to human and animal health, Curr. Top. Med. Chem. 19 (21) (2019) 1868–1871.

[51] E C da Mata, C B Mourao, M Rangel, E F Schwartz, Antiviral activity of animal venom peptides and related compounds, The journal of venomous animals and toxins including tropical diseases 23 (2017) 3.

[52] R Meenakshisundaram, S Sweni, P Thirumalaikolundusubramanian, Hypothesis of snake and insect venoms against human immunodeficiency virus: a review, AIDS Res. Ther. 6 (2009) 25.

[53] J E Burke, E A Dennis, Phospholipase A2 biochemistry, Cardiovasc. Drugs Ther. 23 (1) (2009) 49–59.

[54] S Y Filkin, A V Lipkin, A N Fedorov, Phospholipase superfamily: structure, functions, and biotechnological applications, Biochemistry. Biokhimiia 85 (Suppl. 1) (2020) S177-s195.

[55] A Aloulou, Y B Ali, S Bezzine, Y Gargouri, M H Gelb, Phospholipases: an overview, Methods in molecular biology (Clifton, N.J.) 861 (2012) 63–85.

[56] R K Arni, R J Ward, Phospholipase A2—a structural review, Toxicon 34 (8) (1996) 827–841.

[57] R M Kini, Excitement ahead: structure, function and mechanism of snake venom phospholipase A2 enzymes, Toxicon 42 (8) (2003) 827–840.

[58] S C Austin, C D Funk, Insight into prostaglandin, leukotriene, and other eicosanoid functions using mice with targeted gene disruptions, Prostaglandins & other lipid mediators 58 (5–6) (1999) 231–252.

[59] J M Gutierrez, B Lomonte, Phospholipases A2: unveiling the secrets of a functionally versatile group of snake venom toxins, Toxicon 62 (2013) 27–39.

[60] J Boldrini-Franca, C T Cologna, M B Pucca, K C Bordon, F G Amorim, F A Anjolette, F A Cordeiro, G A Wiezel, F A Cerni, E L Pinheiro-Junior, P Y Shibao, I G Ferreira, I S de Oliveira, I A Cardoso, E C Arantes, Minor snake venom proteins: structure, function and potential applications, Biochim. Biophys. Acta, Gen. Subj. 1861 (4) (2017) 824–838.

[61] C A Nicolau, P C Carvalho, I L Junqueira-de-Azevedo, A Teixeira-Ferreira, M Junqueira, J Perales, A G Neves-Ferreira, R H Valente, An in-depth snake venom proteopeptidome characterization: benchmarking Bothrops jararaca, J. Proteome 151 (2017) 214–231.

[62] R Mendez, F Bonilla, M Sasa, Q Dwyer, J Fernandez, B Lomonte, Proteomic profiling, functional characterization, and immunoneutralization of the venom of Porthidium porrasi, a pitviper endemic to Costa Rica, Acta Trop. 193 (2019) 113–123.

[63] R H Schaloske, E A Dennis, The phospholipase A2 superfamily and its group numbering system, Biochim. Biophys. Acta 1761 (11) (2006) 1246–1259.

[64] D A Six, E A Dennis, The expanding superfamily of phospholipase A(2) enzymes: classification and characterization, Biochim. Biophys. Acta 1488 (1–2) (2000) 1–19.

[65] J M Maraganore, G Merutka, W Cho, W Welches, F J Kezdy, R L Heinrikson, A new class of phospholipases A2 with lysine in place of aspartate 49. Functional consequences for calcium and substrate binding, J. Biol. Chem. 259 (22) (1984) 13839–13843.

[66] Y Angulo, B Lomonte, Biochemistry and toxicology of toxins purified from the venom of the snake Bothrops asper, Toxicon 54 (7) (2009) 949–957.

[67] B Lomonte, J Rangel, Snake venom Lys49 myotoxins: from phospholipases A(2) to non-enzymatic membrane disruptors, Toxicon 60 (4) (2012) 520–530.

[68] J F Wei, X L Wei, Q Y Chen, T Huang, L Y Qiao, W Y Wang, Y L Xiong, S H He, N49 phospholipase A2, a unique subgroup of snake venom group II phospholipase A2, Biochim. Biophys. Acta 1760 (3) (2006) 462–471.

[69] J Polgar, E M Magnenat, M C Peitsch, T N Wells, K J Clemetson, Asp-49 is not an absolute prerequisite for the enzymic activity of low-M(r) phospholipases A2: purification, characterization and computer modelling of an enzymically active Ser-49 phospholipase A2, ecarpholin S, from the venom of Echis carinatus sochureki (saw-scaled viper), The Biochemical journal 319 (Pt 3) (1996) 961–968.

[70] C L Ownby, H S Selistre de Araujo, S P White, J E Fletcher, Lysine 49 phospholipase A2 proteins, Toxicon 37 (3) (1999) 411–445.

[71] R M Kini, H J Evans, A common cytolytic region in myotoxins, hemolysins, cardiotoxins and antibacterial peptides, Int. J. Pept. Protein Res. 34 (4) (1989) 277–286.

[72] C E Nunez, Y Angulo, B Lomonte, Identification of the myotoxic site of the Lys49 phospholipase A(2) from Agkistrodon piscivorus piscivorus snake venom: synthetic C-terminal peptides from Lys49, but not from Asp49 myotoxins, exert membrane-damaging activities, Toxicon 39 (10) (2001) 1587–1594.

[73] A L Ambrosio, M C Nonato, H S de Araujo, A Arni, R J Ward, C L Ownby, D H de Souza, R C Garratt, A molecular mechanism for Lys49-phospholipase A2 activity based on ligand-induced conformational change, J. Biol. Chem. 280 (8) (2005) 7326–7335.

[74] B Lomonte, Y Angulo, E Moreno, Synthetic peptides derived from the C-terminal region of Lys49 phospholipase A2 homologues from viperidae snake venoms: biomimetic activities and potential applications, Curr. Pharm. Des. 16 (28) (2010) 3224–3230.

[75] G Lambeau, P Ancian, J P Nicolas, S H Beiboer, D Moinier, H Verheij, M Lazdunski, Structural elements of secretory phospholipases A2 involved in the binding to M-type receptors, J. Biol. Chem. 270 (10) (1995) 5534–5540.

[76] A Akalu, A Cretu, P C Brooks, Targeting integrins for the control of tumour angiogenesis, Expert Opin. Investig. Drugs 14 (12) (2005) 1475–1486.

[77] E Jimenez-Charris, D S Lopes, S N C Gimenes, S C Teixeira, L Montealegre-Sanchez, L Solano-Redondo, L Fierro-Perez, V M Rodrigues Avila, Antitumor potential of Pllans-II, an acidic Asp49-PLA2 from Porthidium lansbergii lansbergii snake venom on human cervical carcinoma HeLa cells, Int. J. Biol. Macromol. 122 (2019) 1053–1061.

[78] M L Massimino, M Simonato, B Spolaore, C Franchin, G Arrigoni, O Marin, L Monturiol-Gross, J Fernandez, B Lomonte, F Tonello, Cell surface nucleolin interacts with and internalizes Bothrops asper Lys49 phospholipase A2 and mediates its toxic activity, Sci. Rep. 8 (1) (2018) 10619.

[79] R M Kini, H J Evans, A model to explain the pharmacological effects of snake venom phospholipases A2, Toxicon 27 (6) (1989) 613–635.

[80] R Diniz-Sousa, C A S Caldeira, A M Kayano, M V Paloschi, D C Pimenta, R Simoes-Silva, A S Ferreira, F B Zanchi, N B Matos, F P Grabner, L A Calderon, J P Zuliani, A M Soares, Identification of the molecular determinants of the antibacterial activity of LmutTX, a Lys49 phospholipase A2 homologue isolated from Lachesis muta muta snake venom (Linnaeus, 1766), Basic Clin. Pharmacol. Toxicol. 122 (4) (2018) 413–423.

[81] C Prinholato da Silva, T R Costa, R M Paiva, A C Cintra, D L Menaldo, L M Antunes, S V Sampaio, Antitumor potential of the myotoxin BthTX-I from Bothrops jararacussu snake venom: evaluation of cell cycle alterations and death mechanisms induced in tumor cell lines, The journal of venomous animals and toxins including tropical diseases 21 (2015) 44.

[82] F V Azevedo, D S Lopes, S N Cirilo Gimenes, D C Ache, L Vecchi, P T Alves, O Guimaraes Dde, R S Rodrigues, L R Goulart, M Rodrigues Vde, K A Yoneyama, Human breast cancer cell death induced by BnSP-6, a Lys-49 PLA(2) homologue from Bothrops pauloensis venom, Int. J. Biol. Macromol. 82 (2016) 671–677.

[83] F V P de Vasconcelos Azevedo, M A P Zoia, D S Lopes, S N Gimenes, L Vecchi, P T Alves, R S Rodrigues, A C A Silva, K A G Yoneyama, L R Goulart, V de Melo Rodrigues, Antitumor and antimetastatic effects of PLA2-BthTX-II from Bothrops jararacussu venom on human breast cancer cells, Int. J. Biol. Macromol. 135 (2019) 261–273.

[84] A Bazaa, J Luis, N Srairi-Abid, O Kallech-Ziri, R Kessentini-Zouari, C Defilles, J C Lissitzky, M El Ayeb, N Marrakchi, MVL-PLA2, a phospholipase A2 from Macrovipera lebetina transmediterranea venom, inhibits tumor cells adhesion and migration, Matrix Biol. 28 (4) (2009) 188–193.

[85] D.C. Nunes, M.M. Figueira, D.S. Lopes, D.L. De Souza, L.F. Izidoro, E.A. Ferro, M.A. Souza, R.S. Rodrigues, V.M. Rodrigues, K.A. Yoneyama, BnSP-7 toxin, a basic phospholipase A2 from Bothrops pauloensis snake venom, interferes with proliferation, ultrastructure and infectivity of Leishmania (Leishmania) amazo-nensis, Parasitology 140(7) (2013) 844–54.

[86] I P Borges, L E Castanheira, B F Barbosa, D L de Souza, R J da Silva, J R Mineo, K A Tudini, R S Rodrigues, E A Ferro, V de Melo Rodrigues, Anti-parasitic effect on Toxoplasma gondii induced by BnSP-7, a Lys49-phospholipase A2 homologue from Bothrops pauloensis venom, Toxicon 119 (2016) 84–91.

[87] J P Rodrigues, F V P Vasconcelos Azevedo, M A P Zoia, L P Maia, L I V Correia, J M Costa-Cruz, V de Melo Rodrigues, L R Goulart, The anthelmintic effect on Strongyloides venezuelensis induced by BnSP- 6, a Lys49-phospholipase A2 homologue from Bothrops pauloensis venom, Curr. Top. Med. Chem. 19 (22) (2019) 2032–2040.

[88] V D Muller, R R Russo, A C Cintra, M A Sartim, M Alves-Paiva Rde, L T Figueiredo, S V Sampaio, V H Aquino, Crotoxin and phospholipases A(2) from Crotalus durissus terrificus showed antiviral activity against dengue and yellow fever viruses, Toxicon 59 (4) (2012) 507–515.

[89] V D Muller, R O Soares, N N dos Santos Jr., A C Trabuco, A C Cintra, L T Figueiredo, A Caliri, S V Sampaio, V H Aquino, Phospholipase A2 isolated from the venom of Crotalus durissus terrificus inactivates dengue virus and other enveloped viruses by disrupting the viral envelope, PLoS One 9 (11) (2014) e112351.

[90] J F Shimizu, C M Pereira, C Bittar, M N Batista, G R F Campos, S da Silva, A C O Cintra, C Zothner, M Harris, S V Sampaio, V H Aquino, P Rahal, A C G Jardim, Multiple effects of toxins isolated from Crotalus durissus terrificus on the hepatitis C virus life cycle, PLoS One 12 (11) (2017) e0187857.

[91] A B Cecilio, S Caldas, R A Oliveira, A S Santos, M Richardson, G B Naumann, F S Schneider, V G Alvarenga, M I Estevão-Costa, A L Fuly, J A Eble, E F Sanchez, Molecular characterization of Lys49 and Asp49 phospholipases A2 from snake venom and their antiviral activities against dengue virus, Toxins 5 (10) (2013) 1780–1798.

[92] H Brenes, G D Loría, B Lomonte, Potent virucidal activity against Flaviviridae of a group IIA phospholipase A(2) isolated from the venom of Bothrops asper, Biologicals 63 (2020) 48–52.

[93] J Prado-Franceschi, O V Brazil, Convulxin, a new toxin from the venom of the South American rattlesnake Crotalus durissus terrificus, Toxicon 19 (6) (1981) 875–887.

[94] G Alexander, J Grothusen, H Zepeda, R J Schwartzman, Gyroxin, a toxin from the venom of Crotalus durissus terrificus, is a thrombin-like enzyme, Toxicon 26 (10) (1988) 953–960.

[95] R A Hendon, H Fraenkel-Conrat, Biological roles of the two components of crotoxin, Proc. Natl. Acad. Sci. U. S. A. 68 (7) (1971) 1560–1563.

[96] K Rubsamen, H Breithaupt, E Habermann, Biochemistry and pharmacology of the crotoxin complex. I. Subfractionation and recombination of the crotoxin complex, Naunyn-Schmiedebergs Archiv fur Pharmakologie 270 (3) (1971) 274–288.

[97] V G Villarrubia, L A Costa, R A Díez, Fosfolipasas A2 segregadas (sPLA2):¿amigas o enemigas? ¿Actores de la resistencia antibacteriana y antivirus de la inmunodeficiencia humana?, Med. Clin. 123 (19) (2004) 749–757.

[98] A C Cintra, S Marangoni, B Oliveira, J R Giglio, Bothropstoxin-I: amino acid sequence and function, J. Protein Chem. 12 (1) (1993) 57–64.

[99] R R Russo, N N Dos Santos Junior, A C O Cintra, L T M Figueiredo, S V Sampaio, V H Aquino, Expression, Purification and Virucidal Activity of Two Recombinant Isoforms of Phospholipase A2 From Crotalus durissus terrificus Venom, 164, 2019, pp. 1159–1171 (4).

[100] R Bartenschlager, V Lohmann, F Penin, The molecular and structural basis of advanced antiviral therapy for hepatitis C virus infection, Nat. Rev. Microbiol. 11 (7) (2013) 482–496.

[101] T Masaki, R Suzuki, K Murakami, H Aizaki, K Ishii, A Murayama, T Date, Y Matsuura, T Miyamura, T Wakita, T Suzuki, Interaction of hepatitis C virus nonstructural protein 5A with core protein is critical for the production of infectious virus particles, J. Virol. 82 (16) (2008) 7964–7976.

[102] D A Higuchi, C M Barbosa, C Bincoletto, J R Chagas, A Magalhaes, M Richardson, E F Sanchez, J B Pesquero, R C Araujo, J L Pesquero, Purification and partial characterization of two phospholipases A2 from Bothrops leucurus (white-tailed-jararaca) snake venom, Biochimie 89 (3) (2007) 319–328.

[103] T Chijiwa, E Tokunaga, R Ikeda, K Terada, T Ogawa, N Oda-Ueda, S Hattori, M Nozaki, M Ohno, Discovery of novel [Arg49]phospholipase A2 isozymes from Protobothrops elegans venom and regional evolution of Crotalinae snake venom phospholipase A2 isozymes in the southwestern islands of Japan and Taiwan, Toxicon 48 (6) (2006) 672–682.

[104] A Alape-Giron, L Sanz, J Escolano, M Flores-Diaz, M Madrigal, M Sasa, J J Calvete, Snake venomics of the lancehead pitviper Bothrops asper: geographic, individual, and ontogenetic variations, J. Proteome Res. 7 (8) (2008) 3556–3571.

[105] L Paramo, B Lomonte, J Pizarro-Cerda, J A Bengoechea, J P Gorvel, E Moreno, Bactericidal activity of Lys49 and Asp49 myotoxic phospholipases A2 from Bothrops asper snake venom—synthetic Lys49 myotoxin II-(115-129)-peptide identifies its bactericidal region, Eur. J. Biochem. 253 (2) (1998) 452–461.

[106] O G Berg, M H Gelb, M D Tsai, M K Jain, Interfacial enzymology: the secreted phospholipase A(2)-paradigm, Chem. Rev. 101 (9) (2001) 2613–2654.

[107] D Fenard, G Lambeau, E Valentin, J C Lefebvre, M Lazdunski, A Doglio, Secreted phospholipases A(2), a new class of HIV inhibitors that block virus entry into host cells, J. Clin. Invest. 104 (5) (1999) 611–618.

[108] G Lambeau, J Barhanin, H Schweitz, J Qar, M Lazdunski, Identification and properties of very high affinity brain membrane-binding sites for a neurotoxic phospholipase from the taipan venom, J. Biol. Chem. 264 (19) (1989) 11503–11510.

[109] L Cupillard, R Mulherkar, N Gomez, S Kadam, E Valentin, M Lazdunski, G Lambeau, Both group IB and group IIA secreted phospholipases A2 are natural ligands of the mouse 180-kDa M-type receptor, J. Biol. Chem. 274 (11) (1999) 7043–7051.

[110] S Chwetzoff, S Tsunasawa, F Sakiyama, A Menez, Nigexine, a phospholipase A2 from cobra venom with cytotoxic properties not related to esterase activity. Purification, amino acid sequence, and biological properties, J. Biol. Chem. 264 (22) (1989) 13289–13297.

[111] G Lambeau, M Lazdunski, Receptors for a growing family of secreted phospholipases A2, Trends Pharmacol. Sci. 20 (4) (1999) 162–170.

[112] F J Joubert, Naja mossambica mossambica venom. Purification, some properties and the amino acid sequences of three phospholipases A (CM-I, CM-II and CM-III), Biochim. Biophys. Acta 493 (1) (1977) 216–227.

[113] T Ahmad, A J Lawrence, Purification and activation of phospholipase A2 isoforms from Naja mossambica mossambica (spitting cobra) venom, Toxicon 31 (10) (1993) 1279–1291.

[114] M Chen, C Aoki-Utsubo, M Kameoka, Broad-spectrum Antiviral Agents: Secreted Phospholipase A(2) Targets Viral Envelope Lipid Bilayers Derived From the Endoplasmic Reticulum Membrane, 7, 2017, p. 15931 (1).

[115] H P Vacklin, F Tiberg, G Fragneto, R K Thomas, Phospholipase A2 hydrolysis of supported phospholipid bilayers: a neutron reflectivity and ellipsometry study, Biochemistry 44 (8) (2005) 2811–2821.

[116] G van Meer, A I de Kroon, Lipid map of the mammalian cell, J. Cell Sci. 124 (Pt 1) (2011) 5–8.

[117] V Monje-Galvan, J B Klauda, Modeling yeast organelle membranes and how lipid diversity influences bilayer properties, Biochemistry 54 (45) (2015) 6852–6861.

[118] Q Zhang, C Hunke, Y H Yau, V Seow, S Lee, L B Tanner, X L Guan, M R Wenk, G Fibriansah, P L Chew, P Kukkaro, G Biukovic, P Y Shi, S G Shochat, G Grüber, S M Lok, The stem region of premembrane protein plays an important role in the virus surface protein rearrangement during dengue maturation, J. Biol. Chem. 287 (48) (2012) 40525–40534.

[119] O Trott, A J Olson, AutoDock Vina: improving the speed and accuracy of docking with a new scoring function, efficient optimization, and multithreading, J. Comput. Chem. 31 (2) (2010) 455–461.

[120] P G Higgs, A four-column theory for the origin of the genetic code: tracing the evolutionary pathways that gave rise to an optimized code, Biol. Direct 4 (2009) 16.

[121] B Lomonte, E Moreno, A Tarkowski, L A Hanson, M Maccarana, Neutralizing interaction between heparins and myotoxin II, a lysine 49 phospholipase A2 from Bothrops asper snake venom. Identification of a heparin-binding and cytolytic toxin region by the use of synthetic peptides and molecular modeling, J. Biol. Chem. 269 (47) (1994) 29867–29873.

[122] J I dos Santos, A M Soares, M R Fontes, Comparative structural studies on Lys49-phospholipases A(2) from Bothrops genus reveal their myotoxic site, J. Struct. Biol. 167 (2) (2009) 106–116.

[123] C A Fernandes, R J Borges, B Lomonte, M R Fontes, A structure-based proposal for a comprehensive myotoxic mechanism of phospholipase A2-like proteins from viperid snake venoms, Biochim. Biophys. Acta 1844 (12) (2014) 2265–2276.

[124] D Mora-Obando, J Fernandez, C Montecucco, J M Gutierrez, B Lomonte, Synergism between basic Asp49 and Lys49 phospholipase A2 myotoxins of viperid snake venom in vitro and in vivo, PLoS One 9 (10) (2014) e109846.

[125] R Vijay, X Hua, D K Meyerholz, Y Miki, K Yamamoto, M Gelb, M Murakami, S Perlman, Critical role of phospholipase A2 group IID in age-related susceptibility to severe acute respiratory syndrome-CoV infection, J. Exp. Med. 212 (11) (2015) 1851–1868.

[126] C Müller, M Hardt, D Schwudke, B W Neuman, S Pleschka, J Ziebuhr, Inhibition of cytosolic phospholipase A(2)α impairs an early step of coronavirus replication in cell culture, J. Virol. 92 (4) (2018).

[127] C Allal, C Buisson-Brenac, V Marion, C Claudel-Renard, T Faraut, P Dal Monte, D Streblow, M Record, J L Davignon, Human cytomegalovirus carries a cell-derived phospholipase A2 required for infectivity, J. Virol. 78 (14) (2004) 7717–7726.

[128] N Menzel, W Fischl, K Hueging, D Bankwitz, A Frentzen, S Haid, J Gentzsch, L Kaderali, R Bartenschlager, T Pietschmann, MAP-kinase regulated cytosolic phospholipase A2 activity is essential for production of infectious hepatitis C virus particles, PLoS Pathog. 8 (7) (2012) e1002829.